学位申請論文

平島崇男

学 位 審 査 報 告

氏　　名	平　島　崇　男
学位の種類	理　学　博　士
学位記番号	理　博　第　　号
学位授与の日付	昭和　　年　　月　　日
学位授与の要件	学位規則　第5条　第1項該当
研究科・専　攻	理学研究科地質学鉱物学専攻

（学位論文題目）

Petrological study of the Sanbagawa metamorphic belt in the Kanto Mountains, central Japan.

（関東山地三波川変成帯の岩石学的研究）

論文調査委員	主　査　坂野昇平 森本信男　亀井節夫

理　学　研　究　科

氏　名	平　島　崇　男

（論文内容の要旨）

申請者の論文は群馬県から埼玉県にかかる関東山地の三波川変成帯の岩石学的研究である。論文は当該地域の地質構造の解析から出発し，変成鉱物の分布の決定とそれによる変成分帯を基礎にして，変成反応の解析と広域変成帯の比較論にいたっている。

地質構造の研究は岩石学的研究の基礎として行ったものである。その問従来知られていなかった，メランジュ帯が三波川変成帯の上に衝上していること，衝上帯にはひすい輝石＋石英の組み合わせ持つ高圧変成岩をはじめとして，三波川帯に知られていない変成岩が含まれていることを明らかにした。その結果いままで断片的にしか知られていなかった，三波川帯としては異質な変成岩が当該地域に存在する理由を明らかにした。

岩石学的研究の中心は御鉾荷緑色類とその上下の三波川結晶片岩類と秩父累層の塩基性岩においた。その結果の主なものは次の通りである。

1）ローソン石は変成はんれい岩を主とするAl_2O_3に富んだ岩石にのみ産する。その種の岩石の分布は偏りが多いので，その産出を変成分帯の指示鉱物としては使えない。

2）ひすい輝石＋石英の組み合わせは三波川変成岩には存在しない。しかしアルカリ輝石はよく産する。そのひすい輝石成分の濃度は一般に，0.2を越えない。

3）研究地域は変成度の上昇により，ブドウ石－パンペリー石相，アルカリ輝石－緑泥石相，パンペリー石－アクチノ閃石相，とアルバイト－緑簾石－角閃岩相の4つの変成相に分けられる。またパンペリー石－アクチノ閃石相はアルカリ輝石－アクチノ閃石－緑簾石－緑泥石の組み合わせを持つ低温の亜相とより高温のアルカリ角閃石－アクチノ閃石－緑泥石－緑泥石亜相とに

区分できる。

以上のような結果を系統的に扱うため，申請者はA－C－F3成分・7相系およびA－C－F－F3（Fe_2O_3）4成分7相系の共生関係をSchreinemakersの方法で解析し，アルカリ輝石の産する温度・圧力領域を決め，新らしくアルカリ輝石－緑泥石相を提唱した。またそれにより高圧中間群の低温部にたいする変成相系列を修正した。申請者はSchreinemakersの方法を複雑な多成分系で展開する上でのいくつかの新しい工夫をしている。

申請者はこの研究の1つの結論として，関東山地の三波川変成帯は他の地域のそれと同じく大きな分類としては，高圧中間群に属するが，後者よりも，やや高圧のもとで起こったという問題提起をおこなっている。また，California，New Caledonia，New Zealandとなどの高圧変成帯との比較論を展開し，高圧中間群である三波川帯の比較変成論における意義を明らかにした。

氏　名	平　島　崇　男

（論文審査の結果の要旨）

１９６０年代の初めに変成相系列の概念が提唱されたとき，関東山地の三波川変成帯はひすい輝石－藍閃石型の高圧変成作用の典型地域とされた。それはローソン石とひすい輝石＋石英の組み合わせが普通に産するとされていたためである。その後世界的に高圧変成岩の研究が進むにつれ，関東山地の鉱物共生関係が他の地域のそれと整合しないことが指摘された。その後，関東山地の研究者たちは１９６０年代初頭とは異なった結果を得ていたが，以前の研究に大幅な修正が必要なのか，あるいは地域的な原岩の化学組成の偏りの影響を除去できなかったために，研究者によって結果が異なるのか不明であった。

申請者はローソン石は変成はんれい岩の一部にのみ産すること，それはその種の岩石がAl_2O_3に富み，Fe_2O_3に乏しいためであり，そのような岩石分布は地域的に偏っているため，ローソン石の分布は変成分帯の指標となりえないことを明らかにした。ひすい輝石については，関東山地の三波川変成岩にはひすい輝石は産しないこと，しかしアルカリ輝石は頻繁に産することを明らかにした。この結果関東山地の三波川変成帯は他の地域の三波川帯と同じように高圧中間群に属することが明らかになった。これは高圧変成作用論の長年の疑問を解決したものであり，単に一地域の岩石の性質が明らかになったにとどまらず，日本列島の形成を論ずるための重要な貢献である。

申請者はさらにアルカリ輝石の産状を多相平衡論で解析し，従来よく認識されていなかった低変成度での輝石固溶帯の役割を明らかにした。すなわち輝石－緑泥石の組み合わせは角閃石－緑簾石の組み合わせより低温で安定であり，圧力にかんしては３－６kbar 程度の高圧中間群で安定化する。その結果関東山地の三波川変成帯をプレーナイトーパンペリー石帯・アルカリ輝石－緑泥石帯・アルカリ角閃石－緑簾石帯・パンペリー石－アクチノ閃石帯・アルバイト－緑簾石－角閃岸帯の５に分帯した。このうち２番目と３番目の

帯はパンペリー石ーアクチノ閃石相の亜相である。この考えは今後多くの地域に適用されるものと思われ，変成相論での注目される貢献である。共生関係解析のためSchreinemakersの方法を用いたが，それを実際の岩石に適用するために，いくつかの新しい工夫がされており，これも今後利用されるであろう。

申請者は以上の成果を世界の広域変成帯の比較し，環太平洋造山帯の中で三波川帯がNew ZealandとNew Caledoniaとの中間の圧力下で形成されたことを明確にした。なお参考論文は本論文にいたる過程での研究を発表したものと，協同研究者と研究中のNorwayのSpitsbergen島の高圧変成岩の研究に関するものでいずれも申請者の岩石学の高い能力を示すものである。

したがって本研究は理学博士の学位論文としてふさわしいものと認める。

なお，主論文及び参考論文に報告されている研究業績を中心とし，これに関連した研究分野について試問した結果，合格と認めた。

主論文 1

PETROLOGICAL STUDY OF THE SANBAGAWA METAMORPHIC BELT IN THE KANTO MOUNTAINS, CENTRAL JAPAN.

A DISSERTATION
SUBMITTED TO THE DEPARTMENT OF GEOLOGY AND MINERALOGY,
FACULTY OF SCIENCE, KYOTO UNIVERSITY
IN PARTIAL FULFILLMENT OF THE REQUIREMENTS
FOR THE DEGREE OF
DOCTOR OF SCIENCE

by

TAKAO HIRAJIMA

December 1984

Content

ABSTRACT

The present paper treats the metamorphic facies series which characterize the lower-grade part of the glaucophanitic metamorphic belt. For this attempt, geologic and petrologic studies were carried out on the metamorphic rocks located in the Kanto Mountains, central Japan. Specimens were collected from the Chichibu Group, the Mikabu Greenrock Complex, the Sanbagawa schists in the strict sense, and the Tochiya and Atokura Klippes which are exposed in Saitama and Gumma Prefecture.

This petrographic study indicates that the Sanbagawa metamorphism affects the constituents of the Chichibu Group, the Mikabu Greenrock Complex and the Sanbagawa schists. The lowest grade rocks of this metamorphism belong to the prehnite-pumpellyite facies. They are exposed in the upper stratigraphic part of the Chichibu Group. The metamorphic grade increases from the sodic pyroxene-chlorite facies, through the pumpellyite-actinolite facies and finally to the epidote-amphibolite facies with descending stratigraphic order. The sodic pyroxene-chlorite facies is characterized by the mineral assemblage of sodic pyroxene + pumpellyite + epidote + chlorite. The pumpellyite-actinolite facies is subdivided into two subfacies; the lower-temperature subfacies is characterized by the mineral assemblage of sodic pyroxene + actinolite + epidote + chlorite, and the

higher-temperature subfacies by that of sodic amphibole + actinolite + epidote + chlorite. The sodic pyroxene-chlorite facies and two subfacies of the pumpellyite-actinolite facies are proposed for the first time by the present study.

Jd (Jadeite component) in sodic pyroxene plays an important role in determining its minimum pressure of equilibration. Sodic pyroxenes in metabasites of both the sodic pyroxene-chlorite facies and the pumpellyite-actinolite facies contain no more than 20 mol% of Jd. The average of Jd in metabasites of the sodic pyroxene-chlorite facies is about 5 mol%, and that in the pumpellyite-actinolite facies is about 10 mol%. The compositional change of sodic pyroxenes indicates that the metamorphic pressure of the Kanto Mountains increases with the metamorphic temperature.

Atokura and Tochiya Klippes are composed of Cretaceous and Miocene sediments, Paleozoic granitic rocks and the mélange. These rocks suffered the prehnite-pumpellyite facies metamorphism during the early Miocene which postdated the Sanbagawa metamorphism. Jadeite-quartz rock associated with ultrabasic rocks was found from the Tochiya Klippe as a tectonic block, not from the Sanbagawa metamorphic rocks.

To define the metamorphic facies series of the glaucophanitic metamorphism, Schreinemakers' analysis was adopted. For the first step, to give an outline of the stability range of the sodic pyroxene-chlorite facies, the

analysis was carried out for the model ACF system with seven phases; diopside, glaucophane, tremolite, zoisite, pumpellyite, lawsonite, and chlorite. This system provides seven independent petrogenetic grids. Two of them can explain the mineral assemblages observed in the glaucophanitic belts and predict that the sodic pyroxene-chlorite facies is stable at lower-temperature range of the pumpellyite-actinolite facies and at lower-pressure range of the lawsonite-albite facies. For the second step, actual mineral assemblages and compositions were used for the partial analysis of the Schreinemakers method for the ACF-F3(Fe^{3+}) system with seven phases; sodic pyroxene, sodic amphibole, actinolite, epidote, pumpellyite, chlorite and hematite. The grid derived from this system inherited the essential character of the two grids of the ACF system, and makes it possible to compare the P-T conditions of various glaucophanitic belts under same criterion. The grid indicates that the formational pressure of the Kanto Mountains is lower than that of the typical glaucophanitic belt, such as New Caledonia, and is higher than those of the Sanbagawa belt of Shikoku and Western Otago, New Zealand.

I. Introduction

Glaucophane schist facies is one of high-pressure metamorphic facies which have been proposed by Eskola (1939) and originally characterized by the critical minerals of glaucophane, lawsonite and pumpellyite. More detailed studies of the glaucophane schist were carried out mainly in the circum Pacific areas since 1950s (Miyashiro and Banno, 1958; Seki, 1958, 1960; Banno, 1964; Ernst, 1965, 1971; Ernst et al., 1971; Brothers, 1970; Black and Brothers, 1977). Based on these works, Miyashiro (1961, 1973) added the jadeite + quartz assemblage to critical minerals of the glaucophane schist facies and proposed to subdivide the glaucophanitic metamorphic belts into two types; the typical subfacies (jadeite-glaucophane type of metamorphism) and the atypical subfacies (high-pressure intermediate group of metamorphism).

Actually, jadeitic pyroxenes associated with quartz commonly occur in metagreywackes, metasiliceous rocks and meta-acidic rocks of the typical glaucophanitic belts, i.e., Franciscan (Essene & Fyfe, 1967), New Caledonia (Black, 1974; Brothers & Yokoyama, 1982), Sesia-Lanzo zone, Western Alps (Compagnoni & Maffeo, 1973), Cyclades Archipelago (Okurash et al., 1978), Caledonian belt of western Spitsbergen (Kanat, 1984; Hirajima et al., in press) and the Kamuikotan Belt (Seki & Shido, 1959; Gouchi, 1983). In these belts, metabasites commonly contain lawsonite,

glaucophane, aragonite and omphacite.

Other glaucophanitic belts, such as Sanbagawa belt of Shikoku, Shuksan, Calabria and Western Otago, are considered to belong to the atypical subfacies (Miyashiro, 1961, 1973; Brown, 1977). In these areas, jadeite-quartz assemblage is absent and metabasites commonly contain actinolite, low-jadeitic pyroxene, epidote, pumpellyite, and chlorite.

In the Kanto Mountains of the Sanbagawa belt, Seki (1957, 1958, 1960) reported the occurrence of lawsonite and jadeite + quartz assemblage. He found these minerals from the middle grade part of the terrane, whereas the critical minerals of the atypical subfacies such as albite, epidote, actinolite, and calcite are stable in both lower and higher grade parts. Although this phenomenon is unique to the other areas of the typical subfacies, Seki's reports led to the speculation that the metamorphic pressure of the Kanto Mountains is higher than that of the other areas of the belt (Miyashiro, 1965, 1973).

Since Seki's petrographic works, quite a few investigators have engaged in petrologic study of the Kanto Mountains, namely Tanaka and Fukuda (1974), Toriumi (1975), Suzuki (1977) and Tanabe et al. (1982). However, they could not confirmed any petrologic evidence of the typical subfacies from the Kanto Mountains and concluded that the metamorphic facies of this area belongs to the atypical subfacies as same as the other areas of the Sanbagawa belt.

Therefore, the two important notions in late 1950s to early 1960s on the petrology of the Kanto Mountains are questioned. First, it was not clear whether or not the jadeite + quartz assemblage did really occurred in the Kanto Mountains. Second, whether or not the physical conditions of metamorphism of the Kanto Mountains differed from the rest of the Sanbagawa belt.

The chaos on the petrologic interpretation of the Kanto Mountains was caused by the ambiguity of the definition of the glaucophane schist facies, or its facies series. The author aims to define the metamorphic facies series which characterizes the glaucophanitic metamorphism in general. For the first step, he initiated the geologic and petrologic studies of the Kanto Mountains to prepare a reliable geologic map and to determine the mineral assemblages of this area. Then, the petrogenetic grid was constructed by the Schreinemakers' method to determine the metamorphic facies.

Geologic and petrologic studies were carried out on the constituents of the Chichibu Group, the Mikabu Greenrock Complex, the Sanbagawa schists, and the Tochiya and Atokura Klippes, which are exposed in Saitama and Gumma Prefecture. He could clarify that jadeite + quartz assemblage is absent in the Sanbagawa metamorphic rocks composing the Chichibu Group, the Mikabu Greenrock Complex and the Sanbagawa schists, but also found that sodic pyroxene (low jadeitic pyroxene) which closely associated with chlorite is

widespread in the metabasites of the Chichibu Group and the Mikabu Greenrock Complex. Actually, along the Kanna-gawa, central part of the Kanto Mountains, the assemblage of sodic pyroxene + pumpellyite + epidote + chlorite in metabasites of the Chichibu Group progressively changes to that of sodic pyroxene + actinolite + epidote + chlorite in those of the Mikabu Greenrock Complex which is stable under the metamorphic condition of the pumpellyite-actinolite facies (Hashimoto, 1966; Coombs et al., 1976). Then, sodic pyroxene + chlorite assemblage becomes rare in metabasites of the Sanbagawa schists with increase of metamorphic grade.

Such common occurrence of sodic pyroxene is unique, and the sodic pyroxene-bearing assemblages found by this study have not been reported from any of regional metamorphic belts. Thus, the stability relations of sodic pyroxene in lower-grade metabasites was chosen as the major petrologic problem.

Stability of the sodic pyroxene-chlorite assemblage was examined with the Schreinemakers' method for a model ACF system and an ACF-F3(Fe^{3+}) system. To reveal the outline of the stability range of the sodic pyroxene-chlorite assemblage, the analysis was carried out for the model ACF system with seven phases; diopside, glaucophane, tremolite, zoisite, pumpellyite, lawsonite and chlorite. Possible petrogenetic grids derived from the model ACF system predict that the assemblage diopside + chlorite is stable in

basaltic composition at the lower-grade part of the high-pressure intermediate group of metamorphism and it becomes rare with increase of metamorphic grade.

Even though the ACF system is capable to clarify some of important feature of the assemblages in question, it fails to reveal the role of $Al\text{-}Fe^{3+}$ substitution which is essential in determining the stability of such minerals as sodic pyroxene and sodic amphibole, especially when one deals with the high-pressure intermediate facies series. The paragenetic relations of sodic pyroxene and sodic amphibole-bearing assemblages were analyzed in terms of four component system with seven phases, in which Fe_2O_3 is added to component and hematite to the phase, but lawsonite is omitted. As this system ignores lawsonite, it is not appropriate to discuss the stability of calc-alumino silicate, but it is sufficient to represent the role of sodic pyroxene solid solution on the paragenesis of four component ACF-F3 system.

A petrogenetic grid for the ACF-F3 system was constructed using the actual data in the Kanto Mountains. The grid defines the stability field of the sodic pyroxene-chlorite facies and that of the pumpellyite-actinolite facies, and indicates that the Chichibu Group and the Mikabu Greenrock Complex of the Sanbagawa belt in the Kanto Mountains are examples of such a hitherto unknown facies. Further, the grid gives a criterion with which we can compare the P-T condition of glaucophanitic metamorphic

belts.

While being engaged in petrologic works, the author found another group of metamorphic rocks in the Kanto Mountains. They are tectonic blocks belonging to the Klippe system that thrusted over the Sanbagawa belt during Miocene. The tectonic blocks are composed of the metamorphic rocks of various grades and P-T histories such as jadeite-quartz rock, jadeite-aragonite-bearing metabasites, and amphibolite. The constituents of the Klippe includes the Cretaceous and Miocene sediments, Paleozoic granitic rocks and the greenrock mélange. They also suffered the prehnite-pumpellyite facies metamorphism which postdated the Sanbagawa metamorphism. As this is new finding, the mode of occurrence and geologic significance of these rocks are described in the thesis.

II. Geology

II-1-1. Geologic outline of the Kanto Mountains

The Kanto Mountains is the cradle of geology in Japan, but its geology has not been well understood yet. In the Kanto Mountains, following geologic units generally occur with regular zonal arrangement from north to south, i.e., the Sanbagawa Group which contains the Sanbagawa schists and the Mikabu Greenrock Complex, the Chichibu Group, the Cretaceous formations in the Sanchu Graben, the Chichibu Group, and the Mesozoic Shimanto Belt. The rocks of the Sanbagawa and Chichibu Groups are mostly late Paleozoic to Mesozoic sedimentary and igneous rocks, and have been metamorphosed. The boundary between the Chichibu Group and the Shimanto Belt is now under dispute. This paper follows that boundary accepted by Geologic Map of Japan (Geological Survey of Japan, 1978). The Atokura Formation and its correlatives distribute in the WNW-ESE trend in the northern part of the Kanto Mountains. They overlie the Sanbagawa and Chichibu Groups with a thrust contact. The Tertiary system is distributed in the Chichibu basin in the central part of the Kanto Mountains. It also covers pre-Mesozoic basements along the eastern and northern margins of the Kanto Mountains. The distribution of the strata mentioned above are shown in Fig. II-2.

This paper describes geologic and petrologic study on the rocks which crop out on the north of the Sanchu Graven, i.e., the northern half of the Chichibu Group, the Mikabu

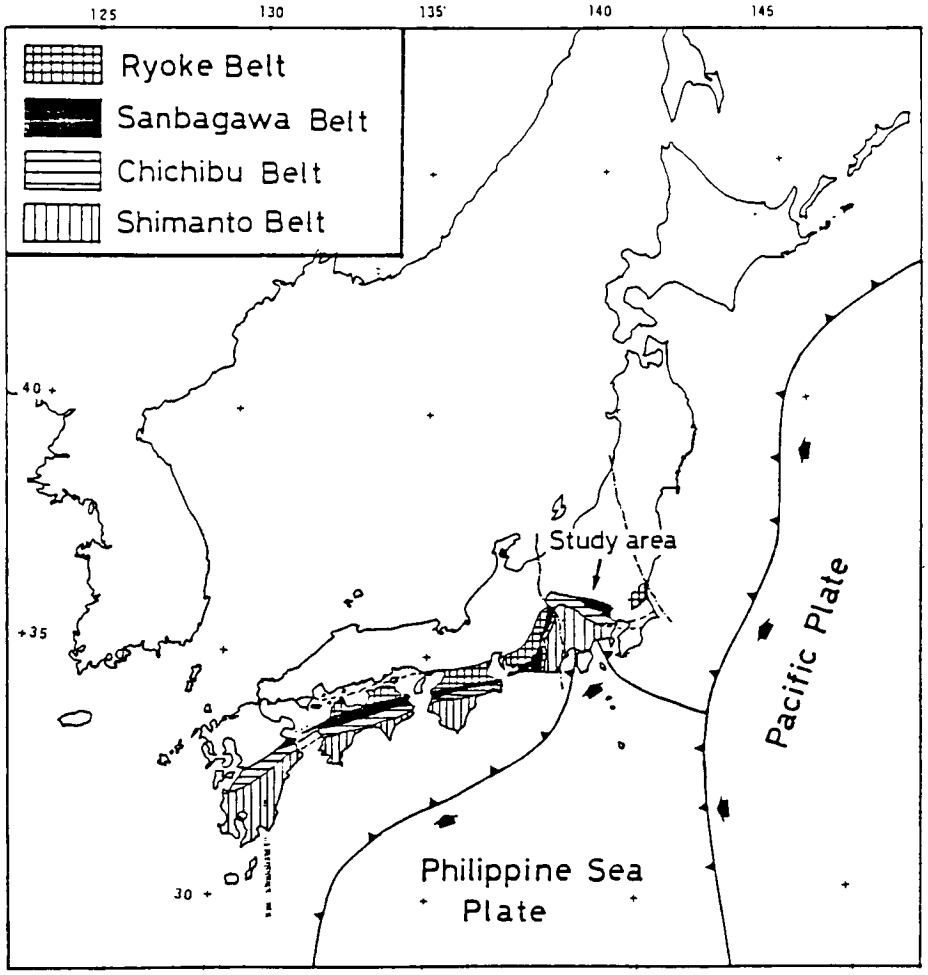

Fig. II-1. Geologic outline of southwest Japan.

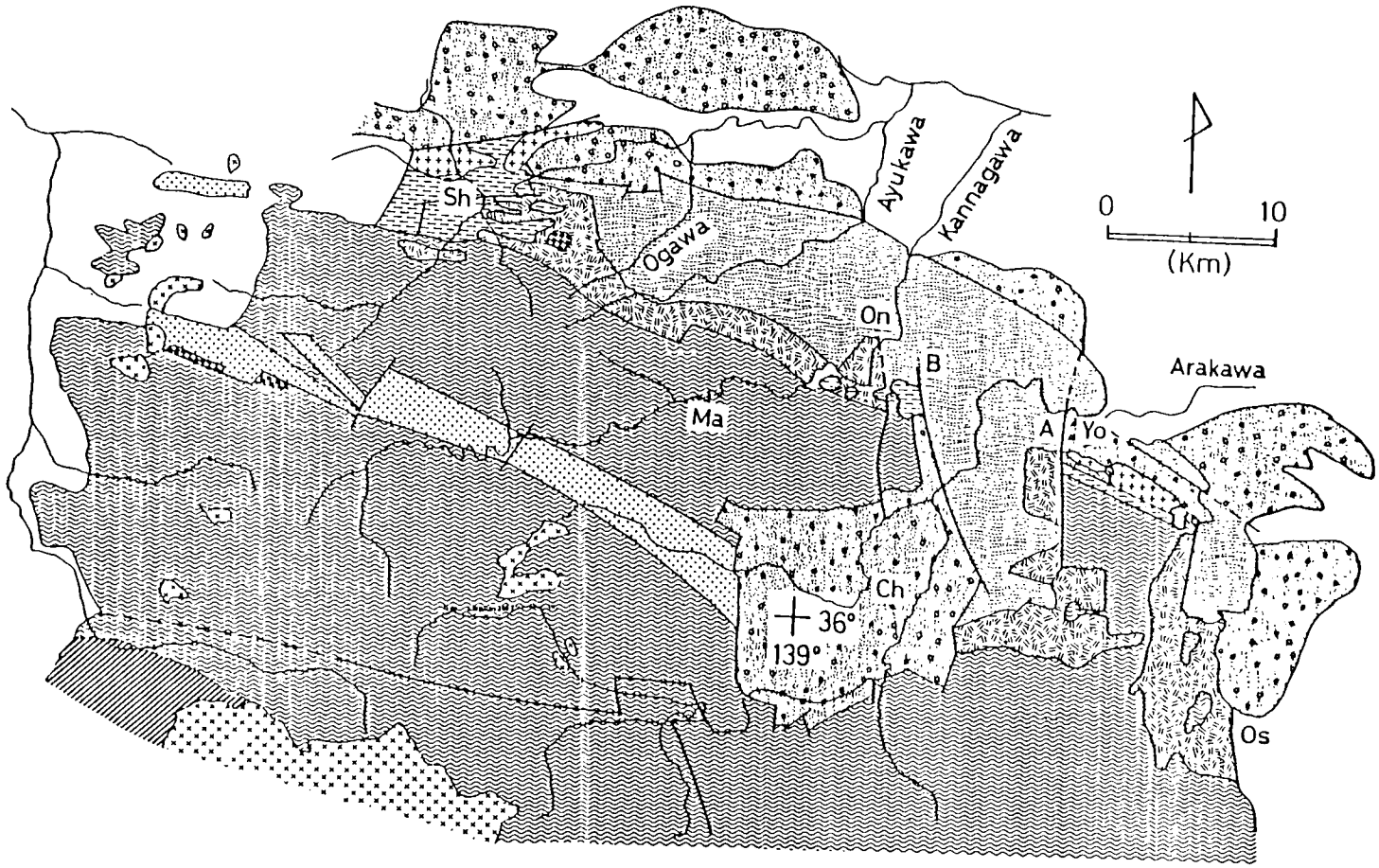

Fig. II-2. Geologic map of the Kanto Mountains.

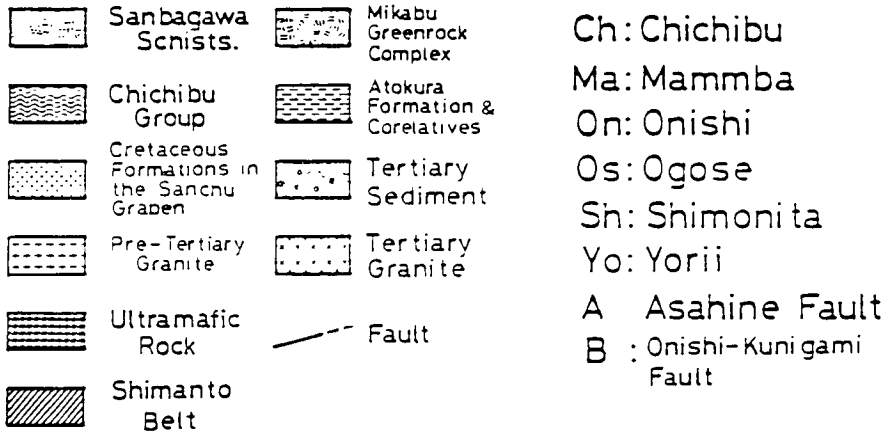

Fig. II-2. (Continue)
Legend of the geologic map of the Kanto Mountains.

Greenrock Complex, the Sanbagawa schists, and the Atokura Formation and its correlatives. In this paper, the Kanto Mountains is subdivided into three parts for simplicity; i.e., eastern, central and western parts. These areas are bounded by rivers such as the Ara-kawa and the Ayu-kawa (Fig. II-2). The mountains and rivers are ordinarily represented by Japanese; i.e. -san and -zan mean a mountain, and -gawa and -kawa do a river.

II-1-2. The Chichibu Group

Huzimoto (1935) divided lithologically the "Titibu (Chichibu) System" along the Kanna-gawa into four formations: the Sakahara, Kashiwagi, Mamba and Kamiyoshida Formations in ascending stratigraphic order. According to him, the age of the Mamba and Kamiyoshida Formations is Permo-Carboniferous, based on the fusulinellae fauna, and four formations of the "Titibu System" are conformable with one another but the "Titibu System" and the "Mikabu System" contact with a fault (so-called Mikabu Tectonic Line). CRG(Chichibu Research Group) (1961) and Ohkubo & Horiguchi (1969) re-defined the "Kashiwagi Formation" comprising the Sakahara and Kashiwagi Formations of Huzimoto (1935) and added a part of the Sakahara Formation around Odokeyama to the Kamiyoshida Formation. The re-defined "Kashiwagi Formation" has been used by subsequent workers: Inoue (1974) and Toriumi (1975). CRG (1961) and Ohkubo & Horiguchi

(1969) demonstrated that the basin-dome structure prevails through the Chichibu terrane, and supported the existence of the "Mikabu Tectonic Line" of Huzimoto (1935). On the other hand, Uchida (1966, 1967) proposed conformable succession between the Sakahara Formation and the Sanbagawa Group. Kimura & Yoshida (1973) and Inoue (1974) found gentle folding of the N-S trend and pointed out that the basin-dome structure after CRG was caused by a combination of E-W trending and N-S trending folds.

Koike et al.(1971) found Triassic conodonts from chert of the Kamiyoshida Formation and concluded that the upper part of the Chichibu Group is of the Late to Middle Triassic ages. Recently, Sato et al.(1977) found Triassic conodonts from chert and limestone beds of the Sakahara Formation and stated that the re-defined "Sakahara Formation", which comprises the Sakahara and Kashiwagi Formations of Huzimoto(1935), overlies the Mamba Formation conformably and some part of the re-defined Sakahara Formation is a contemporaneous heterotopic facies of the Kamiyoshida Formation. Furthermore, Takizawa & Sato (1979) reported that the Kamiyoshida and Mamba Formations are partly unconformable and considered that the Mikabu Formation is correlated to the Mamba Formation. Sashida et al. (1981) found Jurassic radiolarian assemblages from various localities of the Chichibu Group in the Kanto Mountains. Radiolarians are recovered mainly from shales intercalated with Permo-Carboniferous limestones and

Triassic conodont-bearing cherts. They concluded that these limestones and cherts are exotic blocks emplaced by sedimentary slidings during late Jurassic or later age.

II-1-3. The Sanbagawa Group

The Sanbagawa Group, which contains the Sanbagawa schists and the Mikabu Greenrock Complex, is exposed in an about 60 Km long and 10-15 Km wide area containing the town of Shimonita and Onishi of Gunma Prefecture, and of Yorii and Ogose of Saitama Prefecture (Fig. II-2). This group streches from WNW to ESE about 30 Km long from Shimonita to Onishi and it streches out southward to the east of the Onishi-Kunigami fault.

Koto (1889) carried out the first petrographic description of the metamorphic rocks which cropped out along the Sanba-gawa and proposed "Sambagawan (Sanbagawa) Series" and "Mikabu System" to the metamorphic rocks of this district.

Since Koto's classic work, many authors studied the Sanbagawa Group, namely, Huzimoto (1937), Kozima (1944), Seki (1957, 1958, 1960), Tanaka & Fukuda (1974), Toriumi (1975), Hara et al. (1977), Suzuki (1977), Sakai (1980), and so on. Huzimoto (1937) reported that "the Sanbagawa and Mikabu Systems" formed the Ohgiriyama Nappe overlying the "Titibu System" in the northeastern part of the Kanto Mountains, resulting in the Yasudo Window which was formed through dissection of the center of this nappe. Seki

(1958) reported the first metamorphic zoning of the Sanbagawa terrane in the eastern part of the Kanto Mountains. He described that the geologic structure is generally monoclinical with southwestwards dip and that the metamorphic grade increases northwards with descending stratigraphic order. Seki (1960) supplemented the occurrence of jadeite + quartz assemblage in his volcanic formation which is referred to the Mikabu Greenrock Complex in the present paper. His description is quoted by Miyashiro (1961, 1965, 1973) as one of the representative regions of the jadeite-glaucophane type of metamorphism.

Toriumi (1975) performed the metamorphic zoning along the Kanna-gawa in the central part of the Kanto Mountains, consisting of the Chichibu group, the Mikabu Greenrock Complex and the Sanbagawa schists. He also described that the metamorphic grade progressively changed northwards, from Zone I (prehnite-pumpellyite facies), through Zone II (glaucophane schist facies) to Zone III (greenschist facies), and that the boundaries of the zones are roughly in harmony with the stratigraphic boundaries. Progressive metamorphic change along the Kanna-gawa is very similar to that of Shikoku area reported by Banno (1964) and Banno et al. (1978), i.e., the high-pressure intermediate group of metamorphism.

Geologic structures of the Sanbagawa schists were also reported by Tanaka & Fukuda (1974) and Sakai (1980) in the

eastern part, by Suzuki (1977) and Takayama (1984) in the central part, and by Hara et al. (1977) in the western part. Seki (1958, 1960), Tanaka & Fukuda (1974), Toriumi (1975) and Sakai (1980) described that the geologic structure of the Sanbagawa schists is gentle, being usually flat without large-scale folding. On the other hand, Hara et al. (1977) and Suzuki (1977) supposed a large scale overturn structure in the western and central parts of the Sanbagawa schists, respectively.

Geologic and geochemical studies of the Mikabu Greenrock Complex were carried out by Kimura (1977), Uchida (1981), YRG (Yasudo Research Group) (1982) and Yajima et al. (1984). Kimura (1977) reported that the boundary between the Chichibu Group and the Mikabu Greenrock Complex is a decollement in the southeastern part of the Kanto Mountains and denied the Ohgiriyama Nappe of Huzimoto (1937). Uchida (1981) described that the Mikabu type tuff is more magnesian than the Mamba type tuff of the Chichibu Group. YRG (1982) and Yajima et al. (1984) published detailed geologic maps of the Mikabu Greenrock Complex in the southeastern part.

II-1-4. The Atokura Klippe

The Atokura Klippe mainly consists of the Atokura Formation, quartz-diorite and serpentinite. The Atokura Formation, which is mainly composed of sandstone, shale and conglomerate, is exposed near Shimonita, Gunma Prefecture. Huzimoto (1935) distinguished the Atokura conglomerate from

the Chichibu Group as Tertiary sediments. Sugiyama (1943) regarded " the Atokura conglomerate" as a peculiar kind of intrusive igneous rocks which were mistaken for mylonites at a glance. The controversy of the origin of conglomerate continued to Uchida (1962a) and Arai et al.(1963, 1966), who supported the sedimentary origin.

Huzimoto et al.(1953) reported Glauconia sp. which is one of the typical Ryoseki fauna from the Atokura Formation. They also proposed the Atokura Nappe because they found that the Atokura Formation overlay the Mikabu Greenrock Complex with a low angle thrust. Uchida (1962b, 1978) described that the contact relation between the Atokura Formation and the Mikabu Greenrock Complex was due to the folding movement after the deposition of the Atokura Formation and concluded that the former was autochtonous sedimentary rocks.

Arai et al.(1963, 1966) supplemented Cenomanian-Turonian fossils including Trigoniae and Inocerami in the Atokura Formation and considered that the Kawaiyama quartz-diorite intruded into the Atokura Formation and gave contact metamorphism to the surrounding sediments. They concluded that the Atokura Formation, hornfels members and the Kawaiyama quartz-diorite formed the thrust mass, and they were transported to present area in post-Cenomanian age.

Correlatives of the Atokura Formation were reported from other areas in the Kanto Mountains; around Kami-yama, near Onishi (Fujimoto & Sakamoto, 1973), around Mts. Odake and Medake in Minano of Saitama Prefecture (Iijima, 1964),

and from Yorii area (Kosaka, 1979). In the Yorii area, recently, Kadota & Tokunaga (1982) reported Tertiary pollen from the Tochiya Formation which was correlated to the Atokura Formation, and Ono (1983) showed that the K-Ar age of Kinshozan Quartz-Diorite is 251±8Ma, and is not of Cretaceous as considered previously. Further, Hirajima (1983a, 1984) found the jadeite + quartz bearing rock and the mélange zone around the Tochiya Formation in the Yorii area. Geologic and petrologic character of the Yorii area will be discussed in later chapter.

II-2. Description of constituent units.

II-2-1. The Chichibu Group

As mentioned before, stratigraphy of the Chichibu Group is very confused now. This paper follows the lithologic classification of Uchida (1981) who subdivided the Chichibu Group into four formations; Sakahara, Kashiwagi, Mamba and Kamiyoshida formations in ascending stratigraphic order(Fig. II-3). This subdivision was established along the Kanna-gawa. The Chichibu Group which crops out in the eastern part, so called Yasudo Window, and in the western part has not been divided yet.

a) The Kamiyoshida Formation

The uppermost part of the Chichibu Group is the Kamiyoshida Formation, being composed of chert, alternation

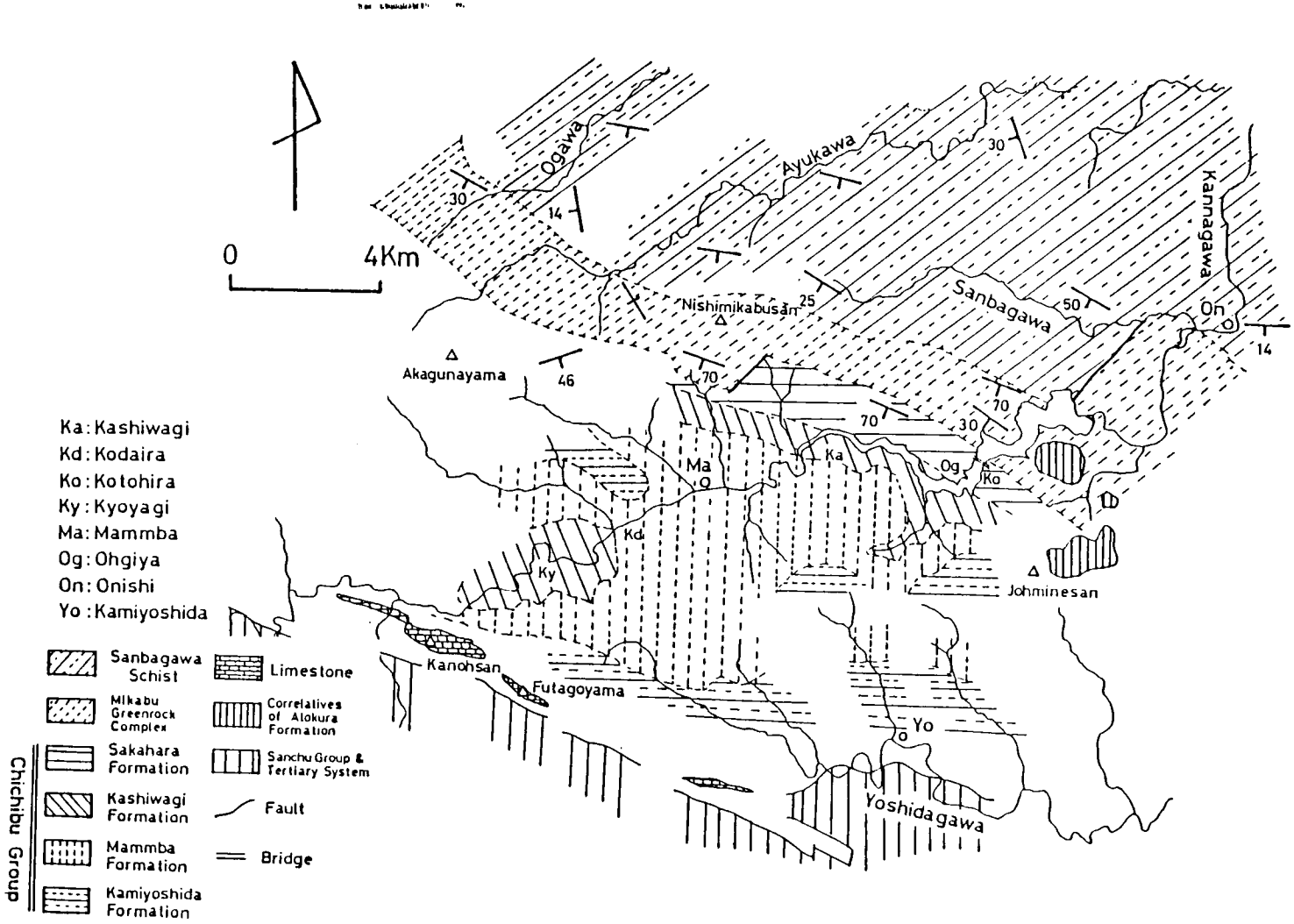

Fig. II-3. Geologic map along the Kanna-gawa. Subdivision of the Chichibu Group follows that of Uchida (1981).

of sandstone and mudstone with large limestone masses which crops out around Kanoh-san, Futago-yama and neighbouring areas (Fig. II-3). The type locality is in the Kamiyoshida area.

b) The Mamba Formation

The Mamba Formation is most abundant in basic materials in the Chichibu Group. This formation consists of mainly basic rocks, such as hyaloclastite, tuff breccia, tuffite, lava and pillow lava, with minor amounts of lenticular limestone, mudstone and bedded chert. Limestone layers often occur in the middle and upper parts of this formation. Typical stratigraphic succession occurs along the Kanna-gawa from Mammba to Kodaira.

c) The Kashiwagi Formation

This formation is characterized by pale green siliceous slate intercalated with thin layers of mudstone, bedded chert and basic rocks. They are described as semi-schists by Ohkubo & Horiguchi (1969). These rocks are exposed along the Kanna-gawa from Ohgiya to Kashiwagi and from Kodaira to Kyoyagi.

d) The Sakahara Formation

Sakahara Formation occupies the lowest part of the Chichibu Group and occurs along Lake Kanna from the Kotohira bridge to Ohgiya. This formation is composed of mainly white-red chert and mudstone with thin layers of basic tuff

and lava. It is also accompanied by massive limestones with 20-30 meters thickness.

e) Undivided Chichibu Group in the Yasudo area

The Chichibu Group of the Yasudo area consists mainly of bedded chert intercalated with thin layers of basic clastic rocks, and the minor constituents of sandstone, limestone and mudstone (Fig. II-4). The lithofacies of this area is similar to those of the Sakahara Formation.

II-2-2. The Mikabu Greenrock Complex

The Mikabu Greenrock Complex is stratigraphically situated between the Chichibu Group and the Sanbagawa schists (Fig. II-2), and is mainly composed of basic rocks intercalated with some layers of mudstone and chert. The basic rocks include gabbro, gabbroic sandstone, ultramafic rock, doleritic dike, basaltic lava, pillow lava, pillow breccia, hyaloclastite and tuffite. Gabbroic rock and lava are predominant in the eastern part, on the south of the Yasudo area, and the western part along the O-gawa and Ayu-kawa. On the other hand, tuffite, pillow breccia and hyaloclastite are rich in the central part along the Kanna-gawa.

Gabbro can be easily distinguished from the other basic rocks as it is coarse-grained (0.1-1.0 mm) and contains pseudomorphs after plagioclase. Gabbro usually occur as lense-shaped body surrounded by tuffaceous matrix. The long

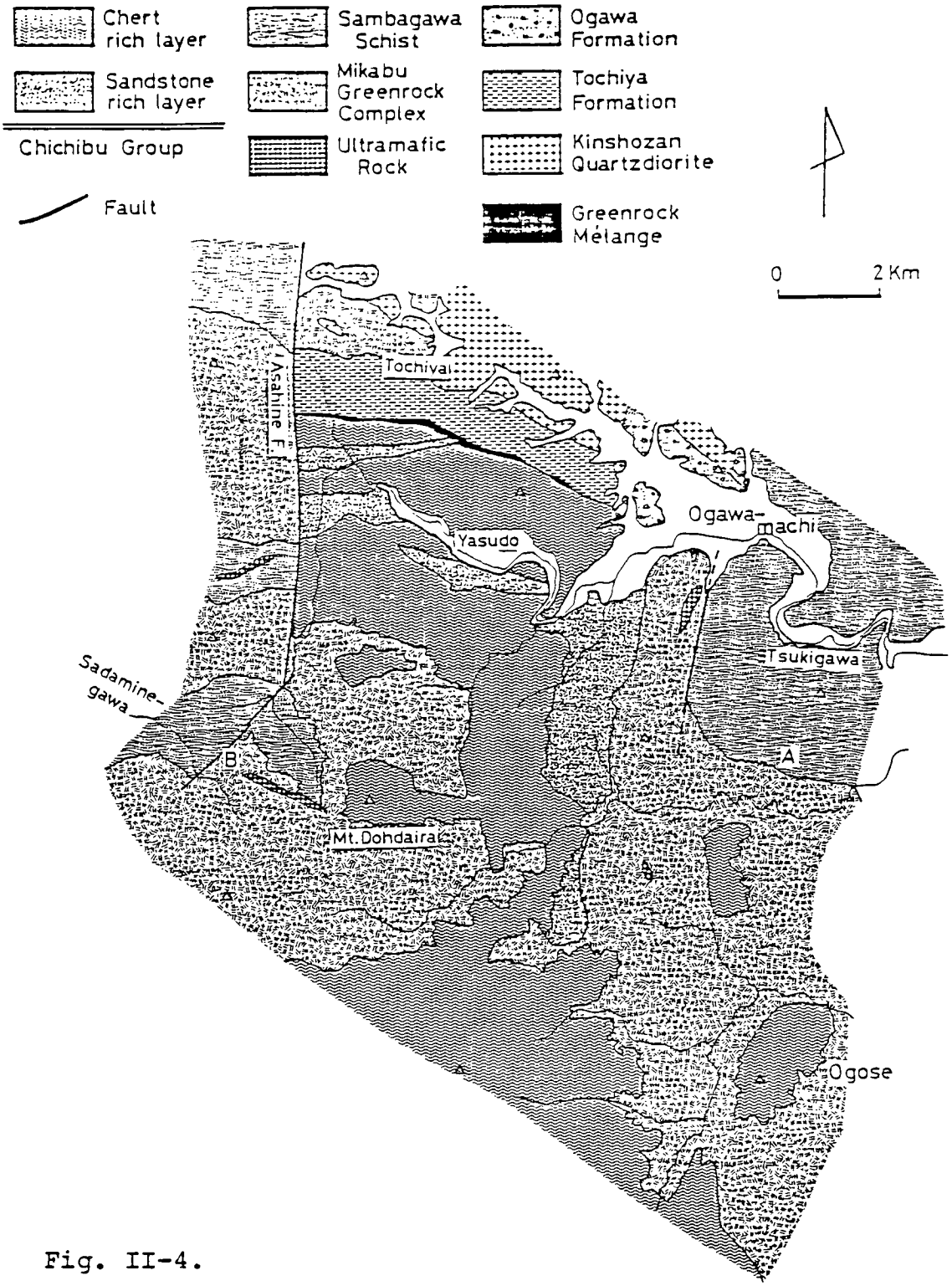

Fig. II-4.

Geologic map of the eastern part of the Kanto Mountains.

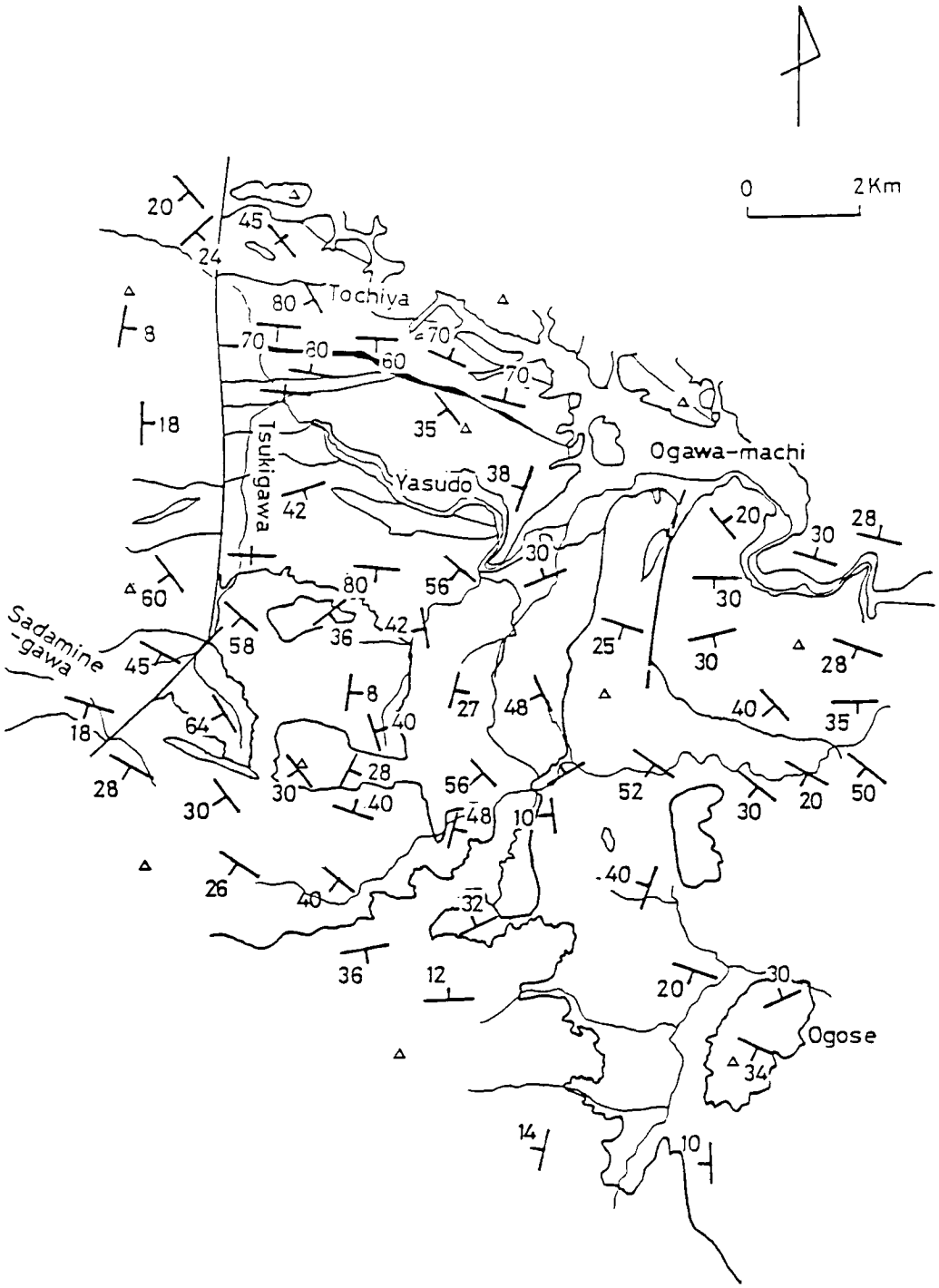

Fig. II-5. Structural outline of the eastern part of the Kanto Mountains. Unit boundaries follow Fig. II-4.

axes of gabbro lenses vary from 4000 meters to a few hundred meters.

Gabbroic sandstone appears as gabbro under unaided eyes, because it is composed of mainly gravels of gabbro. However, it is more foliated than gabbro and is abundant in muscovite which is almost absent in gabbro. Gabbroic sandstone occurs as thin layers, being less than 10 meters thick, interbedded with tuffite and lava.

Pillow lava occurs at several localities in the Mikabu Greenrock Complex. Many of them are closely packed type with minor inter-pillow materials of basaltic tuff, and are devoid of radial joint. Pillow lava cropping out on the southern slope of Higashi-Mikabu-yama preserves radial joints (Plate II-1).

Hyaloclastite contains many volcanic glass patches ranging from a few millimeters to a few centimeters in a cogenetic tuffaceous matrix. Tuffite is defined in this paper as schistose fine-grained rocks which hardly reserve volcanic glass patches.

Pillow breccia is defined as the rock-type containing mainly rounded and angular crusts ranging from 1.0 cm to over 10 cm in diameter with a minor tuffaceous matrix.

Both basaltic lava and doleritic dikes are fine- to medium-grained and massive. Although macroscopic igneous structures are scarcely preserved, these rocks contain relict augite and hornblende. The schistosity scarcely developed in them.

Plate II-1. Closely packed pillow lava at the southern slope of Higashi-Mikabu-yama.

Many ultramafic bodies are scattered in the Mikabu Greenrock Complex. Largest of them measuring about 1.5Km in diameter occurs near Kurouchi-yama southeast of Shimonita. They are composed of dunite, wehrlite, pyroxenite and serpentinite. Ultramafic rocks are pervasively serpentinized. Some of serpentinites are scattered along the fault line.

II-2-3. The Sanbagawa schists

The Sanbagawa schists are mainly composed of metapelites (pelitic schists) intercalated with metasiliceous rocks (quartz schists) and metabasites (basic schists). The schistosity well develops in all lithofacies. Metapelites are generally black in colour on exposure. Albite porphyroblasts and garnets can be observed under unaided eyes in the lower part of the Sanbagawa schists. Hara et al. (1977), Suzuki (1977), Sakai (1980) and Takayama (1984) found three or four layers of relatively thick basic schists (more than 10m) in the western and central part , and the present author found one layer is in the eastern part. They are dark green to pale green colour, and sometimes contain white spots of albite porphyroclasts in green matrix. Relatively thick quartzite layer is exposed along the Sanba-gawa (Suzuki 1977; Takayama 1984). Many other thin layers of quartz schists are distributed here and there. Some of metasiliceous rocks

contain piedmontite.

II-2-4. The Atokura Klippe

a. The Atokura Formation and its correlatives

The Atokura Formation and its correlatives are mainly composed of sandstone, shale, alternation of sandstone and shale, and conglomerate. Its correlatives cropping out near Mt. Medakewere named the Kazo Formation by Iijima (1964), and those of the Yorii area were the Tochiya Formation by Maeda (1954). Sandstone is usually poorly sorted and abounds in lithic fragments of granitic rock and chert, and in detrital grains of garnet, epidote, biotite and zircon. Original sedimentary structures are often reserved (Uchida, 1966; Kosaka, 1979). Conglomerates are mainly composed of pebbles of granitic rocks with minor amounts of sandstone, shale, limestone and chert. Some of conglomerates show mylonitic textures.

b. Quartz-diorite

Quartz-diorites and granitic rocks associated with the Atokura Formation are exposed around Iwa-yama, Yotsumata-yama and Kawai-yama near Shimonita (Uchida, 1966), around Mt. Odake near Minano (Iijima, 1964), and around Kinsho-zan in Yorii area (Kosaka, 1979). Geologic maps of the western part and the Yorii area are shown in Figs.II-6 and II-7, respectively. Quartz-diorite is melanocratic to mesocratic, and is mainly composed of idiomorphic to

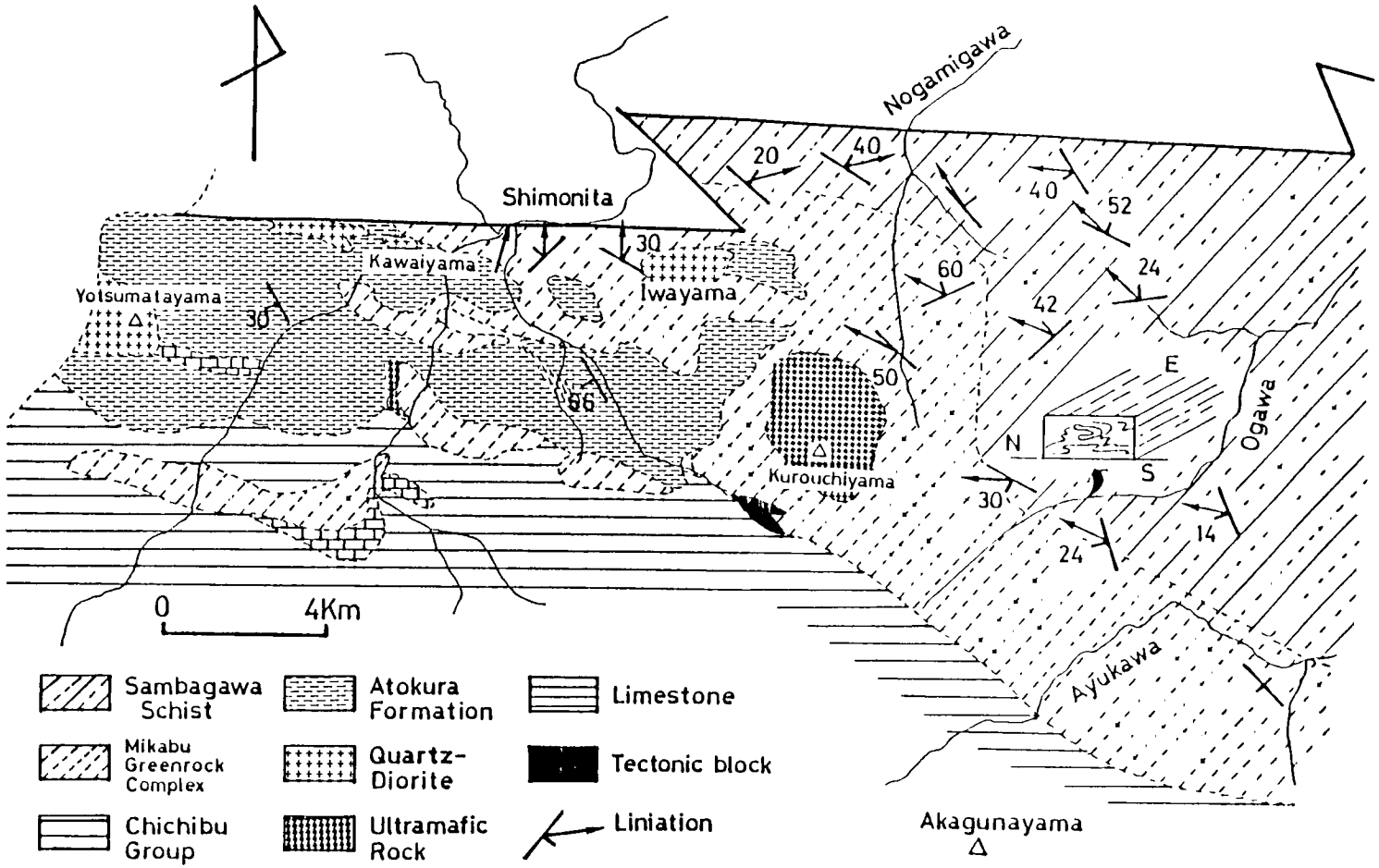

Fig. II-6. Geologic and structural map of the western part of the Kanto Mountains. Eye folding observed along the O-gawa is schematically shown with its locality.

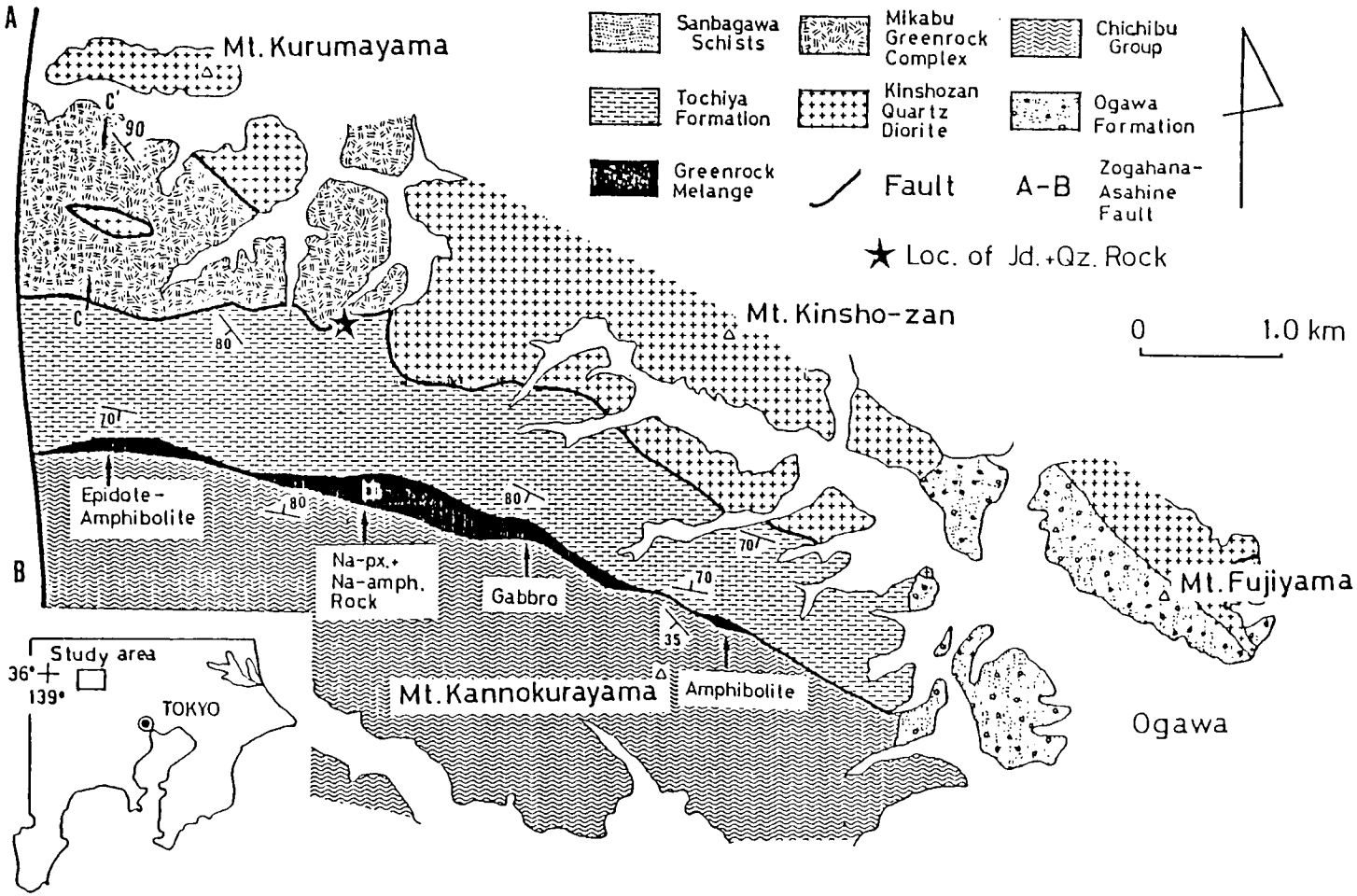

Fig. II-7. Geologic map of the Yorii area with localities of jadeite-quartz rock and other tectonic blocks.

hypidiomorphic crystals of plagioclase and hornblende. Hornblende usually shows the pleochroism of bluish green to pale green colour, and rarely shows pale brown to brown colour. Quartz-diorite also contains minor amounts of quartz, biotite, zircon, apatite and opaque mineral. Some melanocratic dykes with a several ten centimeters in thickness cut into the quartz-diorite. Mineral assemblage of dikes is similar to that of the quartz-diorite, but the grain size of the dikes is smaller than that of the quartz-diorite; 0.1 to 0.5 mm in dikes, 1 to 5 mm in quartz-diorite.

c. Greenrock mélange

Unknown geologic unit is newly found between the Tochiya Formation, correlatives of the Atokura Formation, and the Chichibu Group in the Yorii area (Hirajima, 1984). This geologic unit is mainly composed of actinolite rock. The actinolite rock is usually sheared severely and is composed of actinolite and chlorite whose modal amount exceed 90 %. Gabbro, sodic pyroxene-sodic amphibole-bearing rock, epidote-amphibolite, and amphibolite scatter here and there occurring as lenticular bodies surrounded by sheared actinolite rock. Long diameter of each body varies from several meters to one hundred meters.

The metamorphic rocks mentioned above can not beformed under the same metamorphic condition as that of the Sanbagawa schists to be mentioned later. These rocks had

been mixed up in the matrix of the actinolite rock by tectonic or sedimentary processes. This feature is one of the characters of mélange defined by Silver & Beutner (1980). Therefore, this geologic unit is named greenrock mélange. The greenrock mélange extends WNW-ESE trend about 6 Km long with 200 m width in the Yorii area. Resemblance of this unit was not found in other area of the Kanto Mountains. One of the possibility is the Shimonita area where garnet-sodic pyroxene-bearing rocks and amphibolite occur associated with the jadeite-aragonite-bearing rock (Tanabe et al., 1982).

d. Jadeite-bearing rocks

Jadeite-bearing rocks were newly found in the western and easternparts of the Kanto Mountains by Tanabe et al. (1982)and Hirajima (1983a). In the eastern, part jadeite-quartzrocks associated with ultramafic rocks occur in the terrane of the Tochiya Formation near the boundary with the Sanbagawa Group. A main block of the jadeite-quartz rock which measures about 5x5x10m exists at the top of a small hill, and many other small blocks scatter on the wooded slope. Although the boundary between the jadeite-quartz rock and the surrounding rocks are not found, it is likely that the ultramafic rocks with the jadeite-quartz rock emplaced in solid state into the Tochiya Formation. The detailed sketch map around the locality of the jadeite-quartz rock is shown in Fig. II-8.

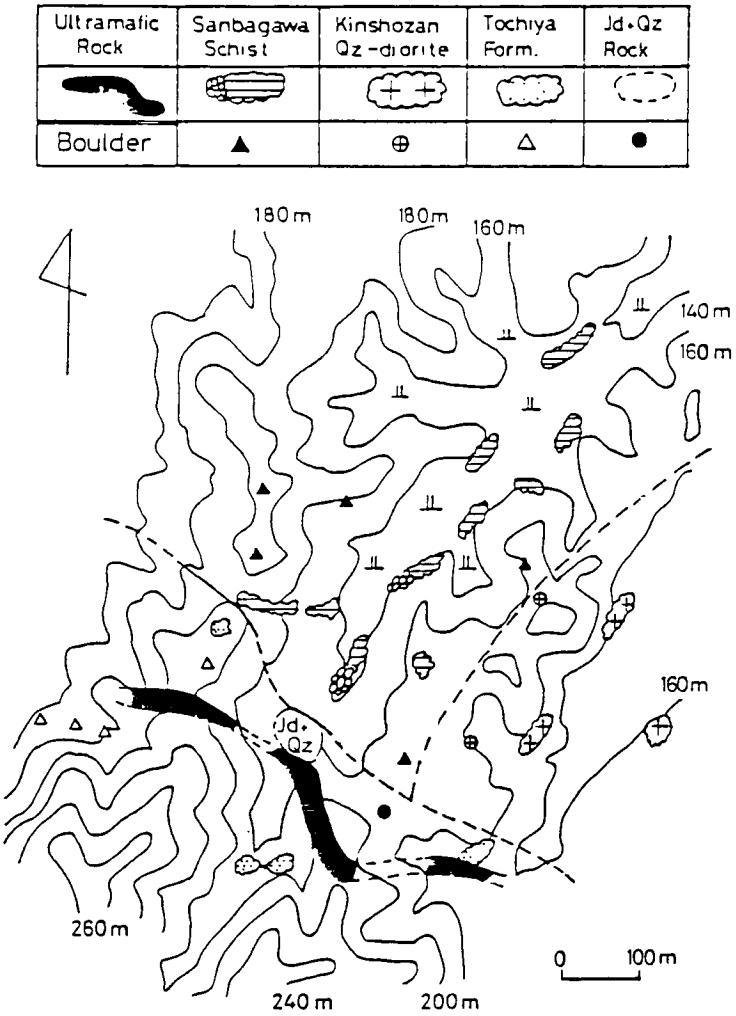

Fig. II-8. Detailed sketch map around the locality of the jadeite-quartz rock.

In the Shimonita area, Tanabe et al. (1982) described that the jadeite-aragonite rocks derived from metavolcanics occur in a block, which measures about 700m by 100m on the surface and extends obliquely to the general trend of the surrounding schists. They considered that the rocks in question were emplaced as a tectonic block, though geological setting of them is not clear.

II-3. Geologic structure

II-3-1 Geologic structure of the Sanbagawa Group

This report intends to discuss the prograde metamorphism in the Kanto Mountains. Therefore, it is necessary to select the place where the geologic section is continuous from lower- to higher-grade parts. This condition is more or less satisfied along the Kanna-gawa in the central part. In this area the general strikes and dips of the Chichibu Group, the Mikabu Greenrock Complex and the Sanbagawa schists, represented by the bedding and schistosity plane, are generally N45^{o}W to EW, and 0-60^{o}S, respectively (Fig. II-3). As reported by CRG (1961), Uchida (1966) and Toriumi (1975), unconformity and fault are not found at the unit boundaries. Unit boundary between the Sanbagawa schistsand the Mikabu Greenrock Complex follows Takayama (1984) who has slightly shifted the previous boundary defined by Toriumi (1977) and Suzuki (1977) southwards.

However, the geologic structures in the eastern and western parts are more complicated. Geologic and structural maps of the eastern part are shown in Figs. II-4 & II-5, respectively. The Chichibu Group, the Mikabu Greenrock Complex, the Sanbagawa schists, and the correlatives of the Atokura Formation are exposed in the eastern part (Fig. II-4). The Chichibu Group which occurs on the east of the Asahine fault (Maeda, 1954) is the so called "Yasudo Fenster(Window)" of Huzimoto (1937). Actually, the Chichibu Group forms the N-S and E-W trending synforms (Fig. II-5) and overlies the Mikabu Greenrock Complex. This observation denied the Huzimoto's idea mentioned before.

On the west of Ogose, the boundary between the Chichibu Group and the Mikabu Greenrock Complex can be traced at nearly same sealevel. Kimura (1977) concluded that this boundary is a flat decollement. The present author agrees with his opinion.

The Mikabu Greenrock Complex conformably overlies the Sanbagawa schists around the locality A in Fig. II-4. However, the boundary between two units is partly in fault contacts. On the south of Ogawa-machi, the strikes and the garnet appearance isograd of the Sanbagawa schists intersect the N-S trending distribution of the Mikabu Greenrock Complex. A fault which crosses the Sadamine-gawa from NE to SW (B in Fig. II-4) can explain the distribution of the

Sanbagawa schists and the Mikabu Greenrock Complex along the river. This fault seems to continue to the Asahine fault which runs in the N-S direction on the west of Tsuki-gawa. These N-S trending faults mentioned above are considered to be formed during Neogene to Quarternary (Kosaka,1979). The original structures of the Sanbagawa Group in the eastern part of the Kanto Mountains should have been disturbed by later tectonic movements.

Mineral and streching lineations of the Sanbagawa schists and the Mikabu greenrocks are ordinarily parallel to the elongation direction of the Sanbagawa Belt (Hara et al., 1977). In the Kanto Mountains, the lineations of the Sanbagawa Group show the WNW-ESE direction, which is also parallel to the Sanbagawa Belt, and they usually plunge westwards. However, the streching lineations of the Mikabu Greenrock Complex near Shimonita show the N-S direction and the mineral lineations of the Sanbagawa schists plunge eastwards on the west of the Nogami-gawa (Fig. II-6). The change of the plunging direction can be explained by the N-S trending syncline proposed by Inoue (1974). N-S trending streching lineations impel the block of the Mikabu Greenrock Complex in the western margin of the Kanto Mountains to rotate along the vertical axis about 90^{o}. The tectonic movement of the latter type is not clarified yet. In any case, the geologic structure of the western part is also disturbed by the later tectonic movements as did in the eastern part.

II-3-2 Geologic structures of the Atokura Klippe and Tochiya Klippe

The author does not agree with the nappe theory of the Sanbagawa schists of Huzimoto (1937), but agrees with the Atokura nappe theory of Huzimoto et al. (1953) and the Tochiya nappe of Kosaka (1979). Following geologic units are exposed in the Yorii area; the Chichibu Group, the Mikabu Greenrock Complex, the Sanbagawa schists, the Tochiya Formation, the Kinshozan quartz-diorite, the greenrock mélange, and the Miocene Ogawa Formation. Except the Ogawa Formation which unconformably covers the Tochiya Formation and the Kinshozan quartz-diorite, the other units are in fault contacts with each other (Fig. II-7). Kosaka (1979) suggested that the Tochiya Formation and the Kinshozan quartz-diorite composed the Klippe which overlay the Mikabu Greenrock complex and the Sanbagawa schists. He reported that the correlatives of the Atokura Formation overlay the Mikabu greenrocks with a low angle fault on the north of Kuruma-yama, and that the Kinshozan quartz-diorites are exposed on swell and the Mikabu greenrocks are on low ground on the north of Kuruma-yama. The detailed route map of this area is shown in Fig. II-9 (around C-C′ in Fig. II-7). The boundary between the Kinshozan quartz-diorite and the Mikabu Greenrock Complex is a nearly flat plane, and the Kinshozan quartz-diorite has the K-Ar age of 251±8Ma (Ono,

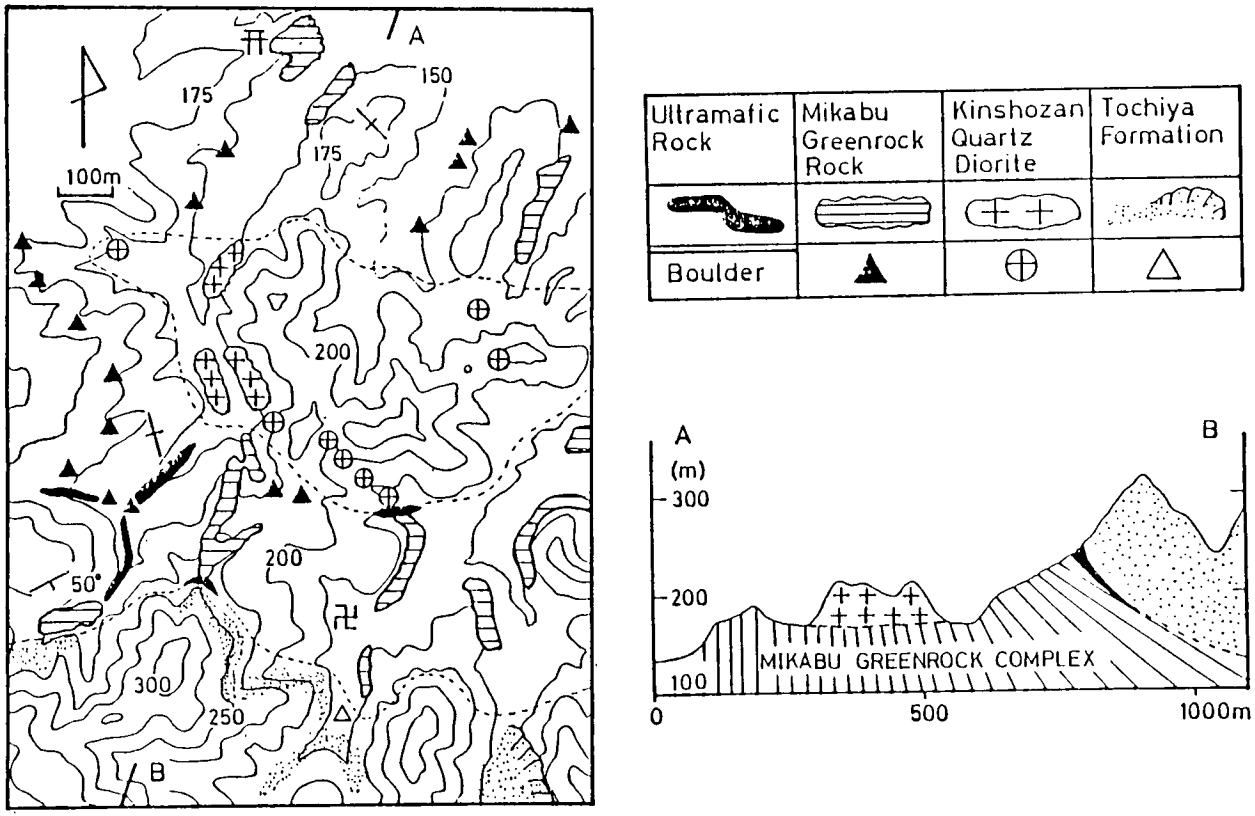

Fig. II-9. Detailed sketch map of the southern part of Kuruma-yama (C-C' in Fig. II-7), and the N-S cross section along A-B.

1983). Thus, geologic and age data support the nappe theory of Kosaka (1979). Our petrologic data to be mentioned in a later section also supports the Klippe theory, but it indicates that the greenrock mélange is also one of the constituents of the Klippe.

III. Petrography

III-1. Petrographic outline of the Kanto Mountains

About four thousand thin sections of samples of the Kanto Mountains were examined in detail under the microscope to determine the mineral assemblage, and about eighty samples were analyzed with an electron microprobe to determine the chemical composition of the rock-forming minerals.

The metamorphic minerals which occur in the study area are epidote, lawsonite, pumpellyite, prehnite, chlorite, sodic pyroxene, sodic amphibole, actinolite, barroisitic hornblende, garnet, biotite, stilpnomelane, muscovite, albite, quartz, hematite, magnetite, rutile, and Fe-sulfides. Relict clinopyroxene and hornblende are commonly comprized in the volcanic rocks of the Chichibu Group and the Mikabu Greenrock Complex.

Among these minerals, chlorite, albite, quartz, and muscovite occur commonly in the various kinds of lithofacies. Epidote and actinolite usually occur in metabasites of all geologic units. Pumpellyite exists in various lithofacies of the Chichibu Group, the Mikabu Greenrock Complex, and the Atokura Formation and its correlatives, and metabasites of the upper-most horizon of the Sanbagawa schist along the Kanna-gawa. Sodic amphibole and sodic pyroxene mainly occur in metabasites of the Chichibu Group and the Mikabu Greenrock Complex. Jadeitic pyroxene and sodic amphibole

are also found from some of tectonic blocks in the Atokura Formation and its correlatives, but they do not belong to the Sanbagawa metamorphic rocks. Lawsonite mainly occurs in metabasites of the Mikabu Greenrock Complex of the eastern part and rarely does in metapelites of the Sanbagawa schists. Prehnite is usually found as veins in the Atokura Formation and its correlatives, but rarely in rocks of the Chichibu Group which are exposed near the Sanchu Graven (Fig. III-1). In the Sanbagawa schists, barroisitic hornblende instead of sodic amphibole occurs in metabasites, and garnet and biotite occur in metapelites. First appearance isograds of garnet and biotite are defined in the eastern and western parts of the Kanto Mountains, respectively. Frequency of the occurrence of these metamorphic minerals and the distribution of them are shown in Table III-1 and Fig. III-1, respectively.

III-2. Comparison to the previous works in the Kanto Mountains

Seki (1958) divided the eastern part of the Kanto Mountains into six zones based on the distribution of metamorphic minerals. Further, the same author (1960) supplemented the occurrence of jadeite + quartz assemblage to his Zone IV. His zonal mapping and the mineral assemblages are shown in Fig. III-2 & Table III-2. His Zone III which is the same area as the Mikabu Greenrock Complex used in this paper, was defined on the basis of the

Table III-1. Frequency of occurrence of metamorphic minerals in the Kanto Mountains.

AREA	No.	Ep	Act	Preh	Pum	Law	Na-am	Na-px	Gar	Bi
Eastern Part	814	490	471	34	269	38	116	99	16	0
	(%)	60.2	57.9	4.2	33.0	4.5	14.3	12.2	2.0	0
Mikabu Chichibu	612	356	417		250	36	112	95		
	(%)	58.2	68.1		40.8	5.9	18.3	15.5		
Sanbagawa	67	58	25			1	2		16	
	(%)	86.6	37.3			1.5	3.0		23.9	
Tochiya	135	76	29	34	19	1	2	4		
	(%)	56.3	21.4	25.2	14.1	1.5	1.5	3.0		
Central Part	904	387	305	11	125	2	58	96	51	40
	(%)	42.8	33.7	1.2	13.8	0.2	6.4	10.6	4.3	3.2
Western Part	2088	808	797	117	209	7	87	211	90	66
	(%)	38.7	38.2	5.6	10.0	0.3	4.2	10.1	4.3	3.2
TOTAL	3806	1685	1573	162	603	47	259	406	157	106
	(%)	44.3	41.3	4.3	15.8	1.2	6.8	10.7	4.1	2.8

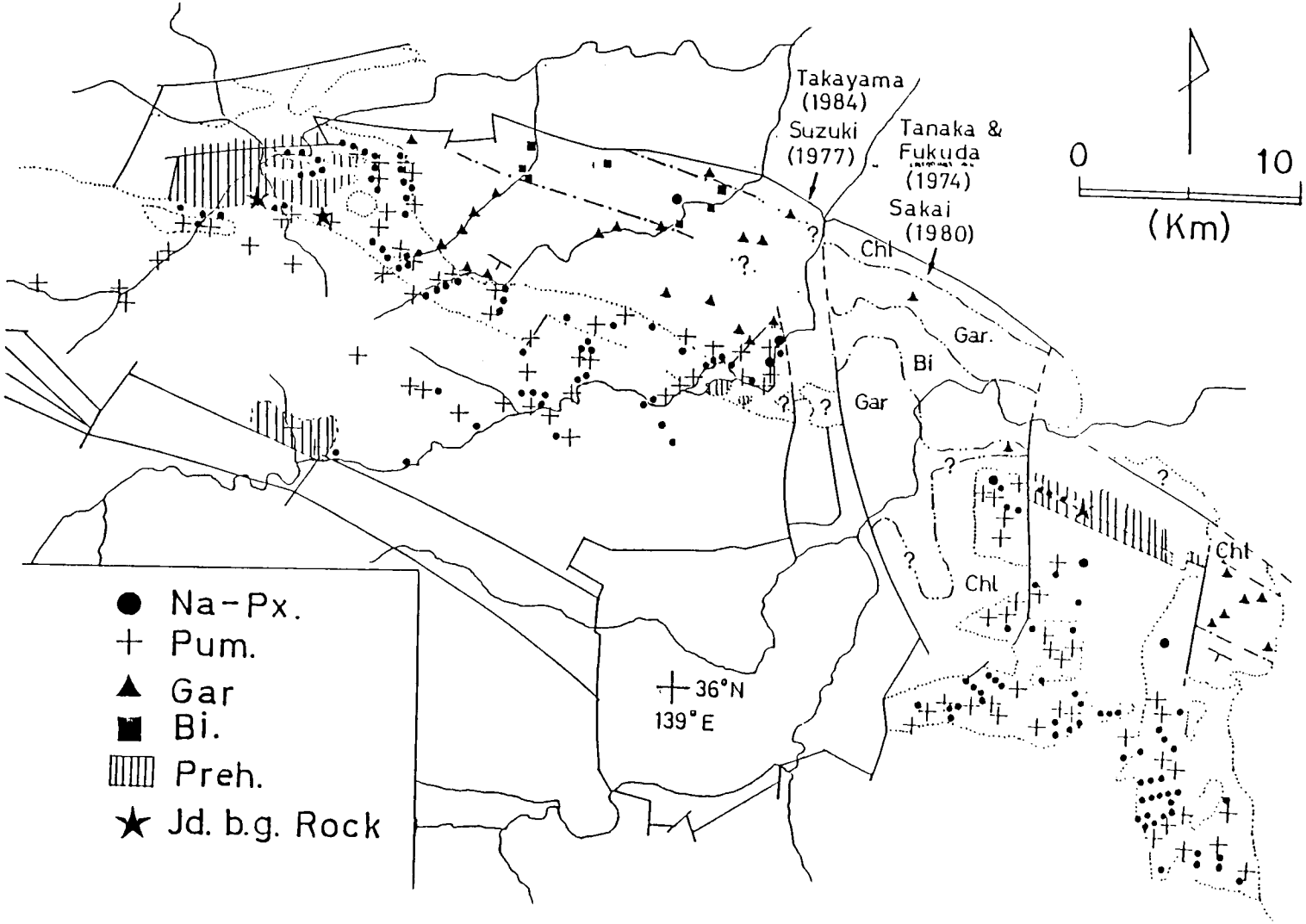

Fig. III-1. Distribution of metamorphic minerals in the Kanto Mountains.

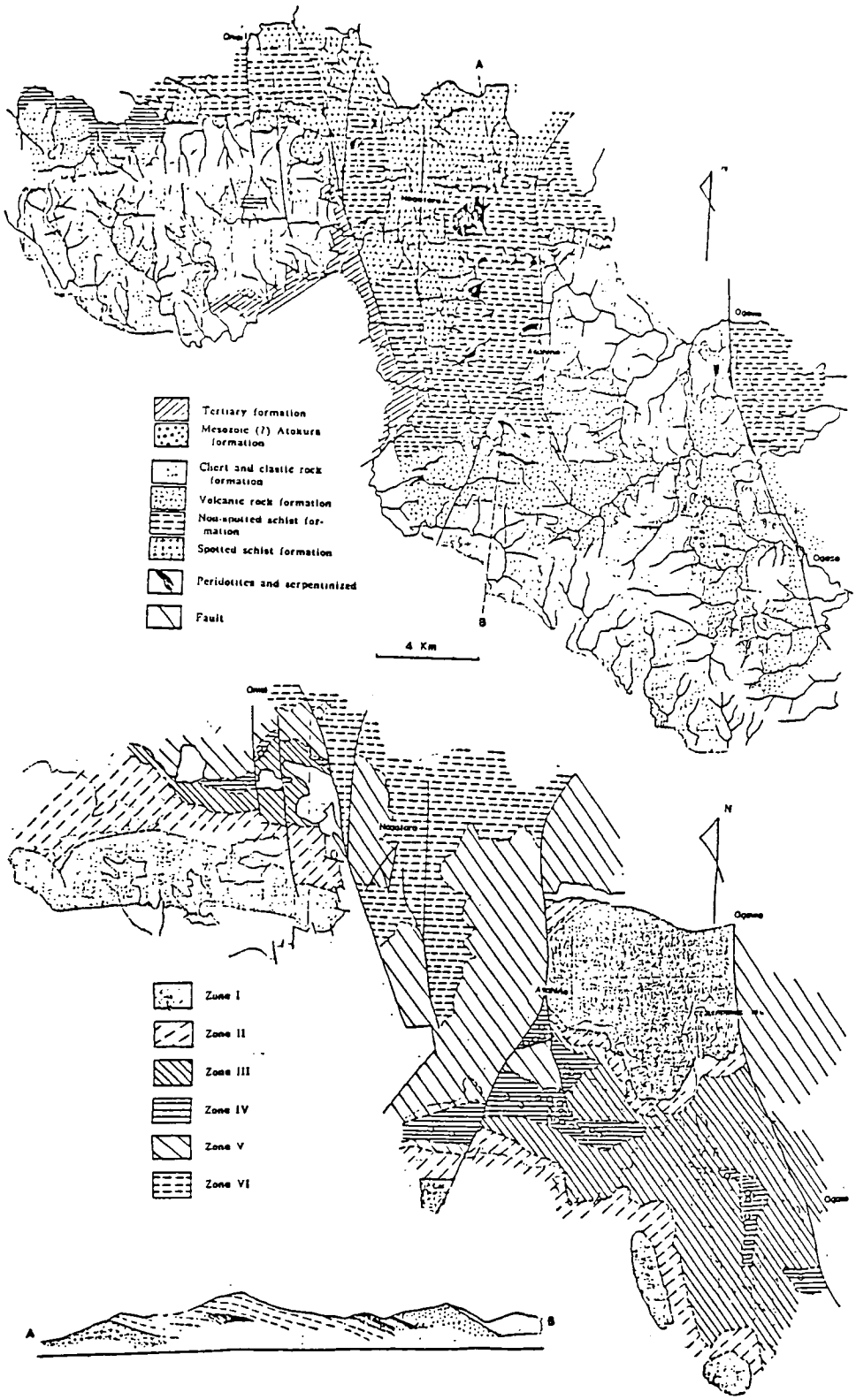

Fig. III-2. Geologic map and metamorphic zonal mapping of the eastern part of the Kanto Mountains by Seki(1960).

Table III-2. Stability ranges of metamorphic minerals of the Kanto Mountains.

A) SEKI(1960)

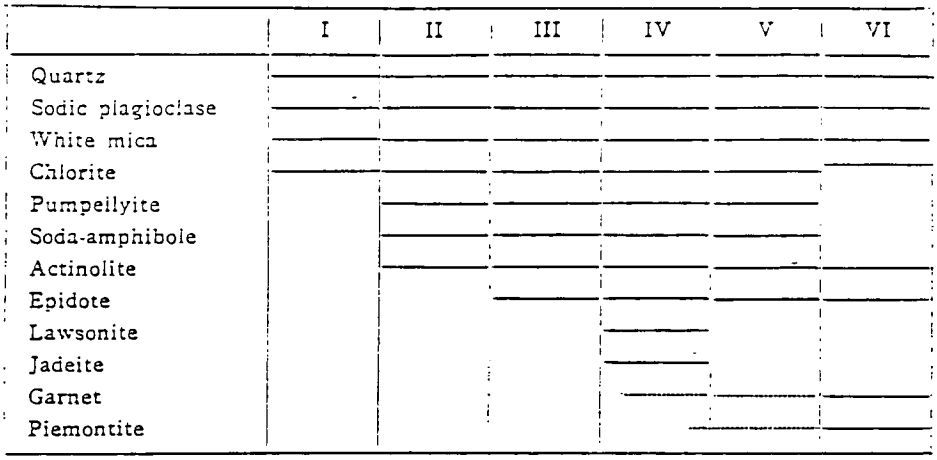

B) THIS STUDY

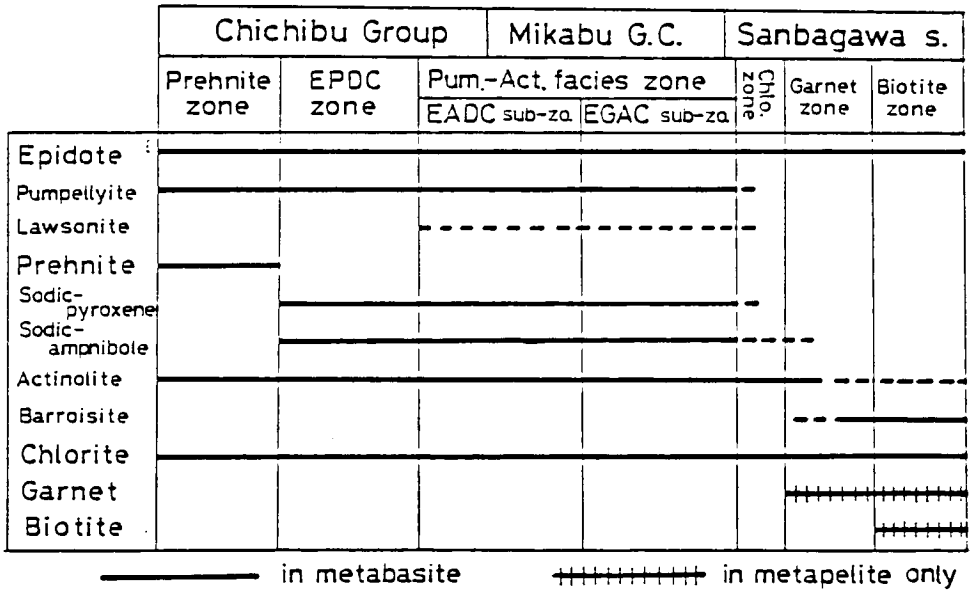

first appearance of epidote, and his Zones I & II, mostly corresponding to the Chichibu Group, on the basis of absence of pumpellyite and epidote, respectively. However, the present author found epidote, pumpellyite and sodic pyroxene from metabasites of the Chichibu Group which belong to his Zone I (Figs. III-1 & III-3). Therefore, it is impossible to distinguish Zones I & II from Zone III.

First definition of Zone IV was based on the occurrence of lawsonite and parallel-symmetric sodic amphibole (b=Y). However, the author found jadeite + quartz assemblage not from Zone IV, but from some of tectonic blocks which were distributed in the Tochiya Formation (Hirajima, 1983a). Instead of jadeite, sodic-augite and aegirine-augite defined by Essene & Fyfe (1967) are commonly comprized in metabasites of Seki's Zone IV and surrounding areas (Fig. III-1). Hence, we cannot serve sodic pyroxene as an index mineral of zonal mapping. In this sense, the only characteristic mineral of Seki's Zone IV is the widespread occurrence of lawsonite. Actually, lawsonite occurs in metabasites with lower Fe_2O_3 and higher Al_2O_3 than those of representative basalt (Kuno et al., 1957; Miyashiro et al., 1969) as will be discussed in later chapter. Hence, the use of lawsonite as an index mineral of zonal mapping is improper. Therefore, the author could not distinguish Zone IV from Zones I, II & III.

Seki's Zones V & VI correspond to the non-spotted zone

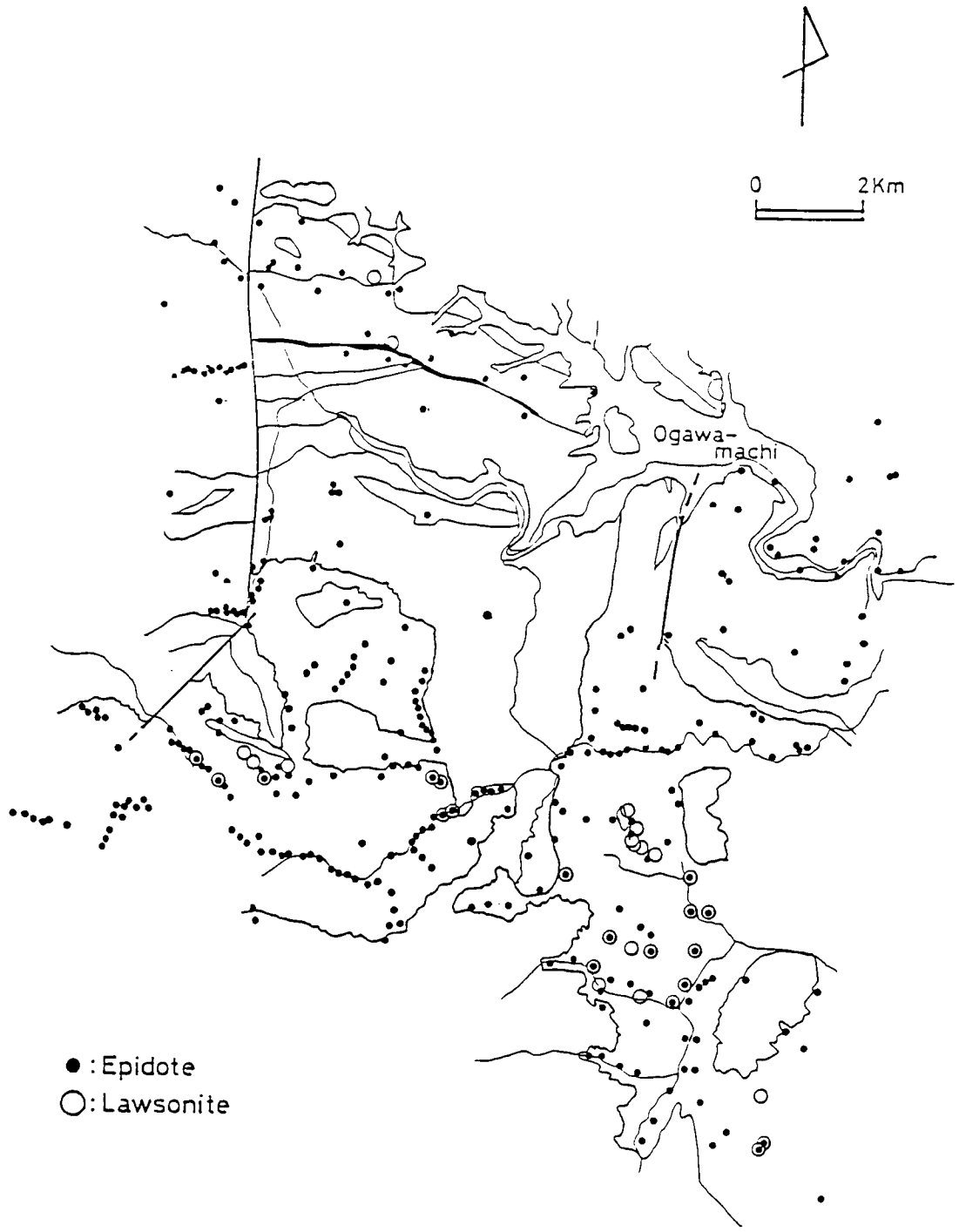

Fig. III-3. Distribution of epidote and lawsonite in the eastern part of the Kanto Mountains.

and spotted zone of the Sanbagawa schists, respectively. Mineral assemblage of Zone V is almost same as that of Zone III, and his Zone VI is similar to the garnet zone of Higashino (1975). In the eastern part, the author confirmed that garnet, albite and chlorite commonly occur in metapelites of the lower stratigraphical part of the Sanbagawa schists, but garnet is absent in its upper part (Fig. III-1). Then, he defines the chlorite zone and the garnet zone in this area on the basis of mineral assemblages of metapelites after Higashino (1975).

Toriumi (1975) divided the metamorphic terrane along the Kanna-gawa into four Zones I, II, IIb & III by the mineral assemblages of metabasites. His Zone I is characterized by the prehnite + pumpellyite + chlorite assemblage and the absence of sodic amphibole, and his Zone III is by the disappearance of pumpellyite, sodic amphibole, lawsonite, and omphacite and the appearance of barroisitic hornblende in basic schists. Toriumi's Zone I is situated in the southern marginal zone of the Chichibu Group along the upper stream of the Kanna-gawa, and his Zone III roughly corresponds to the Sanbagawa schists of the central part of the Kanto Mountains except for the upper most part of the Sanbagawa schists.

However, the distinction of his Zones IIa & IIb, that roughly correspond to the Chichibu Group and the Mikabu Greenrock Complex, respectively, is not clear. He described that the representative mineral assemblages of Zones IIa &

IIb are that of pumpellyite + chlorite + actinolite + magnesioriebeckite and that of epidote + actinolite + chlorite + glaucophane, respectively. Hence, he decided the isograd reaction between these zones as following;

$$\text{Pumpellyite} + \text{Chlorite} + \text{Quartz} = \text{Actinolite} + \text{Clinozoisite} + H_2O \quad ---(1)$$

In Shikoku, this reaction defines the high-temperature limit of the pumpellyite - actinolite facies which is represented by the assemblage of pumpellyite + actinolite + epidote + chlorite (Nakajima et al., 1977 and Banno et al., 1978). Toriumi (1975) described that this assemblage is one of the characteristic ones of Zone IIb. Therefore, the present author does not agree with the subdivision of Zone II into IIa & IIb, and he will propose a new definition of mineral zones based on the assemblages in the ACF-F3 system in next section (III-3).

It is convenient to use the mineral assemblages of metapelites for zonal mapping of the Sanbagawa schists as shown by Higashino (1975). In the central and western parts of the Kanto Mountains, the author found the assemblage of biotite + garnet + chlorite + muscovite + quartz + albite in metapelites of lower stratigraphical part of the Sanbagawa schists and that of garnet + chlorite + muscovite + quartz + albite in its upper part. These parts are defined as biotite zone and garnet zone (Fig. III-1), respectively.

Suzuki (1977) subdivided the Sanbagawa Group of the central part into three zones. His Zone I corresponds to the Mikabu Greenrock Complex and Zones II & III to the Sanbagawa schists. Zone I is characterized by the occurrence of pumpellyite in metabasites. Zone II is characterized by the disappearance of pumpellyite and by the occurrence of garnet in metapelites, and Zone III is by the occurrence of biotite in metapelites. He considered that the highest grade part defined by biotite-bearing layer was located in the stratigraphically middle part, and concluded that the observed thermal structure was formed by the large scale overturn after the prograde metamorphism.

However, our petrographic data indicate that the highest grade part exists in the lower part of the Sanbagawa schists as described before. This problem was examined by Takayama (1984) in detail. He has analyzed the minerals of metapelites which were collected from the same area as studied by Suzuki (1977) with an electron microprobe, and he has shown that biotite occurs only in the stratigraphically lower part and not in the middle part. He concluded that Suzuki (1977) misunderstood oxidized chlorite as biotite. The author agrees with Takayama (1984).

III-3. Mineral assemblage and mineral zone

The author's metamorphic zonal mapping in the Chichibu Group and the Mikabu Greenrock Complex is not concordant to those of Seki (1958) and Toriumi (1975), although that of

the Sanbagawa schists roughly matches the previous works. The discordance mainly owes to the use of the appearance or disappearance isograds of metamorphic minerals for subdivision. In the lower-grade metabasites, stabilities of many minerals sensibly depend both on the bulk rock composition and the metamorphic condition. Therefore, mineral appearance isograds not carefully examined by the phase rule do not serve to define mineral zones of lower-grade metabasites.

The author divides the Chichibu and Sanbagawa Groups by mineral assemblages of metabasites. Silicate minerals of metabasites have to be discussed in the eleven components system; i.e., SiO_2-TiO_2-Al_2O_3-Fe_2O_3-FeO-MnO-MgO-CaO-Na_2O-K_2O-H_2O system. The number of components is reduced as follows. Since quartz, albite and muscovite are usually present in metabasites, the effective components of the system can be reduce to eight. TiO_2-rich minerals in metabasites are sphene, rutile and ilmenite. Sphene is common in the lower-grade rocks and ilmenite is in the higher-grade ones. Except these minerals, TiO_2 scarcely affects the stability of other minerals, and hence TiO_2 can be ignored. MnO plays an important role in determining the stability of garnet, but garnet is very rare in metabasites of the study area. Thus, it can be ignored in our discussion as well. Although the role of fluid phase was not clarified in this paper, H_2O is assumed to be an

externally controlled or a perfectly mobile component. Accordingly, mineral assemblages of metabasites can be discussed in the following five components system; (Al_2O_3-Na_2O-$3K_2O$)-Fe_2O_3-FeO-MgO-CaO, with excess albite, quartz, muscovite and fluid phase.

Mineral assemblages of five component system in lower-grade metabasites are not fully understood to establish the correlation of the bulk rock chemistry and the physical condition. Metabasites belonging to this system generally consist of five phases. However, because of extensive Fe^{2+}-Mg substitutions in chlorite and amphibole, there is a large volume of four phase regions in this system. Let us take $Fe^{2+}/(Fe^{2+}+Mg)$ ratio of chlorite ($=X_{Fe}^{Chl}$) as the index of $Fe^{2+}/(Fe^{2+}+Mg)$ ratio of the system. If a four phases assemblage occurs under a range of X_{Fe}^{Chl}, its equilibrium relations may be approximated by the four phases region of the four component system, providing that the degree of other substitutions such as Fe^{3+}-Al, Si(Mg,Fe)-AlAl, or Ca-(Mg,Fe) are not sensitive to Fe^{2+}-Mg substitution. In this paper we will discuss the mineral assemblages in following ACF-F3 system;

A= Al_2O_3-(Na_2O+$3K_2O$)

C= CaO

F= FeO + MgO

F3= Fe_2O_3

Mineral assemblages of this system are shown in

tetrahedron of which apexes are represented by A,C,F, and F3, respectively (Fig. III-4). In this tetrahedron, four phases assemblages are represented by small tetrahedrons, and three phases assemblages are by triangular planes of a small tetrahedron. Generally, the transition from one of four phases assemblages to another in the original five component system is not univariant, but as we fixed the value of X_{Fe}^{Chl} in the reduced system, the transition is univariant.

Mineral assemblages observed in the study area are tabulated in Table III-3. These assemblages are composed of minerals, epidote (E), pumpellyite (P), lawsonite (L), prehnite (Pr), actinolite (A), sodic amphibole (G), sodic pyroxene (D), garnet (G), chlorite (C). and stilpnomelane (S) associated with albite + muscovite ± quartz ± calcite ± sphene ± ilmenite in metabasites. Metapelites and metacherts of the Chichibu Group and the Mikabu Greenrock Complex ordinarily contain chlorite + muscovite + albite + quartz and those of the Sanbagawa schists contain garnet and biotite associated with the minerals mentioned above. Garnet and biotite are ignored in this section. Therefore, the mineral assemblages of metapelites and metacherts are automatically excluded.

Among twenty-three observed assemblages of four phases, we discuss the high frequency assemblages which are observed more than ten times. They are as follows;

(A) ACF-F3 Diagram

$A = Al_2O_3 - (Na_2O + 3K_2O)$

$C = CaO$

$F = FeO + MgO$

$F3 = Fe_2O_3$

Act : Actinolite
Cross: Crossite
Gl: Glaucophane
Ri: Riebeckite
Di: Diopside
Ac: Acmite
Ep: Epidote
Pum: Pumpellyite
Chl: Chlorite

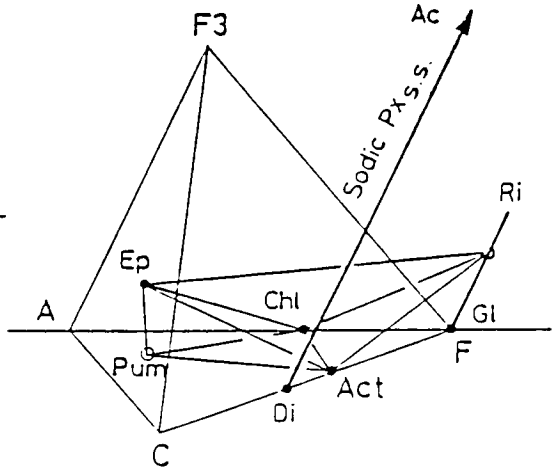

● : Situated on edge or surface of ACF-F3 tetrahedron

○ : Situated outside or inside of ACF-F3 tetrahedron

(B)

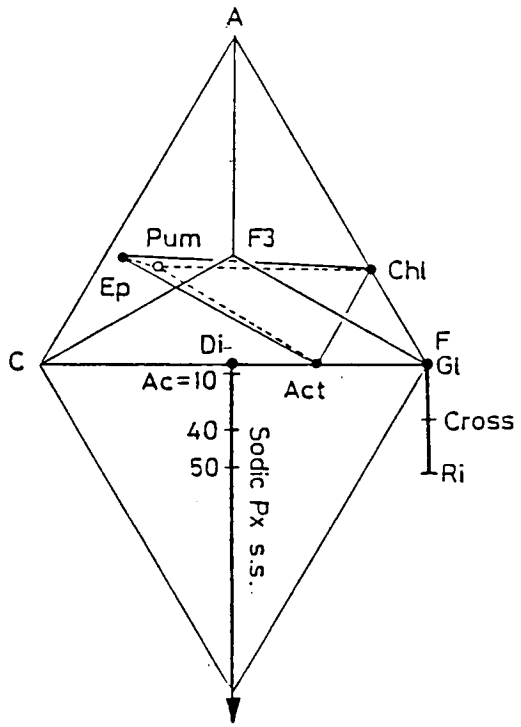

Fig. III-4. (A) ACF-F3 diagram, (B) Projection from F3 apex to ACF plane. Sodic pyroxene and sodic amphibole situate on lines which project from Di and Gl parallel to the A-F3 edge, respectively.

Table III-3. List of mineral assemblages in the Kanto Mountains.

3-Phases

	EAST	CENTRAL	WEST
E.A.C.	153	131	303
E.P.C.	27	20	33
E.L.C.	1	1	
E.G.C.	2	5	4
A.P.C.	25	27	27
A.G.C.	5	1	2
A.L.C.	1		1
G.L.C.	2		
E.G.S.		1	
G.P.C.		1	1
D.E.C.	2	18	52
D.A.C.	6	8	34
D.P.C.	2	25	6
D.G.C.		1	11**
E.Pr.C.	14	3	43
A.Pr.C.	2		8
P.Pr.C.	5		6

4-Phases

	EAST	CENTRAL	WEST
E.A.P.C.	80	14	40
E.A.G.C.	20	26	14
E.A.L.C.	3		
E.P.G.C.	7		3
E.G.C.S.	1		
A.P.G.C.	4		2
A.G.L.C.	1		
A.L.P.C.	1		
E.A.C.S.			1
G.C.S.Ga.			3
E.A.D.C	11	19	21
E.P.D.C.	7	10	23
E.G.D.C.		4	*8
P.G.D.C.			1
G.A.D.C.	3		2
G.L.D.C.			1
P.L.D.C.			2
G.S.D.C.			1
L.E.C.D.			1
E.P.Pr.C.	4	1	12
E.A.Pr.C.	1		4
E.D.Pr.C.			1
A.P.Pr.C.	1		1

Table III-3 Continue.

5-Phases

	EAST	CENTRAL	WEST
E.A.G.D.C	4	10	7
E.L.G.D.C.	3		
E.P.G.D.C.	2	1	2
E.P.L.D.C.	2		
E.P.A.D.C.	13	1	6
P.G.L.D.C.	2		
P.G.A.D.C.	4		1
G.A.L.D.C.	1		1
G.L.S.D.C.	1		
P.D.C.Ga.S.			1
E.A.G.C.S.			1
G.D.C.Ga.S.			2
E.P.C.D.S.	1		
E.A.G.L.C.	2		
E.A.G.P.C.	14		4
L.A.G.P.C.	3		
E.P.G.C.S.			2
E.A.P.Pr.C.	2		1

6-Phases

	EAST	CENTRAL	WEST
E.A.G.P.D.C.	12		3
E.A.G.L.P.C.	1		
E.L.G.P.D.C.	3		
E.L.G.A.D.C.	1		
L.A.G.P.D.C.	4		
G.A.D.C.Ga.S.			3
P.D.C.G.Ga.S.			1

7-Phases

	EAST	CENTRAL	WEST
E.L.A.G.P.D.C.	9		

Abbreviations; E:Epidote, A:Actinolite, G:Sodic-amphibole, D:Sodic-pyroxene, P:Pumpellyite, L:Lawsonite, C:Chlorite, S:Stilpnomelane, Ga:Garnet,

*: Mineral assemblage of three samples is epidote + taramite + jadeite + chlorite.

**: Jadeite + Taramite + Chlorite.

epidote+ actinolite + pumpellyite + chlorite (EAPC)

epidote + actinolite + sodic amphibole + chlorite (EAGC)

epidote + actinolite + sodic pyroxene + chlorite (EADC)

epidote + pumpellyite + sodic pyroxene + chlorite (EPDC)

epidote + pumpellyite + sodic amphibole + chlorite (EPGC)

epidote + pumpellyite + prehnite + chlorite (EPPrC)

EPPrC assemblage occurs only in the Atokura Formation and its correlatives. The author considers that this assemblage postdated the Sanbagawa metamorphism as will be discussed in a later section.

Distributions of main four phases assemblages and some of five phases assemblages are shown in Fig. III-5. EAPC (epidote + actinolite + pumpellyite + chlorite) assemblage commonly occurs in metabasites of the Mikabu Greenrock Complex and rarely in the lower part of the Chichibu Group and the upper most part of the Sanbagawa schists. This mineral assemblage characterizes the pumpellyite-actinolite facies (Coombs et al., 1976) and commonly occurs in the lower grade rocks of the Sanbagawa belt in Shikoku (Nakajima et al., 1977 and Aiba, 1982). Consequently, these facts indicate that the Mikabu Greenrock Complex of the Kanto Mountains belongs to the pumpellyite-actinolite facies same as in Shikoku, but main areas of the Sanbagawa schists and the Chichibu Group do not.

Along the Kanna-gawa, EAGC (epidote + actinolite + sodic amphibole + chlorite), EADC (epidote + actinolite +

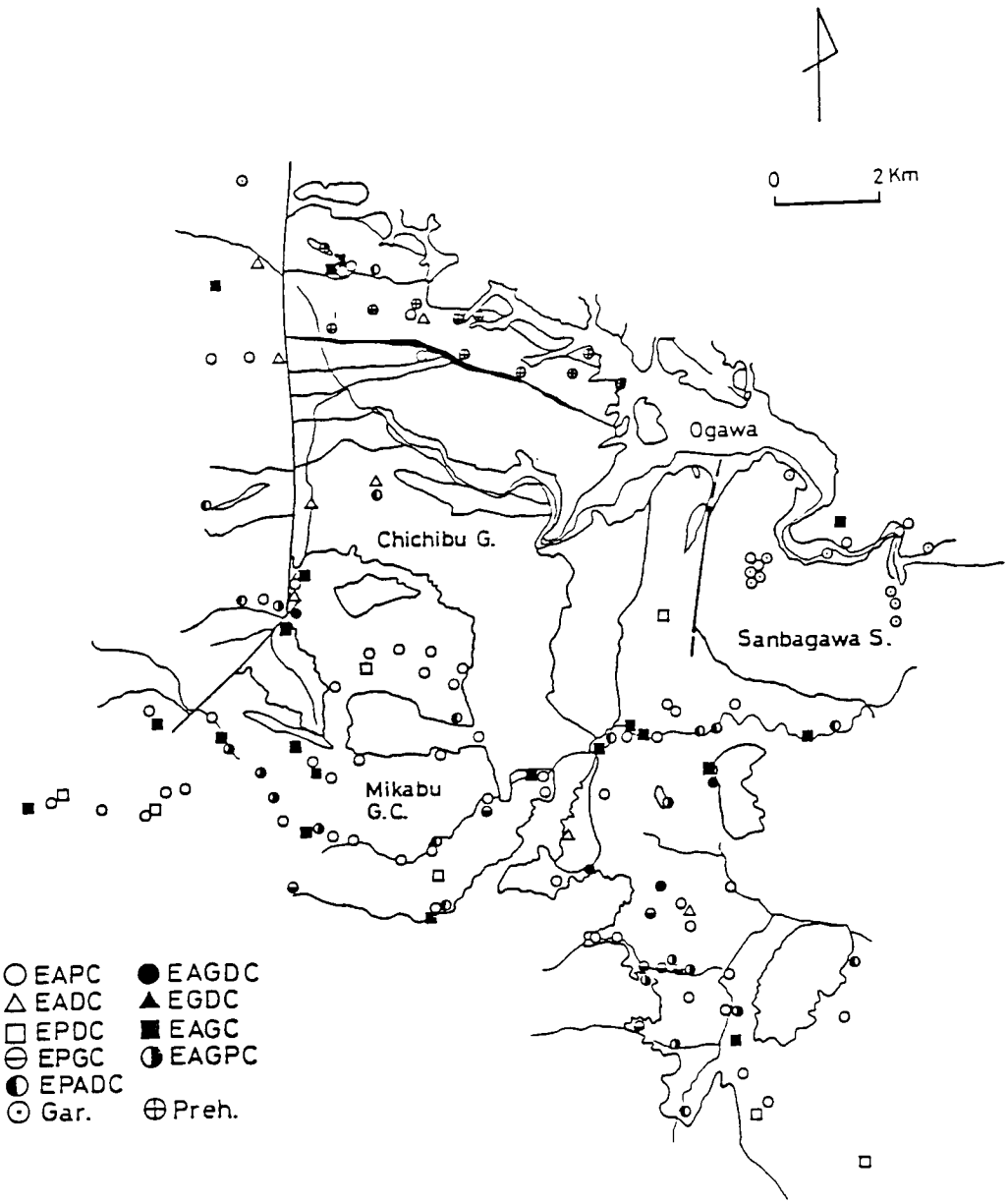

Fig. III-5a. Distribution of mineral assemblages and index minerals in the eastern part of the Kanto Mountains.

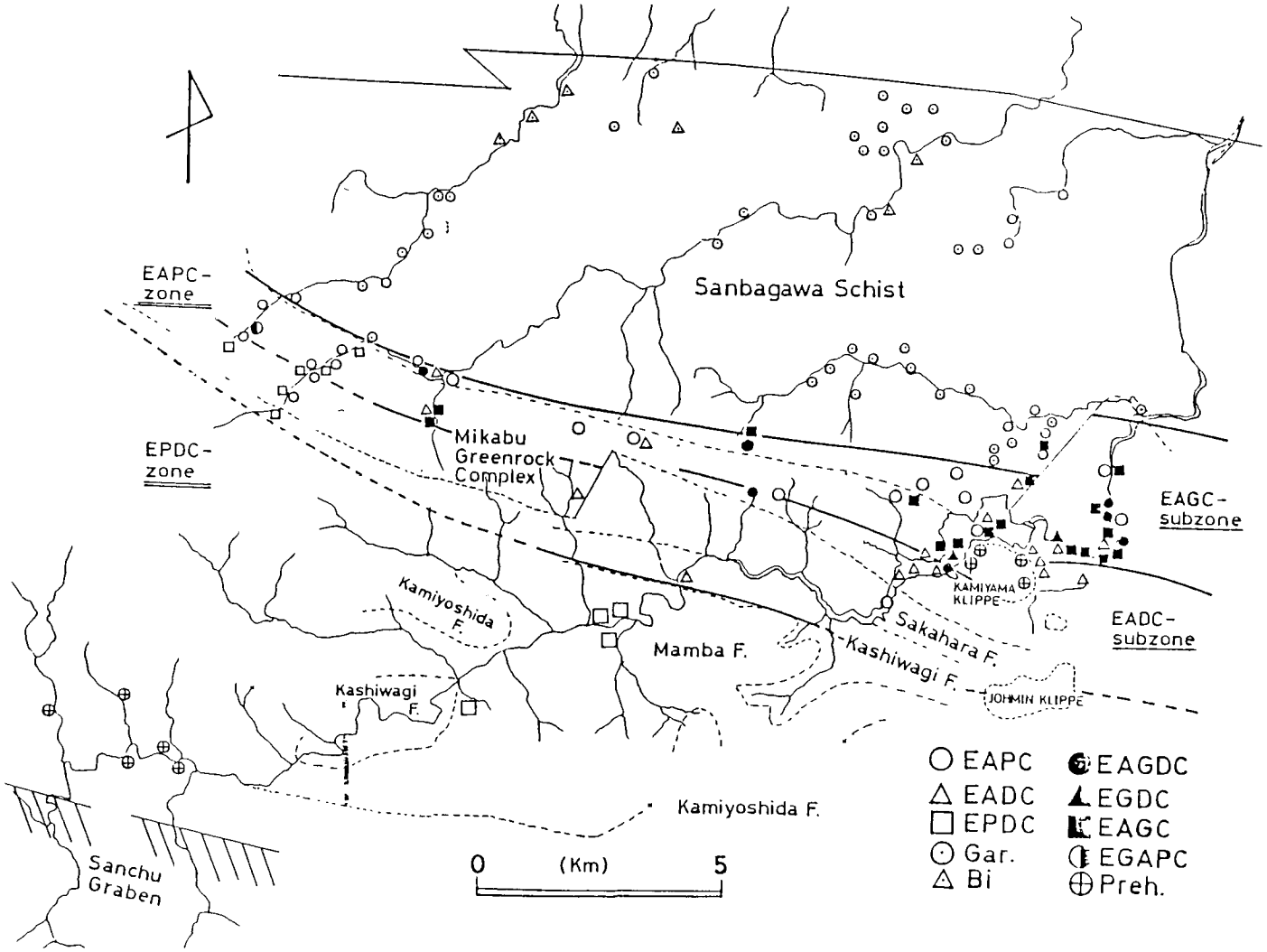

Fig. III-5b. Distribution of mineral assemblages and index minerals in the central part of the Kanto Mountains.

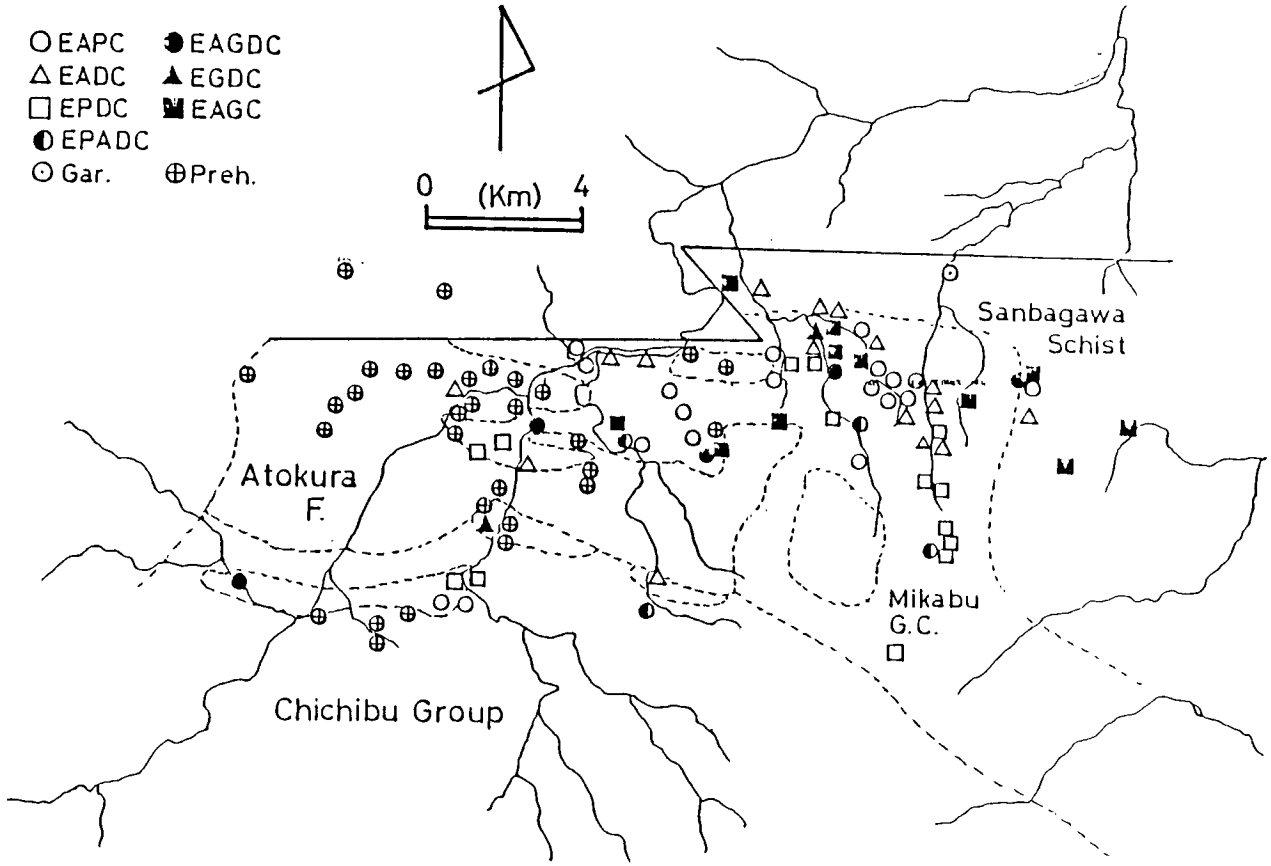

Fig. III-5c. Distribution of mineral assemblages and index minerals in the western part of the Kanto Mountains.

sodic pyroxene + chlorite), and EPDC (epidote + pumpellyite + sodic pyroxene + chlorite) assemblages distribute regularly from north to south; i.e., EAGC assemblage occurs in metabasites of the Sanbagawa schists and the stratigraphically lower part of the Mikabu Greenrock Complex, EADC assemblage occurs in the upper part of the Mikabu Greenrock Complex and the Kashiwagi Formation of the Chichibu Group, and EPDC assemblage is predominant in the Mamba Formation of the Chichibu Group (Fig. III-5-b).

Topological relationships among EAPC, EAGC, EADC, and EPDC assemblages in the ACF-F3 diagram are shown in Fig. III-6. We must know accurately the chemical compositions of constituent minerals to determine the position of minerals in the ACF-F3 tetrahedron. Topology of mineral assemblages mentioned above is analysed qualitatively in this section. Chemical compositions of minerals are assumed as follows with F standing for (Fe^{2+} + Mg) or (Fe^{2+},MG);

epidote	(E)	$Ca_2Al_2Fe^{3+}Si_3O_{12}(OH)$
actinolite	(A)	$Ca_2F_5Si_8O_{22}(OH)_2$
pumpellyite	(P)	$Ca_4FAl_5Si_6O_{23}(OH)_3 2H_2O$
sodic amphibole	(G)	$Na_2F_3AlFe^{3+}Si_8O_{22}(OH)_2$
sodic pyroxene	(D)	$CaNaFAl_{0.2}Fe^{3+}_{0.8}Si_4O_{12}$
chlorite	(C)	$F_5Al_2Si_3O_{10}(OH)_8$

EAPC assemblage forms a partial tetrahedron near the triangular surface defined by the apexes of A, C, and F in

the ACF-F3 tetrahedron (Fig. III-6). EAPC tetrahedron is not crosscut by any edge or triangular plane of the partial tetrahedrons of EAGC or EADC. Partial tetrahedrons of EAGC and EADC share the EAC triangular plane of EAPC tetrahedron and occupy the F3- and F- richer subspace in the ACF-F3 tetrahedron. Therefore, EAGC and EADC assemblages are stable under the P-T condition of EAPC assemblage; i.e., pumpellyite-actinolite facies.

However, EAGC and EADC assemblages can not coexist under the same P-T condition, because sodic pyroxene-chlorite edge of the EADC tetrahedron crosscuts the triangular plane of actinolite-epidote-sodic amphibole of EAGC tetrahedron. This relationship is represented as follows;

$$310\ CaNaFAl_{0.2}Fe^{3+}_{0.8}Si_4O_{12} + 117\ F_5Al_2Si_3O_{10}(OH)_8 + 30\ NaAlSi_3O_8 + 529\ SiO_2 =$$
$$77\ Ca_2F_5Si_8O_{22}(OH)_2 + 78\ Ca_2Al_2Fe^{3+}Si_3O_{12}(OH) + 170\ Na_2F_3AlFe^{3+}Si_8O_{22}(OH)_2 + 182\ H_2O$$

sodic pyroxene + chlorite + albite + quartz =

actinolite + epidote + sodic amphibole + H_2O ---- (2)

This reaction indicates that EADC assemblage is stable at lower temperature than EAGC assemblage. Consequently, pumpellyite-actinolite facies is subdivided into two subfacies, EADC and EAGC.

EPDC assemblage can not coexist with EAPC assemblage, because epidote-actinolite edge of EAPC tetrahedron

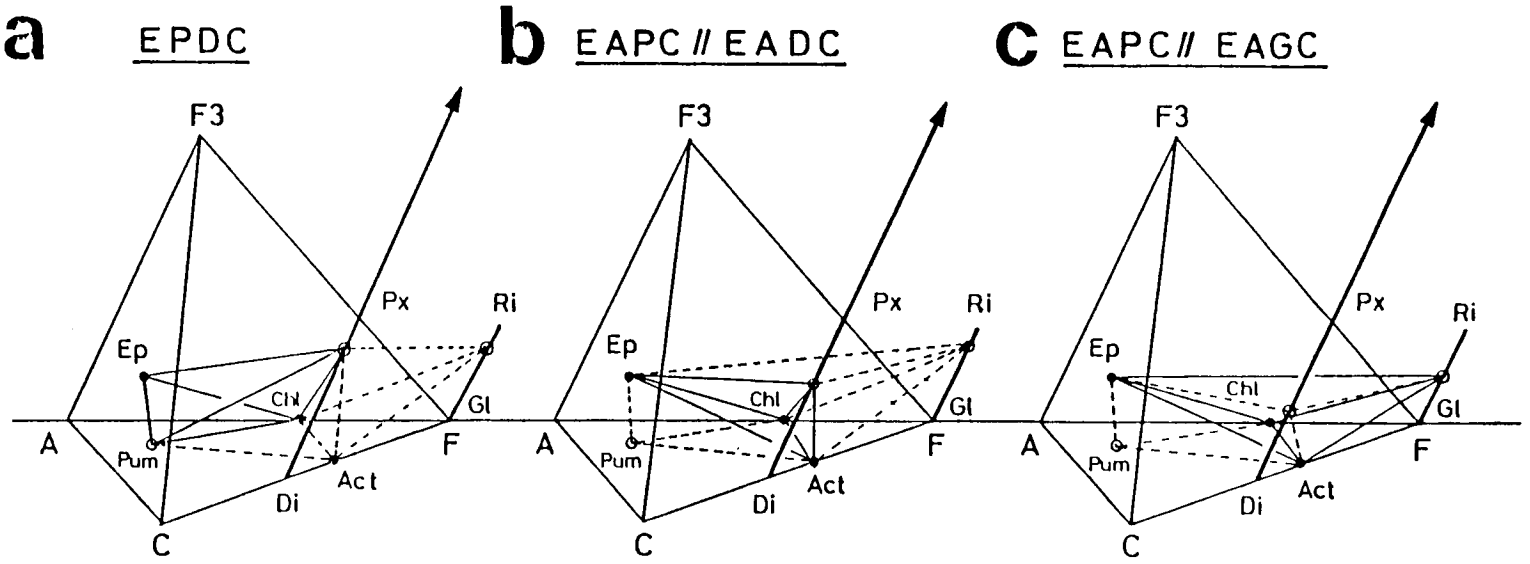

Fig. III-6. Mineral paragenesis of metabasites in the ACF-F3 diagram.
(a) sodic pyroxene-chlorite facies.
(b) sodic pyroxene-chlorite subfacies of pumpellyite-actinolite facies.
(c) epidote-sodic amphibole subfacies of pumpellyite-actinolite facies.

crosscuts the pumpellyite-sodic pyroxene-chlorite triangular plane of the EPDC tetrahedron. This relation is represented as following;

$$170\ Ca_4FAl_5Si_6O_{23}(OH)_3 2H_2O + 430\ CaNaFAl_{0.2}Fe^{3+}_{0.8}Si_4O_{12} + 91\ F_5Al_2Si_3O_{10}(OH)_8 + 997\ SiO_2 =$$
$$344\ Ca_2Al_2Fe^{3+}Si_3O_{12}(OH) + 211\ Ca_2F_5Si_8O_{22}(OH)_2 + 430\ NaAlSi_3O_8 + 576\ H_2O$$

pumpellyite + sodic pyroxene + chlorite + quartz =

epidote + actinolite + albite + H_2O ---------(3)

This reaction indicates that EPDC assemblage is stable at lower temperature condition than EAPC assemblage, i.e., pumpellyite-actinolite facies.

The existence of sodic pyroxene + pumpellyite + chlorite assemblage in the lower grade part of the high-pressure intermediate group of metamorphism is predicted by the Schreinemakers' analyses in the ACF system with seven phases of lawsonite, epidote, pumpellyite, sodic pyroxene, sodic amphibole, actinolite, and chlorite by Hirajima (1983b). Predicted mineral assemblage is actually confirmed as EPDC assemblage found in the study area.

EGDC assemblage and five phases assemblage of EAGDC are observed in the Mikabu Greenrock Complex along the Kanna-gawa. EGDC tetrahedron shares the DCE plane of EADC tetrahedron and occupies the Ca-poor subspace in ACF-F3 tetrahedron (Fig. III-6). Therefore, EGDC assemblage can

be stable under the pumpellyite-actinolite facies condition. Rocks containing EAGDC assemblage are associated with those containing EAGC assemblage. This five phases assemblage may preserve the transitional state from the EADC subfacies to the EAGC subfacies of the pumpellyite-actinolite facies.

Regular distribution of four phases mineral assemblages is observed along the Kanna-gawa, but not so clear in the other areas of the Kanto Mountains. Both in the eastern and western parts of the Kanto Mountains, EADC assemblage occurs in the Chichibu Group and the Mikabu Greenrock Complex, and EAGC assemblage does in the Mikabu Greenrock Complex and the Sanbagawa schists. This tendency is same as that of the Kanna-gawa. However, EPDC assemblage occurs mainly in the Mikabu Greenrock Complex in these areas.

Pumpellyite + sodic amphibole assemblage, such as EPGC and AGPC assemblages, are also observed in the Mikabu Greenrock Complex of the western and eastern parts of the Kanto Mountains which belong to the pumpellyite-actinolite facies. Coexistence of pumpellyite and sodic amphibole is inconsistent with the mineral assemblages of the pumpellyite-actinolite facies, because of following reaction;

$$31\ Ca_4FAl_5Si_6O_{23}(OH)_32H_2O + 43\ Na_2F_3AlFe^{3+}Si_8O_{22}(OH)_2 + 48\ SiO_2 =$$
$$19\ Ca_2F_5Si_8O_{22}(OH)_2 + 43\ Ca_2Al_2Fe^{3+}Si_3O_{12}(OH) + 13\ F_5Al_2Si_3O_{10}(OH)_8 + 86\ NaAlSi_3O_8 + 59\ H_2O$$

pumpellyite + sodic amphibole + quartz =

actinolite + epidote + chlorite + albite + H_2O ----(4)

Graphical representation of the reaction (4) is shown in Fig. III-7. Although EAPC assemblage is mainly observed in tuffites, tuff breccias and lavas, all sodic amphibole - pumpellyite assemblage are observed in coarse-grained rocks, such as gabbro and dolerite. In coarse-grained rocks, actinolite and sodic amphibole replace rims or cracks of relict mafic minerals, and pumpellyite and epidote do relict plagioclase. Such mafic metamorphic minerals and metamorphic Ca-Al silicates do not contact with each other as shown in photomicrograph of a gabbro which contains both pumpellyite and sodic amphibole (Plate III-1). This texture indicates that these two minerals were formed under the pumpellyite-actinolite facies condition, because of insufficient material mixing. EPDC assemblage in the eastern and western parts also occurs in the coarse-grained rocks same as those containing pumpellyite-sodic amphibole assemblage. Coarse-grained rocks such as gabbro and dolerite are more abundant in the western and eastern parts than the central part of the Kanto Mountains. These coarse-grained rocks are not suited to use in metamorphic zonal mapping.

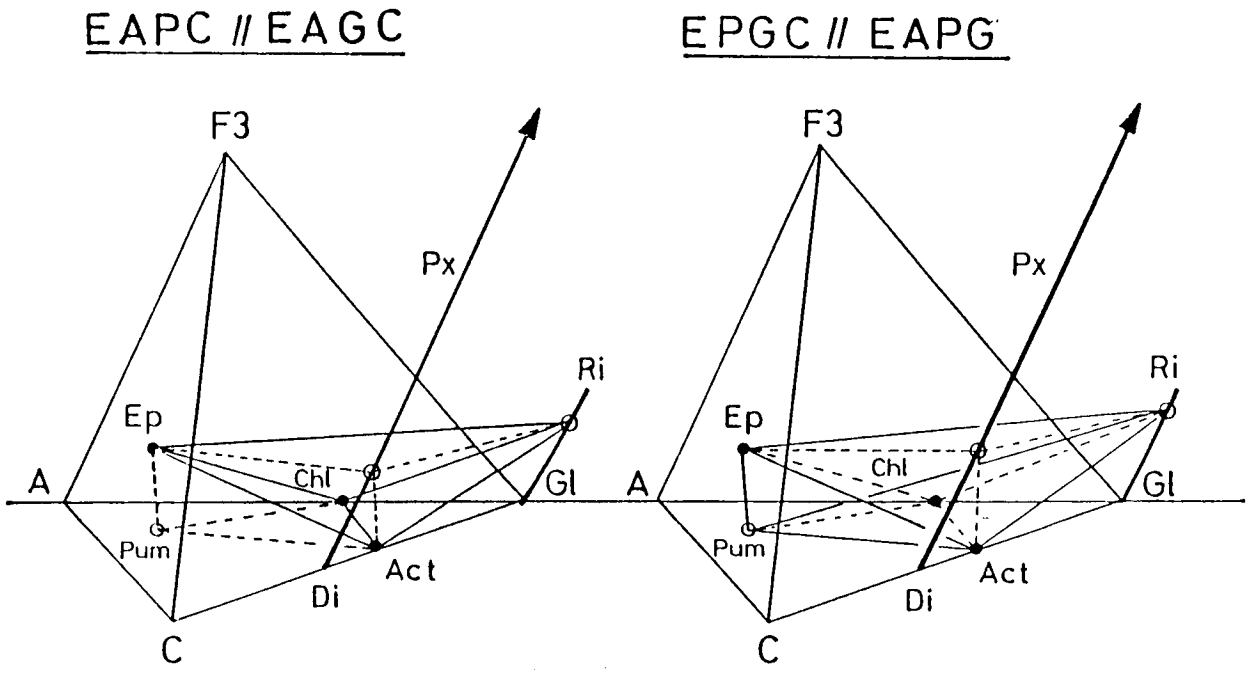

$$Ep + Act + Chl + H_2O = Pum + Gl$$
$$(EAC) \quad = (PG)$$

Fig. III-7. Relationship of mineral paragenesis between pumpellyite-actinolite facies and pumpellyite-sodic amphibole assemblage.

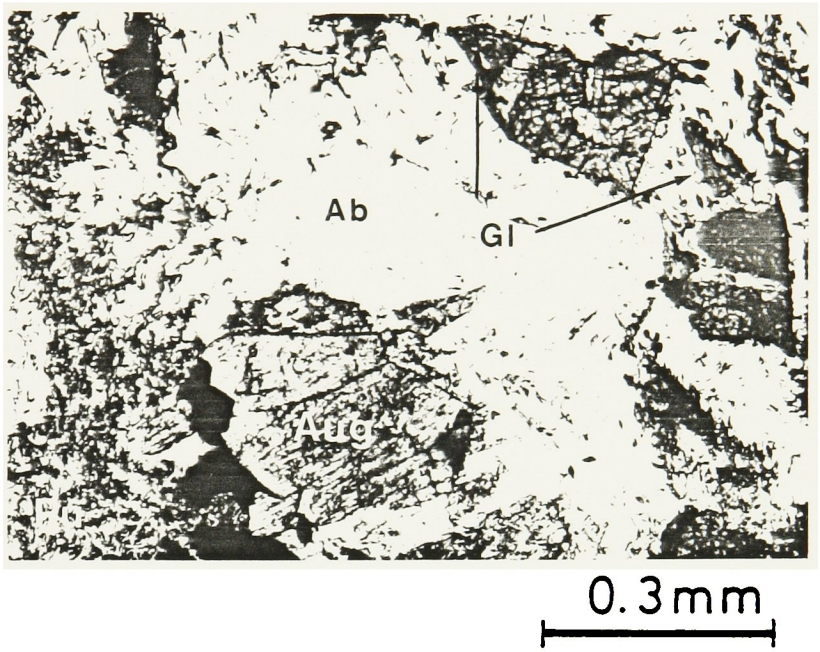

Plate III-1. Photomicrograph of gabbro, rock No.535. Sodic amphibole (Gl) and pumpellyite (Pu) grow at the different place. Ab: albite. Opened nicol.

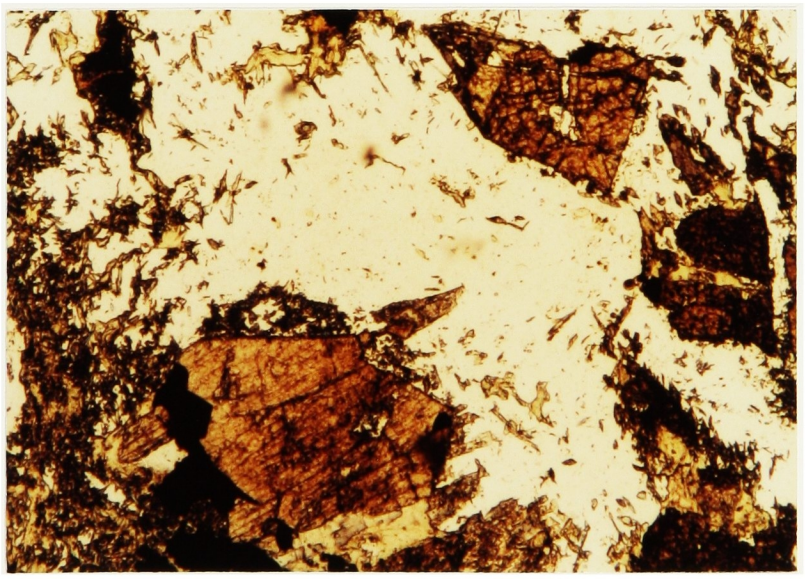

IV. Mineralogy

IV-1 Analytical method

The mode of occurrence and chemical compositions of minerals will be discussed in this chapter. Detailed mineralogical studies were carried out on about eighty specimens. Among them, twenty-seven specimens were analyzed by an electron microprobe of Kanazawa University (Hitachi XMA 5A), and the others were by Hitachi-S550 scanning electron microscope with Kevex energy dispersion system of Kyoto University. Analytical procedures of each microprobe are briefly described.

Hitachi XMA 5A microprobe is equipped with three channels detection system of 38^{o} take off angle. Working standards were used as follows; quartz for Si, kaersutite for Ti, hematite for Fe, corundum for Al, Mn-metal for Mn, wollastonite for Ca, albite for Na, and orthoclase for K. The accelerating voltage, specimen current and beam diameter were kept at 15 KV, 0.02 micro ampere and 3-5 microns, respectively. The background intensity was estimated assuming the linearity between the background intensity and mean atomic numbers of samples. The observed intensities were corrected for the dead time and then the intensity ratios of unknown to standards were corrected by the alpha factors of Albee and Ray (1970). Banno (pers. comm.) re-calculated some of the alpha factors of Albee and Ray (1970) by the method described in Bence and Albee (1968).

Corrected alpha factors are as followings;

a^{SiO2}_{Mg}=1.16, a^{CgO}_{Mg}=1.31, a^{Mg}_{Si}=1.40, a^{Al2O3}_{Si}=1.50, a^{CaO}_{Si}=1.05, and a^{SiO2}_{Ca}=1.18

Microprobe analysis using Hitachi-S550 with Kevex energy dispersion system was carried out under the condition of 15 KV acceleration voltage, 300 picoamperes of beam current and less than 0.1 microns in beam diameter Quantitative analyses were completed by correction subroutines (MAGIC V) of KEVEX QUANTEX-RAY SYSTEM program. Working standards were as follows; albite for Na, Mn-metal for Mn, and natural augite (KH-1) analyzed by Obata (pers. comm.) for Si, Ti,Al, Fe, Mg, and Ca.

Present technique does not allow the routine distinction of Fe^{2+} from Fe^{3+}, hence total iron is reported as FeO for calcic amphibole, pumpellyite, chlorite and relict pyroxene, and Fe_2O_3 for epidote, lawsonite and albite. The estimating method of ferric content in sodic amphibole and sodic pyroxene is described later. Volatile contents can not be determined quantitatively, hence atomic proportions of minerals are calculated on the anhydrous basis.

IV-2 Minerals in the Sanbagawa metamorphic rocks

IV-2-1 Pyroxene

(2-1-1) Mode of occurrence

Because relic pyroxenes commonly occur in basic rocks of the Chichibu Group and the Mikabu Greenrock Complex in the Kanto Mountains, it is necessary to distinguish metamorphic pyroxenes from relic ones. On the microscopical observation and the microprobe analysis, the mode of occurrence of metamorphic pyroxenes in basic rocks is as follows;

(a) Tabular pale-green grains in albite vein. When relic pyroxenes are crosscut by albite vein, a part of them extending into albite vein becomes tabular shaped and pale green, though the rest in the matrix is tabular to rounded shaped and colorless (Plate VI-1).

(b) Pale brown or pale green pyroxenes replacing rims and cracks of relic colorless clinopyroxene in the matrix.

(c) Unhedral fine-grained (about 0.1 mm in diameter) pyroxenes partially or perfectly replacing relic clinopyroxene. Dusty aggregates composed of very fine grained sphene and rutile (less than 0.01 mm in diameter) usually exist around this type of metamorphic pyroxenes (Plate IV-2).

(d) Omphacite vein, as described by Hashimoto (1964).

(e) Coarse-grained pyroxenes associated with Mn-rich garnet, sodic amphibole, stilpnomelane, magnetite, hematite, albite and quartz in the Mn-rich nodule in the Sanbagawa schists

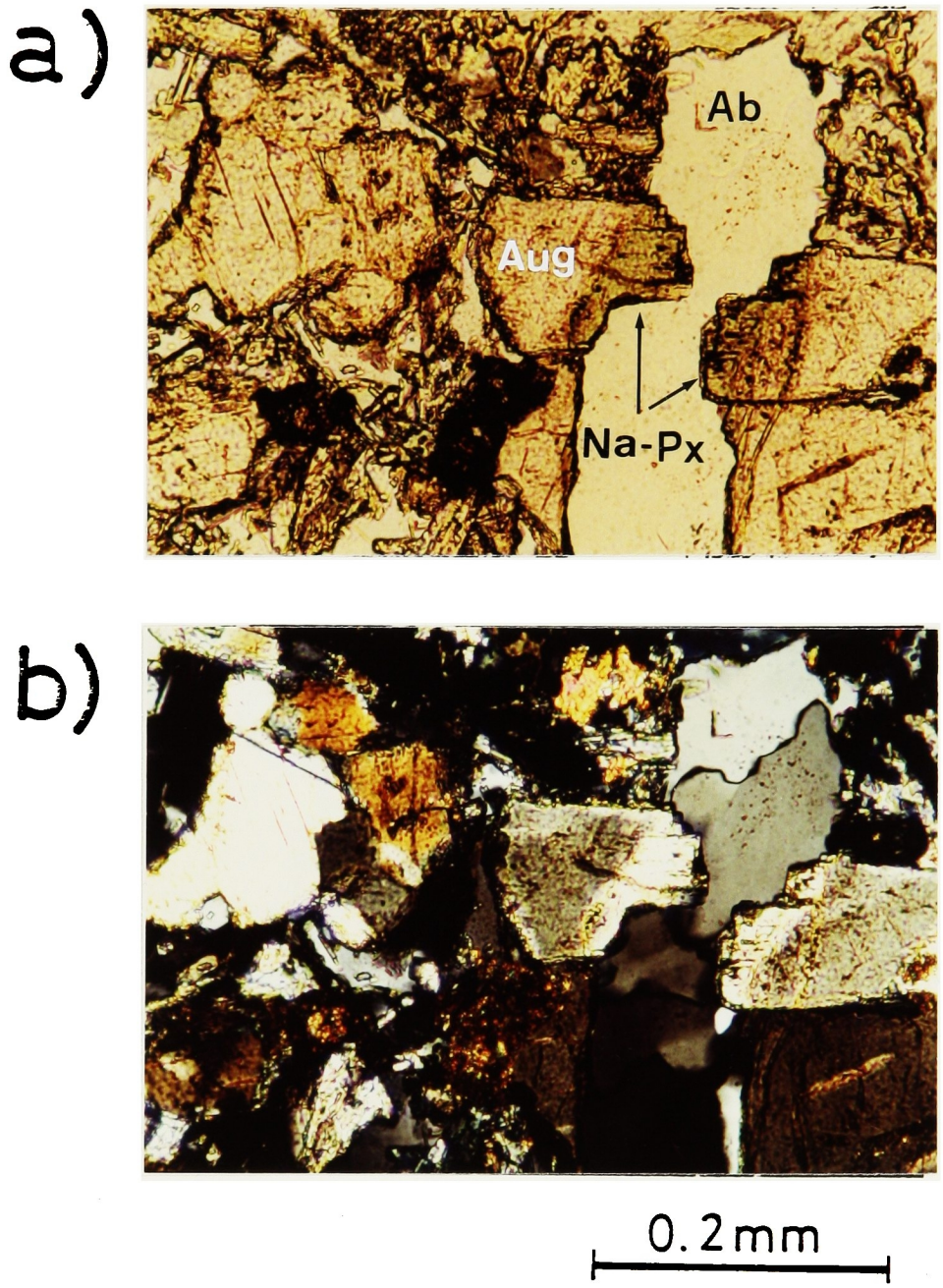

Plate IV-1. Photomicrographs of sodic pyroxenes(Na-Px) partially replace relict augite (Aug) in albite (Ab) vein. a) opened nicol. b) crossed nicols. Rock. No.285. Dolerite in Mikabu Greenrock Complex.

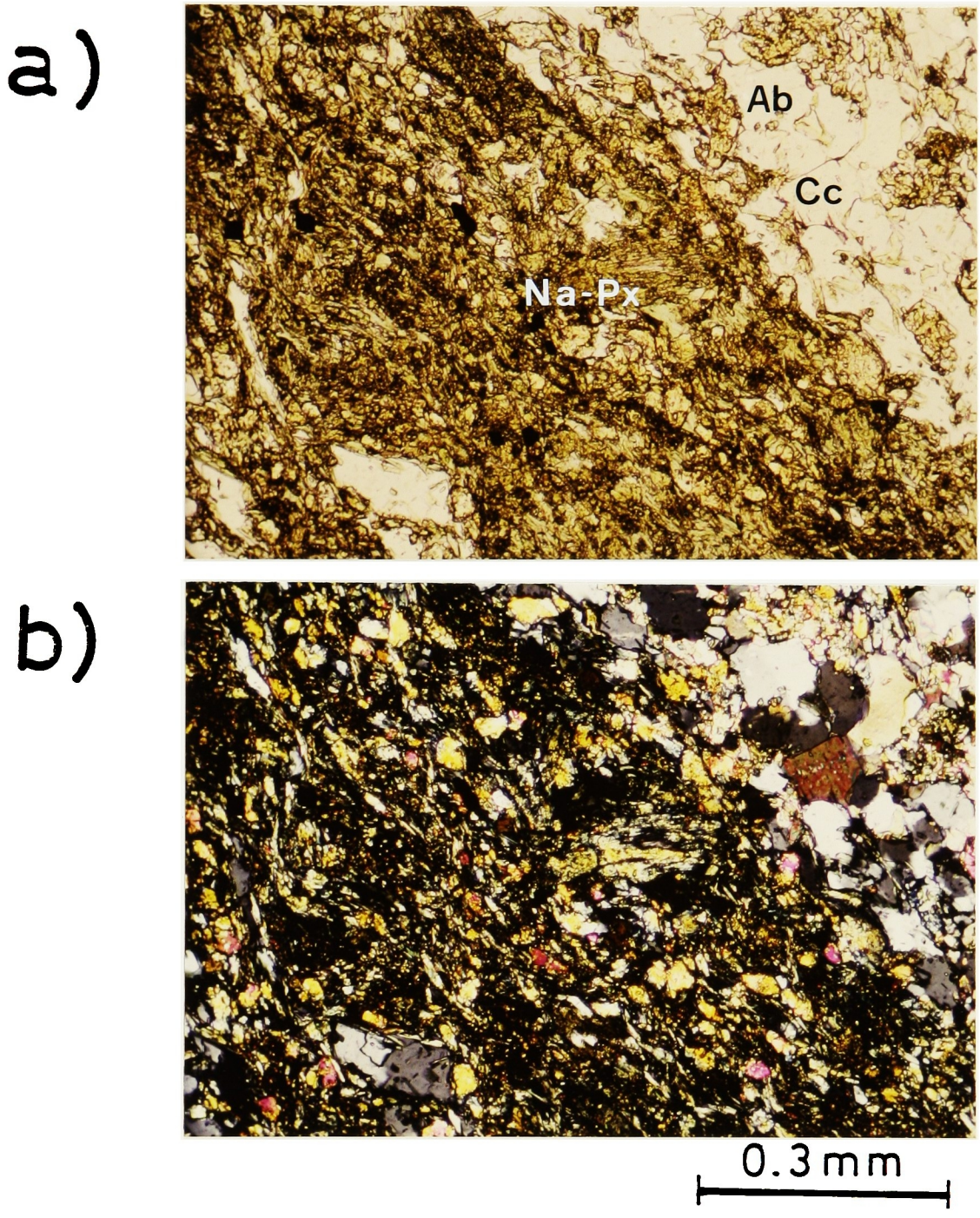

Plate IV-2. Photomicrographs of sodic pyroxenes (Na-Px) completely replacing relict pyroxene. Ab:albite, Cc:calcite, Ep:epidote. a)opened nicol. b)crossed nicols. Rock No. K1404. Mikabu Greenrock Complex.

(Plate IV-3).

Pyroxenes of types (a) and (b) are common in metabasites of the Chichibu Group and the Mikabu Greenrock Complex, and (c) type is in metabasites of the Mikabu Greenrock Complex, especially in epidote + actinolite + sodic amphibole + sodic pyroxene + chlorite -bearing rocks. Omphacite and chloromelanite lamellae are often observed in (a) type pale green sodic augite (Plate IV-4).

(2-1-2) Chemical composition

Metamorphic pyroxenes are distinguished from relict pyroxenes on Si-Al and Ti-Al variation diagrams (Figs IV-1 and IV-2). Metamorphic pyroxenes are usually poorer in TiO_2 and Al_2O_3, and richer in SiO_2 than those of relict ones. The difference in chemical composition between them is easily recognized in secondary electron image. The secondary electron image of the same pyroxene grain as in Plate IV-4 is shown in Plate IV-5. Metamorphic salite growing in the albite vein is brighter part and relict augite is darker part in the secondary electron image. Darker fine lamellae in brighter part are chloromelanite. Chemical compositions of metamorphic and relict pyroxenes are shown in Table IV-1. This paper follows Banno (1959) in recalculating Fe^{2+}/Fe^{3+} ratio from microprobe analyses; Jd (jadeite)=$Al^{VI}/(Na+Ca)$, Ac (acmite)=$Fe^{3+}/(Ca+Na)=(Na-Al^{VI})/(Na+Ca)$ and Di (diopside)=$Ca/(Na+Ca)$.

Metamorphic pyroxenes in metabasites of the Chichibu

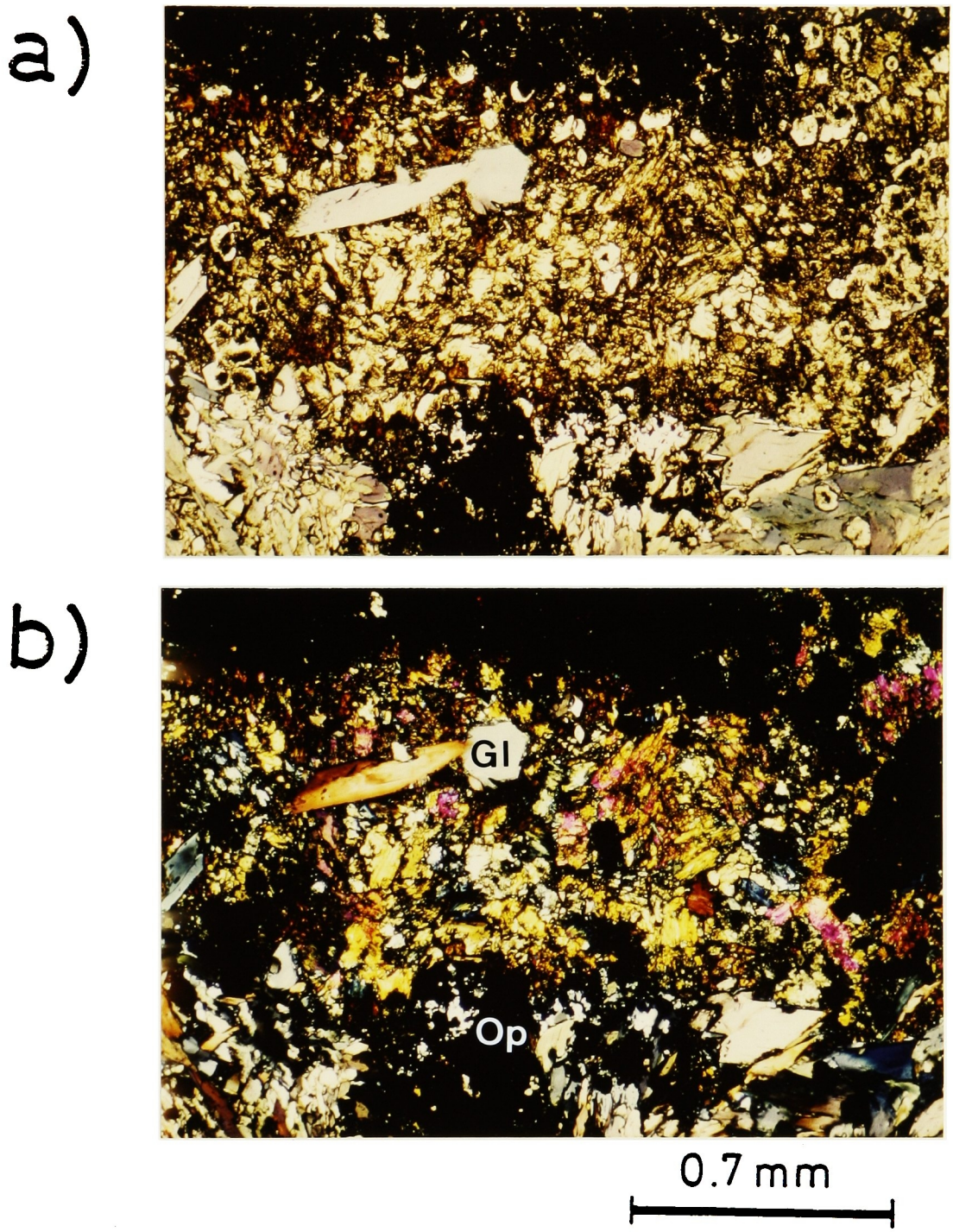

Plate IV-3. Photomicrographs of sodic pyroxene (Aeg-Jd) in the Mn-rich nodule of the Sanbagawa schists. Gl: sodic amphibole. Op: hematite and magnetite. a)opened nicol. b)crossed nicols.

Plate IV-4. Photomicrograph of salite (Na-Px) with aegirine-augite (Aeg-Aug) lamellae. Opened nicol.

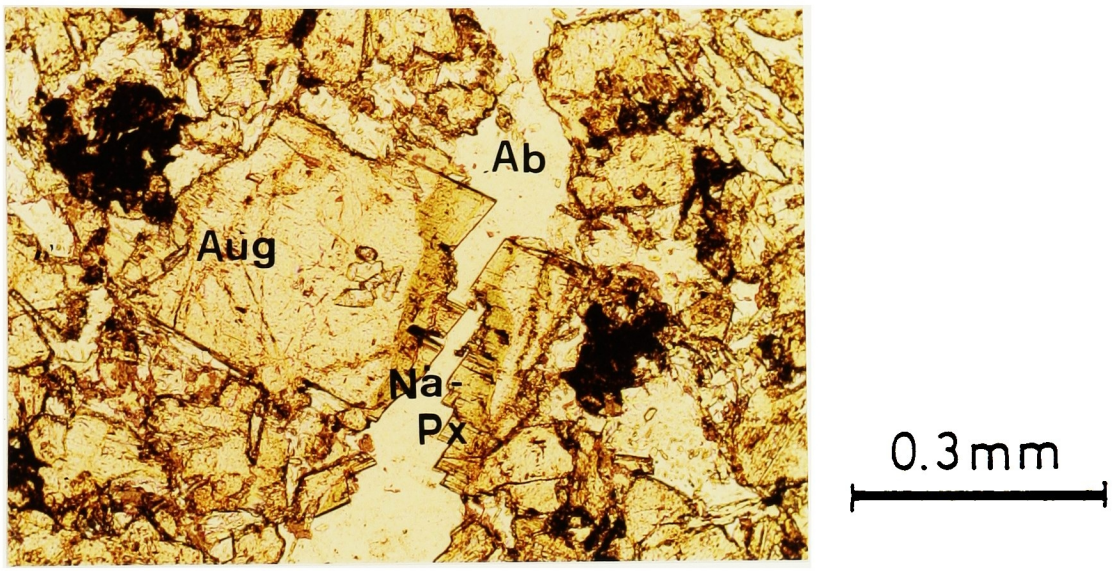

Plate IV-5. Secondary electron image of the same grain in Plate IV-4. Aug:relict augite, Ab:albite.

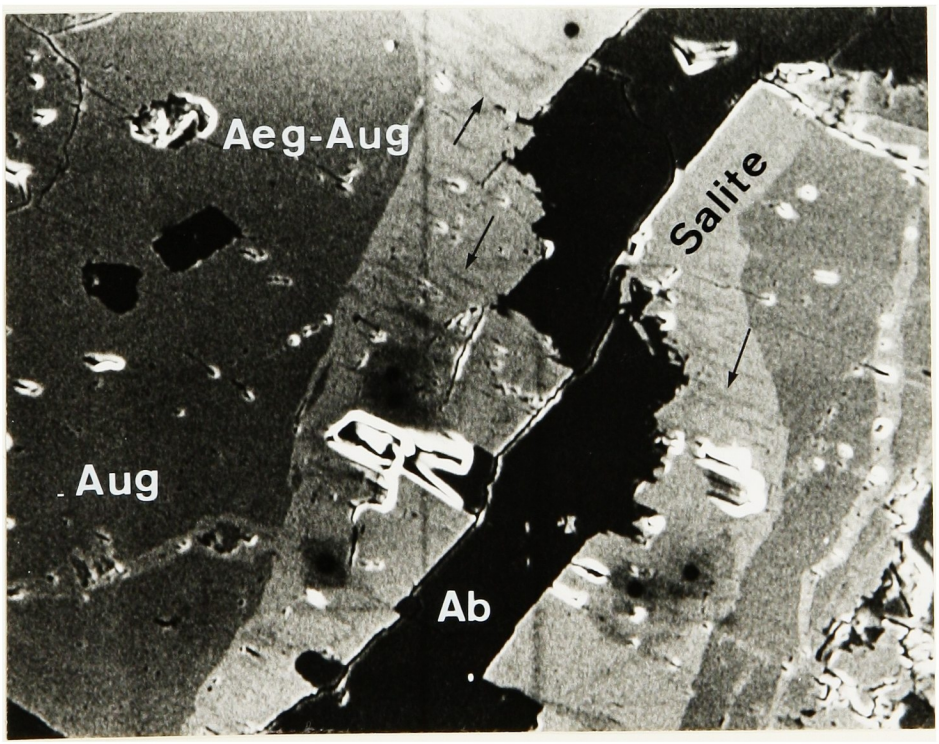

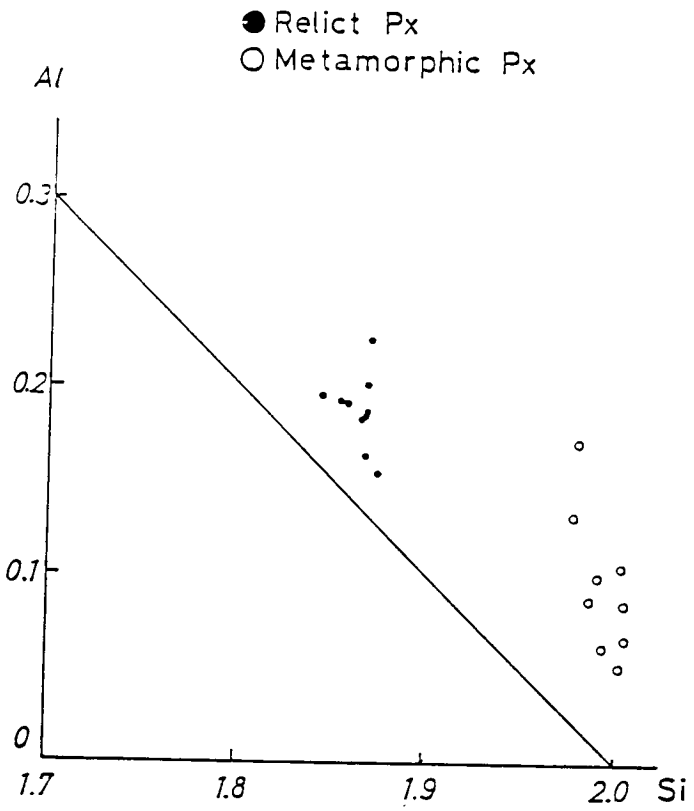

Fig. IV-1. Si-Al diagram of relict(solid circle) and metamorphic (open circle) pyroxenes in metabasites of the Mikabu Greenrock Complex.

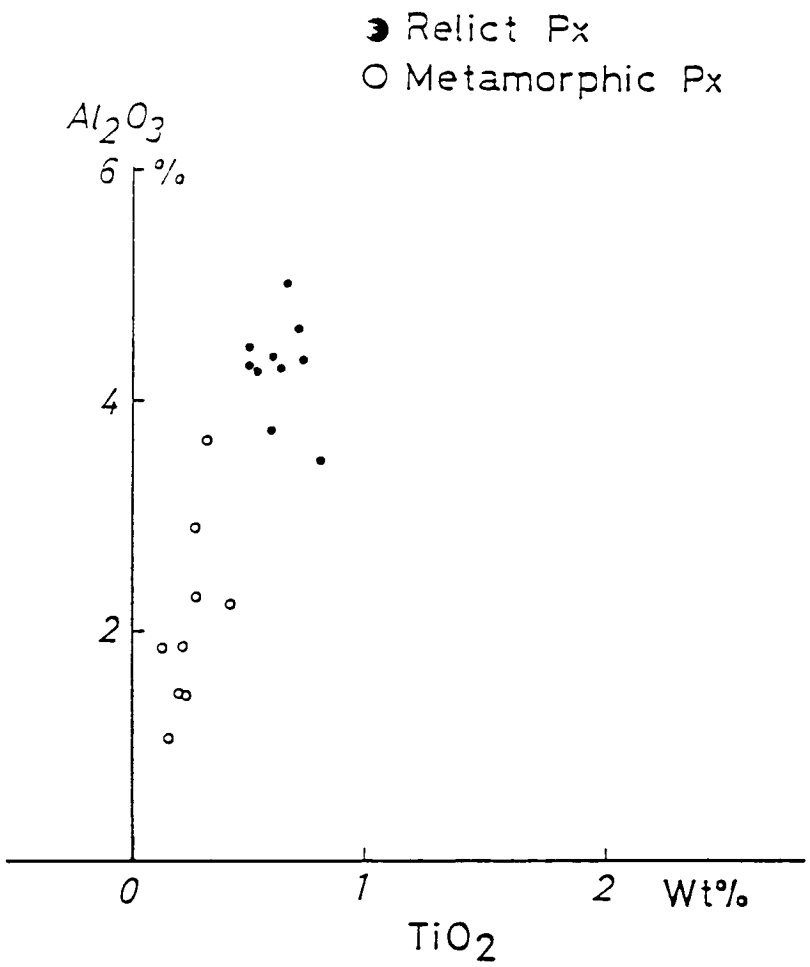

Fig. IV-2. TiO2-Al2O3 diagram of relict (solid circle) and metamorphic (open circle) pyroxenes in metabasites of the Mikabu Greenrock Complex.

Group and the Mikabu Greenrock Complex are plotted in Jd - Ac - Di diagram (Fig. IV-3) proposed by Essene and Fyfe (1967). The Jd contents of them are ordinarily less than 20 mol%, about 10 mol% in average. Pyroxenes of which Jd contents exceed 20 mol% usually form composite grains or the exsolution texture mentioned above. Omphacite or chloromelanite contact metamorphic salite with distinct chemical gap which was proposed by Carpenter (1980).

The Ac contents of metamorphic pyroxenes are controlled by oxygen fugacity in host rocks. As shown in Fig.IV-4, metamorphic pyroxenes associated with hematite are richer in Ac content than those with Fe-sulfides, instead of hematite. Exsolution texture in sodic pyroxenes is not observed in hematite-bearing rocks. Miscibility gap between omphacite and sodic augite seems to close around Ac=50 mol% and Jd=10 mol% in Jd-Ac-Di diagram under the metamorphic condition of the pumpellyite-actinolite facies.

The Jd contents of metamorphic pyroxenes generally increase with descending stratigraphic order; from 5 mol% in average of the Chichibu Group, 10 mol% in Mikabu Greenrock Complex, to 25 mol% in Sanbagawa schists (Fig. IV-4). The systematic increase of Jd content means an increase in pressure (P) at constant temperature (T), a decrease in T at constant P, and/or an increase in both P and T, as predicted from experimental data on the reaction of jadeite + quartz = albite (Holland, 1980) and theoretical calculation (Essene

and Fyfe, 1967; Holland, 1983).

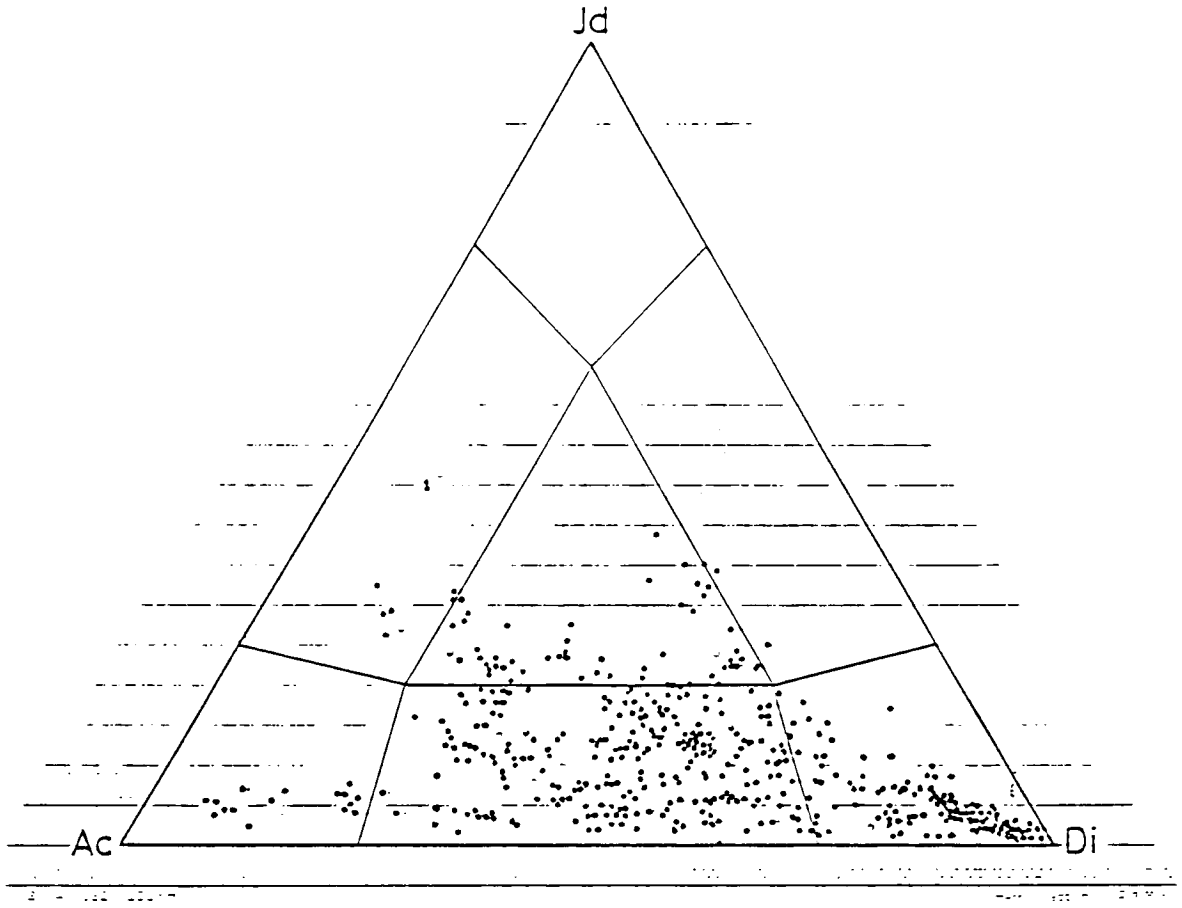

Fig. IV-3. Metamorphic pyroxenes from the Sanbagawa metamorphic rocks in the Kanto Mountains.

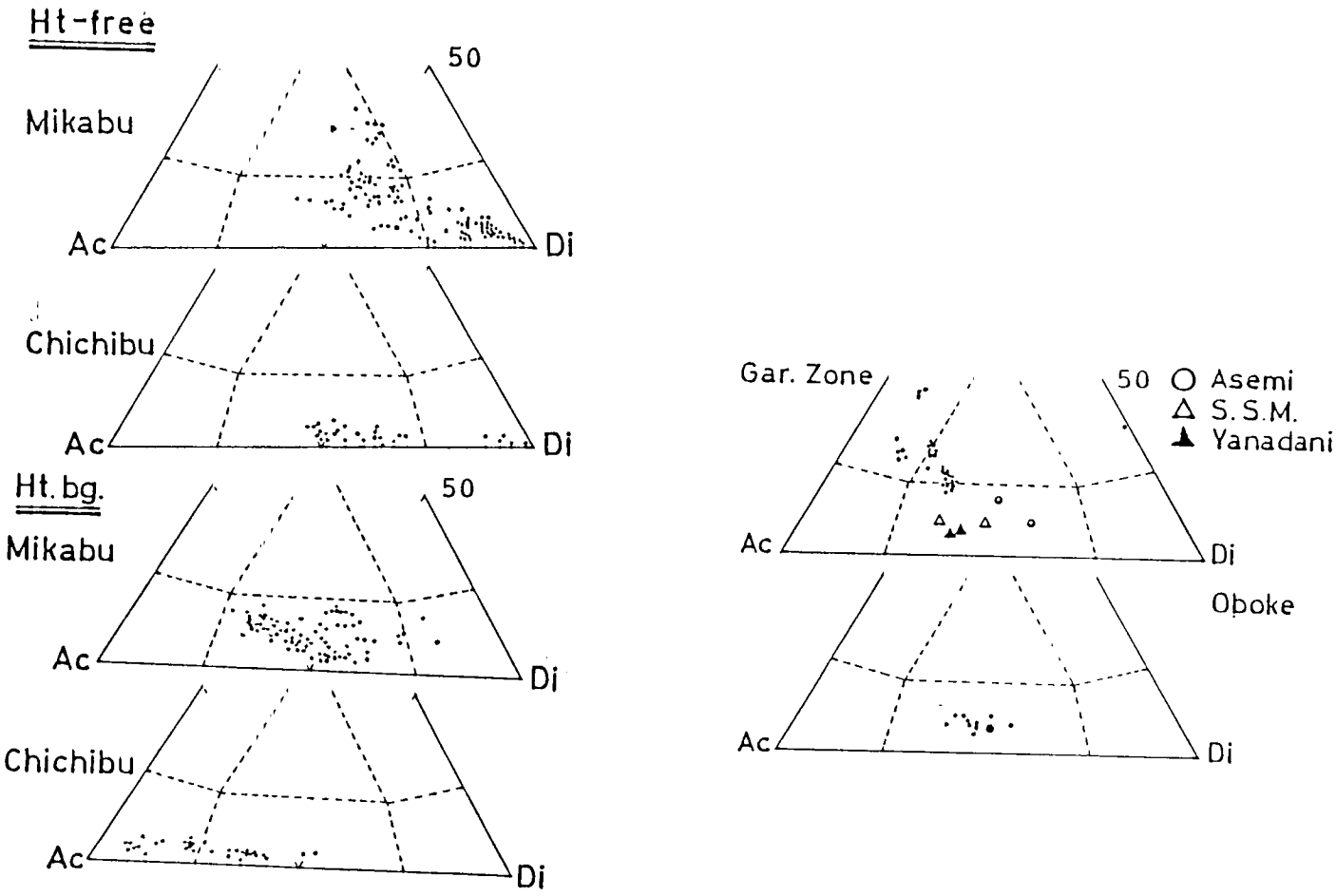

Fig. IV-4. Compositional variation of sodic pyroxenes in each geologic unit.

Table IV-1 Chemical composition of relic and metamorphic pyroxenes in the Sanbagawa metamorphic rocks

Sample No.	116		K444			285		423	
Zone	Chichibu		Chichibu			Mikabu		Mikabu	
Assemblage	EAC		EPDC			Px-lamella		Px-lamella	
Point. No.	17	23	15	16	22	44	45	19	18
Me./Re.	Meta	Relic	Meta	Relic	Meta	Meta	Meta	Meta	Meta
SiO2	50.41	47.23	53.06	51.31	52.23	52.46	53.96	52.06	53.42
TiO2	.99	1.92	.16	.95	.00	.00	.42	.00	.00
Al2O3	1.18	4.45	.97	2.92	.46	.30	4.23	.28	4.28
FeO*	29.36	15.16	18.44	6.70	19.93	16.24	15.94	16.02	14.79
MnO	.31	.40	.40	.19	.39	.71	.08	1.94	.09
MgO	.0	8.74	6.07	16.98	5.27	7.75	5.54	7.22	6.24
CaO	8.85	21.00	14.01	19.84	13.49	21.82	11.13	22.62	11.62
Na2O	7.88	.79	5.97	.00	6.35	1.64	8.14	.45	6.75
Total	98.98	99.68	99.08	98.89	98.16	100.91	99.44	100.59	97.19
O=6									
Si	2.067	1.834	2.072	1.906	2.079	2.016	2.056	2.014	2.066
Al	.057	.204	.045	.128	.022	.014	.190	.013	.195
Ti	.030	.056	.005	.027	.000	.000	.012	.000	.000
Fe	1.009	.492	.602	.208	.664	.522	.508	.518	.478
Mn	.017	.013	.013	.006	.013	.023	.003	.064	.003
Mg	.0	.506	.353	.940	.313	.444	.314	.416	.360
Ca	.479	.874	.586	.790	.575	.898	.455	.937	.482
Na	.546	.059	.452	.000	.490	.122	.601	.034	.506
Total	4.185	4.038	4.128	4.007	4.156	4.039	4.139	3.996	4.092
X(Jd)	.6		.04		.02	.01	.18	.01	.17
X(Ac)	.34		.40		.44	.11	.39	.02	.29
X(Di)	.60		.56		.54	.88	.43	.97	.54

*:Total iron as FeO

Table IV-1. Chemical composition of relic and metamorphic pyroxenes in the Sanbagawa metamorphic rocks. (Continue)

Sample No.	K1431			K357		K1404		US3705	
Zone	Mikabu			Mikabu		Mikabu		Sanbagawa	
Assemblage	EADC			EGDC		EAGDC		Px+Garnet	
Point. No.	23	26	35	21	25	10	21	110	142
Me/Re	Meta	Meta	Meta	Meta	Meta	Meta	Meta	Meta	Meta
SiO2	52.74	53.75	52.60	54.20	54.11	54.37	53.54	54.70	54.49
TiO2	.19	.00	.00	.00	.00	.00	.00	.00	.00
Al2O3	2.84	4.58	2.05	3.68	2.94	3.84	2.17	5.36	6.09
FeO*	16.15	14.34	18.45	21.42	19.64	14.49	19.47	16.72	18.02
MnO	.24	.25	.32	.02	.11	.11	.50	.64	2.45
MgO	6,86	6.31	5.48	2.83	4.26	6.97	4.77	4.78	2.69
CaO	12.89	12.95	13.04	5.90	8.88	12.29	10.31	6.93	3.75
Na2O	5.91	6.93	6.86	10.89	9.28	7.17	7.98	10.39	11.35
Total	98.43	99.10	98.94	98.94	99.22	99.23	98.74	99.53	99.50
O=6									
Si	2.045	2.044	2.059	2.113	2.098	2.062	2.092	2.077	2.084
Al	.130	.206	.095	.169	.134	.171	.100	.240	.274
Ti	.006	.000	.000	.000	.000	.000	.000	.000	.019
Fe	.543	.456	.604	.698	.637	.459	.636	.531	.576
Mn	.008	.008	.011	.001	.004	.004	.017	.021	.079
Mg	.396	.357	.320	.164	.246	.394	.278	.270	.155
Ca	.535	.578	.547	.246	.369	.499	.432	.282	.154
Na	.444	.511	.521	.823	.697	.527	.605	.765	.842
Total	4.107	4.110	4.157	4.214	4.185	4.116	4.160	4.186	4.183
X(Jd)	.13	.20	.09	.16	.13	.17	.10	.23	.28
X(Ac)	.33	.29	.40	.61	.53	.34	.48	.50	.57
X(Di)	.55	.51	.51	.23	.34	.49	.42	.27	.15

*:Total iron as FeO

VI-2-2 Amphibole

(2-2-1) Introduction

Many kinds of metamorphic amphiboles, such as calcic (actinolite, edenite), sodic (glaucophane, crossite, riebeckite), and sodic-calcic (winchite, barroisite, taramite) are distinguished optically and chemically in the metabasites of the study area, in addition to relict hornblende and kaersutite in gabbroic and doleritic rocks. In this study, the nomenclature of amphiboles defined by Leake (1978) is used, except for "hornblende" defined as solid solution in the "Ha'" (hypothetical Hastingsite $Ca_2Na_2Mg_5Al_2Si_6O_{22}(OH)_2$)- "Ts" (Tschermakite $Ca_2Mg_3Al_4Si_6O_{22}(OH)_2$)- "Tr" (Tremolite $Ca_2Mg_5Si_8O_{22}(OH)_2$) triangle (Hallimond, 1943), and the standard amphibole formula;

$$A_{0-1}B_2C_5^{VI}T_8^{IV}O_{22}(OH,F,Cl)_2$$

is adopted. The following substitutions are important to understand the compositional variation of amphiboles in this area;

$MgSi=Al^{IV}Al^{VI}$ (Tschermakite substitution)

$Si=Na^{A}Al^{IV}$ (Edenite substitution)

$Ca^{B}Mg=Na^{B}Al^{VI}$ (Glaucophane substitution)

$Mg=Fe^{2+}$

$Al^{VI}=Fe^{3+VI}$

The compositional variations of amphiboles under metamorphic condition have been studied by many authors, such as

Miyashiro and Banno (1958), Banno (1964), Leake (1965, 1978), Ernst et al. (1970), Black (1973b), Brown (1974, 1977a), Rasse (1974), Laird (1980), Laird and Albee (1981), and Thompson et al. (1982). From these works, the following general consensus of amphibole stability in metamorphism was established.

(1) Glaucophane substitution in amphiboles increases with metamorphic pressure, and sodic amphibole occurs commonly in high-pressure type metamorphic rocks.

(2) Edenite and Tschermakite substitutions increase with metamorphic temperature.

(3) The Ti content of amphibole in coexistence with Ti-rich phases such as sphene and rutile increases with metamorphic temperature.

(2-2-2) Calcic amphibole ---- $(Ca+Na)^B > 1.34$, $Na^B < 0.67$

i) Actinolite

Most of calcic amphiboles in the Sanbagawa metamorphic rocks in the study area are actinolite, but edenitic amphiboles associated with actinolite and albite do occur in meta-hyaloclastite of the Mikabu Greenrock Complex. The modes of occurrence of actinolites are classified into following groups;

a) Colorless or pale green fibrous crystals in the matrix, and interstices of relic pyroxenes of metabasites, mainly in gabbroic rocks, doleritic rocks, and lavas.

b) Mostly colorless amphiboles growing at rims or cracks of

relict pyroxenes, relict hornblendes, and sodic amphiboles.
c) Isolated prismatic or columnar grains scattering in the matrix of schistose metabasites. They are usually pale blueish green or colorless. When they occur in albite-quartz rich layer of metabasites, they are usually coarser-grained than those in epidote-chlorite rich layer.
d) Fibrous colorless crystals showing radial or interlacing textures. This mode of occurrence is often found in metahyaloclastites of the Mikabu Greenrock Complex.

Actinolites of a) and b) types occur in metabasites of both the Chichibu Group and the Mikabu Greenrock Complex, and c) type in both the Mikabu Greenrock Complex and stratigraphically higher part of the Sanbagawa schists.

ii) Metamorphic hornblende

e) Isolated tabular or columnar amphiboles with dark green or bluish green color in the matrix of metahyaloclastite of the Mikabu Greenrock Complex (Plate IV-6). Under the microscope, they coexist with actinolite, chlorite and albite, but not with quartz. They occasionally contact with chlorite or epidote, or are isolated in the chlorite rich part of the rock. Some of them form composite columnar grains with actinolite which occur penetrating from amygdules of albites to a chlorite rich matrix. Amphibole grains are not rimmed by other minerals.
f) Pale-green amphiboles surrounding a dark brown coarse-grained hornblendes (Plate IV-7). Pale-green ones are also

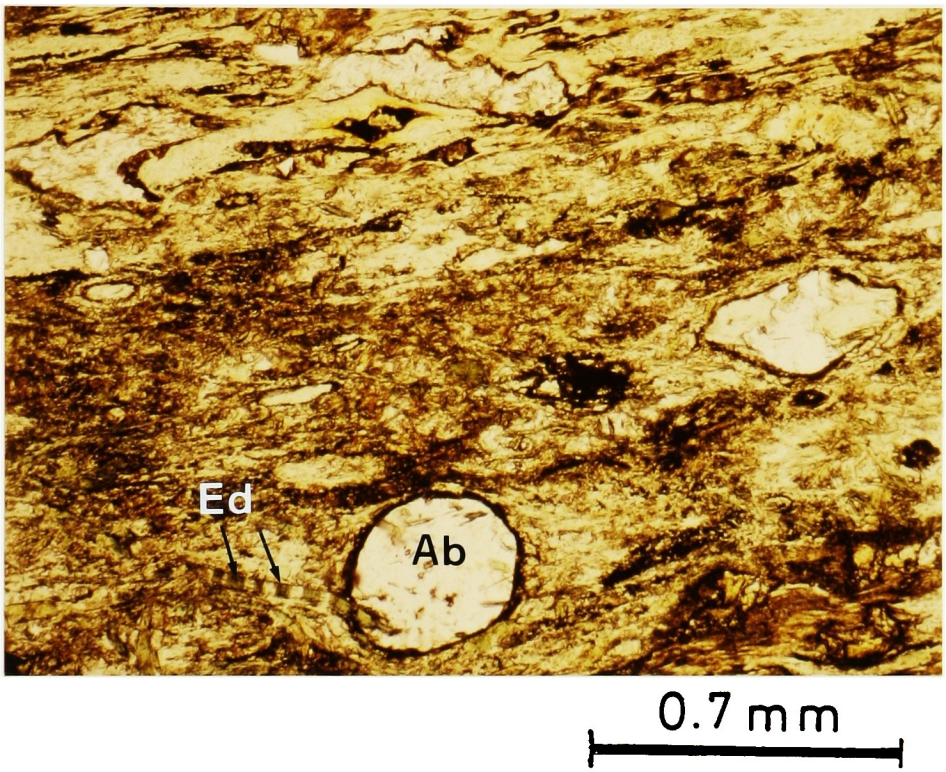

Plate IV-6. Photomicrograph of metamorphic edenite (Ed) in metahyaloclastite of the Mikabu Greenrock Complex. Edenite (pale green)forms a composite grain with actinolite (colorless). Opened nicol. Ab:albite.

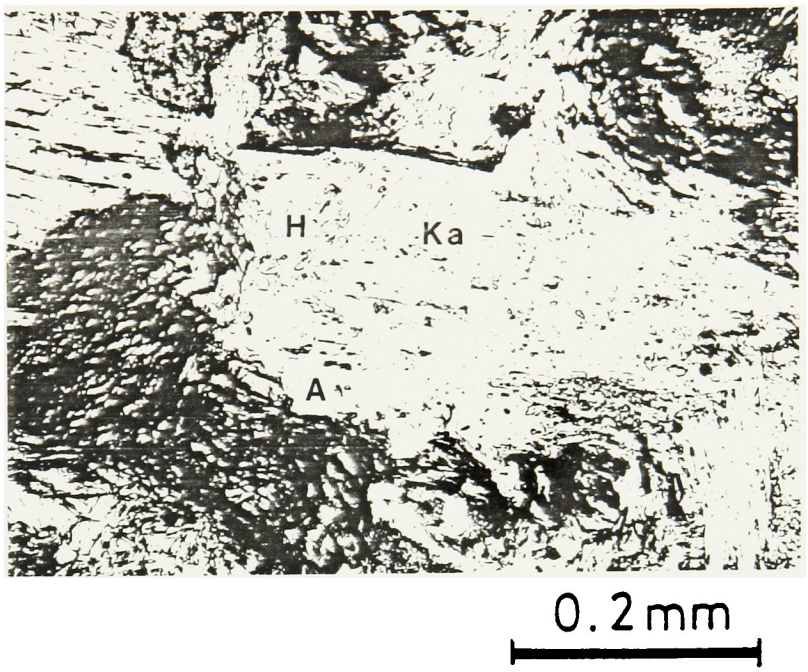

Plate IV-7. Photomicrograph of metamorphic hornblende (H) replacing kaersutite (Ka). Metamorphic hornblende mantled by colorless actinolite (A). The line profile of this grain is shown in Fig. IV-6. Opened nicol.

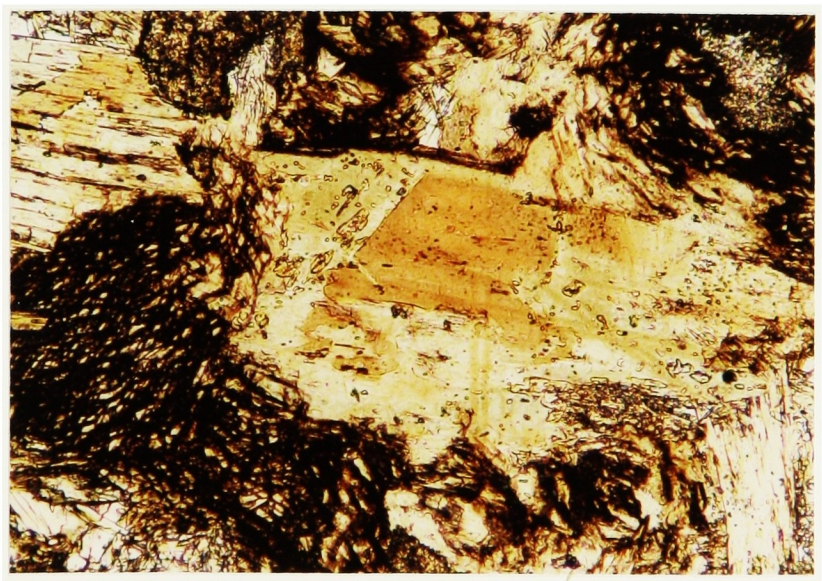

mantled by colorless actinolite. This type amphibole commonly occurs in metagabbros of the Mikabu Greenrock Complex.

iii) Igneous amphiboles

The last types of calcic amphibole is relict igneous amphiboles. Prismatic coarse amphibole grains, from 0.1 cm to 2.0 cm in diameter, are often preserved in gabbros, doleritic rocks, and tuffites of the Chichibu Group and the Mikabu Greenrock Complex, and rarely in the metabasite of the Sanbagawa schists. They are dark green, bluish green or dark brown, and are usually mantled by colorless metamorphic actinolites as mentioned above. The small crystals of clinopyroxene are sometimes preserved in the center of large crystals of relict amphiboles.

iv) Chemical compositions of calcic amphiboles

Microprobe analyses of calcic amphiboles are shown in Table IV-2. Pale-green to colorless actinolites are relatively homogeneous in each thin section. Hence, averaged compositions of actinolite in representative specimens are plotted in Actinolite (Ca)-Glaucophane (Al^{VI})-Riebeckite (Fe^{3+}=Na-Al^{VI}) diagram (Fig. IV-5). This figure indicates that the Ribeckite substitution (CaMg=$NaFe^{3+}$) increases with descending stratigraphic order.

The analyses of metamorphic hornblendes are listed in Table IV-2. The average of five analyses of the e) type

Table IV-2. Chemical composition of calcic amphiboles.
Actinolite --average in each thin section-----

Sample No.	116	K1431	K127	K387	K1404	US2764	444	443	5071
Zone	Chichi	----------		Mikabu	----------		-----	Sanbagawa	---
Assemblage	EAC	EADC	EADC	EAGDC	EAGDC	EAGDC	EAC	EAC	EAC
No.	9	5	5	10	9	6	11	15	8**
SiO2	53.47	54.76	55.27	53.65	55.14	54.91	53.46	53.64	54.00
TiO2	.01	.00	.00	.00	.00	.00	.00	.00	.00
Al2O3	.77	.57	1.11	1.78	1.45	1.14	1.77	2.55	1.82
FeO*	15.12	16.42	13.10	15.55	14.06	11.82	14.31	12.63	16.78
MnO	.28	.26	.23	.23	.26	.33	.22	.25	2.16
MgO	14.21	13.19	15.89	14.04	14.89	16.82	14.86	15.66	12.73
CaO	11.94	10.80	11.05	10.10	10.55	10.55	10.49	10.91	6.59
Na2O	.83	.92	1.22	1.95	1.66	1.77	1.51	1.39	4.11
K2O	.21	.00	11	.00	.00	.10	.00	.00	.14
Total	96.84	96.92	97.98	97.30	98.01	97.44	96.61	97.03	98.33
O=23									
Si	7.859	7.994	7.860	7.760	7.875	7.802	7.734	7.683	7.715
Al	.133	.098	186	.303	.244	191	.302	.430	.306
Ti	.001	.000	.000	.000	.000	.000	.000	.000	.000
Fe3	.111	.275	.372	.500	.318	.488	.554	.470	1.081
Fe	1.747	1.730	1.186	1.381	1.361	.917	1.178	1.043	.924
Mn	.035	.032	.028	.028	.031	.040	.027	.030	.261
Mg	3.114	2.871	3.369	3.028	3.170	3.563	3.205	3.344	2.712
Ca	1.880	1.689	1.684	1.565	1.614	1.606	1.626	1.674	1.009
Na	.237	.260	.336	.547	.460	.488	.424	.386	1.139
K	.039	.000	.020	.000	.000	.018	.000	.000	.026
Total	15.156	14.950	15.040	15.112	15.074	15.112	15.050	15.060	15.173
X(Gl)	.00	.24	.02	.03	.06	.00	.02	.05	.01
X(Ri)	.06	14	18	.23	.15	.23	.25	.21	.51
X(Ac)	.94	.82	.80	74	.79	.77	.73	.74	.48

*:Total iron as FeO
**:Winchite
Fe3/Fe ratio was estimated as assumption of Total cations in T- and M- sites are 13.00

Table IV-2. (Continue)

Chemical composition of calcic amphiboles.
Metamorphic and relic hornblende
-average in each thin section -

Sample No.	828		42	Tanabe(1982)
Zone	Chichibu		Mikabu	Tectonic block
Lithofacies	Gabbro		Hyalo.	
Me/Re	Meta	Relic	Meta	Meta
No.	4(a)	2(b)	5(c)	1(d)
SiO2	38.44	39.02	45.94	37.76
TiO2	.03	6.40	.12	.51
Al2O3	10.69	12.83	8.29	12.89
FeO*	29.04	14.41	12.48	24.29
MnO	.70	.00	.16	.40
MgO	3.32	10.72	14.73	5.33
CaO	6.72	11.72	12.01	7 66
Na2O	3.63	3.17	2.23	4.72
K2O	3.65	.85	.28	1.96
Total	96.12	99.12	96.24	95.59
O=23				
Si	6.169	5.808	6.761	6.124
Al	2.027	2.250	1.438	2.474
Ti	.004	.715	.013	.062
Fe3	1.428	.000	.537	
Fe	2.480	1.797	.999	3.295
Mn	.095	.000	.020	.056
Mg	.796	2.375	3.232	1.288
Ca	1.159	1.869	1.894	1.331
Na	1.132	.915	.636	1.486
K	.749	.162	.053	.407
Total	16.040	15.891	15.583	16.523

*:Total iron as FeO

(a):Ferri-Taramite
(b):Kaersutite
(c):Edenite
(d):Taramite

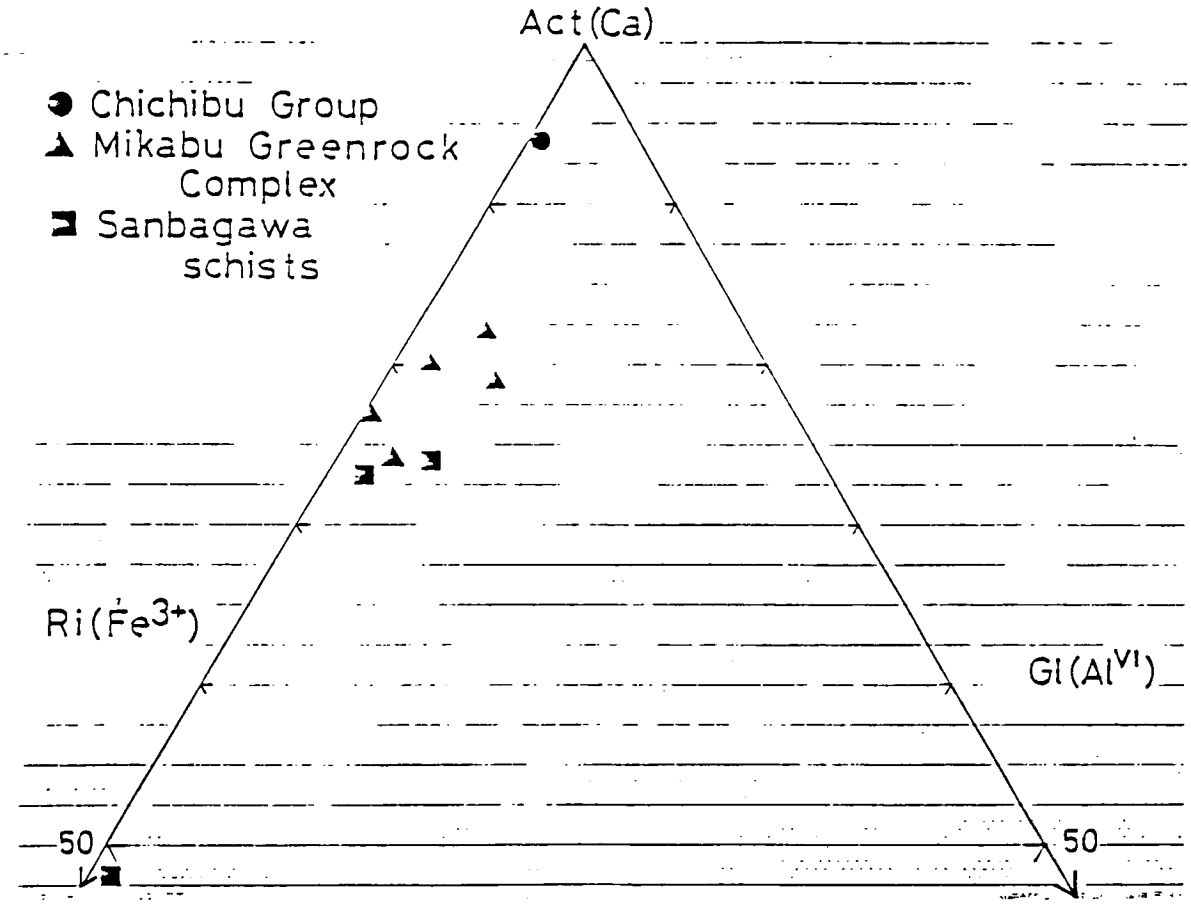

Fig. IV-5. Averaged compositions of actinolite in each thin section. Fe3+/Fe2+ ration of amphiboles are recalculated on the basis of total cations = 13.0 in B, C, and T sites of amphibole formula (Leake, 1978).

hornblende in metahyaloclastite, specimen No.42, gives the following formula;

$$Na_{0.65}K_{0.05}Ca_{1.9}(Fe^{2+}_{1.5}Mn_{0.02}Mg_{3.2}Ti_{0.01}Al^{VI}_{0.30})$$
$$Si_{6.8}Al^{IV}_{1.2}O_{22.0}(OH)_2$$

Although they contain a small amount of tschermakite component, these calciferous amphiboles are named edenite following Leake (1968, 1978).

The metagabbro, specimen No.427-9, contains pale green hornblende <f) type> and brown hornblende, besides chlorite, epidote, albite and actinolite. Under the microscope, pale green hornblende is observed as a platy mantle surrounding a dark brown and coarse-grained hornblende core. A platy mantle is composed of colored-part (green hornblende) and colorless one (actinolite). Colorless actinolite usually mantles pale green hornblende and the chemical composition changes gradually at the boundary between them as shown in Fig. IV-6. However, actinolite rarely occurs between pale green hornblende and dark brown one. Based on the average of three analyses of brown hornblende, eight of green hornblende and three of actinolite in specimen No.427-9, averaged structural formula of each amphibole for O=23.0 are also shown as follows;

Brown hornblende

$$Na_{0.85}K_{0.04}Ca_{1.72}(Fe_{1.84}Mn_{0.03}Mg_{2.83}Ti_{0.34}Al^{VI}_{0.16})$$
$$Si_{6.53}Al^{IV}_{1.53}O_{22}(OH)_2$$

Green hornblende

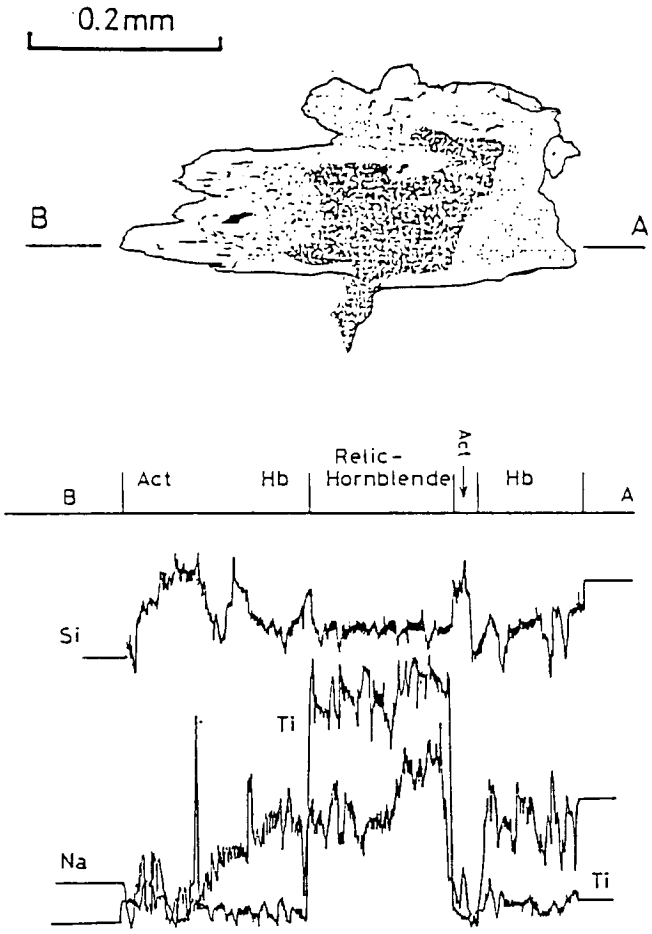

Fig. IV-6. Line profile of amphibole composite grain. Darker part is Ti-rich relict hornblende, and dotted and clear parts are metamorphic hornblende and actinolite, respectively

$Na_{0.77}K_{0.3}Ca_{1.85}(Fe_{1.85}Mn_{0.03}Mg_{2.59}Ti_{0.02}Al^{VI}_{0.44})Si_{7.08}Al^{IV}_{0.92}O_{22}(OH)_2$

Actinolite

$Na_{0.28}K_{0.03}Ca_{1.88}(Fe_{1.89}Mn_{0.04}Mg_{2.93}Ti_{0.03}Al^{VI}_{0.13})Si_{7.75}Al^{IV}_{0.25}O_{22}(OH)_2$

v) Discussion on metamorphic hornblende

Miyashiro (1973) stated that the mineral assemblage intermediate or calcic plagioclase + hornblende was diagnostic of the amphibolite facies and the mineral assemblage albite + epidote + hornblende was of the epidote-amphibolite facies.

Edenite has been found mainly from such metamorphic rocks as amphibolites coexisting with plagioclase (anorthite contents 20-55%) in intermediate- or low-pressure type metamorphic belt (Leake, 1968), but it was not yet reported from the glaucophane schists and the greenschist facies. In the greenschist and low-pressure glaucophane schist facies, albite + actinolite, which is the chemical equivalent of edenite + quartz as shown in the following equation, is stable;

actinolite + albite = edenite + quartz

$$Ca_2Mg_5Si_8O_{22}(OH)_2 + NaAlSi3_3O_8 = NaCa_2Mg_5Si_7AlO_{22}(OH)_2 + 4SiO_2 \quad \text{---------(5)}$$

However, there is no reason to deny that edenite not associated with quartz is stable in such low-temperature facies. Sodic pyroxene (diopside) + chlorite assemblage,

which is common in the lower-grade metabasites of the study area, is equivalent to the edenite + epidote assemblage;

diopside + chlorite = edenite + epidote

$$50\ CaMgSi_2O_6 + 9\ Mg_5Al_2Si_3O_{10}(OH)_8 + 19\ NaAlSi3_3O_8 = 19\ NaCa_2Mg_5Si_7AlO_{22}(OH)_2 + 6\ Ca_2Al_3Si_3O_{12}(OH) + 33\ SiO_2 + 14\ H_2O \quad -----(6)$$

Therefore, only if silica is highly deficient, edenite can be a stable amphibole in the Sanbagawa metamorphic rock.

Further discussion supports the metamorphic origin of the edenite described in this paper;

First, specimen No.42 is mainly composed of chlorite with minor amount of epidote, actinolite, albite, and green hornblende, without quartz. The bulk composition of this rock is high in MgO and low in SiO_2 judging from the modal composition. Green hornblendes occur as a tabular and columnar grain in the chlorite-rich matrix and albite amygdules. Some of them occur crossing over from albite amygdules to the chlorite matrix (Plate IV-6). Moreover, it is not rimmed by other minerals. This texture indicates that green hornblende is not detrital grains but was formed during the Sanbagawa metamorphism.

Second, the texture and scanning profile of zoning around relict brown hornblende suggest that the edenite in metagabbro, specimen No.427-9 was formed simultaneously with actinolite, because relict of igneous brown hornblende is rarely rimmed by actinolite, which is again armoured by edenite. As actinolite is a common mineral in the matrix of

metagabbros, most plausible interpretation is that actinolite and edenite was formed by one and the same metamorphism, the Sanbagawa metamorphism. The compositional gap between actinolite and edenite may represent the solvus between them.

Third, the TiO_2 content of the edenite is extremely low, indicating low temperature origin. The relict brown hornblende in specimen No.427-9 contains about 3.0 wt% of TiO_2 as expected for igneous origin, but the associated edenite contains only less than 0.3 wt% of TiO_2. This value is much lower than those in the amphibolites of the amphibolite facies and the epidote-amphibolite facies. That TiO_2 content is too low for medium- and high-grade hornblende is also reflected by the fact that sphene is common in these rocks, and the edenite never grew in TiO_2-depleted chemical environments. Therefore, it can be concluded that edenite is easily recrystallized in the SiO_2-poor and Na_2O-rich bulk compositions under lower temperature of the pumpellyite-actinolite facies than those of the amphibolite facies or the epidote-amphibolite facies.

When green hornblendes were formed as a platy mantle around brown hornblende core in metagabbro, specimen No.427-9, the selective transfer of elements was recognized. As shown in Table IV-2, FeO, MgO and CaO scarcely moved from relict hornblende core to metamorphic amphibole mantle. However, TiO_2 abruptly decreases at the boundary from relict

core to metamorphic mantle, and is scarcely contained in the mantle. This feature is well represented in the scanning profile of one composite amphibole grain (Fig. IV-6). TiO_2-rich plateau corresponds to the dark brown hornblende core, and TiO_2 poor lowlands do to the amphibole mantle. The brown color of amphiboles has been ascribed to higher contents of TiO_2, as suggested by Binns (1965).

In basaltic rocks, TiO_2 has been known to be the most immobile element during alterlation or metamorphism (Cann, 1970). However, TiO_2 was most rapidly removed from the relict hornblende core to the matrix of rocks among major elements. TiO_2 emitted from relict hornblende may be fixed in sphene which commonly occurs near the composite amphibole grain. Therefore, TiO_2 content of the rock may remain unchanged throughout processes of weathering and metamorphism.

(2-2-3) Sodic amphibole $Na^B \geq 1.34$

Sodic amphibole occurs commonly in metabasites of the Chichibu Group and the Mikabu Greenrock Complex, and rarely in those of the Sanbagawa schists. The mode of occurrence of sodic amphibole is different in each geologic units.

Sodic amphibole in metabasites of the Chichibu Group occurs as fibrous fine grains or as aggregates of fine needles associated with actinolite, epidote, chlorite, albite, quartz, stilpnomelane and opaque minerals (probably hematite), but not with pumpellyite and sodic pyroxene. In metabasites of the Mikabu Greenrock Complex, sodic amphiboles are larger (0.1 to 0.5 mm in long diameter), and common. The representative modes of occurrence of them are as follows;

a) Idiomorphic tabular or columnar crystal in albite-quartz rich matrix of schistose metabasites derived from tuff or hyaloclastite. They are usually surrounded by colorless actinolite (Plate IV-8).

b) Blueish amphiboles growing at rims and cracks of relic augites and hornblendes, or in the interstices of them. This type amphiboles are often observed at the boundary between albite and relic mafic minerals in gabbroic and doleritic rocks (Plate IV-9).

c) Parallel growth with sodic pyroxene in metabasites of EAGDC (epidote - actinolite - sodic amphibole - sodic pyroxene - chlorite) assemblage, although actinolite, not

sodic amphibole, occurs in the albite-quartz rich matrix of same rocks (Plate IV-10).

d) Unhedral rounded-shaped crystal surrounded by dusty aggregates of sphene and rutile in epidote + chlorite rich matrix of metabasites of EAGC assemblages (Plate IV-11).

e) Deep blueish-green riebeckites surrounded by blueish amphiboles in lawsonite-bearing metabasites. The contact between riebeckite core and blue mantle is rather sharp, and the exsolution sequence is not found (Plate IV-12).

Sodic amphibole occurs in distinctly schistose metabasites in the Chichibu Group and the upper stratigraphic part of the Mikabu Greenrock Complex, i.e. in the EPDC and EADC zones (Fig. III- 5-2), but it occurs in all kind of metabasites in the lower stratigraphic part of the Mikabu Greenrock Complex, i.e. the EAGC zone (Fig. III-5-2).

In the Sanbagawa schists, sodic amphibole scarcely occurs in the matrix, but does so as inclusion minerals in epidote or albite grains <f)>. Exceptionally, it occurs as tabular large grains associated with sodic pyroxene, Mn-rich garnet, stilpnomelane, albite, quartz, magnetite, and hematite in Mn-rich nodules which was found from the garnet zone of the Sanbagawa schists in the central part of the Kanto Mountains <g)>.

Chemical compositions of sodic amphiboles from the Mikabu Greenrock Complex and the Sanbagawa schist are listed in Table IV-3. Averaged compositions of sodic amphiboles

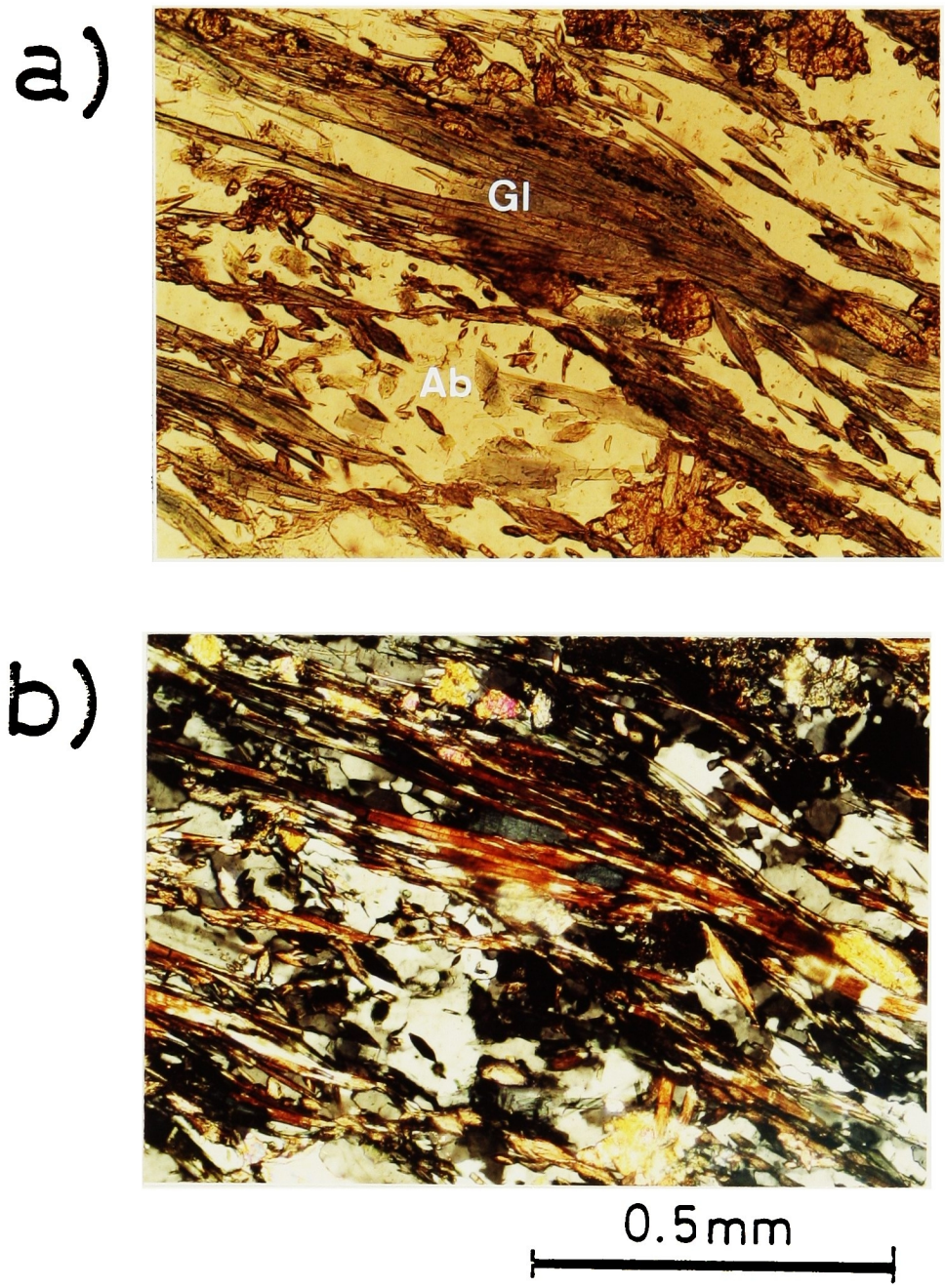

Plate IV-8. Photomicrographs of type a) sodic amphibole (Gl) in albite (Ab)-rich matrix of metabasites. a)opened nicol. b)crossed nicols.

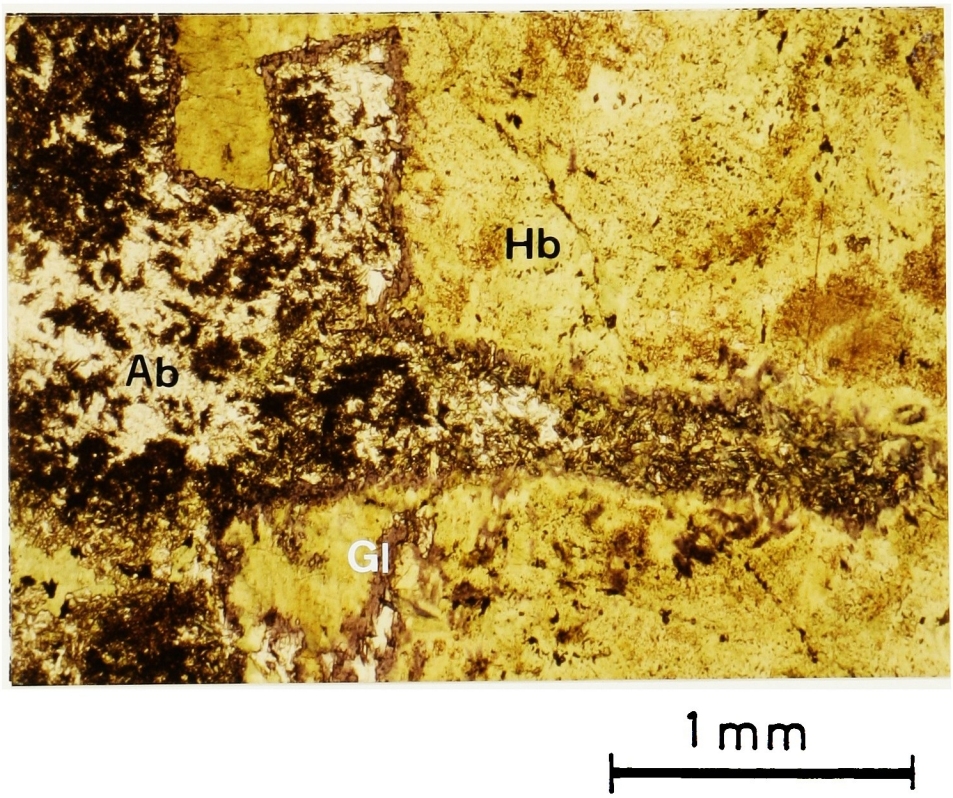

Plate IV-9. Photomicrograph of type b) glaucophane (Gl) growing at the boundary between albite (Ab) and relict hornblende (Hb) in gabbro. Opened nicol.

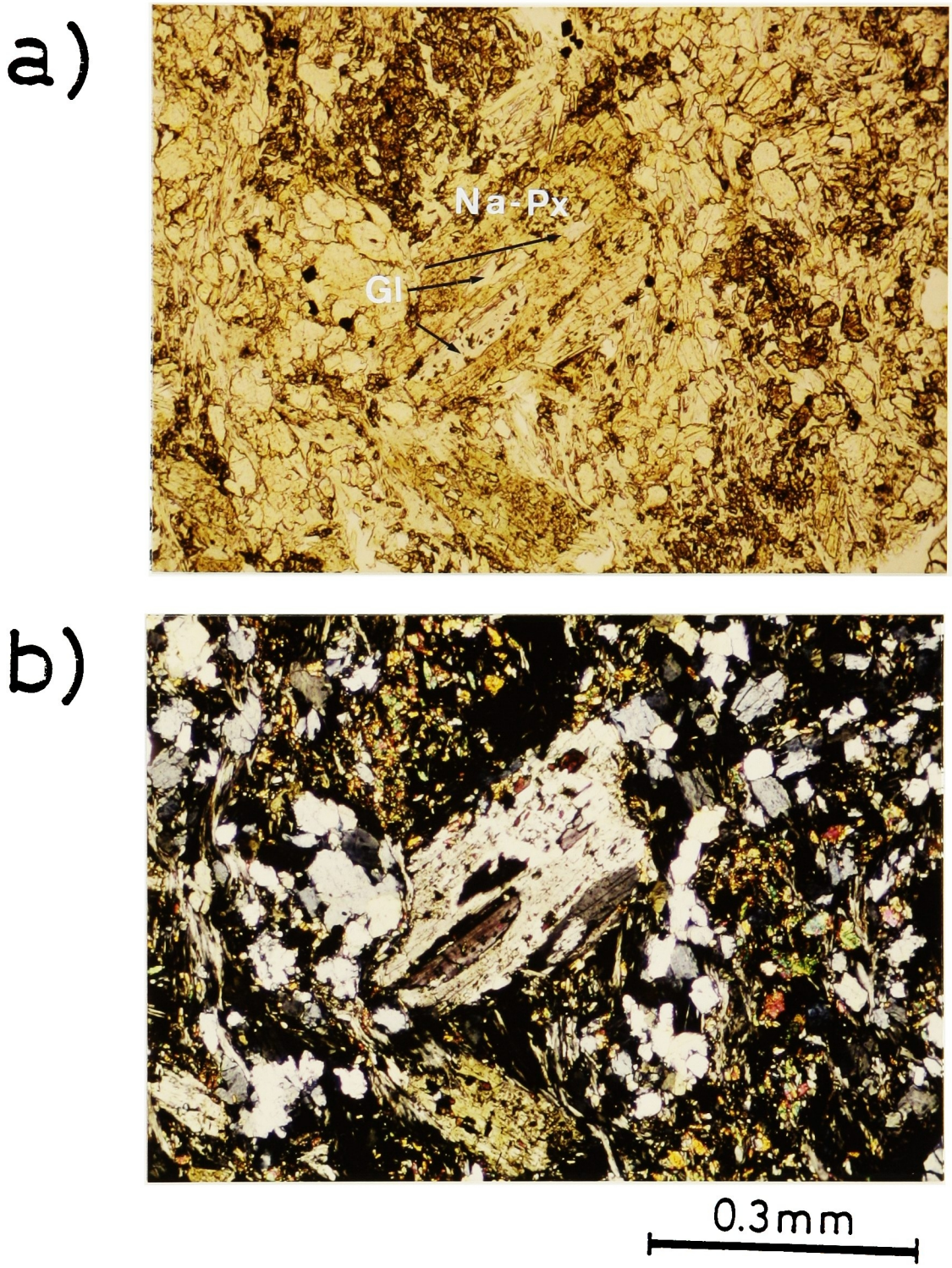

Plate IV-10. Photomicrographs of sodic amphibole (Gl) in parallel growth with sodic pyroxene (Na-Px) in metabasite containing epidote, actinolite and chlorite. a)opened nicol. b)crossed nicols.

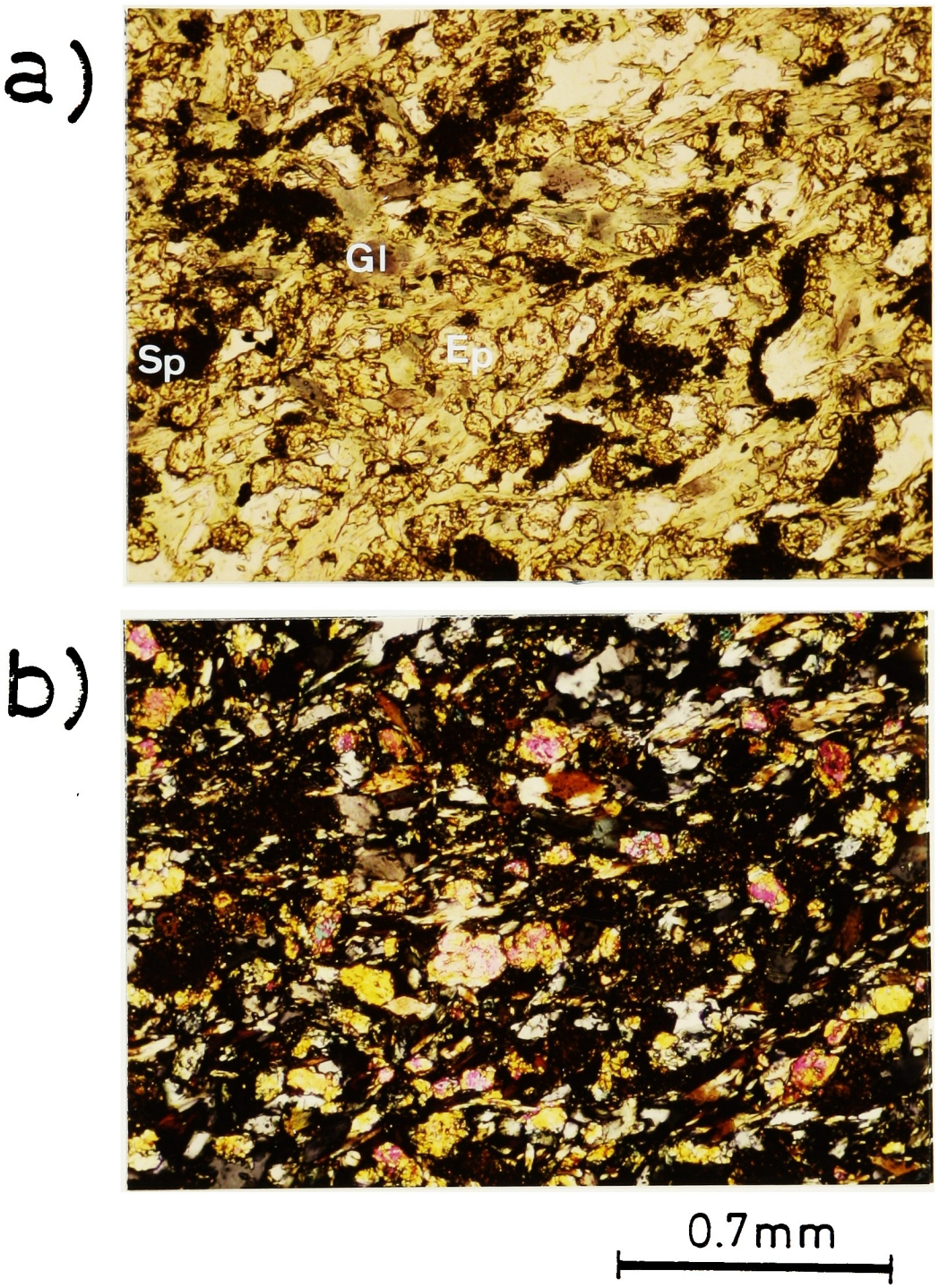

Plate IV-11. Photomicrographs of a metabasite of epidote(Ep) -actinolite-sodic amphibole (Gl)-chlorite assemblage. Sodic amphibole is usually surrounded by dusty aggregate of sphene (Sp) and rutile in this type rock. a)opened nicol. b)crossed nicols.

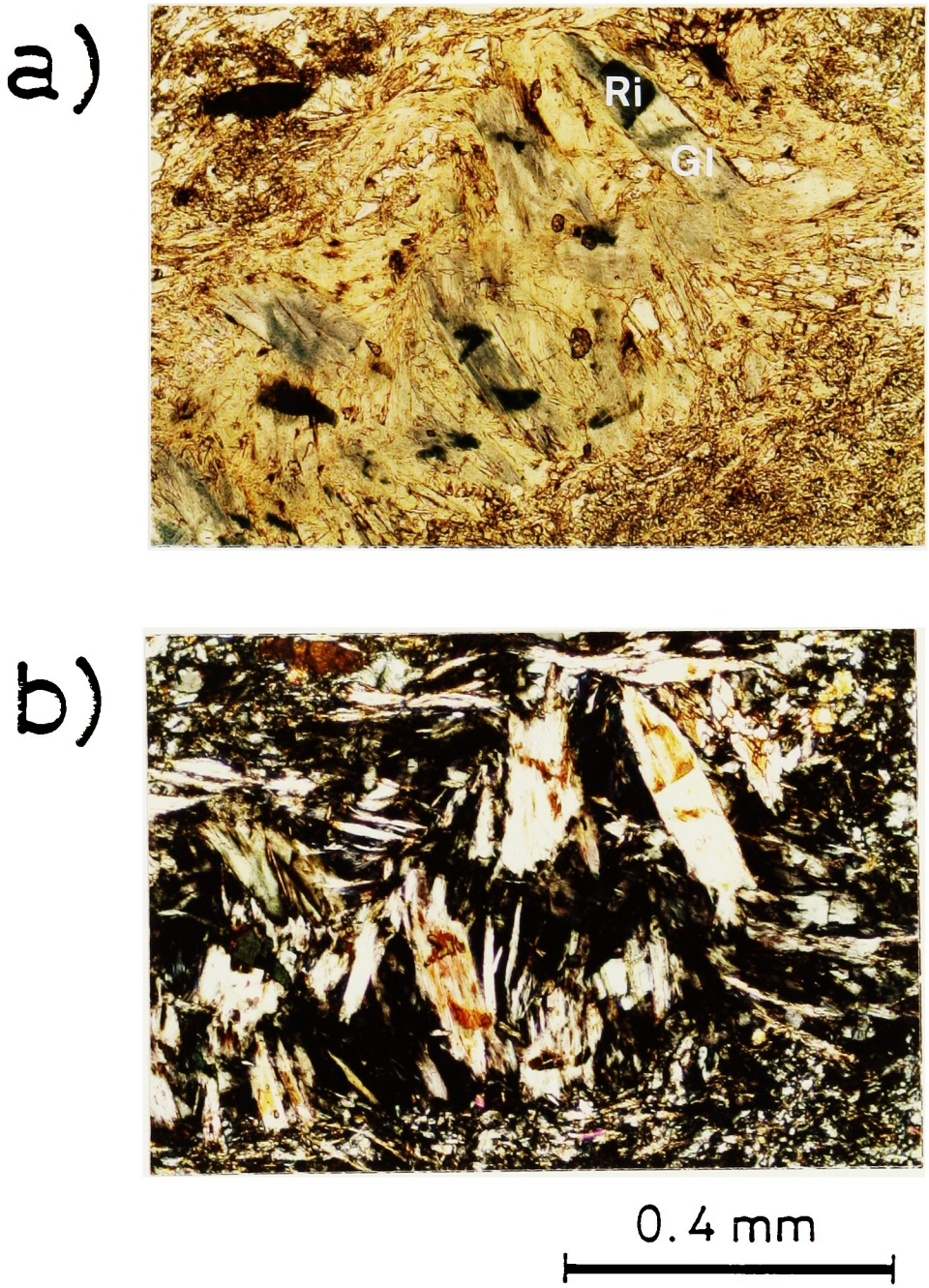

Plate IV-12. Photomicrographs of dark blueish-green riebeckites (Ri) surrounded by crossite or glaucophane (Gl). a)opened nicol. b)crossed nicols.

in each section are plotted in Miyashiro diagram (Fig. IV-7). They are mostly glaucophane, ferro-glaucophane, crossite and magnesioriebeckite, and partly riebeckite. Fe^{3+}/Fe^{2+} ratio of amphiboles is recalculated on the basis of total cations = 13.0 in B, C, and T sites of amphibole formula. Hosotani & Banno (in prep.) showed that the chemical compositions of sodic amphibole were controlled by the univariant mineral assemblages in the epidote-glaucophane schists of the Sanbagawa belt in Shikoku. However, in the study area, the mineral assemblages, either univariant or not, do not affect the chemical compositions of sodic amphiboles, but the local chemical equilibrium and the mode of occurrence of sodic amphibole are more effective. First of all, two types of sodic amphiboles ‹a) and d) types› are observed in the same thin sections associated with sodic pyroxene, actinolite, epidote, chlorite, albite, magnetite, and hematite in a doleritic rock; d) type is riebeckite and a) type is glaucophane as asterisked in Fig. IV-7. d) type riebeckite occurs in epidote and sphene rich layer, and it is not mantled by any other amphiboles as e) type riebeckite described in a later section. Therefore, there is no reason to consider that these sodic amphiboles were formed in different metamorphic events. The formation of these amphiboles owes to the different local chemical compositions of host rock.

Secondary, compositions of sodic amphiboles tend to be as followings; b) and c) types are usually crossite to glaucophane, d) type is crossite to glaucophane, and a) type has a wide chemical variation (Fig. IV-7). The modes of occurrence of sodic amphiboles indicate that following two reactions form sodic amphiboles in the study area;

$310\ CaNaFAl_{0.2}Fe^{3+}_{0.8}Si_4O_{12} + 117\ F_5Al_2Si_3O_{10}(OH)_8 + 30\ NaAlSi_3O_8 + 529\ SiO_2 =$

$77\ Ca_2F_5Si_8O_{22}(OH)_2 + 78\ Ca_2Al_2Fe^{3+}Si_3O_{12}(OH) + 170\ Na_2F_3AlFe^{3+}Si_8O_{22}(OH)_2 + 182\ H_2O$

sodic pyroxene + chlorite + albite + silica =

actinolite + epidote + sodic amphibole + water ------- (2)

$0.5\ Ca_2F_5Si_8O_{22}(OH)_2 + 0.1\ F_{4.5}Al_{2.46}Si_{2.9}O_{10}(OH)_8 + 0.6\ Fe_2O_3 + 2NaAlSi_3O_8 + 0.3\ H_2O =$

$1.0\ Na_2F_3Al_{1.3}Fe^{3+}_{0.7}Si_8O_{22}(OH)_2 + 0.5Ca_2Al_2Fe^{3+}Si_3O_{12}(OH) + 0.8\ SiO_2$

actinolite + chlorite + Fe-oxides + albite + water =

epidote + sodic amphibole + silica ----------(7)

Sodic amphiboles of b) and c) types usually contact with sodic pyroxene or relict augite, suggesting that they were formed by reaction (2). On the other hand, a) type sodic amphiboles usually nucleated in the albite-quartz rich matrix, and they may be formed by reaction (7) as proposed by Brown (1977).

E) type riebeckites were found in lawsonite-bearing metabasites associated with lawsonite, pumpellyite, epidote, sodic pyroxene, actinolite, glaucophane, albite and relict

augite. This mineral shows characteristic pleochroism; X=deep blueish-green, Y=dark green, Z=pale-yellow, and contains significant amounts of K_2O, about 1.1 wt%, although blue amphiboles surrounding riebeckite contains less than 0.05 wt% of K_2O. K_2O-bearing riebeckites were described in lawsonite-bearing metabasalt of New Caledonia (Black, 1970), in alkali granites (Lyons, 1976), in basaltic dikes (Henly, 1978), and in metadolerite of the Iberian pyrite belt (Munhá, 1979). These chemical compositions are shown in Table IV-4.

The glaucophane-riebeckite solid solution has been investigated by many authors (Miyashiro, 1957; Coleman and Papike, 1968). Ernst (1962) determined the continuity of riebeckite-arfvedsonite solid solution by synthetic experiments. He showed that riebeckite is stable to a maximum temperature of 515°C under hematite-magnetite buffer, and under more reducting conditions (wustite-iron buffer) riebeckite-arfvedsonite solid solution is stable to a maximum temperature of about 710°C. Lyons (1976) analysed riebeckites which contained some amount of arfvedsonite component in alkali granites, and concluded that these amphiboles were crystallized under high-temperature condition. Munhá (1979) and Henly (1978) showed that riebeckite-arfvedsonite grew during subsolidus cooling of basalt within the submarine geothermal system which persisted during contemporaneous massive sulfides ore

formation. These reports are not disconcordant with Ernst's phase diagram.

Black (1970) described the K_2O-bearing riebeckite-arfvedsonite in lawsonite-bearing metabasalt from New Caledonia. Chemical composition and mode of occurrence of riebeckite-arfvedsonite and associated minerals are very similar to those of riebeckite in this study. As will be mentioned in a later section, lawsonites commonly occur in the Al_2O_3-rich and Fe_2O_3-poor basic rocks in the study area. Therefore, the amphiboles which coexist with lawsonite should be glaucophane or Al-rich crossite. Hence, it is unlikely that Al-rich glaucophane and Al-poor riebeckite coexist stably in the Al_2O_3-rich basic rocks. The author considers that riebeckite had crystallized before the Sanbagawa metamorphism which formed glaucophane and lawsonite.

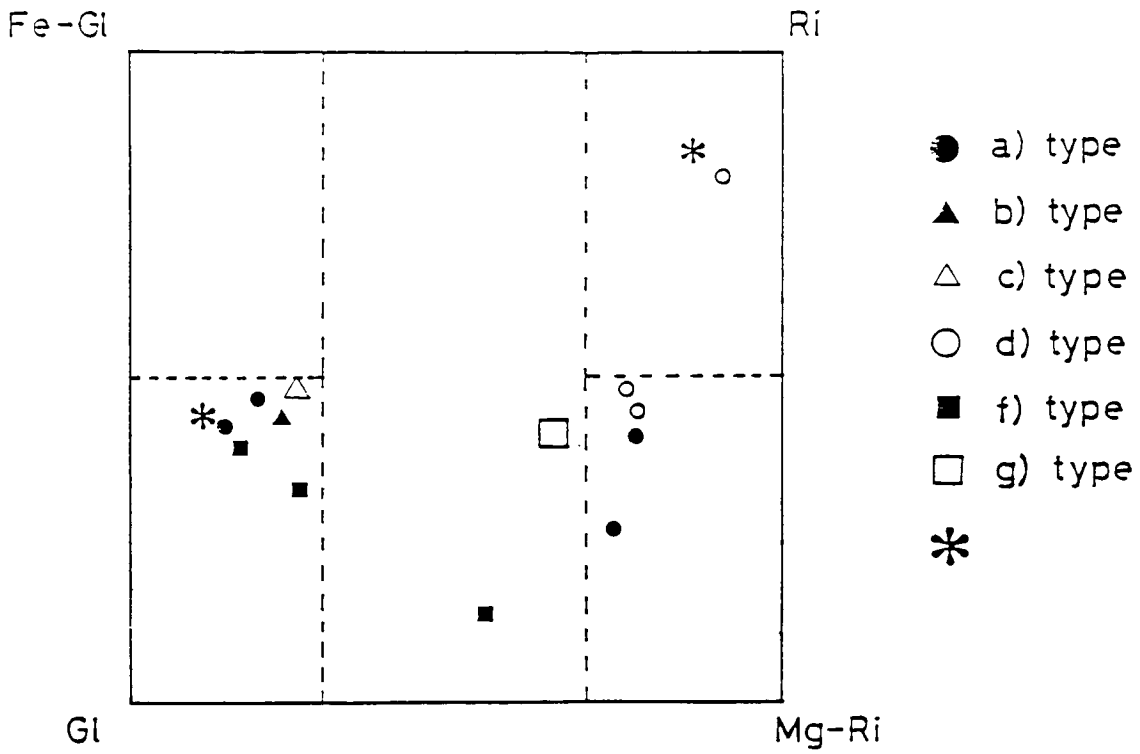

Fig. IV-7. Sodic amphiboles in Miyashiro's diagram. a) to g) correspond to the modes of occurrence of sodic amphibole described in text.

Table IV-3. Chemical composition of sodic amphiboles.
-----average in each thin section------

Sample No.	K387	K1404	US2764	444	443	5071	US3705
Zone	-----	Mikabu	----	----------	Sanbagawa	----------	
Assemblage	EAGDC	EAGDC	EAGDC	EAC	EAC	Bar+EC	Px+Gar
No.	10	4	7	7	10	1	15
SiO2	55.25	56.62	54.59	56.56	56.00	56.89	54.44
TiO2	.00	.12	.00	.00	.00	.00	.00
Al2O3	8.29	8.11	3.52	10.19	10.96	7.54	5.05
FeO*	16.81	16.03	17.34	13.15	12.74	13.49	20.78
MnO	.10	.06	.22	.10	.08	.34	.61
MgO	7.85	8.04	11.61	9.71	9.15	12.08	8.28
CaO	1.22	.90	2.82	1.17	1.16	.90	1.03
Na2O	7.09	7.08	6.21	6.96	7.09	7.07	7 18
K2O	.00	.00	.05	.00	.00	.00	.01
Total	96.61	96.96	96.36	97.84	97.18	98.30	97.38
O=23							
Si	7.904	8.026	7.821	7.811	7.804	7.756	7.809
Al	1.398	1.355	.594	1.659	1.800	1.211	.854
Ti	.000	.013	.000	.000	.000	.000	.000
Fe3	.453	.349	1.163	.509	.329	1.145	1.214
Fe	1.559	1.551	.951	1.010	1.156	.393	1.279
Mn	.012	.007	.027	.012	.009	.039	.074
Mg	1.674	1.699	2.480	1.999	1.901	2.455	1 771
Ca	.187	.137	.433	.173	.173	13	.158
Na	1.967	1.946	1.725	1.864	1.916	1.869	1.997
K	.000	.000	.000	.000	.000	.000	.000
Total	15.154	15.082	15.167	15.037	15.089	15.000	15.157
X(Gl)	.67	.74	.21	.68	76	.43	.40
X(Ri)	.23	.19	.57	.24	.16	.51	.53
X(Ac)	.10	.07	.22	.08	.08	.06	.07

*:Total iron as FeO
Fe3/Fe ratio was estimated as assumption of Total cations in
T- and M- sites are 13.00

Table IV-4. Chemical composition of riebeckite.

Author	This study			Munha(1979)		Black(1970)	Henly(1978)
Area	Kanto Mountain			Iberian pyrite belt		New Caledonia	basalt dike Newfoundland
Point No.	12	17	50				
SiO2	51.89	52.18	53.11	50.57	50.13	50.2	49.80
TiO2	.07	.07	.49	.56	.71	.5	2.14
Al2O3	.64	.44	.71	1.95	3.11	1.7	.78
Fe2O3	*	*	*	10.19	12.57	*	*
FeO	32.69	34.01	31.11	19.35	19.41	30.4	33.90
MnO	.55	.68	.39			.5	.70
MgO	1.86	.95	3.30	4.43	3.15	3.2	1.65
CaO	1.10	.58	3.24	1.23	1.28	2.4	2.09
Na2O	5.57	5.96	5.96	6.65	6.16	5.4	6.86
K2O	1.12	1.15	1.14	1.75	1.59	2.0	.90
Total	95.49	96.02	99.45	96.68	98.11	96.3	98.82
O=23							
Si	8.101	8.154	8.067	7.827	7.671	7.844	7.732
Al	.118	.081	.127	.356	.561	.313	.143
Ti	.008	.008	.056	.065	.082	.059	.250
Fe3	1.387	1.364	.595	1.187	1.447	1.403	.955
Fe	2.880	3.081	3.357	2.505	2.484	2.929	3.446
Mn	.073	.090	.050			.066	.092
Mg	.433	.221	.747	1.022	.719	.745	.382
Ca	.184	.097	.527	.204	.210	.402	.348
Na	1.686	1.806	1.755	1.996	1.828	1.636	2.065
K	.223	.229	.221	.346	.310	.399	.178
Total	15.093	15.132	15.503	15.507	15.312	15.436	15.591

*:Total iron as FeO
Fe3/Fe ratio was estimated as assumption of Total cations in T- and M- sites are 13.00

(2-2-4) Sodic-calcic amphibole. $Ca+Na^B \geq 1.34$,

$0.67 < Na^B < 1.34$

Barroisitic amphiboles instead of calcic and sodic amphiboles become common in metabasites of the garnet zone of the Sanbagawa schists in the Kanto Mountains, as it is in Shikoku (Otsuki, 1980). Barroisitic amphibole forming the schistosity plane is dark green to pale green color and columnar grains, and is associated with epidote, chlorite, muscovite, albite, quartz, and calcite. Some of them are rimmed by colorless actinolite. Chemical compositions of barroisites are shown in Table IV-5.

Other sodic-calcic amphiboles, taramite, are found in gabbroic rocks of the Chichibu Group. Taramite replacing rims and cracks of relict kaersutites and Ti-augites is dark green colored and associated with sodic pyroxene, pumpellyite, chlorite, stilpnomelane, albite, adularia, and sphene, but not with quartz. Although relict mafic minerals contain more than 3.0 wt% of TiO_2, taramite contains only 0.03 wt% of TiO_2 in average of four grains. The texture and chemical composition indicate that taramite was formed in SiO_2 poor and FeO rich system under the lower-temperature of the Sanbagawa metamorphism, same as metamorphic edenites as described in a previous section.

Table IV-5.

Chemical composition of barroisite
-average in each thin section -

Sample No.	5071
Zone	Sanbagawa
Lithofacies	Basic sch.
No.	9
SiO2	49.28
TiO2	.00
Al2O3	5.83
FeO*	18.75
MnO	.37
MgO	11.01
CaO	8.31
Na2O	3.10
K2O	.20
Total	96.86
O=23	
Si	7.234
Al	1.009
Ti	.000
Fe3	.990
Fe	1.312
Mn	.046
Mg	2.410
Ca	1.307
Na	.882
K	037
Total	15.227

*:Total iron as FeO
Fe3/Fe ratio was estimated as
assumption of Total cations in
T- and M- sites are 13.00

(2-2-5) Miscibility gap in amphiboles

The miscibility gap between sodic amphibole and actinolite has been discussed by Klein (1969), Katagas (1974), Brown (1974) and Toriumi (1974, 1975). Toriumi (1974, 1975) described coexisting sodic amphibole and actinolite in an amphibole composite grain in a glaucophane schists of the Kanna-gawa and showed that the miscibility gap existed between these amphiboles.

This problem was examined by the author. The miscibility gap between glaucophane and actinolite is certainly exists in metabasites of the lower stratigraphic part of the Mikabu Greenrock Complex. However, there is no chemical gap between riebeckite and actinolite in metabasites of the same horizon of the Mikabu Greenrock Complex mentioned above and of the Sanbagawa schists (Fig. IV-8). The lack of the gap between actinolite and sodic amphibole was demonstrated by Katagas (1974) and Brown (1974).

Miscibility gap between actinolite and hornblende has been in dispute still now. Miyashiro (1958), Klein (1969), Mish and Rice (1975) and Tagiri (1977) emphasized the presence of the gap in this series. On the other hand, Deer et al. (1963), Ernst (1972), and Grapes and Graham (1978) have denied the presence of such gap. Ernst (1962) suggested that the gap is absent under glaucophanic metamorphism.

In the study area, edenite associated with actinolite

was found from metahyaloclastite of the pumpellyite-actinolite facies zone (see the section 2-2-2). Because edenite forms segmented composite columnar grains with actinolite, the chemical gap observed in this specimen (Fig. IV-9) indicates that the miscibility gap between actinolite and hornblende actually exists in the lower-temperature of the glaucophanitic metamorphism as reported by Miyashiro (1958).

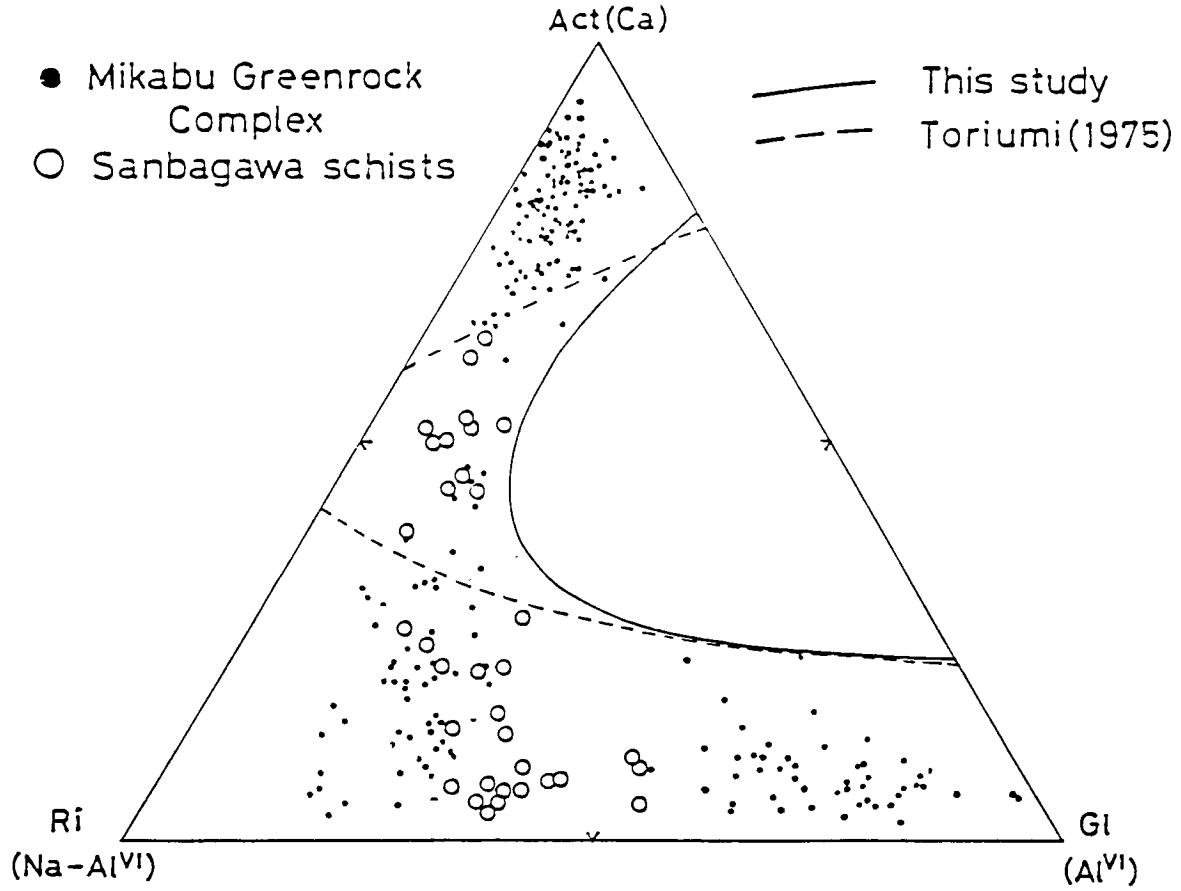

Fig. IV-8. Sodic, calcic and sodic-calcic amphiboles in Act <Ca>-Gl <Al(VI)>-Ri <Fe3+=Na-Al(VI)> diagram.

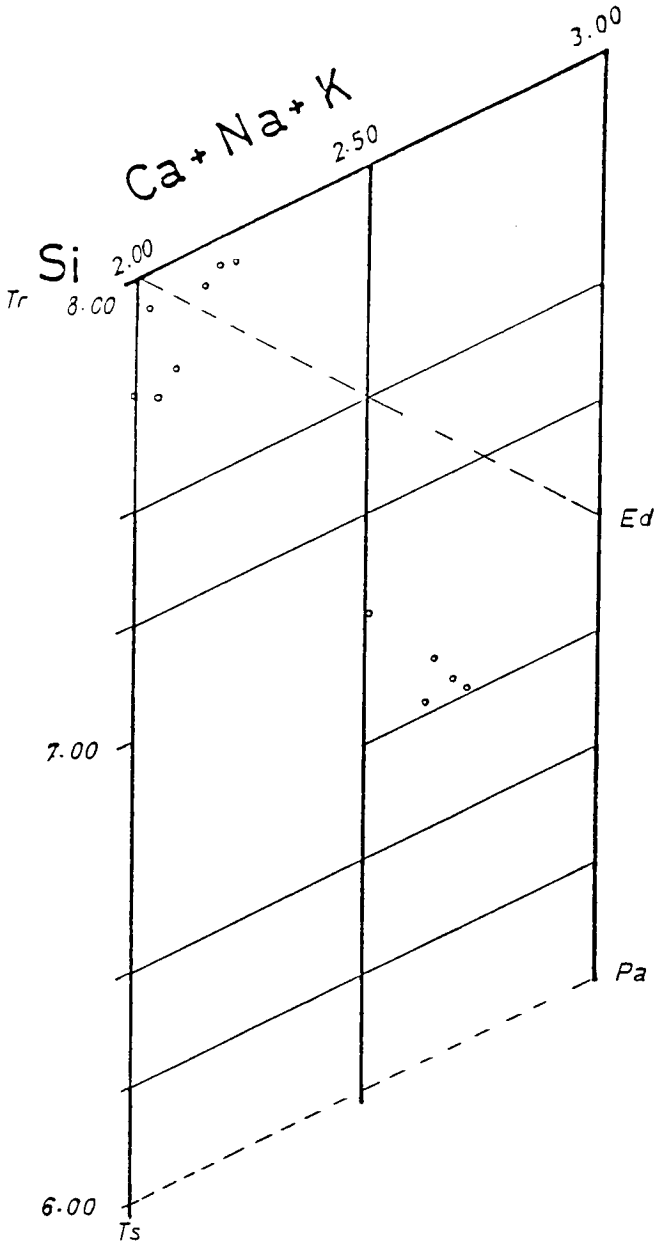

Fig. IV-9. Coexisting actinolite and metamorphic edenite in Si and Ca+Na+K diagram for the half unit cell of the calciferous amphiboles.

IV-2-3. Epidote

Epidote occurs widely and abundantly in all kinds of rocks in the study area as shown in Tables III-1 and III-2b. This mineral is usually irregular and fine-grained, but partly idiomorphic tabular and coarse-grained. Radially twinned and coarse-grained epidotes grew after relict plagioclase in metagabbro of the Mikabu Greenrock Complex. Most grains of epidotes in the Chichibu Group and the Mikabu Greenrock Complex show no noticeable zoning. However, those in the Sanbagawa schists are larger and show a complex zoning. Sector-zoned epidotes, which were found in lower-grade metabasite of the Sanbagawa schists in Shikoku by Yoshizawa (1984), were also found in metabasites of the Mikabu Greenrock Complex of the study area.

Miyashiro and Seki (1958) described that epidote tended to have compositions near $Ca_2Al_2Fe^{3+}Si_3O_{12}(OH)$ at very low temperature, and the compositional range became larger with rising temperature. Recently, Ernst et al.(1970), Toriumi (1975), Kawachi (1975), Nakajima et al.(1977), and Otsuki (1980) also described the enlargement of compositional range of epidote with increasing metamorphic temperature in Sanbagawa belt and in the Wakatipu area of New Zealand. They concluded that Al-enrichment of epidote with increasing metamorphic temperature is due to the decomposition of pumpellyite.

Chemical compositions of epidote are shown in Table IV-6 and Fig. IV-10. Al-enrichment in epidote is also

observed in hematite-bearing metabasites of the study area (Fig. IV-10). Otsuki (1980) described that the oxidation state of rocks influenced the composition of epidote; i.e., epidote coexisting with hematite has high-X_{Fe}^{Ep} $<=Fe^{3+}/(Al+Fe^{3+})>$ on the one hand, and that coexisting with pyrrhotite low-X_{Fe}^{Ep}, on the other. Epidotes of the Mikabu Greenrock Complex in this study coexist mainly with pyrite or chalcopyrite, and partly with hematite. However, epidotes of the Mikabu Greenrock Complex were not so strongly influenced by the oxidation state of host rocks as reported by Otsuki (1980). One of possible explanation for this phenomenon is provided by the schematic phase diagram of hematite, pumpellyite and epidote in a model system by Nakajima et al.(1977). They showed that only epidote with X_{Fe}^{Ep} =0.35 can coexist with hematite, actinolite and chlorite at the lower stability limit of epidote, and that X_{Fe}^{Ep} of epidote not coexisting with hematite decreases more rapid with increasing temperature than that coexisting with hematite. This diagram suggests that epidote formed at relatively low-temperature is not affected by the oxidation state of host rocks.

Fig. IV-10. Frequency distribution of XFe=<Fe/(Fe+Mg)> ratios in epidote of the Sanbagawa metamorphic rocks.

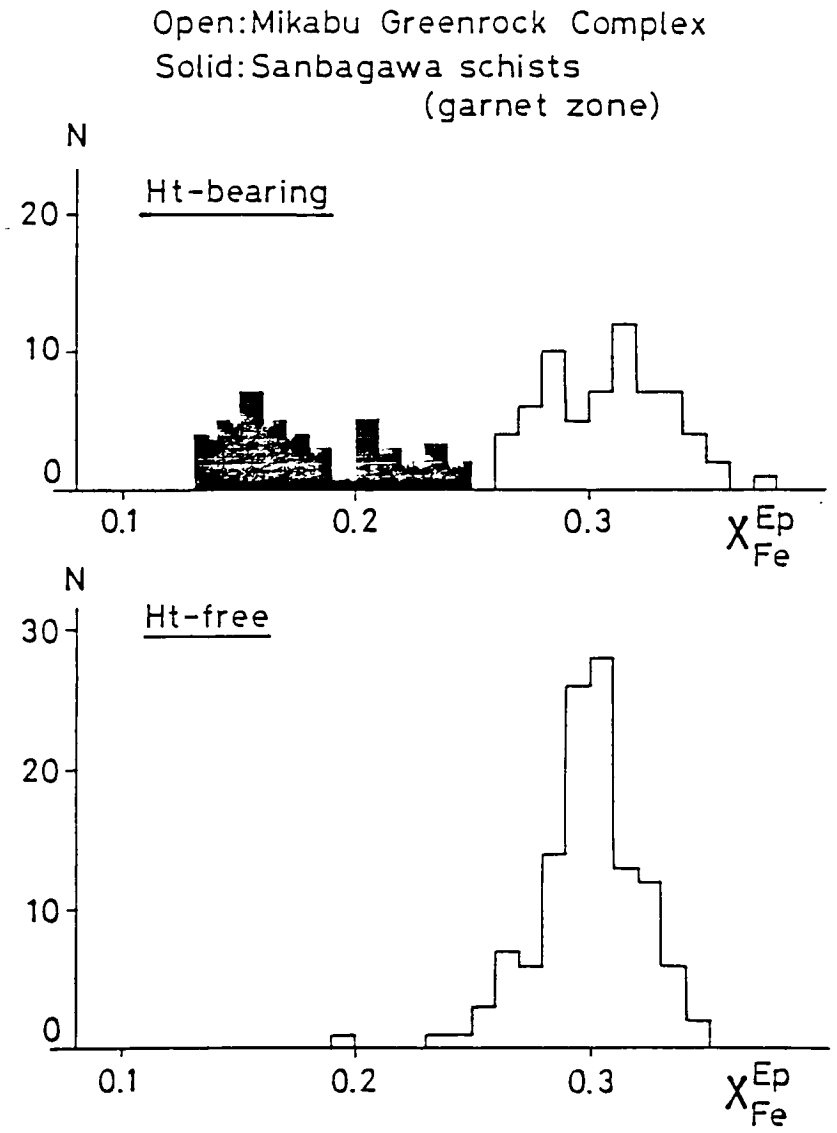

Table IV-6. Chemical composition of epidote

Rock No.	K778			K362			K1431		
Zone	Mikabu								
Assemblage	EDC			EAGC+Ilt			EADC+Fe-sulfide		
Point No.	12	17	50	6	17	37	3	21	24
SiO2	37.32	37.34	37.44	37.48	37.17	36.89	37.14	37.48	36.63
Al2O3	21.75	22.20	22.18	22.19	21.46	21.82	22.33	22.69	22.37
Fe2O3	15.40	15.34	15.40	15.73	15.98	16.88	15.75	15.14	15.45
MnO	.00	.00	.00	.27	.19	.13	.00	.00	.00
CaO	23.10	22.92	22.98	23.49	23.44	23.51	23.26	23.19	22.93
Total	97.57	97.83	98.01	99.17	98.24	99.28	98.49	98.50	97.38
O=12.5									
Si	3.005	2.995	2.998	2.977	2.986	2.943	2.967	2.984	2.975
Al	2.064	2.099	2.093	2.078	2.032	2.051	2.102	2.129	2.129
Fe3	.933	.926	.928	.941	.966	1.013	.947	.907	.939
Mn	.000	.000	.000	.018	.013	.009	.000	.000	.000
Ca	1.993	1.972	1.972	1.999	2.018	2.009	1.991	1.978	1.984
Total	7.996	7.992	7.991	8.013	8.015	8.025	8.008	7.998	8.009

Table IV-6. (Continue)
Chemical composition of epidote

Rock No.	K387			5071			444		
Zone	Mikabu			Sanbagawa					
Assemblage	EAGDC+Ht			Barroisite+EC			EAC+Mt		
Point No.	12	34	47	7	33	37	11	14	28
SiO2	37.92	37.56	37.81	37.52	37.36	38.61	37.50	37.46	38.98
Al2O3	22.66	21.49	22.30	21.13	21.47	22.62	25.64	24.75	27.71
Fe2O3	14.03	15.55	15.03	15.42	16.65	14.91	10.54	11.84	7.72
MnO	.13	.26	.00	.00	.41	.44	.24	.20	.20
CaO	23.13	22.89	23.68	22.95	23.40	22.67	23.52	23.21	24.19
Total	97.88	97.75	98.82	97.02	99.28	99.28	97.47	97.46	98.80
O=12.5									
Si	3.026	3.021	3.003	3.028	2.976	3.041	2.974	2.981	3.012
Al	2.131	2.037	2.087	2.016	2.016	2.100	2.396	2.321	2.524
Fe3	.843	.942	.899	.940	.999	.884	.629	.709	.449
Mn	.009	.018	.000	.000	.028	.029	.016	.013	.013
Ca	1.978	1.972	2.015	1.991	1.997	1.913	1.998	1.979	2.003
Total	7.987	7.990	8.004	7.984	8.016	7.967	8.014	8.006	8.001

IV-2-4 Pumpellyite

Pumpellyite occurs widely and abundantly in matrix of the basic rocks of the Mikabu Greenrock Complex and the Chichibu Group, and rarely of the upper most part of the Sanbagawa schists, as shown in Tables III-1, III-2b, and Fig. III-5. Pumpellyite veins frequently occur in coarse-grained rocks of the Mikabu Greenrock Complex. This mineral occurs as anhedral, polysynthetic-twinned grain, and as idiomorphic needles or tabular grains. In schistose rocks pumpellyite forms matrix associated with amphiboles, epidote, and chlorite , and in massive rocks it does monomineralic amygdules or grows as pseudomorph after plagioclase or volcanic glass. The axial color of pumpellyite is almost colorless and rarely pale blueish-green (=Y). The assemblage pumpellyite-sodic amphiboles is often observed in coarse-grained basic rocks of the study area, whereas this assemblage is extremely rare in the Sanbagawa belt in Shikoku and is inconsistent with the mineral assemblages of the pumpellyite-actinolite facies. As mentioned in previous section, pumpellyite replaces plagioclase and does not contact directly with sodic amphibole in coarse-grained rocks of the study area. These minerals should be formed depending upon the local chemical composition under the pumpellyite-actinolite facies condition.

Nakajima et al.(1977) and Aiba (1982) described that

the maximum Al content of pumpellyite tendes to increase and the maximum Fe^{3+} content decreases with increasing metamorphic temperature in rocks with the same Fe^{2+}/Mg ratio. Al contents of pumpellyite in this study increase from the Chichibu Group to the Mikabu Greenrock Complex (Fig. IV-11 and Table IV-7). Al-enrichment with descending stratigraphic order is also observed in epidote as described in a previous section (IV-2-3). These facts indicate that the metamorphic temperature of the Kanto Mountains increases with descending stratigraphic order.

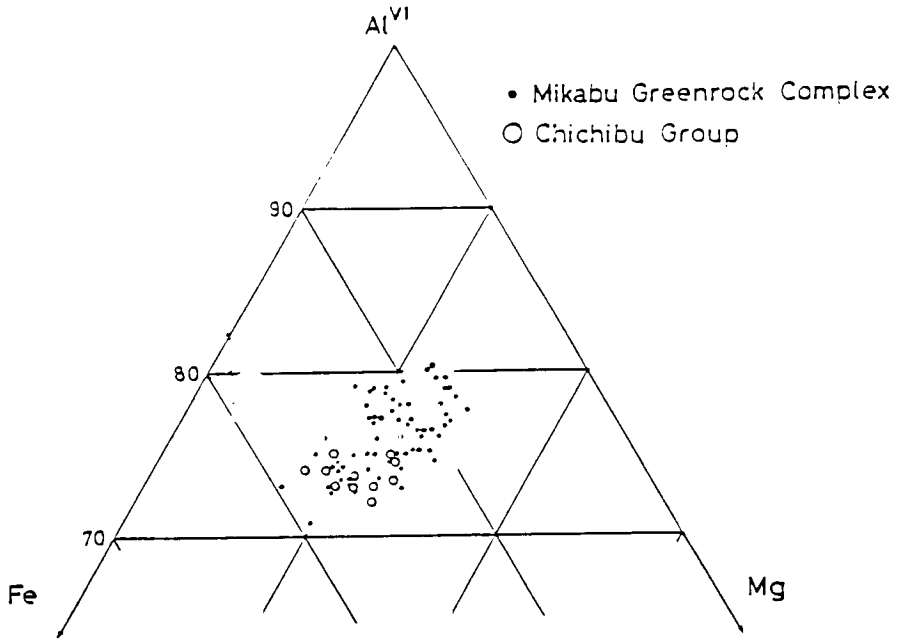

Fig. IV-11. Pumpellyite in Al(VI)-Fe(total)-Mg diagram.

Table IV-7. Chemical composition of pumpellyite.

Rock No.	828		US3537		US576		US1038		
Zone	- Chichibu -		Mikabu						
Point No.	74	76	22	27	21	27	22	25	48
SiO2	36.21	35.76	37.46	37.47	36.79	36.65	36.83	36.92	36.50
TiO2	.00	.00	.05	.03	.00	.00	.00	.00	.00
Al2O3	23.42	24.32	25.25	24.64	25.34	24.58	24.23	24.77	25.00
FeO*	6.58	5.82	3.47	4.34	3.44	5.60	6.30	5.77	5.57
MnO	.00	.00	.11	.17	.40	.17	.11	.15	.00
MgO	3.07	3.04	3.34	3.38	3.25	2.52	2.45	2.40	2.28
CaO	22.89	22.66	22.62	22.65	22.30	22.90	22.65	22.86	22.60
Total	92.17	91.59	92.68	93.23	91.54	92.43	92.57	92.85	91.95
O=49									
Si	11.954	11.826	12.056	12.066	11.991	11.983	12.048	12.009	11.967
Al	9.114	9.477	9.592	9.342	9.734	9.470	9.343	9.495	9.659
Ti	.000	.000	.012	.006	.000	.000	.000	.000	.000
Fe	1.816	1.608	.934	1.170	.939	1.532	1.725	1.569	1.528
Mn	.000	.000	.032	.048	.110	.047	.031	.040	.000
Mg	1.152	1.498	1.604	1.620	1.581	1.228	1.193	1.165	1.112
Ca	8.094	8.027	7.800	7.814	7.787	8.023	7.940	7.966	7.937
Total	32.490	32.436	32.032	32.414	32.142	32.283	32.280	32.249	32.203

*:Total iron as FeO

IV-2-5 Lawsonite

Lawsonite occurs rarely in the metabasites and psammites of the Mikabu Greenrock Complex and in the siliceous rocks of the chlorite zone of the Sanbagawa schists (Tables III-1 and III-2b). This mineral occurs with sodic pyroxene, sodic amphibole, actinolite, pumpellyite, epidote, chlorite, phengite, and albite, with or without quartz in matrix of metabasites. This mineral is colorless and is clearer than epidote under opened-nicols. Anhedral lawsonite with (101) polysynthetic twin always coexists with the irregular to tabular shaped lawsonite. In naked eyes, lawsonite-bearing basic rocks are massive and fine-grained, and have a characteristic splashed pattern which is composed of white fine needles of lawsonite scattered in green matrix.

When both lawsonite and epidote occur in the same thin section, lawsonite is almost always irregular shaped, whereas lawsonite occurs not accompanied with epidote, lawsonite is clear and an idiomorphic-tabular grain. Lawsonite could not stably coexist with epidote.

The chemical composition of lawsonite is remarkably uniform and closely approximates to the ideal structural formula with the only noticeable substitution being Al byFe (0.33-1.93 wt% of Fe_2O_3, about 0.78 wt% in average)

Lawsonite-bearing basic rocks are common only in the restricted area of the Mikabu Greenrock Complex in the eastern part of the Kanto Mountains. Even in this area,

the volume of lawsonite-bearing rocks is far less than that of lawsonite-free rocks. The bulk composition of lawsonite-bearing rocks are clearly in richer-Al_2O_3 and in poorer-Fe_2O_3 than those of lawsonite-free rocks, except one sample which contains larger amount of phengite than the other lawsonite-bearing rocks (Fig. IV-12a).

The bulk compositions of metabasites from the Mikabu Greenrock Complex and the Mamba Formation of the Chichibu Group in the central and western parts of the Kanto Mountains (Uchida, 1981) are shown in Figs. IV-12b and IV-12c, respectively. Fig. IV-12b indicates that rocks with appropriate composition to crystallize lawsonite under the pumpellyite-actinolite facies condition occur rarely in these areas. This is one of possible explanations for lack of lawsonite in the central and western parts of the Kanto Mountains. On the other hand, the appropriate rocks to crystallize lawsonite exist in the Mamba Formation (Fig. IV-12c). However, as the metamorphic grade of the Mamba Formation is lower than the pumpellyite-actinolite facies as mentioned in chapter III, lawsonite is not formed in the Mamba Formation.

Fig. IV-12. Al_2O_3-Fe_2O_3 diagram of the bulk rock compositions in metabasites of the Kanto Mountains.
a) Metabasites in the eastern part. Lawsonite-bearing rocks are shown as solid symbols.
b) Metabasites of the Mikabu Greenrock Complex in the central and western parts (Uchida,1981).
c) Metabasites of the Mamba Formation of the Chichibu Group in the central and western parts (Uchida, 1981).
Lawsonite was not found in the analyzed rocks by Uchida (1981). Symbols of rock types are in common with b) and c).

Fig. IV-12.

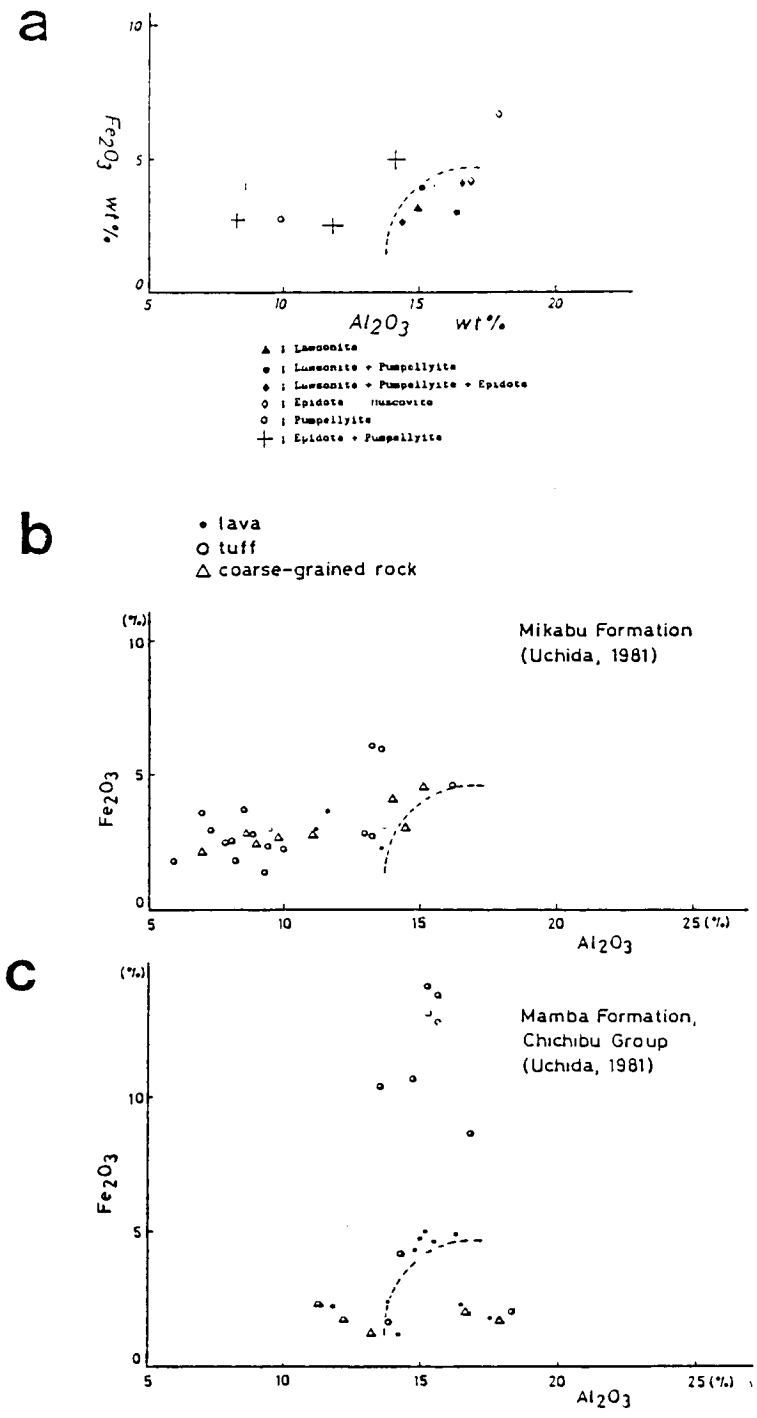
a
Fe_2O_3 wt%
Al_2O_3 wt%
▲ ; Lawsonite
● ; Lawsonite + Pumpellyite
◆ ; Lawsonite + Pumpellyite + Epidote
◇ ; Epidote Muscovite
○ ; Pumpellyite
+ ; Epidote + Pumpellyite
b
• lava
○ tuff
△ coarse-grained rock
Mikabu Formation
(Uchida, 1981)
Fe_2O_3
Al_2O_3
c
Mamba Formation,
Chichibu Group
(Uchida, 1981)
Fe_2O_3
Al_2O_3

Table IV-8. Chemical composition of lawsonite.

Rock No.	11		40		343	
Zone	Mikabu					
Point No.	44	67	33	35	13	24
SiO2	38.25	36.59	38.27	37.74	38.02	38.30
TiO2	.44	.04	.07	.13	16	08
Al2O3	31.65	31.04	30.95	31.32	29.93	31.04
Fe2O3	.84	.90	.52	40	2.14	1.28
MnO	.00	.30	.00	00	.06	01
MgO	.02	00	00	00	.00	00
CaO	16.97	17 17	17 96	17.60	17 76	17 50
Na2O	.12	1 18	.00	01	.02	03
K2O	.03	.10	.00	02	.07	.05
Total	88.32	87.68	87 77	87.22	88.16	88.29
O=8						
Si	2.008	1.956	2.025	2.008	2.041	2.024
Al	1.958	1.979	1.930	1.964	1.860	1.933
Ti	.018	.002	.003	.005	.007	.003
Fe3	.033	.036	.021	.016	.087	.051
Mn	.000	.014	.000	.000	.030	.000
Mg	.002	.000	.000	.000	.000	.000
Ca	.954	.984	1.018	1.003	1.022	.991
Total	4.987	5.100	4.997	4.998	5.029	5.008

*:Total iron as Fe2O3

IV-2-6 Chlorite

Chlorite commonly occurs in all kinds of rocks in the study area. Chemical compositions of chlorite in metabasites of the study area are shown in Table IV-9, and the chemical variation are represented in the Hey's diagram (Fig. IV-13) and in a histogram of Al-content in each geologic unit (Fig. IV-14). These diagrams indicate the slight decrease of Si-content and the slight increase of Al-content in chlorite with descending stratigraphic order, i.e., from the Chichibu Group to the Sanbagawa schists, although X_{Fe} <=Fe/(Fe+Mn+Mg)> of chlorite shows a wide variation reflecting the wide range of bulk rock composition. Compositional range of chlorite in the same thin sections are plotted in Al^{VI}-Fe^{total}-Mg diagram (Fig. IV-15) suggesting that chlorite is relatively homegeneous in the same thin sections.

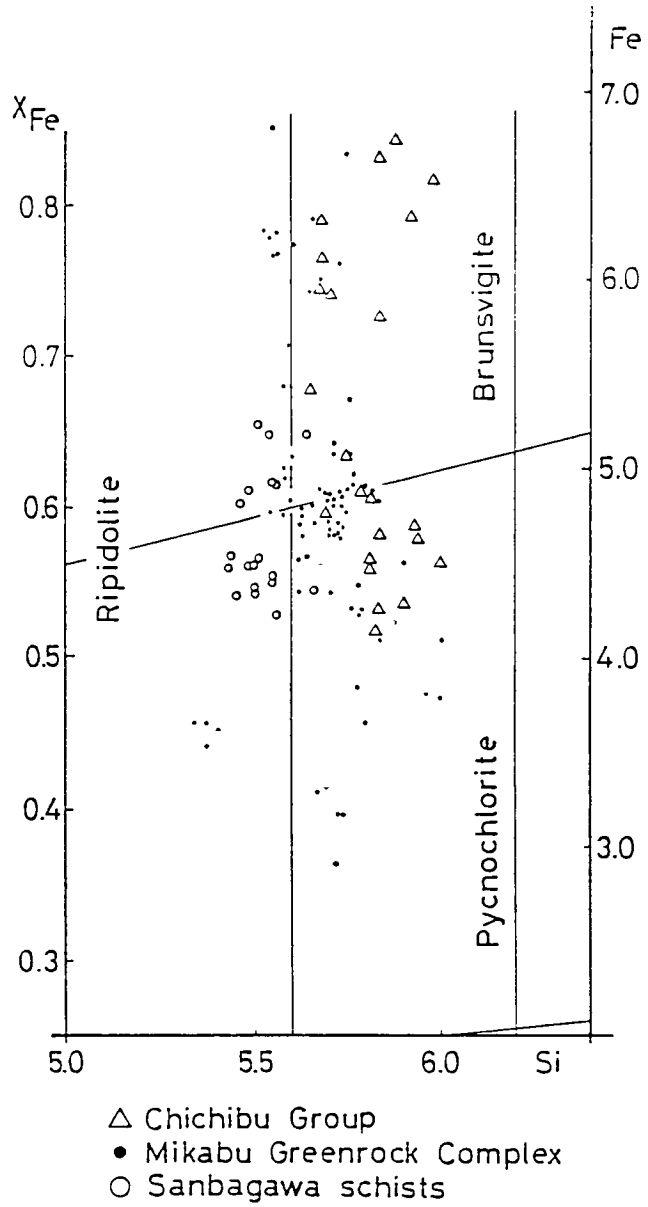

Fig. IV-13. Chlorite in Hey's diagram.

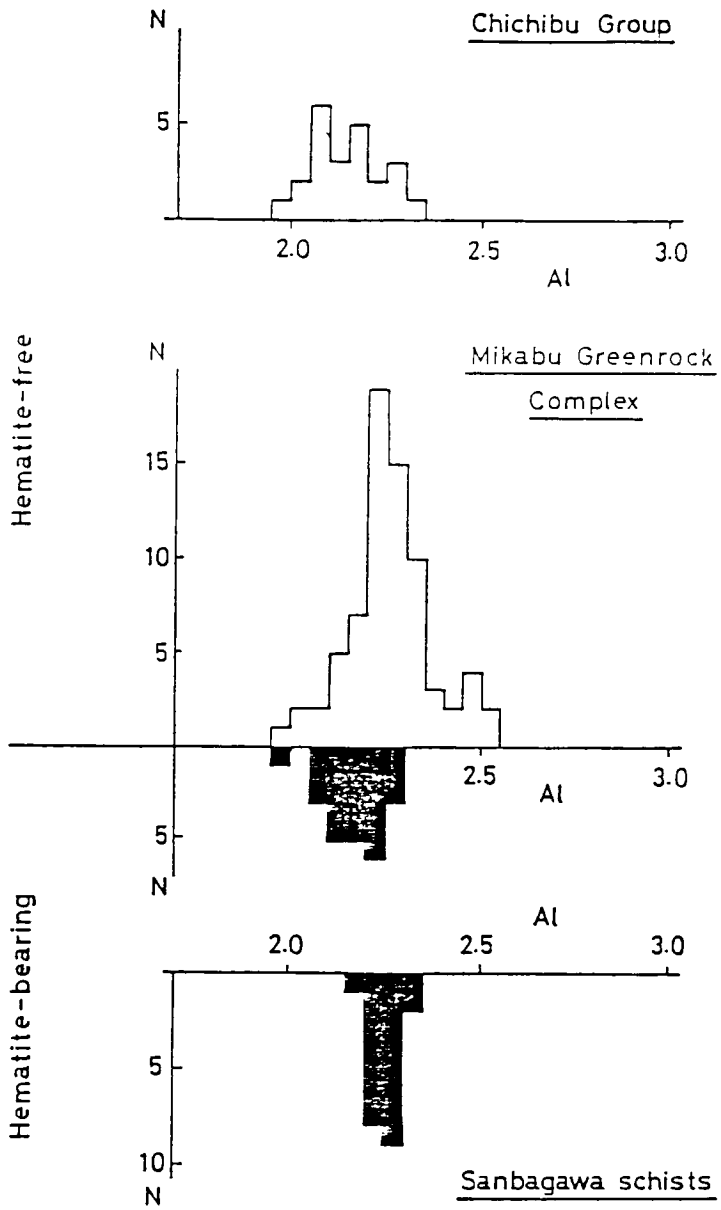

Fig. IV-14. Frequency distribution of Al-content in chlorite of the Sanbagawa metamorphic rocks.

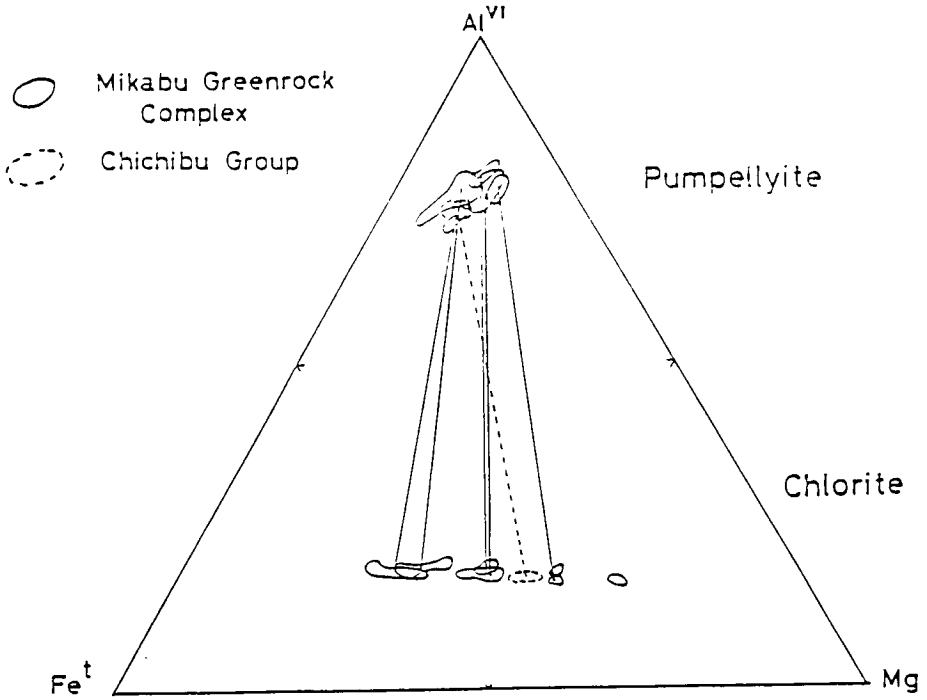

Fig. IV-15. Compositional range of chlorite and pumpellyite in each thin section in Al(VI)-Fe(total)-Mg diagram. Tie lines bind the averaged compositions of chlorite and pumpellyite in the same thin section.

Table IV-9. Chemical composition of chlorite.

Rock No.	K444		US516		834		5071	
Zone	- Chichibu -		---------- Mikabu ----------				--Sanbagawa--	
Point No.	14	21	6	38	108	128	2	11
SiO2	27.70	28.18	26.68	26.49	26.95	26.32	26.17	26.04
Al2O3	16.29	17.28	18.39	18.14	17.40	18.39	18.63	17.65
FeO*	24.16	23.91	26.58	26.97	27.44	28.50	27.85	28.59
MnO	.42	.41	.39	.31	.38	.49	.50	.69
MgO	17.98	18.80	15.79	15.58	15.29	14.94	15.52	14.43
Total	86.54	88.58	87.84	87.50	87.46	88.63	88.68	87.40
O=14								
Si	2.948	2.916	2.830	2.830	2.887	2.798	2.773	2.820
Al	2.044	2.108	2.300	2.284	2.196	2.304	2.327	2.253
Fe	2.150	2.069	2.358	2.408	2.458	2.534	2.468	2.589
Mn	.037	.036	.035	.028	.034	.044	.045	.063
Mg	2.852	2.900	2.496	2.480	2.440	2.368	2.451	2.329
Total	10.048	10.031	10.019	10.030	10.015	10.048	10.064	10.054

*:Total iron as FeO

IV-2-7 Garnet

Idiomorphic fine-grained garnets occur ubiquitously in pelitic schists in the central and western parts of the Kanto Mountains. In the eastern part, they occur only in the lower part of the Sanbagawa schists (Fig. III-1, Tables III-1 and III-2b). Garnet stably associates with epidote, phengite, calcite, chlorite and quartz. The garnets show the zoning with the Mn-rich core and Mn-poor rim (Table IV-10 and Fig. IV-16), and the zoning profile of them are very similar to that of the garnet zone in Shikoku (Banno and Kurata, 1972; Kurata and Banno, 1974; Higashino, 1975; Otsuki, 1980; Sakai, 1982).

Garnets with an optical anomaly were found in Mn-rich nodule in the garnet zone of the Sanbagawa schists in the central part (Plate IV-13). They associate with sodic pyroxene, sodic amphibole, magnetite, hematite, stilpnomelane, albite and quartz. They are composed of wide and homogeneous core (pure spessartine), and very thin rim which has very similar composition to that of garnet in the surrounding pelitic schists (Fig. IV-17).

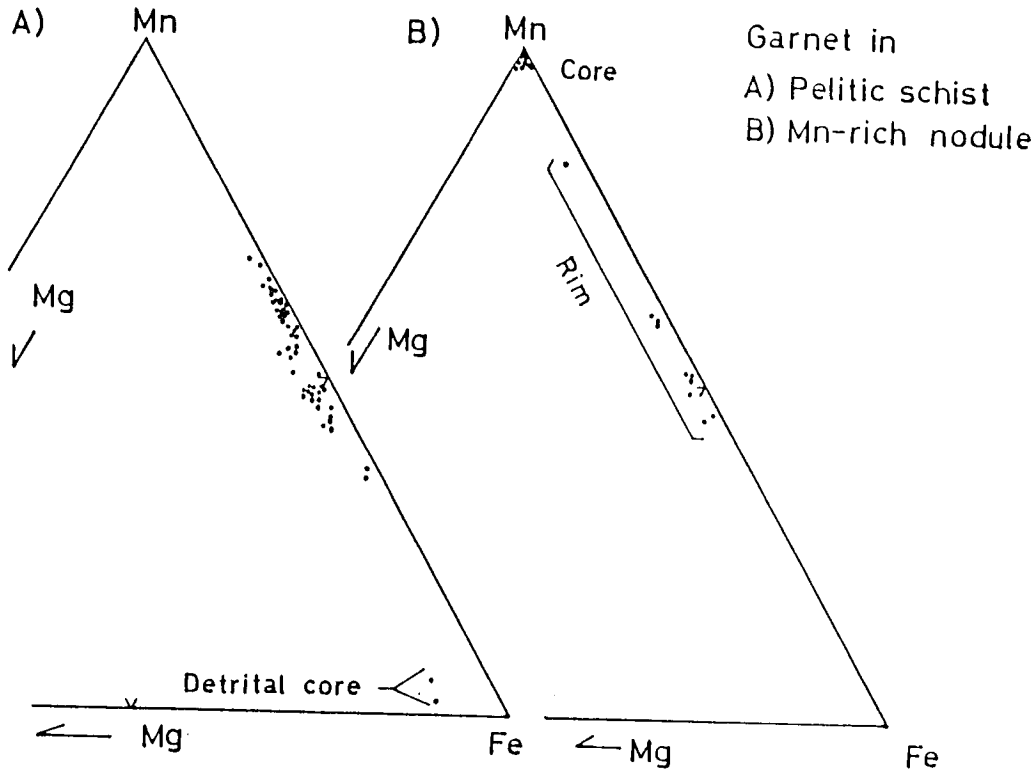

Fig. IV-16. Garnet in Mn-Mg-Fe diagram.

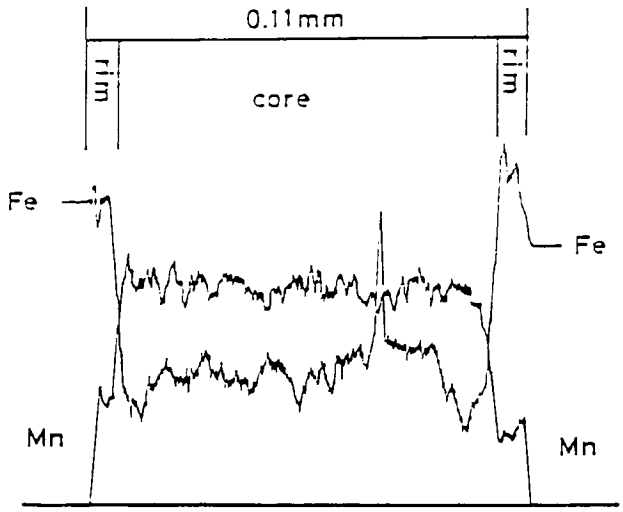

Fig. IV-17. Line profile of spessartine garnet in Mn-rich nodule of the garnet zone.

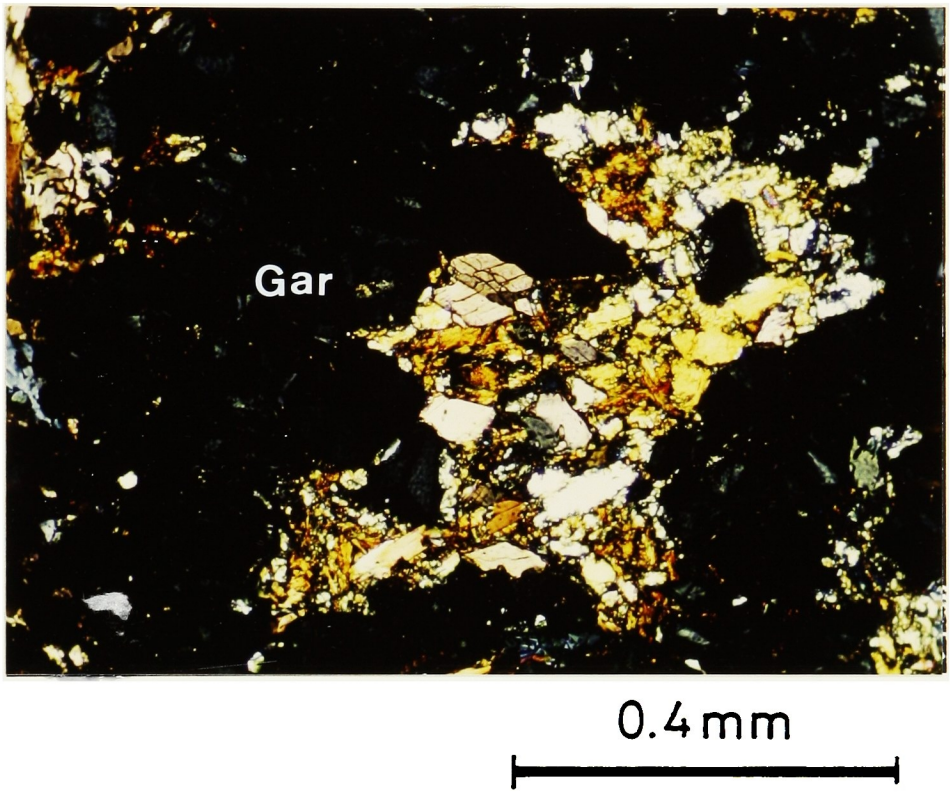

Plate IV-13. Photomicrograph of optical anomaly garnet (Gar) in Mn-rich nodule in the garnet zone of the Sanbagawa schists. a)opened nicol. b)crossed nicols.

Table IV-10. Chemical composition of garnet

Rock No.	448		472		US3705	
Zone	Sanbagawa					
Point No.	17	19	10	16	103	104
Core/Rim	core	rim	core	rim	core	rim
SiO2	37.07	37.58	37.23	37.01	37.78	36.36
TiO2	.00	.00	.00	.00	.15	.64
Al2O3	20.28	20.50	20.44	20.40	19.82	17.60
FeO*	15.71	20.11	10.97	12.45	17.11	3.55
MnO	21.24	11.31	24.77	21.40	16.01	36.06
MgO	.29	.43	.37	.30	.45	.07
CaO	5.48	10.02	7.06	8.03	7.71	4.30
Total	100.07	99.78	100.83	99.59	99.03	98.58
O=12						
Si	3.018	3.026	3.002	3.008	3.071	3.051
Ti	.000	.000	.000	.000	.009	.040
Al	1.945	1.946	1.942	1.953	1.899	1.741
Fe	1.070	1.354	.739	.846	1.163	.249
Mn	1.464	.760	1.691	1.473	1.102	2.563
Mg	.036	.052	.044	.037	.054	.009
Ca	.478	.865	.610	.699	.672	.387
Total	8.011	8.003	8.026	8.016	7.970	8.040

*:Total iron as FeO

IV-2-8 Other minerals

(8-1) Quartz

Since the distinction of quartz from albite in lower-grade metabasites is very difficult under the microscope, untwinned colorless minerals were identified by the microprobe. Quartz was found in five polished sections among about fifty analyzed sections of the Mikabu Greenrock Complex and the Chichibu Group, but it commonly occurs in metabasites of the Sanbagawa schists.

(8-2) Albite and K-feldspar

Albite occurs as pseudomorphs after plagioclase in all basic rocks, and as vein or compositional banding composing the leucocratic layers. The An (=anorthite) content in albite ranges 0.1 to 1.0 mol%, and oligoclase was not found in the study area.

K-feldspar was found in metabasites of the Chichibu Group. This mineral has a composition of nearly $KAlSi_3O_8$ and occurs as composite veins with albite.

(8-3) Prehnite

Prehnite rarely occurs in rocks of the Chichibu Group which are exposed near the Sanchu Graben (Fig. III-1). It commonly occurs in the Atokura Formation and correlatives, however. Prehnite of the Chichibu Group occurs as veins or aggregates of fine-tabular grains in the matrix associated with calcite, albite, epidote and chlorite. Some prehnite

veins are crosscut by albite or calcite veins (Plate IV-14), indicating that prehnite of the Chichibu Group was formed by the Sanbagawa metamorphism as pointed out by Toriumi (1975).

(8-4) Phengite

Phengitic muscovite is a minor constituent mineral in basic rocks, but is major in pelitic schists. The chemical compositions of phengite are shown in Table IV-11. Paragonite component is very low.

(8-5) Stilpnomelane

Stilpnomelane is sometimes found in basic and siliceous rocks in the study area, but not much attention was paid to this mineral by the author.

(8-6) Sphene

Sphene occurs in most basic rocks. The chemical compositions of sphene are shown in Table IV-11. Minor amounts of Al_2O_3 and Fe_2O_3 are contained.

(8-7) Calcite

Carbonates were tested with the Fiegl's solution. They are calcite in the Sanbagawa metamorphic rocks. Aragonite was found only in the jadeite-aragonite-bearing tectonic blocks reported by Tanabe et al.(1982).

(8-8) Hematite, Magnetite, Ilmenite and Pyrite.

These minerals were identified by both the reflecting microscope and the microprobe. Among opaque minerals,

pyrite is most common in metabasites of the Mikabu Greenrock Complex and the Chichibu Group, and hematite and magnetite are predominant in those of the Sanbagawa schists. Sodic amphibole usually coexists with hematite even in the Mikabu Greenrock Complex and the Chichibu Group.

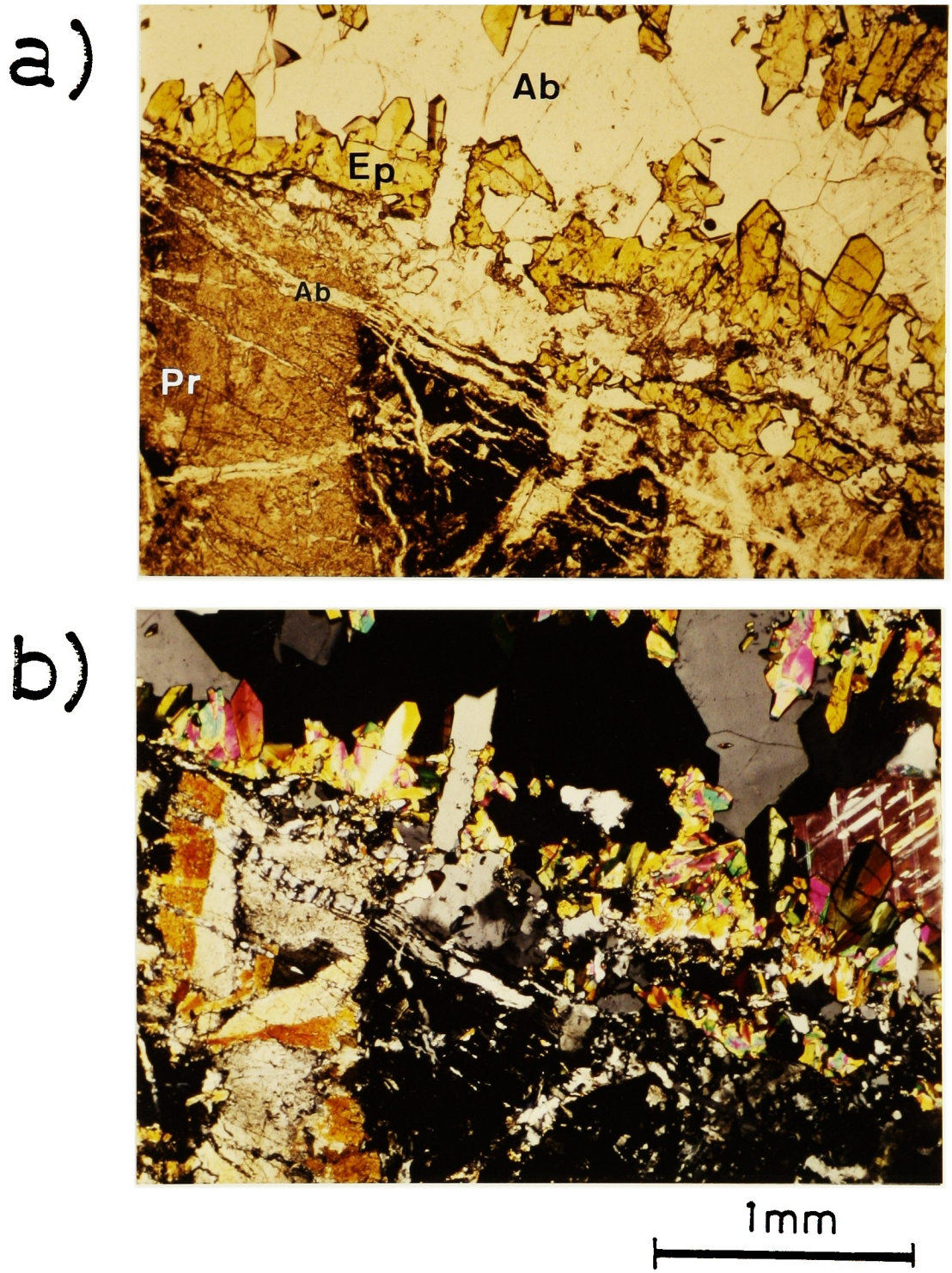

Plate IV-14. Photomicrographs of prehnite (Pr) vein in volcanic rocks of the Chichibu Group. Prehnite vein is crosscut by albite (Ab) and epidote (Ep) veins. a)opened nicol. b)crossed nicols.

Table. IV-11. Chemical composition of other minerals

Mineral	- Phengite -		--------- Stilpnomelane ---------				-Sphene-
Rock No.	324		828		K387	US3705	14
Zone	-- Mikabu --		----Mikabu --		--------	Sanbagawa	-Mikabu-
SiO2	50.33	54.54	44.18	45.25	49.73	50.01	30.17
TiO2	.02	.01	.00	.10	.00	.00	38.61
Al2O3	18.72	18.09	6.53	6.32	5.71	5.61	1.89
FeO*	7.37	6.52	28.73	28.80	24.56	18.90	1.63
MnO	.01	.04	1.14	1.30	1.88	12.78	.00
MgO	7.63	6.99	4.94	5.22	9.41	5.36	.49
CaO	.04	.01	.00	.00	.00	.00	27.04
Na2O	.01	.02	.00	.22	.00	.00	.06
K2O	9.02	8.77	1.06	1.33	3.00	.99	.05
Total	93.15	94.99	86.58	88.54	94.29	93.65	99.92
O=	O=22.0		---------- O=22.0 ----------				O=5.0
Si	7.047	7.379	7.311	7.327	7.411	7.578	.986
Al	3.090	2.885	1.274	1.207	1.003	1.002	.073
Ti	.002	.000	.000	.012	.000	.000	.950
Fe	.862	.738	3.976	3.900	3.061	2.395	.044
Mn	.002	.005	.160	.178	.237	1.640	.000
Mg	1.592	1.410	1.220	1.260	2.089	1.210	.024
Ca	.005	.002	.000	.000	.000	.000	.947
Na	.002	.005	.000	.038	.000	.000	.004
K	1.612	1.514	.224	.275	.590	.192	.002
Total	14.114	13.938	14.164	14.197	14.371	14.007	3.030

*:Total iron as FeO

IV-3 Minerals in the Atokura and Tochiya Klippes

The constituent rocks of the Atokura and Tochiya Klippes are metamorphosed. Metamorphic minerals from each geologic unit of the klippes are described below.

IV-3-1 The Atokura Formation, its correlatives and quartz-diorites.

A) Prehnite

As described in the previous chapters, prehnite commonly occurs as veins in sandstone, shale and conglomerate of the Atokura Formation and its correlatives, and in quartz-diorites (Fig. III-5 and Table III-1). This mineral associates with epidote, pumpellyite, chlorite, albite and quartz (Plate IV-15). In conglomerates and quartz diorites, prehnite replaces detrital or relict plagioclases and forms an irregular aggregate composed of fine tabular grains. The detailed distribution map of prehnite in the eastern part of the Kanto Mountains (Yorii area) indicates that prehnite occurs only in the Tochiya Formation (correlatives of the Atokura Formation), the Kinshozan-quartz-diorite and the greenrock mélange, but not in the surrounding basements (Sanbagawa schists, Mikabu Greenrock Complex and Chichibu Group) and the tertiary cover (Ogawa Formation)(Fig. IV-18). This tendency was confirmed also in the central and western parts (Fig. III-1).

Fig. IV-18.
A) Geologic map of the Yorii area showing the localities of the tectonic blocks in thegreenrock melange and the jadeite-quartz rock.
B) Distribution of metamorphic minerals around the Tochiya Formation.
Abbreviations: Mt.Ku;Kuruma-yama, Mt.Ki;Kinsho-zan Mt.Fu;Fuji-yama, Mt.Ka;Kannokura-yama.

a

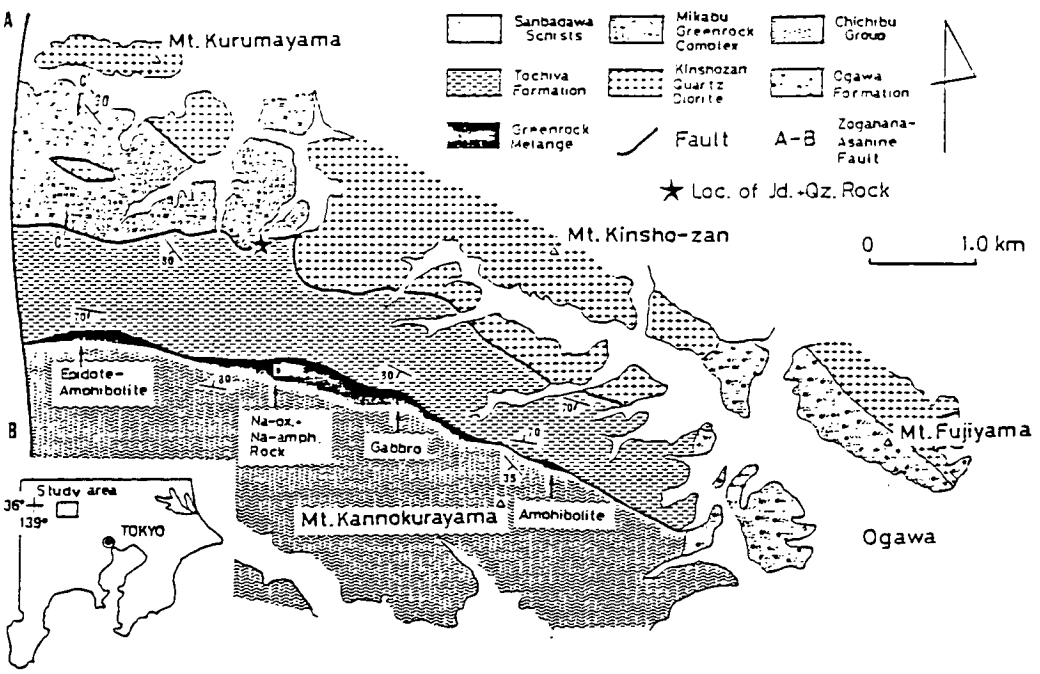

b

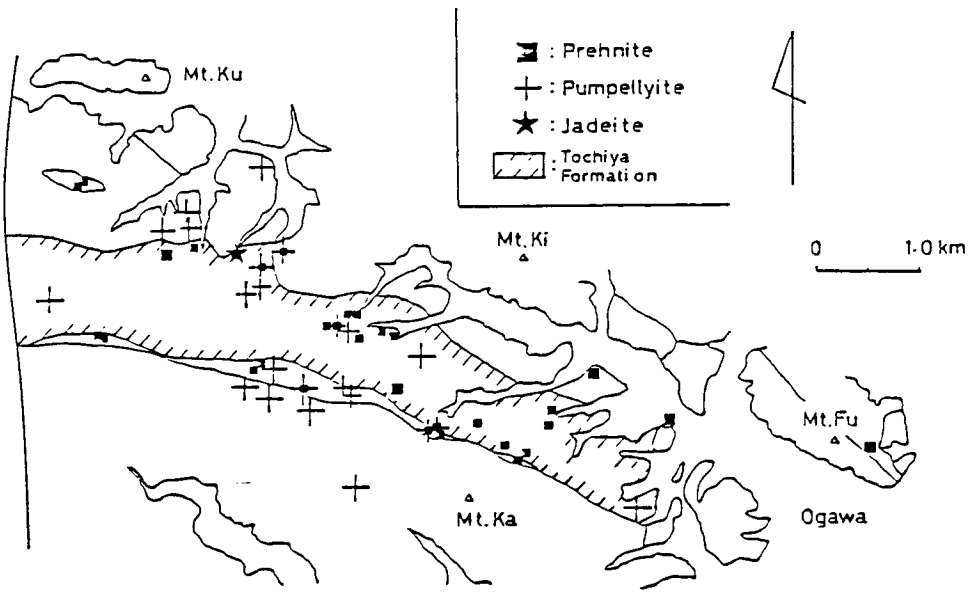

B) Pumpellyite

Pumpellyite often occurs in conglomerates and sandstone of the Atokura Formation and its correlatives and in quartz-diorites. It is colorless to pale-green colored under the microscope. It occurs as aggregates replacing plagioclase in quartz-diorites, and as fine columnar grain in the interstice between albite and quartz in sandstone and conglomerate (Plate IV-14). Submicroscopic-size pumpellyite grains, a few micron in size, in plagioclase are identified by electron microprobe. Pumpellyite replacing plagioclase is close to its Al-end member (Table IV-12).

C) Epidote

Epidote commonly occurs in the most rocks of the Atokura Formation, its correlatives and quartz diorite. However, its grain size is not uniform and it is always irregular-shaped. Therefore, it is very difficult to determine under the microscope whether they are metamorphic origin or detrital. Because the secondary electron image shows that epidote of submicroscopic size together with pumpellyite replaces plagioclase, some epidotes in matrix were metamorphic origin.

D) Garnet

Garnets are common in sandstone and conglomerate of the Atokura Formation and its correlatives. It is usually unhedral, and broken grains of garnet scatter in the interstice of quartz and albite grains. Hence the garnets

were detrital origin.

IV-3-2 Greenrock mélange

This unit is mainly composed of actinolite rocks, except for various tectonic blocks enclosed in it. Actinolite rock is mainly composed of actinolite and chlorite whose modal amount exceed 90 % with minor amount of epidote, albite and sphene. The actinolite rock very resembles to those of the Mg-rich Mikabu type tuff of Uchida (1981) in the lithofacies and the mode of occurrence of mineral. Hence, actinolite rock should be derived from hyaloclastite or tuff.

IV-3-3 Tectonic blocks in the klippes

Several types of tectonic blocks, i.e.,jadeite-quartz rock, sodic pyroxene-sodic amphibole-bearing rock, epidote-amphibolite and etc., were found in the Tochiya Formation and the greenrock mélange (Fig. IV-18). The mode of occurrence of metamorphic minerals in these blocks are as follows;

A) Jadeite-quartz rock

Jadeite-quartz rock associated with ultramafic rocks occurs in the Tochiya Formation near the boundary with the Sanbagawa schists. The detailed sketch map around the locality of this rock is already shown in Fig. II-8.

Essential components of the jadeite-quartz rock are

colorless jadeite, glaucophane, quartz and albite. Pale-green pyroxenes, such as aegirine, aegirine-augite, aegirine-jadeite and chloromelanite, occur enclosed in albite, and Na-Ca amphiboles occur replacing glaucophane. Zircon and allanite are minor accessories.

The majority of the rock is grayish-white for unaided eyes, with grayish-blue glaucophane veins and colorless quartz veins. The grayish-white part is mainly composed of quartz aggregates and jadeite-albite aggregates, 3-5 mm in diameter.

Jadeite is always enclosed by albite, hence jadeite does not contact directly with quartz aggregates. However, submicroscopic quartz grains, a few micron in size, enclosed in jadeite with direct contact, are identified by electron microprobe.

Jadeite is in blade shapes. Sometimes coarse jadeite is surrounded by albite which contains fine grained jadeites in the same optical orientation as the coarse-grained one (0.5 x 1.0 mm) (See Plate IV-16). On the other hand, pale-green pyroxenes are tabular and fine-grained (0.03 x 0.2 mm). Majority of them occur within the jadeite-albite aggregates near the boundary to quartz aggregates.

Chemical compositions of sodic pyroxenes are tabulated in Table IV-13 and Fig. IV-19. Jd contents of colorless pyroxene exceed 80 mol% and those of pale-green pyroxenes range from 10 to 30 mol%, with 20 mol% as average (Fig. IV-19). Both jadeite and pale-green pyroxenes near the

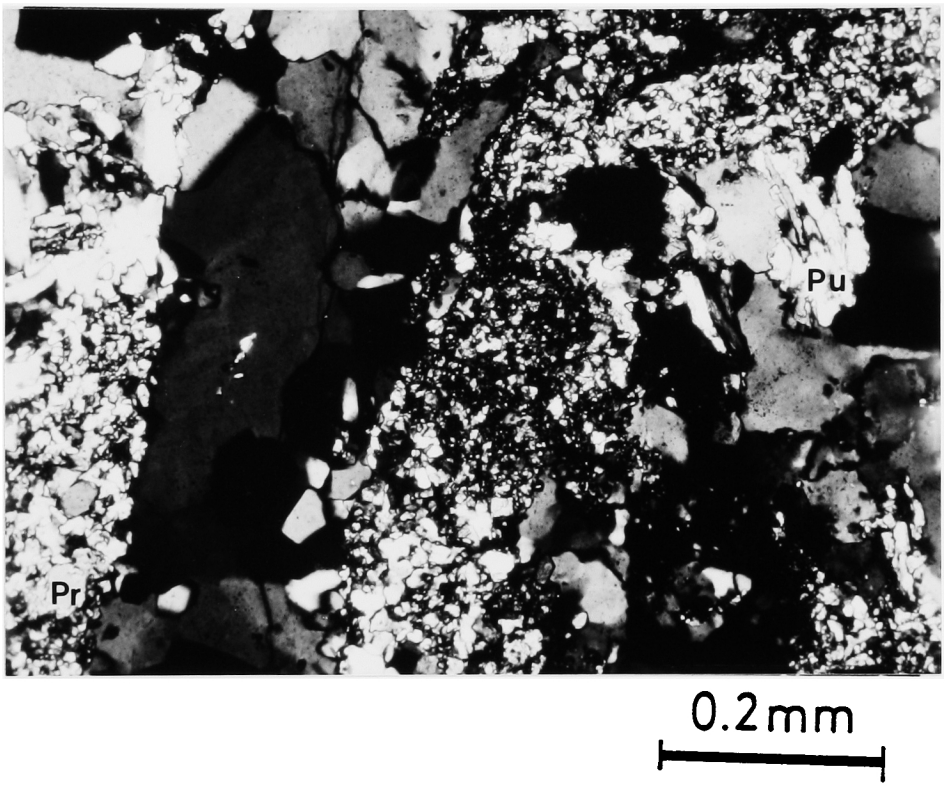

Plate IV-15. Photomicrograph of prehnite (Pr) and pumpellyite (Pu) in the interstice of quartz (Qz) grains of a coarse sandstone of the Tochiya Formation. Opened nicol.

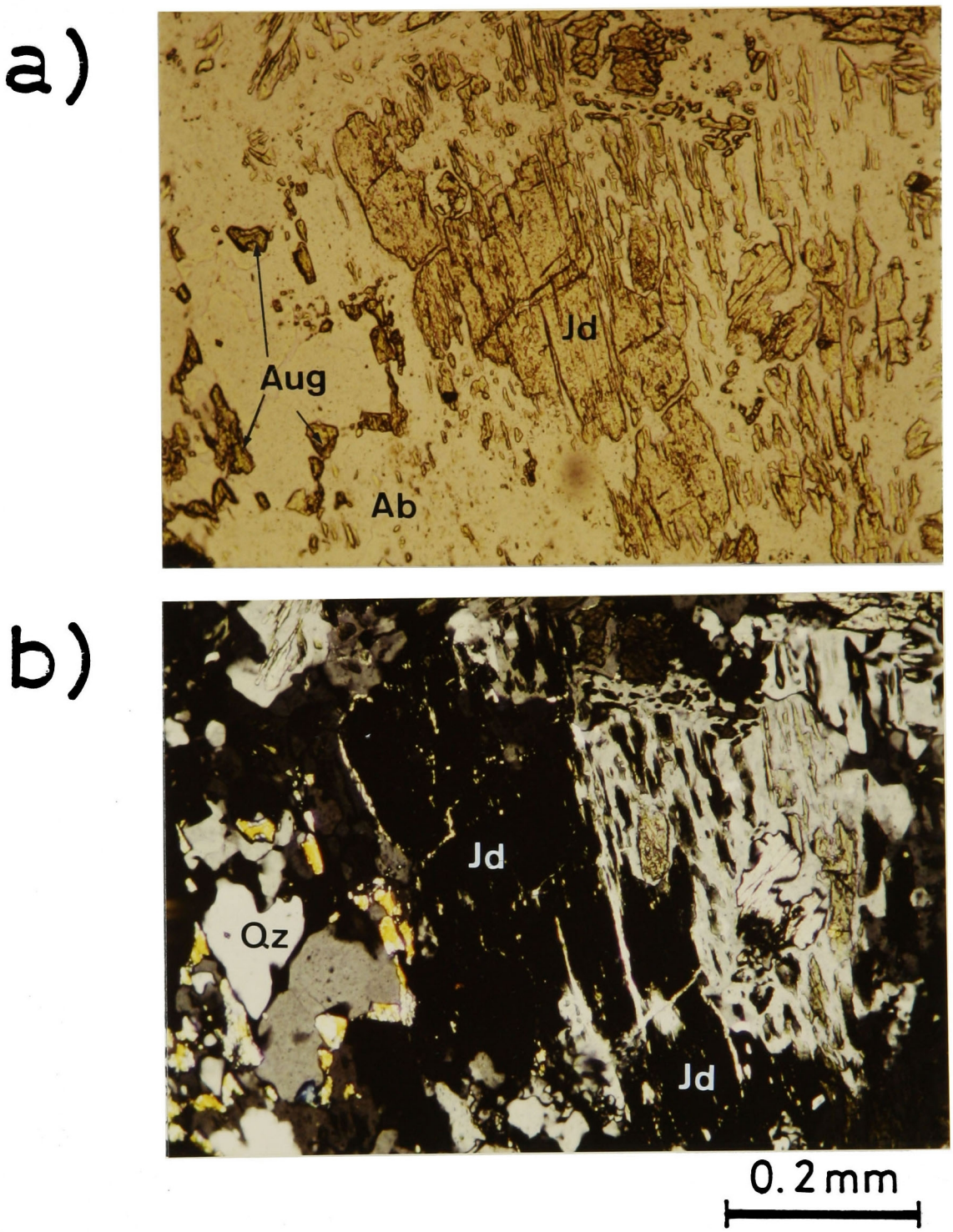

Plate IV-16. Photomicrographs of the jadeite-quartz rock. Coarse jadeite (Jd) and fine-grained one are in the same optical orientation. Aeg: second stage pyroxene. Ab: albite. Qz: quartz.
a)opened nicol. b)crossed nicols.

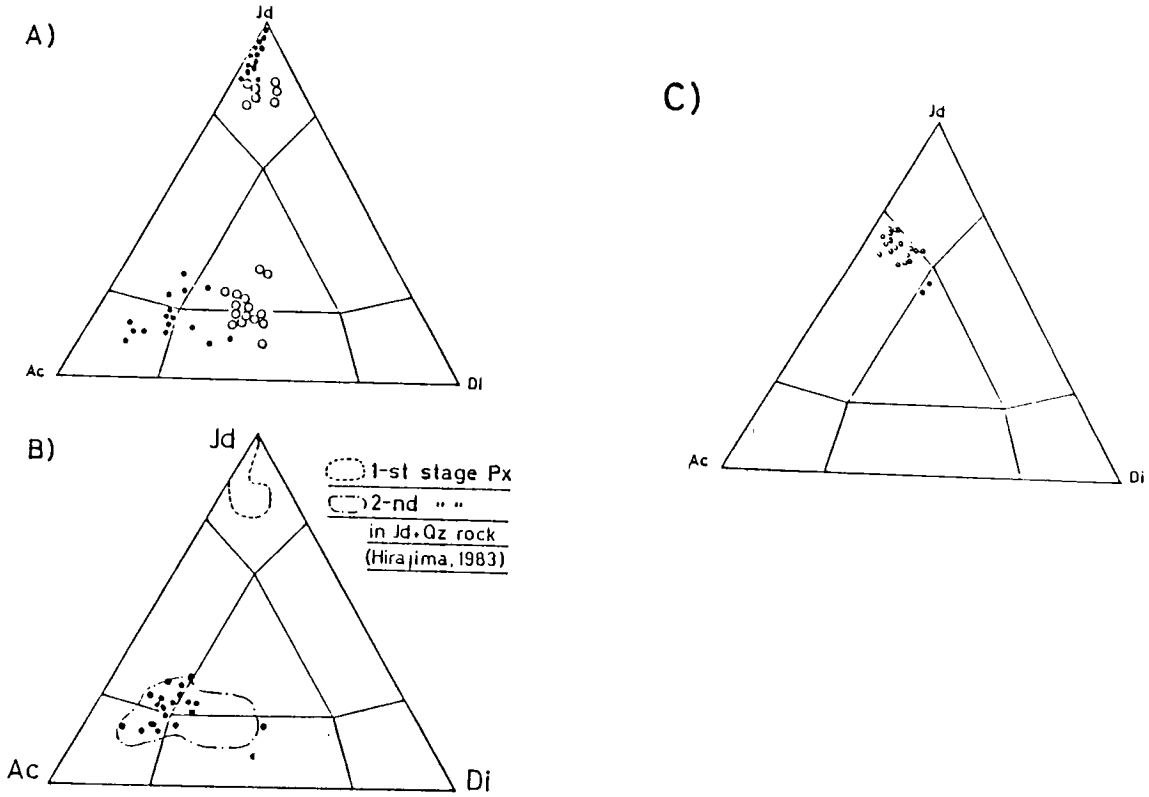

Fig. IV-19. Sodic pyroxenes from tectonic blocks in the Atokura and Tochiya Klippes.
A) Jadeite-quartz rock in the Tochiya Formation.
Solid circle; pyroxenes near glaucophane vein.
Open circle ; pyroxenes in the grayish-white part.
B) Sodic pyroxene-sodic amphibole-bearing rock in the greenrock mélange.
C) Jadeite-analcite rock in the western part.

glaucophane vein are slightly richer in Di content than those of grayish-white part (Fig. IV-19). Obviously, the variation of Di contents in jadeite is inherited in secondary pale-green pyroxenes (Plate IV-16). These facts indicate that impure-jadeite decomposed to albite and pale-green pyroxenes, i.e. components not permitted by albite. The reaction is as follows;

Impure Jadeite + Quartz =

Pale-green Pyroxene (Aegirine) + Albite ------(8)

Replacement textures of glaucophane are not so clear as those of pyroxenes. However, thin films of retrograded amphiboles (less than 10 μm in width) surround the glaucophane. They are crossite, riebeckite, winchite and actinolite (Fig. IV-20). Clearly amphibole coexisted with jadeite is glaucophane, and those with pale-green pyroxenes are retrograded amphiboles.

B) Sodic pyroxene-sodic amphibole-bearing rock

This rock is mainly composed of sodic pyroxene, sodic amphibole, actinolite, albite and sphene. Minor amount of epidote, pumpellyite and lawsonite are included only in albite. Sodic pyroxene usually occurs as granular, columnar or irregular ameba-shaped grains, and rarely as a parallel growth with sodic amphibole. Some sodic pyroxenes are green to pale yellowish green. However, pleochroism of the majority of them is very weak, hence they are easily misunderstood with epidote under the

Fig. IV-20. Amphiboles from tectonic blocks of the klippes.
A) Jadeite-quartz rock.
Solid circle; host glaucophane.
Open circle; retrograded amphiboles.
B) Sodic pyroxene-sodic amphibole-bearing rock.
Stars connected by tie lines show the amphiboles with distinct chemical gap.

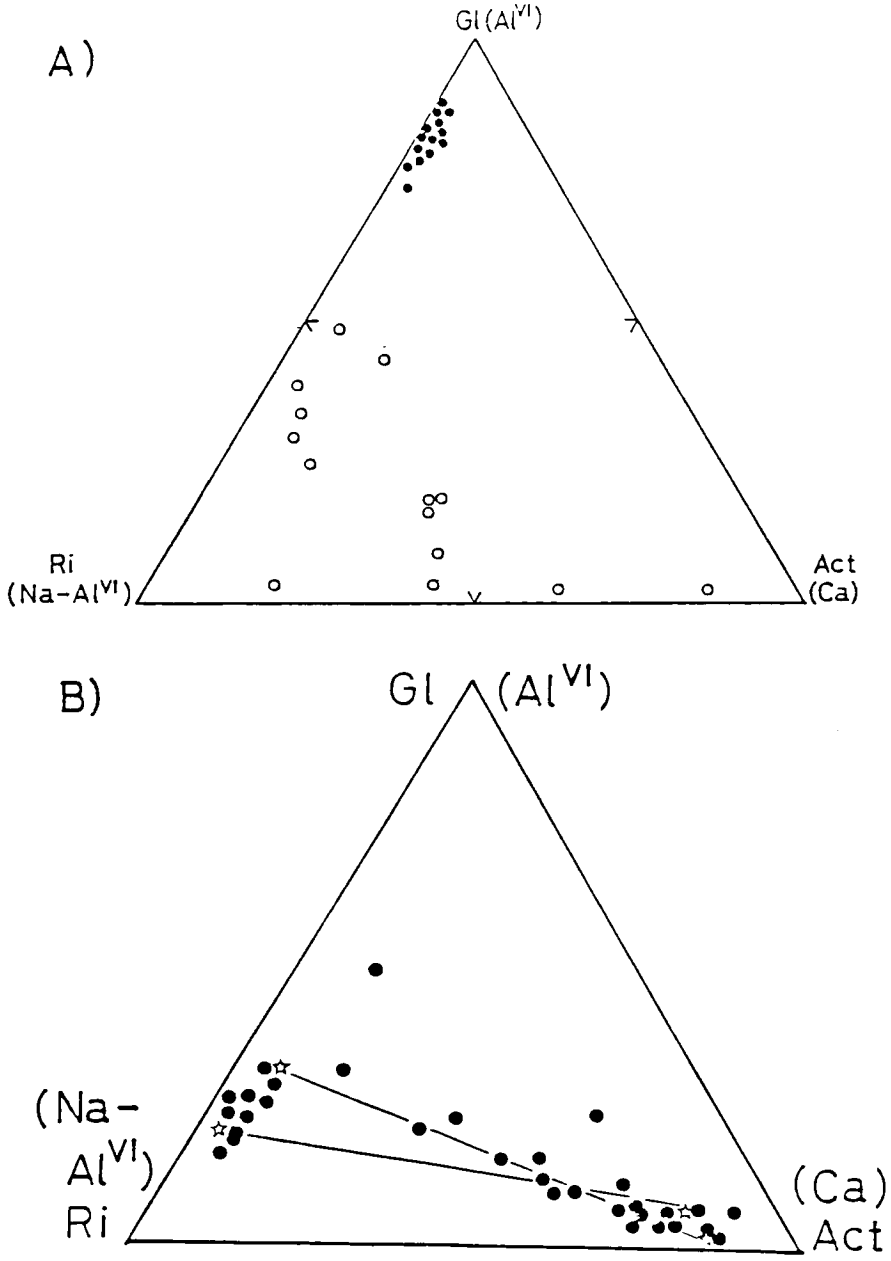

microscope. Sodic pyroxenes slightly variate their chemical composition within each grain, in the range very similar to secondary pale-green pyroxenes in the jadeite-quartz rock. The average composition of them is X_{Jd}=0.2, X_{Ac}=0.6 and X_{Di}=0.2 (Fig. IV-19).

Sodic amphibole is dark blue to pale blueish green color. It is surrounded by colorless actinolite, and vice versa. When sodic amphibole contacts to actinolite with a sharp boundary, the chemical composition changes discontinuous between them. However, some amphiboles have intermediate composition between sodic amphibole and actinolite (Fig. IV-20).

Chemical composition of epidote, and those of pumpellyite and chlorite are shown in Figs. IV-21 and IV-22, respectively. These values are similar to those of the surrounding Mikabu Greenrock Complex.

C) Epidote-amphibolite

Epidote-amphibolite occurs as a relatively large block, about 100 m in long diameter, in the greenrock mélange. It is dark green for unaided eyes, and is well schistose and coarse-grained. Many white prehnite veins, less than a few millimeters in width, crosscut the schistosity of the rock. Epidote-amphibolite is mainly composed of hornblende, epidote, albite and sphene with minor amount of secondary minerals, such as actinolite and prehnite.

Hornblende is green to pale yellowish green and coarse

columnar grains (0.1 x 1.0 mm). It is one of the main constituent minerals of schistosity. Actinolite occurs along rims and cracks of hornblende.

Epidote is usually unhedral and compose the matrix with hornblende. Grain size of epidote variates from 0.05 to 1.0 mm in diameter, and coarse grains are often cracked. These epidote is obviously richer in Al-content than those of the Mikabu Greenrock Complex (See Fig. IV-21).

Two other types of sodic pyroxene-bearing tectonic blocks were found in the western part of the Kanto Mountains by this study. One of them is mainly composed of hornblende, grandite garnet, sodic pyroxene and epidote, with minor amount of pumpellyite, chlorite, sphene and albite. Modal amount of hornblende, sodic pyroxene and garnet in this rock type variates at every hand specimen.

The other type is jadeite-analcite rock and is mainly composed of jadeite, white mica, grandite garnet, taramite, and pumpellyite with or without analcite vein. Although aragonite was not found in this rock, mineral assemblage and the mode of occurrence of the rock are similar to those of jadeite-aragonite rock reported by Tanabe et al.(1982). However, the locality of jadeite-analcite rock is about 5 Km westwards to that of Tanabe et al.(1982) (See Fig. III-1). Jadeite usually grows in amygdules of metabasites, about a few millimeters in diameter, associated with muscovite and

taramite. Analcite vein often crosscuts jadeite amygdules and the matrix. The chemical compositions of jadeite in this rock is shown in Fig. IV-20.

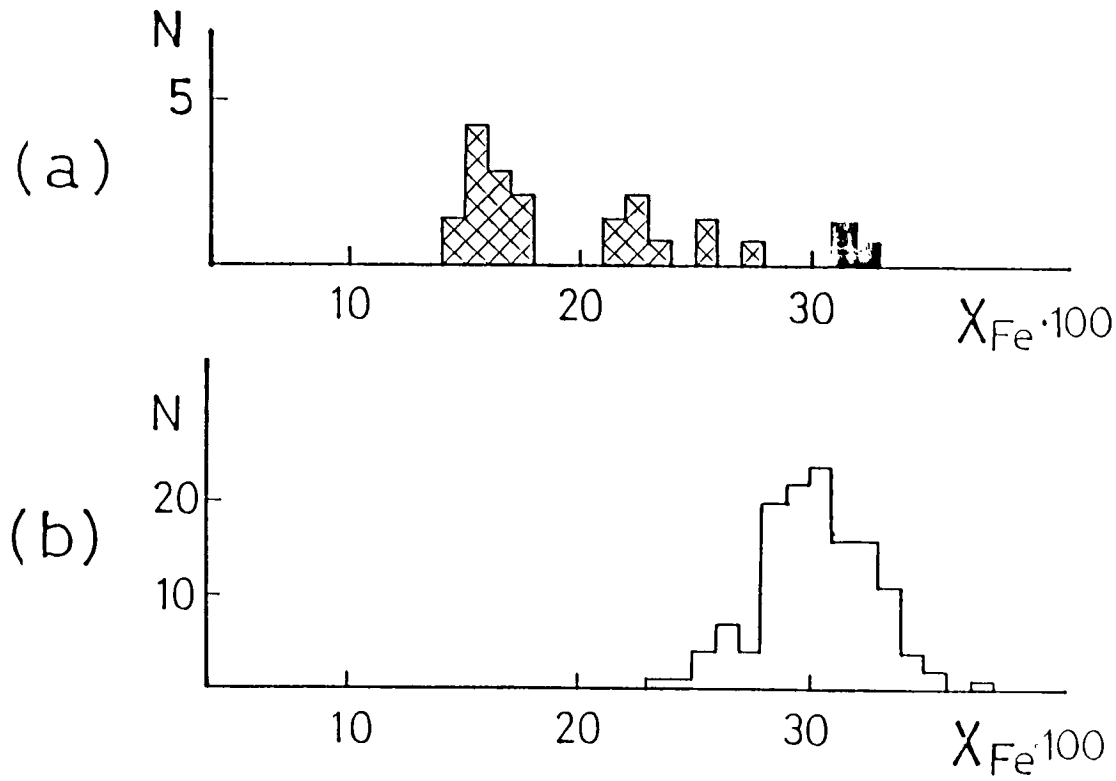

Fig. IV-21. frequency diagrams of XFe=Fe3+/(Al+Fe3+) ratio in epidote of tectonic blocks.
A) Epidote-amphibolite (Cross) and sodicpyroxene-sodic amphibole-bearing rock (Solid) in the greenrock melange.
B) The Mikabu Greenrock Complex.

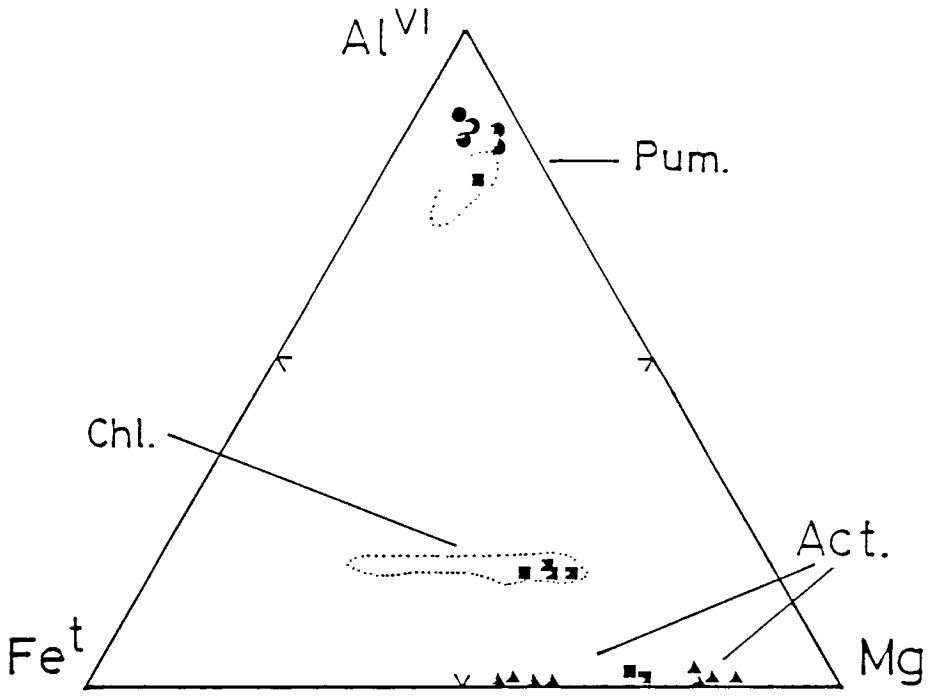

Fig. IV-22. Chemical compositions of chlorite, actinolite and pumpellyite in tectonic blocks. Solid circle; Meta gabbro, Square; sodic pyroxene-sodic amphibole-bearing rock, Triangle; epidote-amphibolite, Dotted area; Compositional range of the Mikabu Greenrock Complex.

Table. IV-12. Compositions of prehnite, pumpellyite and epidote in the constituent rocks of the Tochiya Klippe.

Mineral	Na-px	Na-px	Na-am	Act	Act	Act	Hb	Chl	Pum	Ep	Ep	Pr
Rock No.	727	727	727	727	626	626	626	727	590	590	626	604
Point No.	-14	-96	-50	-51	-31	-32	-18	-59	-120	-118	-8	-10
SiO2	53.35	54.35	53.23	54.62	54.40	52.84	46.37	27.67	38.10	38.44	38.25	43.39
TiO2							.03	.18				
Al2O3	5.48	7.37	2.52	1.19	1.77	.63	11.22	17.90	27.09	23.92	27.06	21.63
Fe2O3*										12.15	8.18	2.79
FeO*	19.89	18.56	23.27	10.64	7.54	14.99	11.42	20.62	1.47			
MnO			.26		.20	.50	.20	.46				
MgO	1.65	1.84	7.83	17.32	18.61	13.49	13.54	20.83	3.10			
CaO	4.17	4.96	.83	11.91	12.80	12.08	12.03		23.66	23.60	23.62	26.74
Na2O	11.70	11.58	7.23	1.18	.63	.44	1.34					
K2O							.09					
Total	96.24	98.66	95.16	96.85	95.96	95.02	96.40	87.47	93.42	98.10	97.11	94.55
O=	6**	6**	23	23	23	23	23	14	24.5	25	25	11
Si	2.012	1.993	8.154	7.854	7.797	7.928	6.793	2.856	6.012	6.076	6.019	3.060
Al	.244	.319	.454	.202	.300	.112	1.937	2.177	5.037	4.456	5.018	1.797
Ti							.004	.020				
Fe3+	.588	.518								1.446	.969	.164
Fe2+	.040	.051	2.981	1.280	.904	1.880	1.400	1.779	.194			
Mn			.033		.024	.064	.025	.040				
Mg	.093	.101	1.787	3.711	3.977	3.017	2.957	3.204	730			
Ca	.169	.195	.136	1.834	1.966	1.942	1.889		3.999	3.996	3.982	2.020
Na	.856	.823	2.148	.328	.175	.129	.380					
K							.017					
Total	4.000	4.000	15.693	15.209	15.153	15.076	15.418	10.056	15.972	15.974	15.988	7.041

Rock No. 727= Na-px + Na-am rock
No. 626= Epidote amphibolite Tectonic blocks in the greenrock melange zone.
No. 590= Gabbro
No. 604= Conglomerate in the Tochiya Formation.

Abbreviations ; Na-am; Alkali-amphibole, Hb; Hornblende, Chl; Chlorite, The others are the same as Table, 1. O=; Numbers of Oxgens in the formula unit.

*; Total iron in epidote and prehnite as Fe2O3, in the other minerals as FeO.

**; Recalculated total cations as 4.000.

Table IV-13 Chemical composition of pyroxenes in the tectonic blocks of the Klippes

Sample No.	US331			5038		EC-6		EC-7	
Area	Shimonita			Shimonita		Shimonita		Shimonita	
Assemblage	EPC+Jd+Hb			PD+Garnet		EPC+Garnet		PC+Garnet	
Point. No.	5	13	37	10	12	8	12	3	8
Me/Re	Meta	Meta	Meta	Meta	Meta	Meta	Meta	Meta	Meta
SiO2	56.70	56.19	57.22	54.91	57.03	55.14	53.97	51.28	55.52
TiO2	.00	.00	.00	.00	.00	.50	.27	.00	.00
Al2O3	16.32	15.05	17.38	6.93	16.47	7.45	6.90	1.10	8.32
FeO*	8.01	11.17	8.97	14.23	10.16	14.16	14.86	23.57	13.45
MnO	.11	.30	.09	.29	.00	.00	.12	.63	.14
MgO	1.55	.43	.57	4.94	.32	4.32	4.55	3.55	4.09
CaO	3.63	3.72	1.43	11.39	2.33	8.06	8.67	13.02	8.12
Na2O	13.41	12.98	14.44	8.26	14.15	9.99	8.86	6.07	9.89
Total	99.72	99.85	100.07	100.95	100.46	99.61	98.20	99.22	99.55
O=6									
Si	2.022	2.033	2.030	2.036	2.032	2.058	2.053	2.053	2.063
Al	.686	.642	.727	.303	.692	.328	.309	.052	.364
Ti	.000	.000	.000	.000	.000	.014	.008	.000	.000
Fe	.239	.338	.266	.441	.303	.442	.473	.789	.418
Mn	.003	.009	.003	.009	.000	.000	.004	.022	.005
Mg	.082	.024	.030	.273	.017	.240	.258	.212	.227
Ca	.139	.144	.054	.453	.089	.322	.353	.559	.323
Na	.927	.911	.991	.594	.977	.723	.653	.471	.712
Total	4.098	4.101	4.101	4.109	4.110	4.129	4.111	4.157	4.112
X(Jd)	.64	.61	.70	.29	.65	.31	.31	.05	.35
X(Ac)	.23	.26	.25	.28	.27	.38	.34	.41	.34
X(Di)	.13	.14	.05	.43	.08	.31	.35	.54	.31

*:Total iron as FeO

V. Graphical representation of prograde metamorphism

(V-1) Schreinemakers' analyses of a model ACF system

(1-1) Introduction

Since the proposal of Miyashiro (1961) to classify regional metamorphism in terms of pressure, the differences and similarities of the glaucophanitic metamorphic belts have been discussed by many petrologists, such as Banno (1964), Ernst et al.(1970), Brothers (1974), Brown (1974, 1977a) and Black (1977).

Brown (1977a) has presented a petrogenetic grid which compares the metamorphic conditions of different belts. Most petrogenetic grids for glaucophanitic metamorphism were based on the synthetic experiments for the main constituent minerals, such as jadeite + quartz = albite, jadeite = albite + nepheline, or aragonite = calcite, and the main mineral assemblages observed in nature. The petrogenetic grids of this type are convenient to compare main mineral assemblages between metamorphic belts, but they can not predict all possible assemblages of the same system.

Actually, sodic pyroxene-bearing mineral assemblages, which have not been found in the Sanbagawa belt of Shikoku (EPDC, and EADC assemblages, see Chapter III), occur in the lower-grade metabasites of the study area. To understand the stability of sodic pyroxene-bearing assemblages, a petrogenetic grid for a basaltic system was produced by the Schreinemakers' method in a model ACF system with seven phases; lawsonite, epidote, pumpellyite, diopside,

actinolite, glaucophane and chlorite. From the topological arguments of the Schreinemakers' bundles, seven possible sets of invariant points, and ten geometrically independent petrogenetic grids of univariant curves are derived. For the basaltic bulk composition, seven independent petrogenetic grids of metamorphic facies are obtained. The comparison with natural mineral assemblages reported from the Sanbagawa, New Caledonia and Franciscan metamorphic belts (Banno et al., 1978; Black, 1977; Ernst et al., 1970) rejects five of them and leaves only two.

Both of possible grids of metamorphic facies predict that the sodic pyroxene-bearing assemblages are stable at a lower-grade of high-pressure intermediate group of metamorphism. The construction of the petrogenetic grids by the Schreinemakers' method will be described in the following sections.

(1-2) Components and phases

The physical conditions of lower-grade metamorphism (less than about 500°C) have been discussed mainly by mineral assemblages in metabasites, which are sensitive to the metamorphic condition. As described in Chapter III, mineral assemblages of lower-grade metabasites were discussed in the following pseudo-four component system; $(Al_2O_3\text{-}Na_2O\text{-}3K_2O)\text{-}Fe_2O_3\text{-}(FeO+MgO)\text{-}CaO$ with excess albite, quartz, muscovite and fluid phase, taking $Fe^{2+}/(Fe^{2+}+Mg)$

ratio of chlorite as the index of $Fe^{2+}/(Fe^{2+}+Mg)$ ratio of the system. However, the correlation between compositions of constituent minerals and bulk rock composition was not fully understood to construct the petrogenetic grids for a four component system. As the first step to construct petrogenetic grids for four and five component systems, the mineral assemblages in the model ACF system will be discussed in this Chapter. For this approximation, component "A" is equal to ($Al_2O_3+Fe_2O_3-Na_2O-3K_2O$), "C" is CaO, and "F" is (FeO+MgO). This treatment harms to discuss the exact stability fields of minerals which involve Fe^{3+}-Al substitution, such as sodic pyroxene, sodic amphibole and Ca-Al silicates, but is still effective to predict the stability fields of some unknown or scarcely noticed assemblages.

Following six phases commonly occur in lower-grade metabasites of the glaucophanitic metamorphic belts; lawsonite, pumpellyite, epidote, glaucophane, actinolite and chlorite. In the typical high pressure belts, such as New Caledonia and Franciscan, sodic pyroxene commonly occurs in various kinds of lithofacies (Black, 1977; Ernst et al., 1970). Earlier part of this thesis pointed out that sodic pyroxene, which is characterized by low X_{Jd}, also occurs in lower-grade metabasites of the Sanbagawa belt. Therefore, it is necessary to add sodic pyroxene to six phases mentioned above for the analysis of the stability relation in lower-grade metabasites of high pressure belts. Fig. V-

Table V-1. Abbreviation, formula and molar volume of seven phases.

Mineral	Abb.	Formular	M.V.(cc/mol)
Lawsonite	(L)	$CaAl_2Si_2O_8 2H_2O$	101.3(5)
Glaucophane	(G)	$Na_2Mg_3Al_2Si_8O_{22}(OH)_2$	259.7(1)
Epidote	(E)	$Ca_2Al_3Si_3O_{12}(OH)$	136.4(2)
Diopside	(D)	$CaMgSi_2O_6$	66.1(5)
Pumpellyite	(P)	$Ca_4MgAl_5Si_6O_{23}(OH)_3 2H_2O$	295.6(3)
Actinolite	(A)	$Ca_2Mg_5Si_8O_{22}(OH)_2$	272.9(5)
Chlorite	(C)	$Mg_5Al_2Si_3O_{10}(OH)_8$	210.0(4)
Quartz	(Q)	SiO_2	22.7(5)
Albite	(Ab)	$NaAlSi_3O_8$	100.1(5)
Water	(W)	H_2O (350°C,3.5Kb)	19.8(6)

Molar Volume(M.V.) reffered from Borg(1967)-(1), Myer(1966)-(2), Schiffman and Liou(1980)-(3), Chernosky(1975)-(4), Robie and Waldbaum(1968)-(5), and Burnham et al.,(1969)-(6)
Abb.:abbreviation.

Fig. V-1. Seven phases on the ACF diagram.

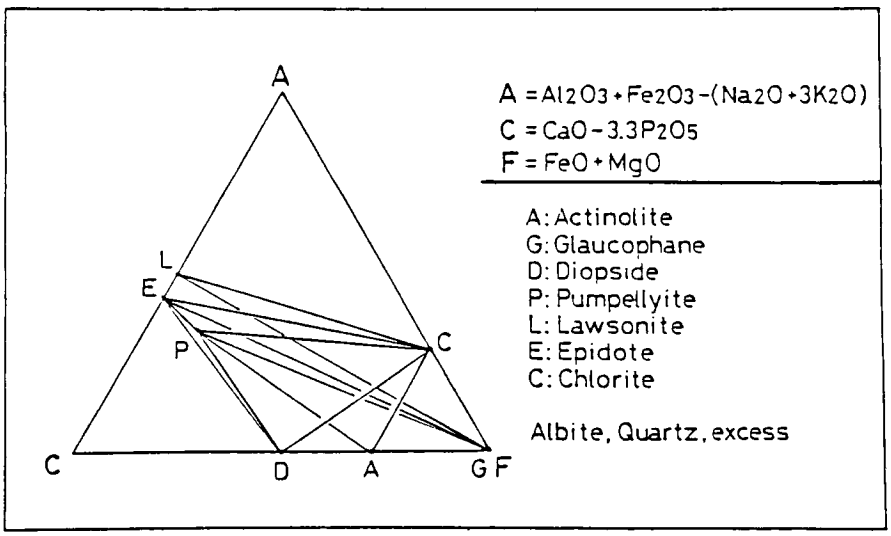

1 shows the seven phases on the ACF diagram, and Table V-1 does abbreviation, formula, and molar volume of them. Al- and Mg-end compositions are used for solid solutions of minerals which contain Fe^{3+}-Al and Fe^{2+}-Mg substitutions, respectively. Al/Si ratio (=2/3) of chlorite is approximated by the actual data of the Kanto Mountains (Toriumi, 1975 and this study). Sodic pyroxene associated with albite is assumed to diopside (D) in this model system and is always plotted at the position of diopside of the ACF diagram, because the Fe^{3+}-Al substitution is considered unimportant.

This model system is applicable to the P-T range from 3 to 10 Kb and 300°C to 500°C, because it assumes the stable existence of albite and quartz, and does not consider garnet, barroisite, hornblende, zeolite nor prehnite (Nitsch, 1968, 1971; Liou, 1971; Black, 1977; Brown, 1977a).

(1-3) Procedure to derive the petrogenetic grids

An invariant point for a 3-component system in P-T field requires that five phases be in equilibrium, and an univariant line requires four phases. For the general case with seven phases taken five at a time, there will be 21 ($_7C_5$) invariant points. They are represented by an abbreviation and a number in Table V-2. As an invariant point involves five of the seven phases, the abbreviation of invariant point is designated by brackets [ ], which contain

Table V-2. Invariant points and 5 univariant reaction lines(4 in the case of degeneration) which radiate from each invariant point.

INVARIANT POINT	REACTION LINES
[1][L,G]	V-1 V-2, V-3, V-4. V-5,
[2][E,G]	V-1, V-6, V-7, V-8, V-9,
[3][D,G]	V-2, V-6, V-10, V-11, V-12,
[4][P,G]	V-3. V-7, V-10, V-13, V-14.
[5][A,G]	V-4, V-8, V-11, V-13, V-15,
[6][C,G]	V-5, V-9. V-12, V-14, V-15,
[7][E,L]	V-1, V-16, V-17, V-18,
[8][D,L]	V-2, V-16, V-19, V-20, V-21,
[9][P,L]	V-3, V-17, V-19, V-22,
[10][A,L]	V-4, V-18, V-20, V-22, V-23,
[11][C,L]	V-5, V-17, V-21, V-23,
[12][D,E]	V-6, V-16, V-24, V-25, V-26,
[13][P,E]	V-7, V-17, V-24, V-27,
[14][A,E]	V-8, V-18, V-25, V-27, V-28,
[15][C,E]	V-9, V-17, V-26, V-28,
[16][P,D]	V-10, V-19, V-24, V-29. V-30,
[17][A,D]	V-11, V-20, V-25, V-29, V-31,
[18][C,D]	V-12, V-21, V-26, V-30, V-31,
[19][A,P]	V-13, V-22, V-27, V-29, V-32,
[20][C,P]	V-14, V-17, V-30, V-32,
[21][C,A]	V-15, V-23, V-28, V-31, V-32,

2 abbreviations for phases not involved. The number of invariant point is also designated in the brackets [ ].

For the general case with seven phases taken four at a time , there will be 35 ($_7C_4$) univariant lines. However, G(glaucophane), A(actinolite) and D(sodic pyroxene) are collineared on the CF edge of the ACF diagram (Fig. V-1). Therefore, following four univariant assemblages which contain them , G+A+D+ C(chlorite), G+A+D+ P(pumpellyite), G+A+D+ L(lawsonite) and G+A+D+ E(epidote), are degenerated and represented by the following reaction,

D(diopside) +G(glaucophane) =A(actinolite) ----(V-17)

$$2CaMgSi_2O_6 + Na_2Mg_3Al_2Si_8O_{22}(OH)_2 + 2SiO_2 = Ca_2Mg_5Si_8O_{22}(OH)_2 + 2NaAlSi_3O_8$$

so there rest 32 independent univariant reaction lines in this system. The 32 independent univariant assemblages and 32 reactions corresponding to each assemblage are tabulated in Table V-3. Five (four in the case of degeneration) univariant reaction lines radiate from each invariant point. Abbreviation numbers of them are also listed in Table V-2. To simplify the description of invariant point and univariant line, the abbreviations of them shown in Tables V-2 and V-3 are used.

Morey-Schreinemakers rule (Zen, 1966a) decides the topology of univariant reaction lines radiating from each invariant point. Zen (1966a) depicted the correlation between the topology of univariant reaction lines around an invariant point and the chemographic relation of phases

Table V-3. 32 independent univariant assemblages and 32 reactions corresponding to each assemblage.

U.A.	NO.	REACTION	dP/dT
DPAC	V-1	15C+86D+67Q=6P+31A+8W	103.8
EAPC	V-2	25P+2C+29Q=43E+7A+67W	53.3
EDAC	V-3	50D+9C+43Q=6E+19A+14W	63.6
EDPC	V-4	19P+10Q=C+31E+14D+47W	52.6
EDPA	V-5	9P+7Q=15E+4D+A+23W	52.9
LPAC	V-6	86L+17A=30P+11C+95Q+40W	26.0
LDAC	V-7	L+2A=5D+C+5Q	0.0
LDPC	V-8	31L+17D=12P+C+21Q+16W	28.1
LDPA	V-9	11D+15L=6P+A+8Q+8W	28.8
LEAC	V-10	10L+A=6E+C+7Q+14W	37.9
LEPC	V-11	14L+5P=17E+C+4Q+33W	44.2
LEPA	V-12	4L+5P+3Q=11E+A+19W	44.4
LEDC	V-13	19L+5D=12E+C+9Q+28W	40.3
LEDA	V-14	9L+5D=6E+A+2Q+14W	41.1
LEDP	V-15	P+Q=L+E+D+W	95.6
GPAC	V-16	12A+15C+86Ab=6P+43G+19Q+8W	-2.7
DGA	V-17	A+2Ab=2D+G+2Q	0.0
GDPC	V-18	24D+15C+62Ab+5Q=6P+31G+8W	-3.8
GEAC	V-19	9C+6A+50Ab=25G+6E+7Q+14W	-9.0
GEPC	V-20	6P+3C+14Ab+5Q=7G+12E+20W	-146.8
GEPA	V-21	2G+9P+11Q=15E+3A+4Ab+23W	39.8
GEDC	V-22	12D+9C+38Ab+5Q=19G+6E+14W	-12.3
GEDP	V-23	9P+2Ab+5Q=6D+15E+G+23W	63.3
GLAC	V-24	A+2C+10Ab=5G+2L	0.0
GLPC	V-25	17G+24L=6P+9C+19Q+34Ab+8W	5.0
GLPA	V-26	30L+9A+22Ab=12P+11G+38Q+16W	-69.8
GLDC	V-27	D+C+4Ab+Q=2G+L	0.0
GLDP	V-28	15L+9D+2Ab=G+6P+10Q+8W	38.8
GLEC	V-29	5G+12L=6E+3C+10Ab+7Q+14W	19.0
GLEA	V-30	3A+18L+10Ab=12E+5G+14Q+28W	86.3
GLEP	V-31	3P+6L+2Ab=G+9E+Q+17W	56.6
GLED	V-32	3D+9L+2Ab=G+6E+4Q+14W	52.0

U.A.; univariant assemblage.

composing the invariant assemblage for the 3 component system. This method provides two possible cases of topology which are related in mirror image. The slope of the univariant reaction lines in the P-T field can be calculatedby using a series ofapproximations. This procedure decides a unique topology around an invariant point, and reduces the number of the possible petrogenetic grids by half. Consider a typical dehydration reaction:

$$A_s + B_s = C_s + D_s + n(H_2O)_f \quad \text{----- (9)}$$

where the subscript "s" indicates a solid phase and the subscript "f" indicates a fluid phase which is herein assumed to be pure H_2O. The slope is given by the equation (Thompson, 1955):

$$\left(\frac{dP}{dT}\right)_{G=0} = \frac{\Delta S}{\Delta V_s + n(H_2O)V_{H2O}(dP_{H2O}/dP_s)} \quad \text{-----(10)}$$

where P_s, ΔV_s and ΔS represent the solid pressure, the change in volume of solid phase and the change in entropy respectively, V_{H2O} is the molar volume of water at specified P_{H2O} and T, and $n(H_2O)$ is the number of moles of H_2O given by the reaction. Assuming that $P_{H2O}=P_s$, Thompson's equation is modified to:

$$\left(\frac{dP}{dT}\right)_{G=0} = \frac{\Delta S}{\Delta V_s + n(H_2O)V_{H2O}} \quad \text{-----(11)}$$

Equation (11) corresponds to that of case I of Albee (1965).

Assuming that the change of the molar volume of the solid phases with the change of P-T conditions, $(dV_s/dP)_T$ and $(dV_s/dT)_P$, is negligible small, the molar volumes of the

solid phases are referred to those at the standard state (Table V-1). V_{H2O} was taken as 19.8 cc/mol, the value at 350°C and 3.5 Kb (Burhnam et al., 1969), because this value roughly represents the median of V_{H2O} under the P-T range considered. Entropy of the complex silicates may be estimated by the addition of the entropies of complex oxides (Fyfe et al., 1958). Hence the entropy change in a dehydration reaction ($\Delta S_{Dehydration}$) is approximated by the entropy of the H_2O in the fluid phase ($S_{(H2O)f}$) minus the entropy of H_2O in the solid phase ($S_{(H2O)s=Ice}$):

$$\Delta S_{Dehydration} = S_{(H2O)f} - S_{(H2O)s=Ice} \quad -----(12)$$

$\Delta S_{Dehydration}$ at 350°C and 3.5 Kb is estimated as about 12 (cal/mol.deg) from Figs.32 and 33 of Fyfe et al.(1958). Slopes of univariant reaction lines calculated from these assumptions are tabulated in Table V-3.

We are mainly interested in the topology of the grid. Sofar as the compositions of constituent minerals are fixed in this model system (Table V-1), the change of slopes, caused by changes of ΔS and ΔV with the P-T conditions or estimated errors in them, are insignificant. Therefore, the univariant reaction lines are straight in P-T space with a slope tabulated in Table V-2 in the following discussion. Although a univariant line of a solid-solid reaction is usually a straight line with small positive slope in the P-T field, this paper regards it as a straight line parallel to the temperature axis, i.e., $dP/dT=0$ as assumption of $\Delta S=0$ in the case of the solid-solid reaction.

Among 32 univariant reactions, only one was determined by the synthetic experiments by Nitsch (1971) and Schiffman and Liou (1980):

P(pumpellyite)+C(chlorite) =

E(epidote) +A(actinolite) + H_2O --- (V-2)

$25Ca_4FAl_5Si_6O_{23}(OH)_32H_2O + 2Mg_5Al_2Si_3O_{10}(OH)_8 + 29Si_2O =$

$43Ca_2Al_3Si_3O_{12}(OH) + 7Ca_2Mg_5Si_8O_{22}(OH)_2 + 67H_2O$

Therefore, there is no invariant point of which stability is established by the synthetic work.

Korzhinskii (1959) outlined the method to examine the stability of invariant points. He regarded a three component - seven phases multisystem with two independent variables as a system with (-2) degrees of freedom, and showed that three independent invariant points share a univariant line of non-degenerate (his Table 2) and that not all of three invariant points are stable at a time.

Different relations are possible among three invariant associations sharing a univariant association in common, excluding degenerate equilibrium. Which part of the line being stable depends on both the relative position of invariant points and the radiating direction of the line from each point. There are two possible relationships between a univariant reaction line and invariant points:

A) radiating in the same direction from three invariant points (case a in Fig. V-2).

B) radiating in the same direction from two of three

invariant points, but in the opposite direction from the other (cases b, c, d and e in Fig. V-2).

In case A, only one invariant point is stable on the univariant line and a stable part of the line is a half line starting from the stable invariant point. In case B, a possible set of two invariant points is stable and the rest is metastable at the same time. A stable part of the univariant line is bounded by two stable invariant points. There will be two possible sets of two stable invariant points on a line, but they are not stable at a time. All possible topological relations between radiating direction and the relative position of invariant points on a univariant line are depicted in Fig. V-2. Case A corresponds to "heterotypical with regard to the stability", and case B to "homotypical with regard to the stability" of Korzhinskii (1959).

Homotypical and heterotypical relations on each univariant line are tabulated in Table V-4. Homotypical invariant points represented by the number in the brackets [ ] are bound by the symbol "-", and heterotypical ones by the symbol "x". Among a set of homotypical points, the point on the left of the symbol "-" is situated at the end point of lower-pressure side on the stable univariant line (if $dP/dT=0$, at the end point of lower-temperature side on the univariant line).

Fig. V-2. Stable part (solid line) on univariant reaction lines. Arrow shows radiating direction of univariant line from each invariant point.
a) radiating in the same direction from three invariant point.
b) - d) radiating in the same direction from two of three points, but in the opposite direction from the other.

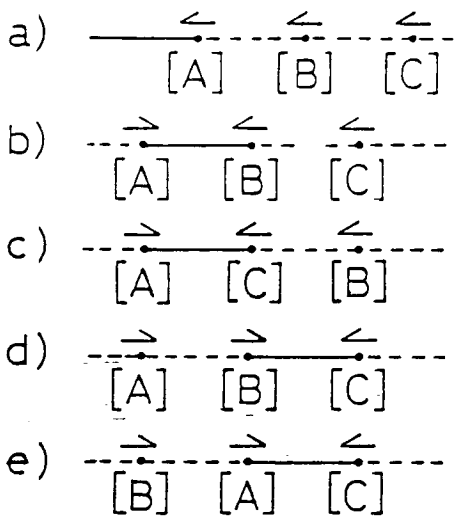

Fig. V-3. Topological relation of the diversion on a tie linein the invariant points circuit. The tie line diverses at a junction symboled as "●". End of it marked with an arrow represents the high-pressure side of the invariant point on a univariant line (if dP/dT=0, high-temperature side one).
a) in the cases of b) and c) in Fig. V-2.
b) in the cases of d) and e) in Fig. V-2.

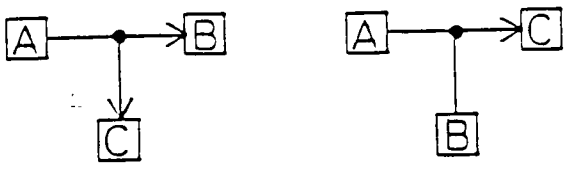

Table V-4. Homotypical or heterotypical relations on each univariant line.

Reaction No.	homo.	hetero.
V-1	[1]-[2] [1]-[7]	[2]x[7]
V-2	[1]-[3] [1]-[8]	[3]x[8]
V-3		[1]x[4]x[9]
V-4		[1]x[5]x[10]
V-5	[1]-[6] [1]-[11]	[6]x[11]
V-6	[2]-[3] [2]-[12]	[3]x[12]
V-7	[13]-[2] [13]-[4]	[2]x[4]
V-8		[2]x[5]x[14]
V-9	[2]-[6] [2]-[15]	[6]x[15]
V-10	[3]-[16] [4]-[16]	[3]x[4]
V-11		[3]x[5]x[17]
V-12	[3]-[6] [3]-[18]	[6]x[18]
V-13	[5]-[4] [5]-[19]	[4]x[19]
V-14	[4]-[20] [6]-[20]	[4]x[6]
V-15		[5]x[6]x[21]
V-16	[8]-[7] [8]-[12]	[7]x[12]
V-17	[7]-[11] [15]-[11] [13]-[15] [13]-[20]	[7]x[9]x[13] [9]x[11]x[20]
V-18	[7]-[14] [10]-[14]	[7]x[10]
V-19		[8]x[9]x[16]
V-20	[8]-[17] [10]-[17]	[8]x[10]
V-21	[8]-[11] [18]-[11]	[8]x[18]
V-22	[9]-[10] [9]-[19]	[10]x[19]
V-23	[10]-[21] [11]-[21]	[10]x[11]
V-24	[13]-[12] [13]-[16]	[12]x[16]
V-25	[12]-[17] [14]-[17]	[12]x[14]
V-26	[12]-[15] [18]-[15]	[12]x[18]
V-27		[13]x[14]x[19]
V-28	[14]-[21] [15]-[21]	[14]x[15]
V-29		[16]x[17]x[19]
V-30	[16]-[18] [16]-[20]	[18]x[20]
V-31	[17]-[21] [18]-[21]	[17]x[18]
V-32		[19]x[20]x[21]

homo; Homotypical
hetero; Heterotypical

(1-4) Invariant points circuit and the petrogenetic grid of the univariant curves

A petrogenetic grid based on the Schreinemakers' method is composed of invariant points and the univariant reaction lines radiating from invariant points. To decide the position of invariant points of the petrogenetic grid in the P-T field, it is necessary to know the all geometrically independent parameters $\langle=2+3(c+2)\rangle$ in the multisystem with (-2) degrees of freedom; "c" is the number of the component in the system (Korzhinskii, 1959), and the geometrically independent parameters are the exact position of an invariant point in the P-T space, 2, the slopes of the univariant reaction lines, (c+2), and the distance between two stable invariant points on a homotypical univariant reaction lines, 2(c+2). As we have the slopes of 32 reaction lines, we can deduce the possible sets of invariant points to constitute the petrogenetic grids.

In a petrogenetic grid by the Schreinemakers' method, the univariant reaction line of homotypical relation binds invariant points, but that of heterotypical one does not. Therefore, all possible sets of invariant points constituting the petrogenetic grid can be derived from the examination of the all permutations and combinations of invariant points in homotypical relation. To solve the problem, an invariant points circuit (Fig. V-4) was proposed by the author. The invariant points circuit is composed of invariant points in homotypical relation,

represented by the number in a square, and solid tie lines binding them, which correspond to stable univariant lines.

There are two possible sets of homotypical invariant points on a univariant line, and hence this relation will be represented by the diversion of a tie line in the invariant points circuit. All possible cases of topological relation of the diversion on a non-degenerate line are depicted in Fig. V-3. The tie line diverses at a junction symboled as "●", and the end of it marked with an arrow represents the high-pressure side of the invariant point on a univariant reaction line (if dP/dT=0, high temperature side one). A set of homotypical invariant points [A] and [B], and that of [A] and [C] is stable alternatively on a line in the cases of b) and c) in Fig. V-2. These relations will be represented in Fig. V-3a on the invariant points circuit, and the cases d) and e) of Fig V-2 in Fig. V-3b. All possible sets of homotypical invariant points in this model system provide the invariant points circuit shown in Fig. V-4.

One end of a tie line with an arrow is defined as "tie line of inflow", and the other end of the tie line without an arrow as "tie line of outflow". An invariant point generally possesses tie lines of both inflow and outflow. However, some invariant points are exclusively composed of tie lines of inflow and are defined as "an invariant point of inflow", and those exclusively composed of tie lines of

Fig. V-4. Invariant points circuit. Invariant points, [1], [5] and [9] are those of outflow, and invariant points, [19], [20] and [21] are those of inflow. Invariant points of out flow are shown by the symbol "⊡". One possible set of invariant points, [9], [10], [14], [17] and [21], is shown by dotted line.

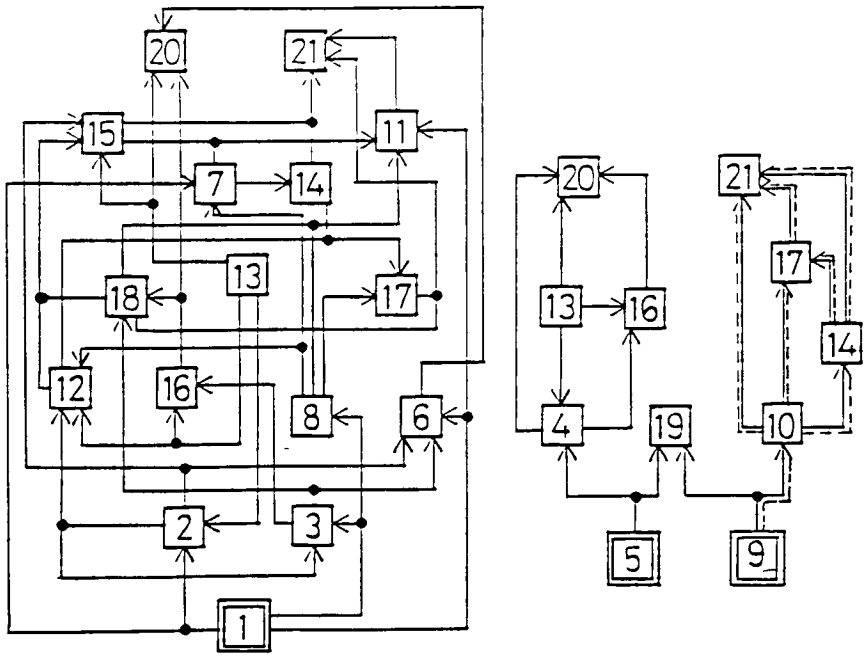

Table V-5. Seven independent sets of invariant points. The abbreviation number of the set and the abbreviation number on invariant points constituting eachset are tabulated.

1,	[5],[9],[19]
2,	[4],[5],[13],[16],[20]
3,	[9],[10],[14],[17],[21]
4,	[1],[2],[3],[6],[13],[16],[20]
5,	[1],[7],[8],[11],[14],[17],[21]
6,	[1],[2],[3],[11],[13],[15],[16],[18],[21]
7,	[1],[2],[8],[11],[12],[13],[15],[17],[21]

outflow are as "an invariant point of outflow". No invariant point exists at lower-pressure field than the position of the invariant point of outflow in the P-T field of petrogenetic grids. The invariant point of inflow means that this point is situated at the highest pressure position among the invariant points constituting petrogenetic grids. In the model system, invariant points [1], [5] and [9] are those of outflow, and invariant points [19], [20] and [21] are those of inflow. Slopes of univariant reaction lines which concentrate to invariant point [13] are always zero (dP/dT=0), and hence this point is situated outside of the P-T area for the model system. Therefore, invariant point [13] is not treated as an invariant point of outflow, nor as that of inflow in this model system, although Fig. V-4 depicted this point as an invariant point of outflow.

A set of invariant points [1] and [9] is in the heterotypical relation on a reaction (V-3), and that of [1] and [5] is also on the same reaction (V-4) (Table V-4). Hence, invariant point [1] can not coexist with invariant point [9] on the reaction line (V-3) , nor with [5] on the reaction line (V-4) at the same time. Therefore, there are two series of invariant points circuit for the model system: one of them contains invariant point [1] as that of outflow and invariant points [20] and [21] as those of inflow. The other does [5] or [9] as invariant points of outflow and [19], [20] and [21] as those of inflow (Fig. V-4).

All possible combinations of invariant points which

construct the petrogenetic grid can be derived from the invariant points circuit in the following procedure. Reaction (V-22) indicates that a set of invariant points [9]-[19], and that of [9]-[10] are homotypical with each other, and one of two sets is stable alternatively. Therefore, one of tie lines corresponding to the reaction (V-22) in the invariant points circuit becomes stable. First, consider the case that the tie line [9] - [10] is stable. This assumption makes invariant point [10] stable, and hence all univariant reactions which concentrate to [10] must be stable. Reactions (V-18), (V-20) and (V-23) indicate that tie lines of [10] - [14], [10] - [17], and [10] - [21] are stable. In the same way, as invariant points [14]-[17] become stable, tie lines [14] - [21], and [17] - [21] are selected from reactions (V-28) and (V-31), respectively (Table V-4). Because there is no tie line which outflows from invariant point [21], the following possible set of invariant points is obtained; (1), a set consisting of invariant points [9], [10], [14], [17] and [21], and this set is shown in Table V-4 adding a dotted line parallel to solid tie lines, and (2), a set in which tie line [9] - [19] is stable instead of [9] - [10].

By continuing this procedure, four independent sets of invariant points are derived from the invariant points circuit which starts from the invariant point of outflow [1], and three sets from the invariant points circuit

starting from points [5] and [9]. They are tabulated in TableV-5 with the abbreviation number of the set and the abbreviation number of invariant point constituting each set.

By combining invariant points by a homotypical univariant line, seven sets of invariant points are obtained. As mentioned in a foregoing section, there is no information about the distance between two stable invariant points on a line, thus one set of invariant points can provide one or plural geometrically independent petrogenetic grid of univariant curves.

Fig. V-5 gives an example of one possible petrogenetic grid of univariant curves derived from a set of invariant points, No.7, tabulated in Table V-5. This petrogenetic grid is composed of eight invariant points, and the relative positions of seven of them in this grid aredecided uniquely from the topology of univariant curves at each invariant point. However, the ambiguity of distance between invariant points on a line gives two possible geometrical positions of invariant point [17][A,D].

Case 1 ; invariant point [17] exists at lower-pressure field of the univariant reaction (V-17) ----D+G=A---- where invariant points [11][C,L] and [15][C,E] are stable.

Case 2; invariant point [17] is stable at higher-pressure field of the reaction (V-17).

Fig. V-5a shows the petrogenetic grid of univariant curves in case 1. As mineral assemblages around invariant point

Fig. V-5a. One possible petrogenetic grid of univariant curves derived from a set of invariant points, No.7 in Table V-5.

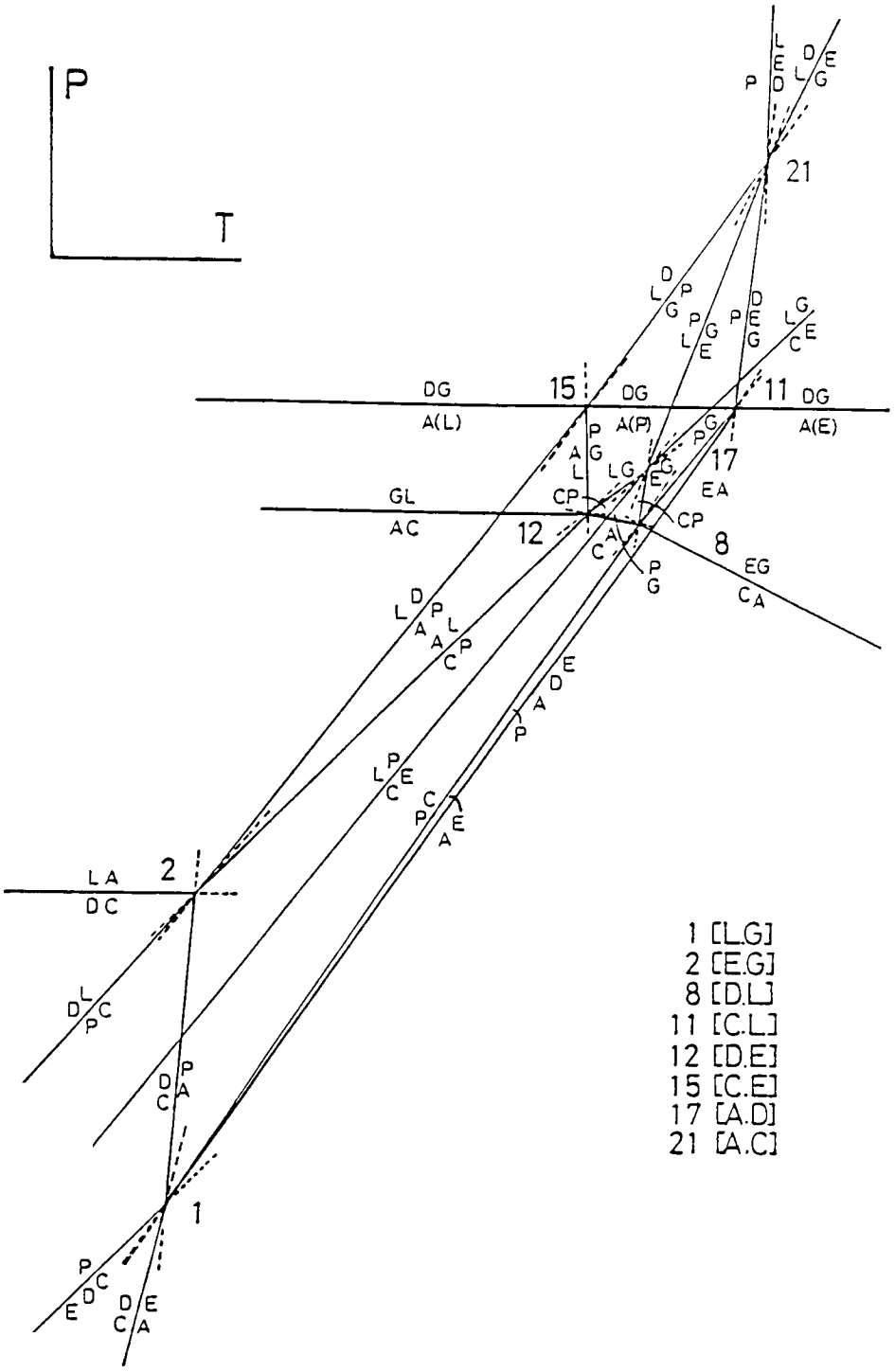

[17] are different between the two cases, one possible set of invariant points, No.7, provides two geometrically independent petrogenetic grids of univariant curves.

Similar situations exist between invariant point [6] [C,G] and the univariant reaction (V-24) --A+C=G+L-- in the set of invariant points, No.4, and between point [16][P,D] and the reaction (V-1) --C+D=P+A-- in No.6. Consequently seven possible sets of invariant points tabulated in Table V-5 provide ten geometrically independent petrogenetic grids of univariant curves.

(1-5) Petrogenetic grids of metamorphic facies

When we study the phase relation in a particular metamorphic belt, we usually give an attention to the mineral assemblages in rocks of common bulk chemical composition. As this paper intends to solve the mineral assemblages in lower-grade metabasites of the Sanbagawa belt in the Kanto Mountains, mineral assemblages and reactions in the basaltic system will be discussed in the petrogenetic grid of univariant curves.

Compositions of representative basaltic rocks and those of the Mikabu Greenrock Complex in the Kanto Mountains are plotted in the ACF diagram (Fig. V-6). Most of them are plotted in a region enclosed by three tie lines of EA, EG, and AC. This fact indicates that we should pay attention to the mineral assemblages and chemical reactions in this compositional field.

Fig. V-5b. Enlargement of the petrogenetic grid of univariant curves (Fig. 5a). Topological relation and divariant mineral assemblage around invariant point [17] are shown.

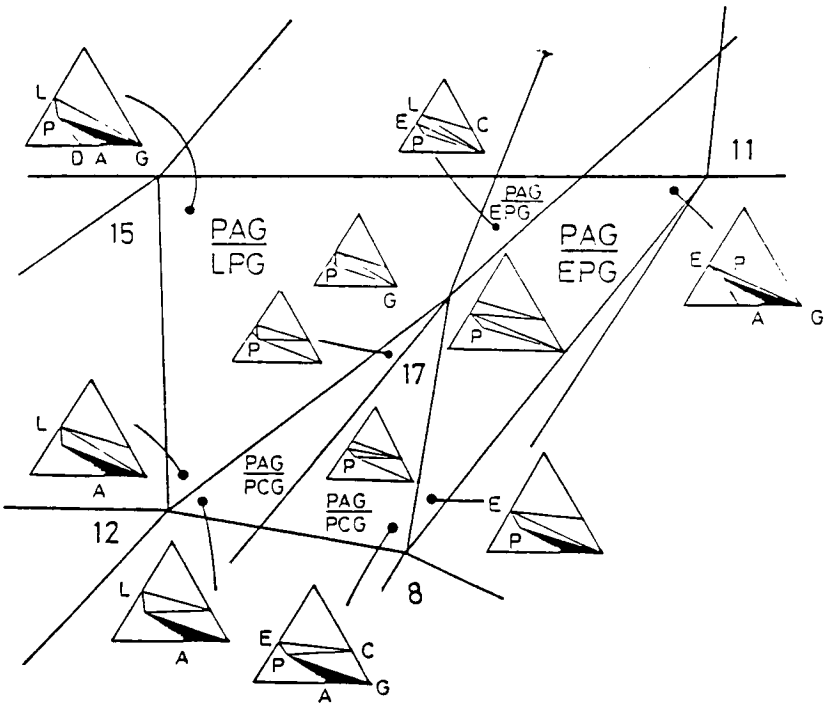

Fig. V-6. Compositions of representative basaltic rocks (solid symbols) and those of the Mikabu Greenrock Complex (open circle) on the ACF diagram.

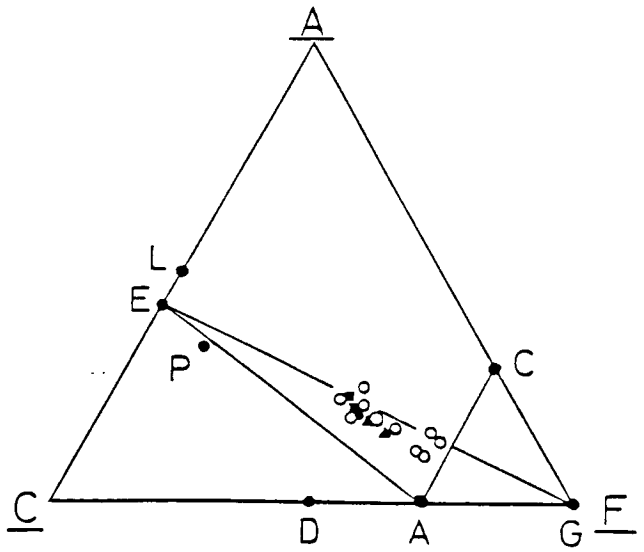

Topological relation and divariant mineral assemblages around invariant point [17] of the petrogenetic grid of univariant curves (Fig. V-5a) are enlarged in Fig. V-5b. Five univariant curves which radiate from invariant point [17] subdivide the square P-T field of which apexes are designated by following four invariant points, [15][C,E], [12][D,E], [8][D,L] and [11][C,L], into five subspaces. As basaltic rocks are plotted along the PG tie line in the ACF diagram, two divariant assemblages described by abbreviations of minerals in Fig. V-5b are possible in each subfield for basaltic rocks. This paper roughly approximates that the basaltic rocks are restricted to "C"-component rich and "A"-component poor side of the PG tie line in the ACF diagram. As this assumption permits PAG (pumpellyite + actinolite + glaucophane) divariant assemblage to be stable exclusively in all of the five subfields, the P-T field designated by invariant points, [15], [12], [8], and [11], is defined as PAG facies. Mineral assemblages defined by invariant point [17] always occur in "A"-component-rich side of the PG tie line. Hence, petrologically this invariant point is not important for the basaltic rocks in this model system, or in other words it is not necessary to distinguish petrologically two petrologic grids of univariant curves derived from the set of invariant points, No.7. Similarly, invariant point [16] in the set of invariant points, No.4, and the univariant

reaction (V-1) in the set of invariant points, No.6, are also unimportant for the model system. Consequently, seven independent petrogenetic grids have petrological significance. A mineral facies corresponds to a region in P-T field bounded by univariant lines. It is not practical to define a mineral facies for all possible regions bounded by univariant lines. It is suffice to define it as a region bounded by the univariant lines corresponding to the reactions which commonly occur in representative rock type in regional metamorphic belts. Basaltic composition has been traditionally regarded as such a common rock type (Eskola, 1920, 1939). Defining a mineral facies for basaltic rocks is also the interest of the author for reasons stated above. The author therefore defines a grid of metamorphic facies by the net of univariant lines relevant for the metamorphic reactions among basaltic original rocks. Hence, seven grids of univariant curves are rewritten by solid tie lines and dotted ones; Solid tie line corresponds to the univariant reaction which is relevant for the basaltic system, i.e., in the PAG field of the ACF diagram, and dotted one not for the basaltic system. They are depicted in Fig. V-7. The univariant mineral assemblages which represent each metamorphic facies are described in corresponding P-T field by the abbreviations of minerals, such as PAC and DPC.

Among seven possible grids of metamorphic facies, that of No.3 (Fig. V-7c) does not include PA (pumpellyite -

actinolite) assemblage which commonly occurs in the Sanbagawa belt. That of No.4 (Fig. V-7d) does not include PG (pumpellyite - glaucophane) assemblage which commonly occurs in New Caledonia and Franciscan belt. Those of No.1 (Fig. V-7a), and No.2 (Fig. V-7b) do neither PA nor PG assemblages. Grids of metamorphic facies, No.5 (Fig. V-7e), No.6 (Fig. 7-f) and No.7 (Fig. V-7g), can represent the observed mineral assemblages in the glaucophanitic metamorphic belts. These three grids are very similar in respect to the topology and constituting invariant points. Similarities and differences among them will be discussed hereafter;

(Similarity)

1) Among Ca-Al silicates, L(lawsonite) is stable at high-pressure field, E(epidote) is at high-temperature field, and P(pumpellyite) is at intermediate field.
2) Among amphiboles, A(actinolite) is stable at low-pressure field, and G(glaucophane) is at high-pressure field.
3) Chlorite disappears at high-temperature and high-pressure field.

(Difference)

1) Stability fields of diopside (D) are divided into two fields by that of LA (lawsonite - actinolite) assemblage in the grids, No.6 and No.7; diopside is stably associated with chlorite in medium-pressure and low-temperature field, and with glaucophane in high-pressure field.

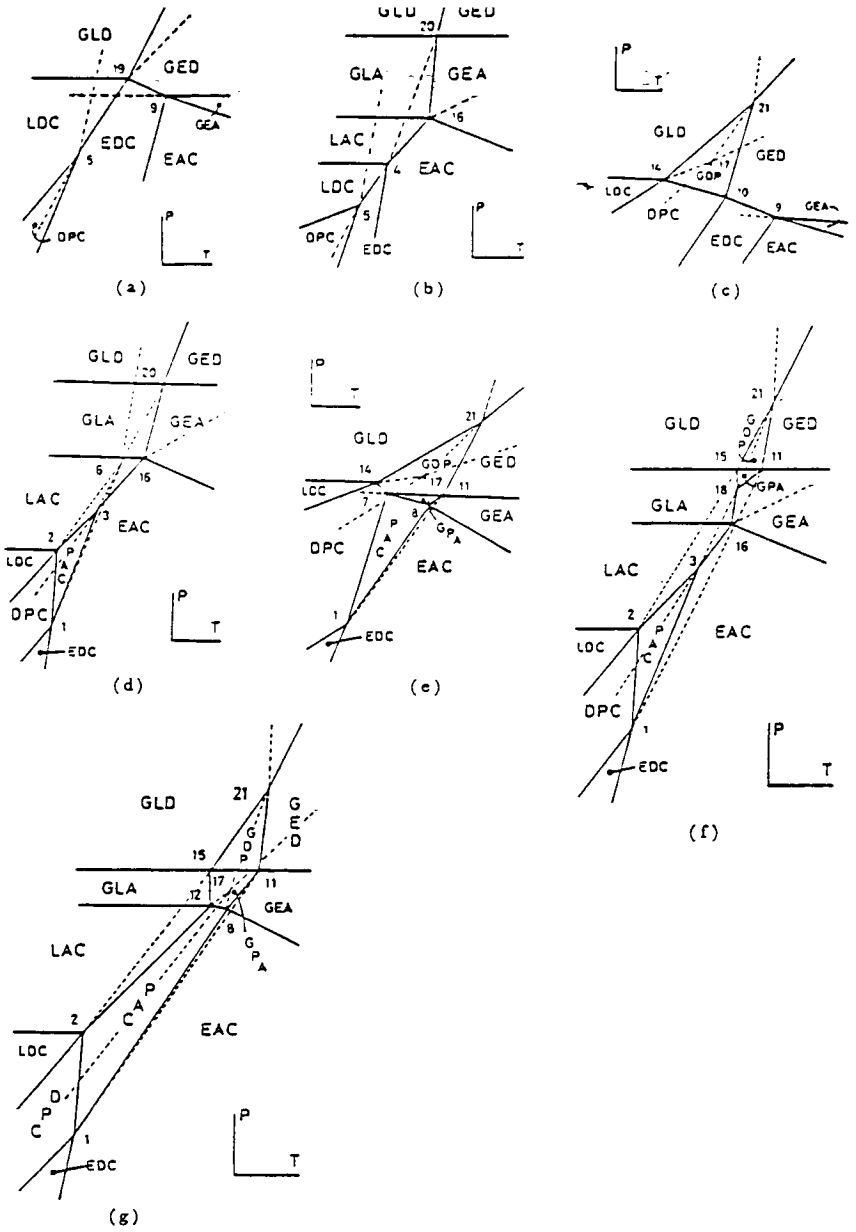

Fig. V-7a. The grid of metamorphic facies, No.1.
Fig. V-7b. The grid of metamorphic facies, No.2.
Fig. V-7c. The grid of metamorphic facies, No.3.
Fig. V-7d. The grid of metamorphic facies, No.4.
Fig. V-7e. The grid of metamorphic facies, No.5.
Fig. V-7f. The grid of metamorphic facies, No.6.
Fig. V-7g. The grid of metamorphic facies, No.7.

However, the grid, No.5, does not include the stability field of LA assemblage, and hence diopside is stable from medium-pressure to high-pressure field.

2) Pumpellyite is rare in the medium-pressure and medium-temperature field of the grid, No.6, but it commonly occurs from low- to medium temperature and high-pressure field in the grids, No.5 and No.7.

Similarities described above are concordant to the mineral assemblages and the mode of occurrence of minerals in nature. More detailed comparison between natural assemblages and those represented in the grids of metamorphic facies will be described in the following section.

(1-6) Comparison three petrogenetic grids of metamorphic facies with natural mineral assemblages

If we discuss the natural mineral assemblages by using the grids of metamorphic facies in the ACF system, it is inevitable to select the natural mineral assemblages arbitrarily. The mineral assemblages which occur frequently in each metamorphic belt are considered to be stable ones in the ACF system.

<New Caledonia>

The detailed petrologic studies on the high-pressure rocks which crop out in the north-eastern part of New Caledonia were reported by Brothers (1970) and Black (1977).

Especially, the isograds of Ca-Al silicates, amphiboles, sodic pyroxene and garnet were decided by them in the Ouégoa district. Among Ca-Al silicates, pumpellyite occurs in the lowest-grade metabasites. Occurrence and disappearance of Ca-Al silicates with increase of metamorphic grade are as follows; occurrence of lawsonite -- disappearance of pumpellyite -- occurrence of epidote -- disappearance of lawsonite. Black (1977) defined the lawsonite zone (lower-grade) and the epidote zone (higher-grade) on the basis of change of Ca-Al silicates in this area. PAC (pumpellyite - actinolite - chlorite) assemblage characterizes the lowest-grade part of this area. Prograde P-T path of New Caledonia can be expressed in the grids of metamorphic facies, No.6 and No.7, as follows (Fig. V-8);

PAC -- LAC -- GLA -- GLD -- GED
(LAC -- GLA: lawsonite zone; GLD -- GED: low-temperature part of epidote zone)

This P-T path will be drawn in the grid of metamorphic facies, No.5 as follow;

PAC -- GPA -- GDP(GLD) -- GED, or
DPC -- LDC -- GLD -- GED

The former path for No.5 cannot represent the common occurrence of sodic pyroxene at the lower-grade part of New Caledonia, and the latter can not do PA assemblage. Therefore the grids of metamorphic facies, No.6 and No.7 are more realistic than that of No.5.

Fig. V-8. Prograde P-T path of New Caledonia (N), Franciscan (F), and Sanbagawa (S) on the grid of metamorphic facies, No.6.

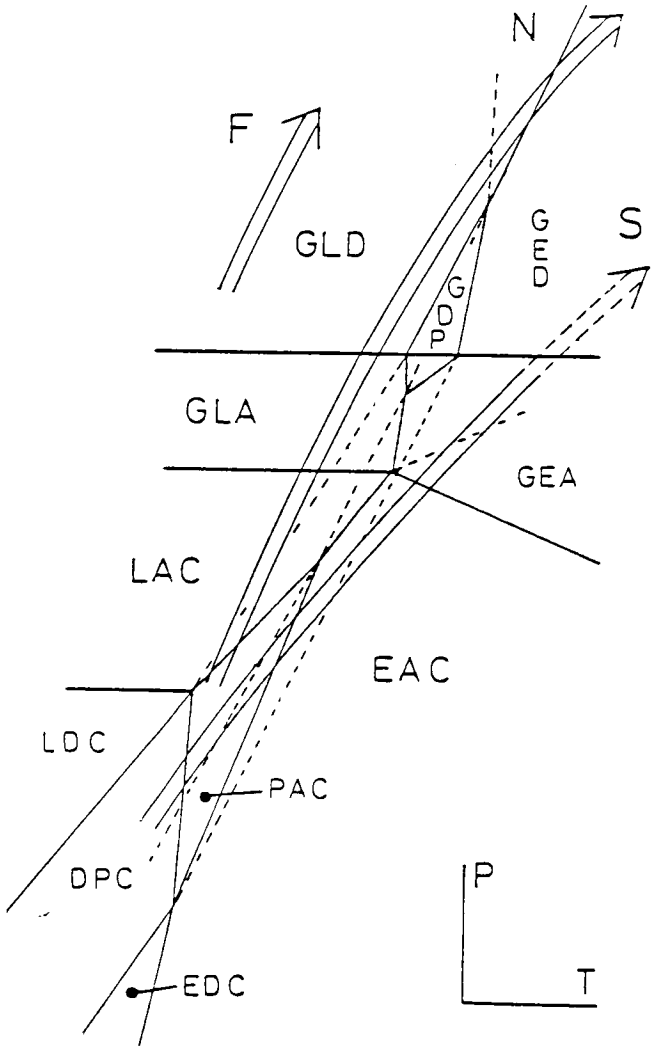

<Sanbagawa belt of Shikoku>

The prograde change of mineral assemblage in the Sanbagawa belt of Shikoku was studied in detail by Banno (1964), Ernst et al.(1970), Higashino (1975), Nakajima et al.(1977), Banno et al. (1978), Otsuki (1980) and Aiba (1982).

Actinolite is rare, but pumpellyite is stable and common in the lowest-grade metabasites of this area (Aiba, 1982). With increase of metamorphic grade, the frequency of actinolite increases, and pumpellyite disappears in due definite grade. This relation is represented by the reaction;

P(pumpellyite) +C(chlorite)
=E(epidote) + A(actinolite) ---------(V-2)

which is considered to define the high-temperature limit of the pumpellyite-actinolite facies. With further increase of metamorphic grade, amphiboles change from actinolite or winchite, through crossite, and finally to barroisite (Otsuki, 1980).

Epidote commonly occurs in metabasites throughout the Sanbagawa belt. The composition of epidote in lower-grade metabasites is rich-in Fe^{3+} and it changes into Al-richer with increase of the metamorphic grade (Miyashiro and Seki, 1958; Nakajima et al., 1977; this study). As this model system uses Al-end composition of epidote, the stability field of epidote is restricted to the higher-temperature

field in the grids.

Prograde change on mineral assemblages of the Sanbagawa belt in Shikoku is represented by the grid of metamorphic facies, No.6 as follows (Fig. V-8);
(D)PC (existence of pumpellyite and lack of actinolite; Aiba, 1982) -- PAC (the coexistence of pumpellyite and actinolite; Nakajima et al.,1977) -- EAC (disappearance of pumpellyite;Banno,1964) -- GEA (occurrence of winchite or crossite; Otsuki,1980) -- barroisite zone (Otsuki, 1980) -- eclogite facies (Takasu, 1984).

The highest-grade part of the Sanbagawa belt is characterizedby the occurrences of barroisite and eclogite. As the petrogenetic grids for this model system do not consider the existence of them, the grids are valuable for the lower-grade part than GEA facies. There is no doubt that lower-half prograde path of the Sanbagawa belt situates at lower-pressure field than that of New Caledonia (Fig. V-8).

<Franciscan belt>

Franciscan belt, which is situated in the western coast of North America, was subdivided into three mineral zones from ocean side to inner-continent on the basis of mineral assemblages in metagraywackes (Bailey et al., 1970; Ernst, 1971);

1. laumontite zone
2. pumpellyite zone

3. lawsonite zone (blueschist belt)

However, the constituent rocks and the geologic structures of the Franciscan belt were usually sheared and disturbed severely. Hence it is very rare that the continuous increase of metamorphic grade is observed in outdoors, but it is very common that rocks belonging to the different metamorphic grades directly contact with each other by a fault. As a rare case, albite disappearance isograd represented by the reaction, albite = jadeite + quartz, which divides the lawsonite zone into albite subzone and jadeite subzone, was reported at Pacheco Pass area in the Diablo Range by Ernst (1965). The representative mineral assemblages of metabasites in albite subzone are:

pumpellyite + lawsonite + sodic amphibole + aragonite

at Pacheco Pass area (Ernst, 1965), and

lawsonite + glaucophane + sodic pyroxene + chlorite

at Panoche Pass area in the Diablo Range (Brown and Bradshow, 1979). These mineral assemblages are considered to be stable in GLD and GDP facies in the grids of metamorphic facies, No.6 and No.7 (Figs. V-7f, V-7g and V-8). The petrogenetic grids for this model system cannot treat the mineral assemblages in jadeite subzone, as albite is not stable in this subzone.

Epidote and actinolite which commonly occur both in the Sanbagawa belt and New Caledonia are very rare in Franciscan belt, except for metabasites of the Black Butte area. The

metamorphic pressure of the Black Butte area is considered to be lower than that of the other areas of Franciscan belt (Brown, 1977a). Metabasites of the Pacheco Pass area in the Diablo Range and those of the Cazadero area contain sodic amphibole, lawsonite, jadeite and aragonite, instead of epidote and actinolite. Metamorphic rocks of these areas are considered to be one of the highest-pressure glaucophane schists in the world (Brown, 1977a). The grids of metamorphic facies for the model system which we have discussed support his view (Fig. V-8).

<The Sanbagawa belt in the Kanto Mountains>

The report on the occurrence of jadeite + quartz assemblage from the Sanbagawa belt by Seki (1960) led to the speculation that the metamorphic pressure of the Kanto Mountains is higher than that of the other areas of the belt (Miyashiro, 1965).

However, the author found jadeite-quartz bearing rock as the tectonic block of the Tochiya Klippe and showed that the formation of jadeite + quartz assemblage had predated the Sanbagawa metamorphism (Hirajima, 1983a). On the other hand, the lower-grade metabasites of the Sanbagawa belt in the Kanto Mountains were divided into three mineral zones based on the mineral assemblages for the ACF-F3 system with descending stratigraphic order as described in Chapter III;

EPDC zone -------- Mamba Formation of the Chichibu Group

EAPC//EADC zone -- Kashiwagi and Sakahara Formations of the Chichibu Group and upper half of

theMikabuGreenrock Complex

EAPC//EAGC zone -- lower half of the Mikabu Greenrock Complex and the uppermost part of the Sanbagawa schists.

EAPC assemblage characterizes the pumpellyite-actinolite facies (Coombs et al., 1976) and EPDC assemblage is newly found at the lower-grade part of the pumpellyite-actinolite facies. Disappearance of sodic pyroxene with increase of the metamorphic grade is defined by the reaction (2) in the Chapter III;

sodic pyroxene + chlorite + albite + quartz =

actinolite + epidote + sodic amphibole + H_2O

Jadeite contents of sodic pyroxenes in the Sanbagawa metamorphic rocks seldom exceed 20 mol% (See Fig. IV-4).

Pumpellyite-actinolite facies is represented as PAC field in the petrogenetic grids of metamorphic facies No.6 and No.7. These grids predict that DC assemblage is stable at the lower-grade part of the PAC field, and that D disappears with increase of metamorphic grade. These predictions from the petrogenetic grids of metamorphic facies are well concordant with the observed natural assemblages. Consequently, the prograde path of the Kanto Mountains is:

DPC -- PAC -- EAC

in the grid of the metamorphic facies, No.6 (Fig. V-8). This path cannot be distinguished from that of the lower-grade part of Shikoku.

(1-7) Concluding remarks on the petrogenetic grids for the ACF system

1) From the topological arguments of the Schreinemakers' bundles for the ACF system with seven phases, seven independent sets of invariant points were derived which constitute the petrogenetic grid of univariant curves. For the basaltic system, seven sets of invariant points provide seven petrogenetic grids of metamorphic facies. Two of them can explain natural mineral assemblages qualitatively and they can distinguish the difference in metamorphic condition among the Sanbagawa belt, new Caledonia and Franciscan belt.

2) The two grids of metamorphic facies predict the existence of DC and LA assemblages (or, facies), which have not been known in low-temperature and medium-pressure field. DC assemblage characterizes the lower-grade part of the high-pressure intermediate group of metamorphism (Miyashiro, 1961). This assemblage is actually found in the Kanto Mountains. LA assemblage is reported in the lawsonite zone of New Caledonia (Black, 1977).

V-2. Prograde mineral assemblages in the ACF-F3 system

Prograde mineral assemblages in the Kanto Mountains were established in four component (ACF-F3) system with six phases, chlorite (C), sodic pyroxene (D), pumpellyite (P), sodic amphibole (G), epidote (E) and actinolite (A), as described in the Chapter III (see Fig. III-6). As six phases in the four component system provide one invariant assemblage, the petrogenetic grid of this system will be discussed in this section. Compositions of six phases defined as in Chapter III are concordant to the observed ones in the Kanto Mountains (see Chapter IV), and they provide six univariant reactions which radiate from the invariant point, composed by DCAEGP phases with excess albite, quartz and water, as follows;

$$D+C = A+E+G+H_2O \quad \text{---------- (2)}$$

$$310CaNaFAl_{0.2}Fe^{3+}_{0.8}Si_4O_{12} + 117\ F_5Al_2Si_3O_{10}(OH)_8 + 30\ NaAlSi_3O_8 + 529\ SiO_2 =$$

$$77\ Ca_2F_5Si_8O_{22}(OH)_2 + 78\ Ca_2Al_2Fe^{3+}Si_3O_{12}(OH) + 170\ Na_2F_3AlFe^{3+}Si_8O_{22}(OH)_2 + 182\ H_2O$$

$$P+D+C = E+A+H_2O \quad \text{---------- (3)}$$

$$170\ Ca_4FAl_5Si_6O_{23}(OH)_32H_2O + 430\ CaNaFAl_{0.2}Fe^{3+}_{0.8}Si_4O_{12} + 91\ F_5Al_2Si_3O_{10}(OH)_8 + 997\ SiO_2 =$$

$$344\ Ca_2Al_2Fe^{3+}Si_3O_{12}(OH) + 211\ Ca_2F_5Si_8O_{22}(OH)_2 + 430\ NaAlSi_3O_8 + 576\ H_2O$$

$$P+G = E+A+C+H_2O \quad \text{---------- (4)}$$

$$31\ Ca_4FAl_5Si_6O_{23}(OH)_32H_2O + 43\ Na_2F_3AlFe^{3+}Si_8O_{22}(OH)_2 + 48\ SiO_2 =$$

$$43\ Ca_2Al_2Fe^{3+}Si_3O_{12}(OH) + 19\ Ca_2F_5Si_8O_{22}(OH)_2 + 13\ F_5Al_2Si_3O_{10}(OH)_8 + 86\ NaAlSi_3O_8 + 59H_2O$$

D+P+G = E+A+H_2O ---------- (9)

$$130CaNaFAl_{0.2}Fe^{3+}_{0.8}Si_4O_{12} + 117\ Ca_4FAl_5Si_6O_{23}(OH)_32H_2O + 91\ Na_2F_3AlFe^{3+}Si_8O_{22}(OH)_2 + 403\ SiO_2 =$$

$$195\ Ca_2Al_2Fe^{3+}Si_3O_{12}(OH) + 104\ Ca_2F_5Si_8O_{22}(OH)_2 + 312\ NaAlSi_3O_8 + 299\ H_2O$$

P+G = D+C+E+H_2O ---------- (10)

$$77\ Ca_4FAl_5Si_6O_{23}(OH)_32H_2O + 211\ Na_2F_3AlFe^{3+}Si_8O_{22}(OH)_2 =$$

$$190\ CaNaFAl_{0.2}Fe^{3+}_{0.8}Si_4O_{12} + 104\ F_5Al_2Si_3O_{10}(OH)_8 + 59\ Ca_2Al_2Fe^{3+}Si_3O_{12}(OH) + 205\ SiO_2 + 232\ NaAlSi_3O_8 + 35H_2O$$

D+C = P+G+A+H_2O ---------- (11)

$$215\ CaNaFAl_{0.2}Fe^{3+}_{0.8}Si_4O_{12} + 97.5\ F_5Al_2Si_3O_{10}(OH)_8 + 129\ NaAlSi_3O_8 + 306.5\ SiO_2 =$$

$$39\ Ca_4FAl_5Si_6O_{23}(OH)_32H_2O + 172\ Na_2F_3AlFe^{3+}Si_8O_{22}(OH)_2 + 29.5\ Ca_2F_5Si_8O_{22}(OH)_2 + 52\ H_2O$$

==========

Calculations of appropriate values of ∇S and ∇V for the six reactions, following the procedures Albee (1965), provide one petrogenetic grid which is shown in Fig. V-9. Divariant assemblages which are stable in each sector divided by univariant reaction lines were labelled by the abbreviations of minerals, as EPDC or EADC, in Fig. V-9.

This petrogenetic grid predicts that pumpellyite-actinolite facies is stable in lower-pressure side than P (pumpellyite) - G (sodic amphibole) assemblage and in higher-temperature side than D (sodic pyroxene)-C (chlorite) assemblage, and that sodic pyroxene disappears with an increase of temperature. These characteristics are inherited from the petrogenetic grids of the ACF system with seven phases. As P-G assemblage was not found in metabasites of the Chichibu Group, prograde mineral assemblages observed in the Kanto Mountains, EPDC -- (EAPC//EADC) -- (EAPC//EGDC), are schematically shown as an arrow in Fig. V-9 without a contradiction.

This grid theoretically supports the existence of sodic pyroxene-chlorite facies and suggests that EPDC assemblage characterizes the lower-grade part of the intermediate-high pressure group of metamorphism.

Fig. V-9. Petrogenetic grid for ACF-F3 system with six phases.

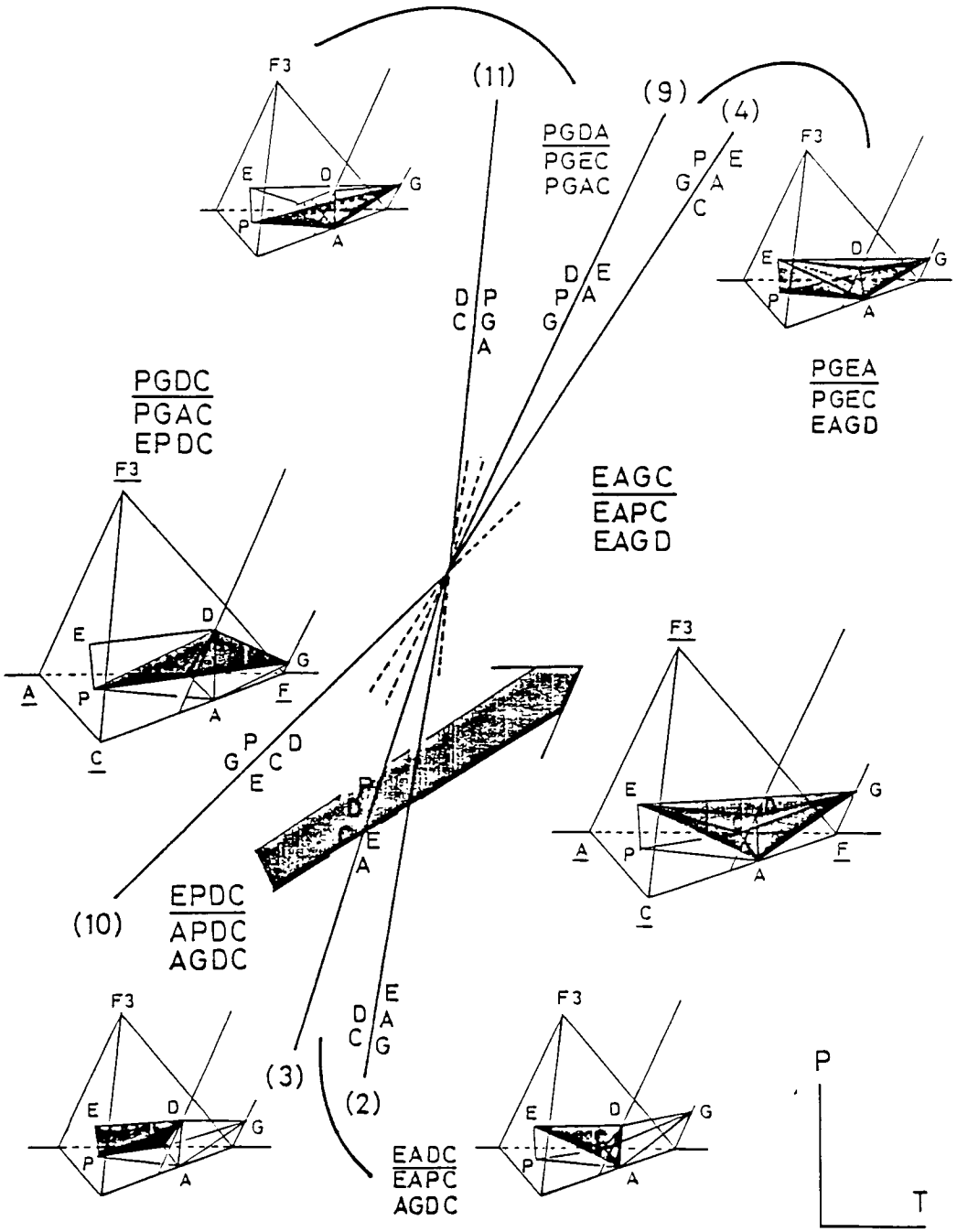

VI. Discussion

(VI-1) Jadeite + quartz problem in the Kanto Mountains.

Sodic pyroxenes are one of common minerals in the typical high-pressure metamorphic belts in the world. Jadeitic pyroxenes have been described from metagraywackes and meta-acidic rocks, acmitic pyroxenes from metacherts, and omphacitic pyroxenes from metabasites and associated eclogites in these belts (Essene and Fyfe, 1967; Coleman and Lee, 1963; Black, 1974; Okay, 1980a and 1980b).

This study demonstrated that sodic pyroxenes commonly occur in lower-grade metabasites of the Kanto Mountains, and that the chemical compositions of them are characterized by low X_{Jd} (Fig. IV-4). The jadeite-quartz rock, however, was found as a tectonic block in the Tochiya Formation, not in the Sanbagawa metamorphic rocks (Figs. II-7 and II-8). The report of the jadeite + quartz assemblage by Seki (1960) in the Kanto Mountains led to the speculation that the metamorphic pressure of the Kanto Mountains is higher than that of the other areas of the Sanbagawa belt. The discovery of the jadeite-quartz rock in a tectonic block by the author provides new information on the metamorphic history of this area.

The jadeite-quartz rock is mainly composed of colorless jadeite, pale-green pyroxene, glaucophane, sodic-calcic amphibole replacing rims of glaucophane, quartz and albite. Zircon and allanite are minor accessories, and mica is scarcely contained. In this rock, K_2O is contained only in

amphiboles, whose K_2O content is no more than 0.1 wt%. Unless the rock suffered any metasomatism which completely removed K_2O from the host rock, the jadeite-quartz rock could not have been derived from ordinary sedimentary rocks. Its possible original rock is an oceanic plagiogranite reported by Aumento (1969), based on the scarcity of K_2O and the occurrence of zircon and allanite.

The jadeite-quartz rock contains two kinds of sodic pyroxenes which are different in composition and texture as describedin the Chapter IV-3-3A. First type is tabular-grained jadeite ($X_{Jd}>0.8$) which coexists with quartz and glaucophane, and the second one is fine-grained pale-green pyroxene ($0.1<X_{Jd}<0.3$) which coexists with albite and sodic-calcic amphiboles mantling glaucophane core. Pale-green pyroxenes occur near the boundary between quartz aggregates and jadeite + albite aggregates, but always in the latter. The photomicrograph (Plate IV-15) indicates that the second pyroxenes are derived from the decomposition of jadeite by the following reaction;

Impure Jadeite + quartz =

Pale-green pyroxenes + albite --------(8)

The P-T condition of the formation of jadeite-quartz assemblage is shown by an open circle in a P-T grid (Fig. VI-1), which is composed of a petrogenetic grid of metamorphic facies for ACF system described in the Chapter

V-1 (Fig. V-7f) and the reaction line of jadeite + quartz = albite (Holland, 1980). Second sodic pyroxenes contain more X_{Jd} than those in the lower-grade metabasites of the Chichibu Group and the Mikabu Greenrock Complex in the Kanto Mountains (Compare Fig. IV-4 with Fig.IV-19). Second pyroxenes in the jadeite-quartz rock and sodic pyroxenes in the Mikabu Greenrock Complex coexist with sodic-calcic amphiboles. The metamorphic pressure of the second pyroxenes was slightly higher than that of the lower-grade metabasite of the Sanbagawa belt, or nearly equal to it. Then, the P-T condition of the second stage is drawn as solid circle in the diopside + chlorite field in Fig. VI-1. Therefore, we concluded that the jadeite + quartz assemblage could not have been formed by the Sanbagawa metamorphism.

Fig. VI-1. A model petrogenetic grid of the glaucophanitic metamorphism and the P-T paths for the jadeite-quartz rock. Abbreviations; A=actinolite, D=diopside, G=glaucophane, L=lawsonite, E=epidote, P=pumpellyite, C=chlorite.

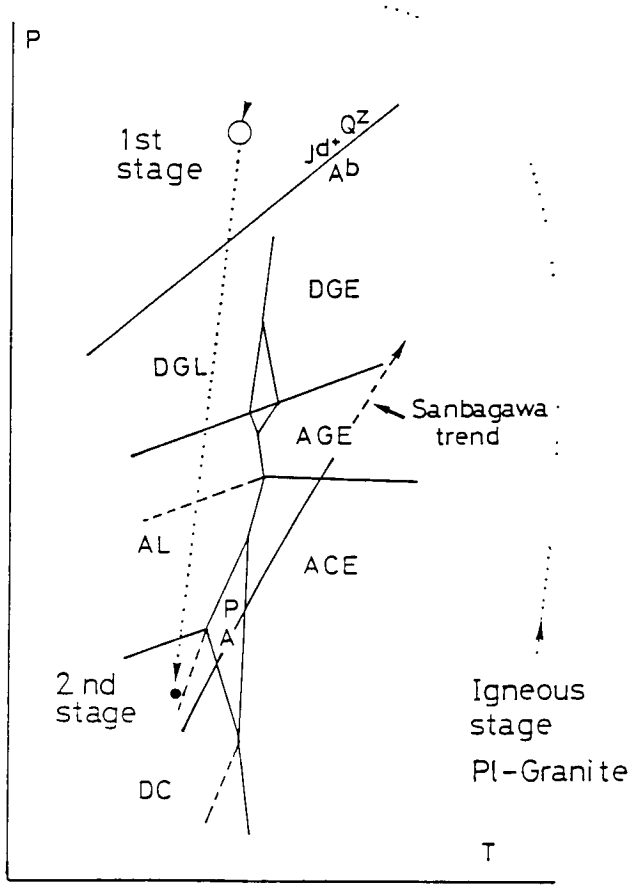

(VI-2) Metamorphic condition of the Kanto Mountains.

The following features of minerals are available for estimating the metamorphic condition of the Sanbagawa metamorphic rocks in the Kanto Mountains;

1) Chemical compositions of sodic pyroxenes do not exceed 20 mol% of jadeite content (Fig. IV-4).

2) Common occurrence of the assemblage of epidote, pumpellyite, actinolite and chlorite, which characterizes the pumpellyite-actinolite facies (Table III-3).

3) Carbonate minerals are always calcite, not aragonite.

4) Lawsonite occurs associated with albite and pumpellyite in Al_2O_3-rich and Fe_2O_3-poor metabasites of the Mikabu Greenrock Complex.

5) Prehnite was observed in the lowest grade part, but zeolite was not found.

The published experimental results which treat the stability of the minerals mentioned above provide a P-T grid as shown in Fig. VI-2. The metamorphic condition of the Kanto Mountains is approximately estimated to be in the dotted region of Fig. VI-2; lower-pressure side of the reaction, --calcite = aragonite-- (Johannes and Punha, 1971; Crowford and Hoersch, 1972), high-temperature side of --heulandite = lawsonite + quartz-- (Nitsch, 1968), and high-pressure side of the zeolite decomposition reactions by Liou (1971). As pumpellyite is scarcely contained in metabasites of the Sanbagawa schists, the high-temperature limit of the

Fig. VI-2. P-T diagram for numerous critical reactions in low-grade metamorphic rocks. The reaction jadeite+quartz=albite from Newton & Smith (1967). and those of zeolites from Liou (1971). P.P. :prehnite-pumpellyite facies. P.A. :pumpellyite-actinolite facies. L.A. :lawsonite-albite facies B.S :blueschist facies.

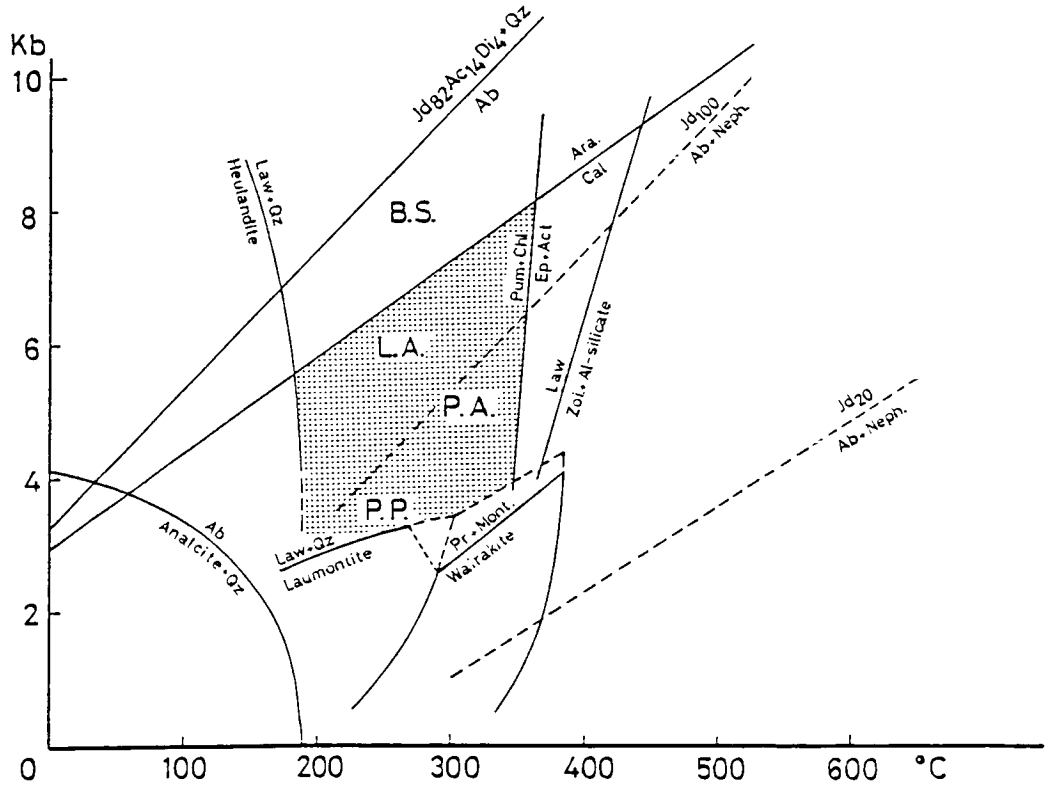

Mikabu Greenrock Complex is roughly defined by the reaction, --pumpellyite + chlorite = epidote + actinolite + H_2O-- (Nitsch, 1971). This dotted region corresponds to two metamorphic facies; lawsonite-albite (LA) facies on high-pressure side (Winkler, 1965) and pumpellyite-actinolite (PA) facies on low-pressure side (Hashimoto, 1966; Coombs et al., 1976).

Impure jadeite not associated with quartz can stably occur in the dotted region by the reaction, -- jadeite = albite + nepheline -- (Curtis and Griffins, 1979). Seki (1960) reported the coexistence of impure jadeite and quartz by the X-ray diffraction method. He probably found impure jadeites not associated with quarts, which are similar to what were reported in a metagabbro of the Mikabu Greenrock Complex of the Oshika area by Watanabe (1974).

Prograde mineral assemblages of the Kanto Mountains were established as follows (Chapters III and V-2);

EPDC	Chichibu
EAPC//EADC	Chichibu and Mikabu
EAPC//EAGC	Mikabu and Sanbagawa

As the reactions which define mineral zones have a steep positive slope in the petrogenetic grid (Fig. V-9), the observed assemblages indicate that the metamorphic temperature increases with descending stratigraphic order.

The compositional change of constituent minerals provides a more detail information on P-T condition in the

study area. Pumpellyite is associated with sodic pyroxene, epidote and chlorite in the metabasites of the Chichibu Group. It has X_{Al}^{Pum} ratio <=Al(VI)/(Al+Fe^{3+}) of pumpellyite> in the range from 0.90 to 0.93. The maximum value of this ratio slightly increases with descending stratigraphic order, and the range of ratio is from 0.90-0.97 in the metabasites of the Mikabu Greenrock Complex (Fig. IV-15). Epidote of the Mikabu Greenrock Complex has relatively homogeneous composition about X_{Al}^{Ep} <=Al/(Al+Fe3) of epidote> =0.7, but that ratio increases with descending order to about 0.85 in metabasites of the Sanbagawa schists (Fig.IV-10). According to the schematic phase diagram of epidote and pumpellyite proposed by Nakajima et al.(1977), the compositional changes of epidote and pumpellyite also indicate that the metamorphic temperature of the Kanto Mountains increases with descending stratigraphic order.

For a long time, petrologists tried to estimate the formation pressure of sodic pyroxenes as a function of $NaAlSi_2O_6$ activity in them. Early work by Essene and Fyfe (1967) assumed that diopside-jadeite-acmite solid solution series behaved as an ideal ionic mixture for lack of natural data, and considered that the $NaAlSi_2O_6$ activity in jadeite-acmite solid solution and diopside-jadeite solid solutions as follows;

$$\mu_{Jd}(\text{in acmite}) = \mu^0_{Jd} + RT\ln(X_{Jd})$$

$$\mu_{Jd}(\text{in diopside}) = \mu^0_{Jd} + 2RT\ln(X_{Jd})$$

However, Carpenter (1980) pointed out that omphacite under the transition temperature, about 850°C, are largely ordered and possesses a primitive cell symmetry, probably P2/n space group, and that the miscibility gaps exist between P2/n omphacite and C2/c pyroxenes. Recently, Holland (1983) gave an isopleths of X_{Jd} in jadeite-diopside system, with ordering and exsolution into P2/n omphacite near to $Jd_{50}Di_{50}$ (Fig. VI-3). Isopleths of jadeite-diopside-acmite system by the ideal solution model (Essene and Fyfe, 1967) taking V=17.34cc and the reaction line of jadeite + quartz = albite of Newton and Smith (1967) was shown in Fig. VI-4. Minimum formation pressures of sodic pyroxenes in the diopside-jadeite system, especially in low X_{Jd} pyroxenes, calculated on the basis of the ideal solution model (less than 1 Kb at 400°C and X_{Jd}=0.05) were unrealistically lower than that of the ordering and exsolution model (4.1Kb at 400°C and X_{Jd}=0.05) (Compare Figs. VI-3 and VI-4).

However, in spite of this ambiguity, it is selfevident that the increase of X_{Jd} means an increase of formation pressure at constant temperature, or with an increase of temperature, at least in jadeite-diopside-quartz system. Although it is difficult to estimate the effect of ordering and exsolution on X_{Jd} isopleths in jadeite-acmite-diopside system, this paper assumed that the ideal solution model is valid for C2/c single phase region and principal character observed in both jadeite-diopside and jadeite-acmite joins is inherited in jadeite-acmite-diopside system.

Fig. VI-3. Isopleths of NaAlSi2O6 with ordering to P2/n allowed for omphacites near to Jd50Di50 (Holland 1983).

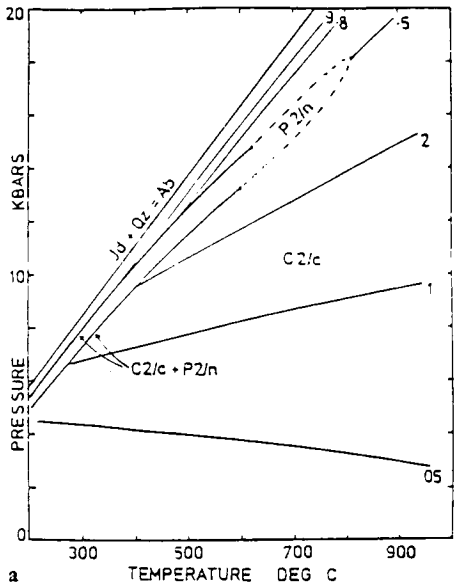

Fig. VI-4. Isopleths of NaAlSi2O6 by the ideal mixing model for jadeite-acmite-diopside system.

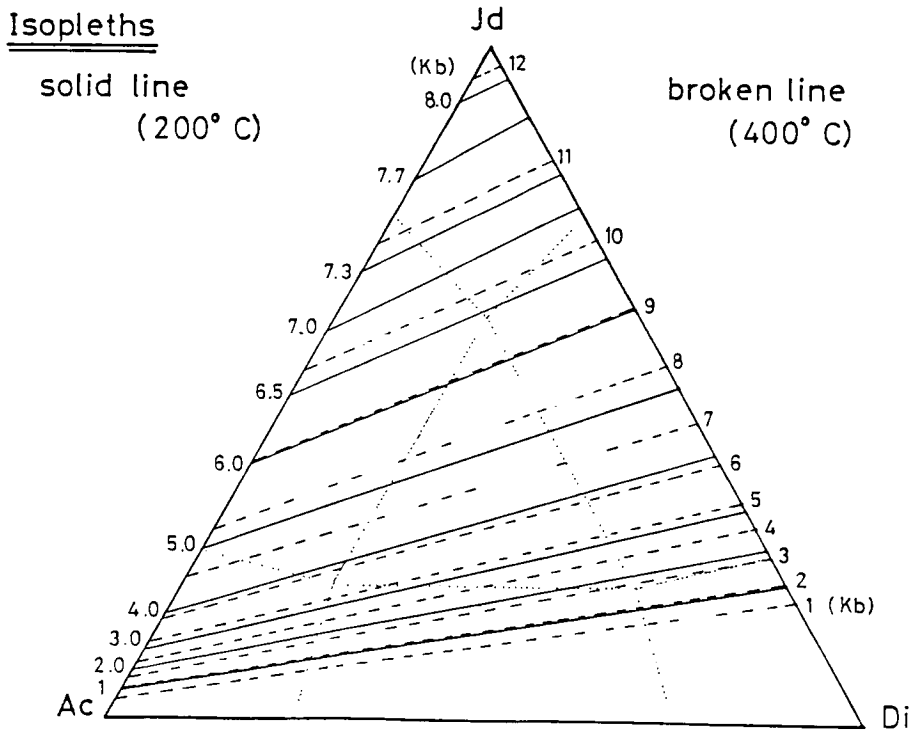

X_{Ac} in sodic pyroxenes is affected by the oxidation state of host rocks in the study area. Actually, aegirine-augite and sodic augite mainly occur in hematite-free metabasites, and aegirine-augite and aegirine do in hematite-bearing ones (Fig. IV-4). Chemical gap between chloromelanite (omphacite)-sodic augite was observed in hematite-free metabasites of the Kanto Mountains, but not in hematite-bearing ones. Therefore, diopside-omphacite miscibility gap proposed by Carpenter (1980) probably expands to chloromelanite field from jadeite-diopside join under low-temperature condition, but not to aegirine-augite. We regard sodic pyroxene in hematite-bearing rocks to be in C2/c pyroxene field. X_{Jd} in sodic pyroxenes in hematite-bearing rocks continuously increases with descending stratigraphic order (Fig. IV-4). As chemical change of Ca-Al silicates and the progression of mineral assemblages indicate that the metamorphic temperature increase with descending order, chemical variation of sodic pyroxenes means that the metamorphic pressure of the Kanto Mountains gradually increases with the metamorphic temperature.

A few data of sodic pyroxenes were reported from lower-grade metabasites of the Asemi River area (Otsuki, 1980), Oboke area (Yoshizawa, 1984), Omoiji-Nagasawa area (Nakajima, 1975) and Yanadani-Mikawa area (Aiba et al., 1982). These data suggest the increase of X_{Jd} in sodic pyroxenes with increase of metamorphic temperature in

Shikoku (Fig, IV-4). X_{Jd} of Oboke and Asemi areas, belonging to the chlorite zone of the Sanbagawa schists, are very similar to that of the Mikabu Greenrock Complex in the Kanto Mountains.

The tendency for pyroxenes to become more jadeitic with increase of metamorphic grade has also been described in metabasites of the lawsonite and epidote zones of New Caledonia (Black, 1974). Pyroxenes in metabasites of these areas are mainly chloromelanite and omphacite on the one hand, and those in metabasites of the Kanto Mountains are aegirine-augite and sodic augite on the other. Pumpellyite stably occurs both in metabasites of the Kanto mountains and of the lawsonite zone of New Caledonia. These mineralogical data indicate that the metamorphic pressure of the Kanto Mountains is lower than those of the New Caledonia at the same temperature.

(VI-3) Stability of sodic pyroxene-chlorite facies, in comparison with the pumpellyite-actinolite facies.

(A) The definition and the type locality of the sodic pyroxene-chlorite facies

Hashimoto (1966) proposed the pumpellyite-actinolite facies which is an independent facies located between the prehnite-pumpellyite facies on the one hand, and the greenschist and the glaucophane schist facies on the other, by showing that rocks of such a facies occupy well mappable area. This proposal is widely supported by subsequent workers such as Seki (1969, 1972), Coombs (1971) and Zen (1974).

The pumpellyite-actinolite facies was originally defined by the presence of pumpellyite, actinolite and stilpnomelane and by the absence of prehnite and lawsonite. Nakajima et al.(1977) regarded that this facies is characterized by the common presence of PAC (pumpellyite-actinolite-chlorite) assemblage in metabasites of the ACF-F3 system, and they defined the higher-temperaturelimit of this facies by the disappearance of PC (pumpellyite-chlorite) assemblage, replaced by EA (epidote-actinolite) assemblage by sliding equilibrium. Aiba (1982) has shown that the lower-grade part of the pumpellyite-actinolite facies of Nakajima et al.(1977) is characterized by PHtEC (pumpellyite-hematite-epidote-chlorite) assemblage instead of EAC (epidote-actinolite-chlorite) one.

The common occurrence of sodic pyroxene associated with PAC assemblage is newly found and it requires a new phase relation in lower-grade metabasites. The petrogenetic grids of metamorphic facies in the three component (ACF) system with seven phases (Fig. V-7) indicate that the independent metamorphic facies characterized by the common occurrence of sodic pyroxene-chlorite assemblage exists on a lower-temperature part of the pumpellyite-actinolite facies (PAC field of the grid). For the detail discussion, a Schreinemakers' bundle around the invariant point of the four component (ACF-F3) system with six phases was examined; sodic pyroxene(D) - chlorite(C) - actinolite(A) - epidote(E) - sodic amphibole(G) - pumpellyite(P) (Fig. V-9). Their compositions are taken from the natural data as described in Chapters III-3 and V-2. As stilpnomelane is rare in lower-grade metabasites of the Kanto Mountains and it has been known to occur only in metabasites of high Fe/(Fe+Mg) ratio (Aiba, 1982), it is excluded in the following discussion.

The Schreinemakers' bundle around the invariant point (Fig. V-9) indicates that the PAC assemblage is stable all around it, and that PG (pumpellyite-sodic amphibole) assemblage which is incompatible with EAC (epidote-actinolite-chlorite) assemblage is stable in the higher-pressure part of two univariant lines, -- PG=EAC -- (4) and -- PG=DCE -- (10). Therefore the definition of the

pumpellyite-actinolite facies by Nakajima et al.(1977) is insufficient to discuss the mineral assemblage in the four component system, and the definition should be improved for this system.

The definition of metamorphic facies in the four component system follows the method described in the section (V-1-5). The positions of the bulk composition of representative basalts in ACF-F3 system is roughly estimated from that of the ACF diagram (Fig. V-6). As A component ($=Al_2O_3+Fe_2O_3-3K_2O-Na_2O$) in the ACF system is subdivided into $A'=Al_2O_3-3K_2O-Na_2O$ and $F3=Fe_2O_3$ in the ACF-F3 system, representative basalts are plotted slightly away from the ACF plane to the F3 apex of ACF-F3 tetrahedron.

The stability field of EAPC assemblage is bounded by two univariant lines, PG=EAC -- (4) and PDC=EA -- (3), in the grid (Fig.V-9). Since we define the metamorphic facies in the four component system by the common occurrence of the divariant assemblage, the sector surrounded by the reaction lines,(3) and (4), in this grid is defined as the pumpellyite-actinolite facies. This sector is further divided by the univariant line, DC=EAG -- (2), into two fields. On higher-temperature side of the reaction (2), EAGC assemblage stably occurs in Fe^{3+}-rich rocks and EAPC assemblage in Fe^{3+}-poor rocks. Similarly, on lower-temperature side of the reaction (2), EPDC assemblage occurs in Fe^{3+}-rich rocks and EAPC assemblage in Fe^{3+}-poor rocks. This phase relation is the same as that observed in the

Kanto Mountains (Fig. III-5-2). The occurrence of EAPC assemblage is more frequent than those of EAGC and EADC assemblages (Table III-3) in the Kanto Mountains.

The new grid for the four component system indicates that EPDC or PADC assemblages is stable in a lower-temperature side of the newly defined pumpellyite-actinolite facies. Actually, EPDC assemblage was observed in metabasites of the Chichibu Group along the Kanna-gawa. We defined this area as the sodic pyroxene-chlorite facies. Fundamentally, we use the metamorphic facies defined in the four component system in the following discussion.

Mineral zones of the sodic pyroxene-chlorite facies and the pumpellyite-actinolite facies were mapped from south to north with descending stratigraphic order along the Kanna-gawa, i.e., with increase of both metamorphic pressure and temperature (Fig. III-5-2). Zone boundary between the sodic pyroxene-chlorite and the pumpellyite-actinolite facies is determined by the first appearance of EADC assemblage with ascending grade. The boundary between two subzones of the pumpellyite-actinolite facies is determined by the first appearance of EAGC assemblage or EAGDC assemblage. The higher-grade limit of the pumpellyite-actinolite facies is determined by the disappearance of pumpellyite in metabasites. The isograd of the pumpellyite disappearance roughly corresponds to the lithologic zone boundary of between the Sanbagawa schists and the Mikabu Greenrock

Complex in the Kanto Mountains. Prehnite occurs in the lowest grade part of the Chichibu Group along the Kanna-gawa (Fig. III-1). However, the phase relations between the lower limit of the sodic pyroxene-chlorite assemblage and the prehnite zone was not determined exactly.

(B) Comparison of the sodic-pyroxene facies with the pumpellyite-actinolite facies

Aiba (1982) pointed out that the lower-grade part of the pumpellyite-actinolite facies is characterized by pumpellyite-hematite assemblage. To examine the phase relation between pumpellyite-hematite and sodic pyroxen-chlorite assemblages, the petrogenetic grid will be constructed for the ACF-F3 system with seven phases; DCAEPG + hematite (Ht). For the general case of four component system with seven phases, there will be 7 ($_7C_6$) invariant points. They are represented by an abbreviation in Table VI-1. The abbreviation of invariant point is designated by brackets [ ], which contain 1 abbreviation for a phase not involved. DCAEPG invariant system discussed in the previous section corresponds to the invariant point [Ht] in this system; i.e., the invariant point not containing hematite.

Four component system with seven phases corresponds to the case of -1 degree of freedom (Korzhinskii, 1959). In this system, there are two possible sets of invariant points. ΔV and ΔS derived by the same method of Chapter V-2

Table VI-1. Invariant points and 6 univariant reaction lines which radiate from each invariant point for ACF-F3 system with 7 phases.

INVARIANT POINT	REACTION LINES
[Ht]	2, 3, 4, 9. 10, 11,
[G]	3, 102, 103, 104, 105, 106,
[P]	2, 105, 107, 108, 109. 110,
[A]	10, 102, 107, 111, 112, 113,
[D]	4, 104, 109, 112, 114, 115,
[E]	11, 106, 110, 113, 114, 116,
[C]	9, 103, 108, 111, 115, 116,

Abbreviations:

MINERALS	FORMULA						
	Na	Ca	F	Al	F3	Si	H
Ht:hematite	0	0	0	0	2	0	0
G :sodic amphibole	2	0	3	1	1	8	2
P :pumpellyite	0	4	1	5	0	6	7
A :actinolite	0	2	5	0	0	8	2
D :sodic pyroxene	1	1	1	0.2	0.8	4	0
E :epidote	0	2	0	2	1	3	1
C :chlorite	0	0	5	2	0	3	8
Ab:albite	1	0	0	1	0	3	0
Q :quartz	0	0	0	0	0	1	0
W :water	0	0	0	0	0	0	2

determine the unique topological relation of univariant lines around invariant points, and give two possible sets of invariant points; one set is composed of four invariant points, [Ht], [G], [P] and [A], and the other is of three points, [D], [E], and [C]. As the invariant system, DCAEPG, i.e., [Ht], is found in the Kanto Mountains, we consider that the set containing the invariant point [Ht] is stable. Univariant reactions composing the new petrogenetic grid are tabulated in Table VI-2.

Many important informations are provided by the petrogenetic grid for the four component system with seven phases (Fig. VI-5);

(1) Pumpellyite-hematite assemblage stably occurs in lower-temperature condition and sodic pyroxene-chlorite assemblage in medium-temperature condition.

(2) Pumpellyite-sodic amphibole assemblage is stable in high-pressure field and actinolite-hematite assemblage in low-pressure field.

(3) EAPC assemblage is stable in higher-temperature field of reactions (104) --PA+Ht=EC--, (3) --PDC=EA--, and (4) --PG=EAC--. The pumpellyite-actinolite facies (the stability field of EPAC assemblage) is subdivided into three subfacies by the reactions, (2) --DC=EAG--, (105) --DEC=A+Ht-- and (109) --EG=CA+Ht--: high-temperature and high-pressure (H-T/H-P) subfacies defined by the occurrence of EAGC assemblage, medium-temperature and high-pressure (M-T/H-P) subfacies by EADC assemblage and low-

Table VI-2. 21 independent univariant assemblages and 21 reactions corresponding to each assemblage for ACF-F3 system with seven phases.

U.A.	NO.	REACTION
(Ht,P)	2	310D+117C+529Q+30Ab=77A+78E+170G+182W
(Ht,G)	3	170P+430D+91C+997Q=344E+211A+430Ab+576W
(Ht,D)	4	31P+43G+48Q=43E+19A+13C+86Ab+59W
(Ht,C)	9	117P+91G+403Q+130D=195E+104A+312Ab+299W
(Ht,A)	10	77P+211G=190D+104C+59E+205Q+232Ab+35W
(Ht,E)	11	430D+165C+258Ab+613Q=78P+344G+59A+104W
(G,A)	102	220P+60D+211Ht+198Q=470E+56C+60Ab+311W
(G,C)	103	20P+20D+13Ht+50Q=42E+8A+20Ab+41W
(G,D)	104	40P+60A+43Ht+12Q=86E+14C+47W
(G,P)	105	4E+80D+28C+176Q=44A+34Ht+80Ab+70W
(G,E)	106	10P+430D+147C+949Q=235A+172Ht+430Ab+388W
(P,A)	107	20D+8C+7Ht+20Ab+26Q=10E+20G+7W
(P,C)	108	78E+20D+140G+170Q=88A+117Ht+300Ab+91W
(P,D)	109	22E+40G+36Q=2C+22A+31Ht+80Ab+21W
(P,E)	110	110D+39C+233Q=55A+10G+39Ht+90Ab+91W
(A,C)	111	11P+10D+13Ht+4Ab+19Q=27E+7G+18W
(A,D)	112	22P+6G+19Ht+12Q=44E+8C+12Ab+29W
(A,E)	113	4840D+2376C+649Ht+5500Ab+5632Q =1210P+5170G+99W
(D,E)	114	14P+82G+6C=28A+41Ht+164Ab+42Q+127W
(D,C)	115	14G+12E+12Q=2P+8A+13Ht+28Ab+5W
(E,C)	116	26P+98G+40D+184Q=72A+65Ht+236Ab+117W

U.A.; univariant assemblage. Two abbreviations of minerals, which are not contained for the univariant system, are drawn in ( ).

Fig. VI-5. A petrogenetic grid of univariant curves derived from an ACF-F3 system with seven phases.

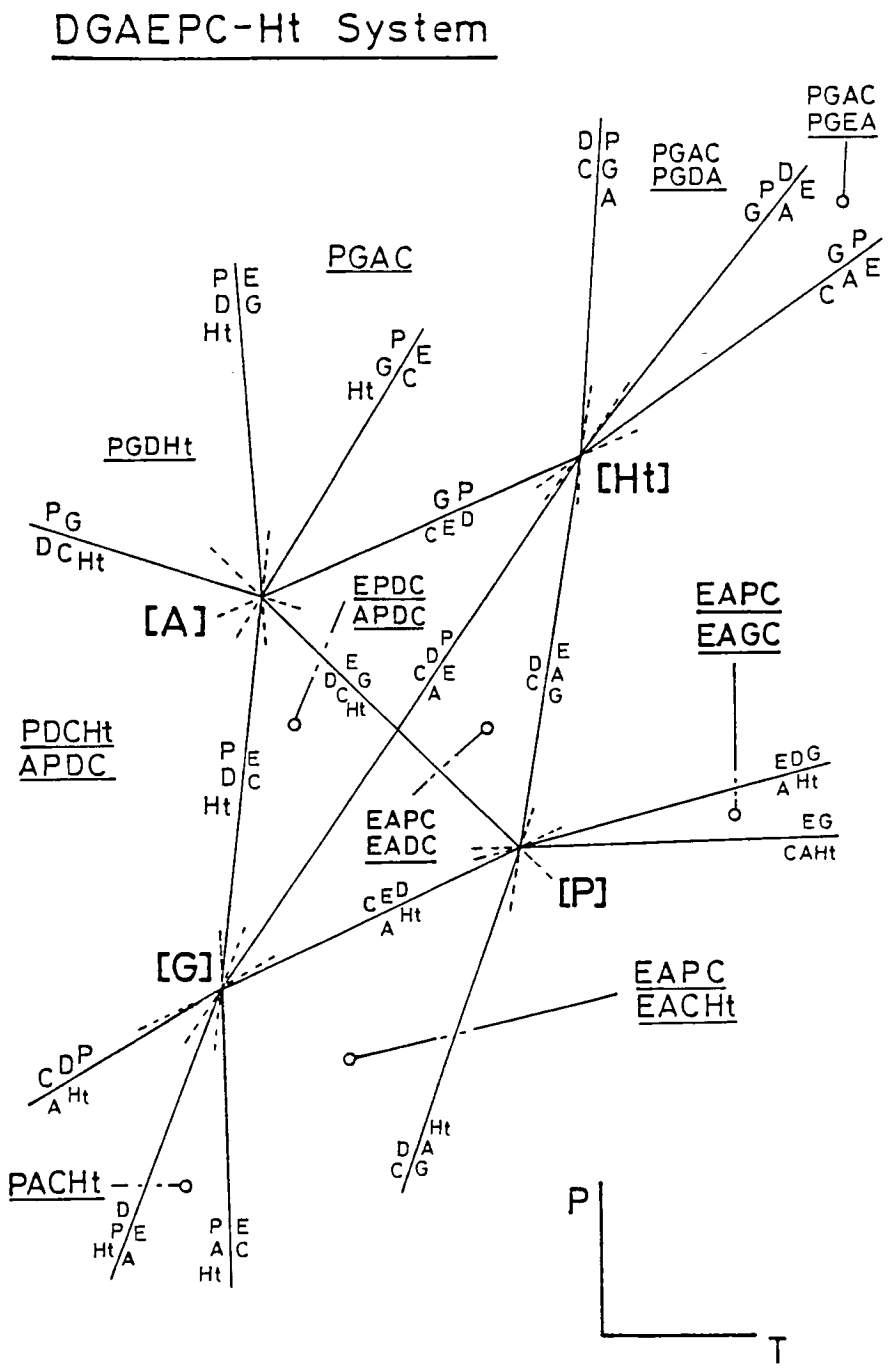

pressure (L-P) subfacies by EAC-Ht assemblage.

The petrogenetic grid for four-component system with seven phases indicates that the metamorphic condition of the Kanto Mountains belongs to the M-T/H-P subfacies of the pumpellyite-actinolite facies.

Watanabe (1975), Nakajima (1975), Otsuki (1980), Aiba (1982) and Yoshizawa (1984) reported the occurrence of sodic pyroxenes in lower-grade metabasites of the Sanbagawa belt. However, they did not consider that sodic pyroxene is one of common minerals in lower-grade metabasites, and hence there is no systematic description on sodic pyroxene-bearing mineral assemblages in the Sanbagawa belt, except for the Kanto Mountains. Nakajima et al. (1977) described that EAPC and EAC-Ht assemblages commonly occur in metabasites of the Omoiji-Nagasawa area in central Shikoku. If there is no oversight of common occurrence of sodic pyroxene in Shikoku, the metamorphic condition of Shikoku belongs to the L-P subfacies of the pumpellyite-actinolite facies. Therefore, new petrogenetic grid clarifies that the P-T path of the Kanto Mountains (trend S.K. in Fig. VI-6) is slightly higher in pressure than that of the Shikoku (trend S.S.) even in the same pumpellyite-actinolite facies.

EAPC assemblage was reported from the following regional metamorphic belts; Western Otago (Kawachi, 1975), Shuksan (Brown, 1977a) and Calabria, South Italy, (De Roever, 1972). Kawachi (1975) reported the occurrence of

Fig. VI-6. Prograde P-T paths of representative glaucophanitic belts on the petrogenetic grid for ACF-F3 system with seven phases. N.C :New Caledonia, W.O. :Western Otago, S.S. :Sanbagawa belt, Shikoku. S.K. :Sanbagawa belt, Kanto Mountains.

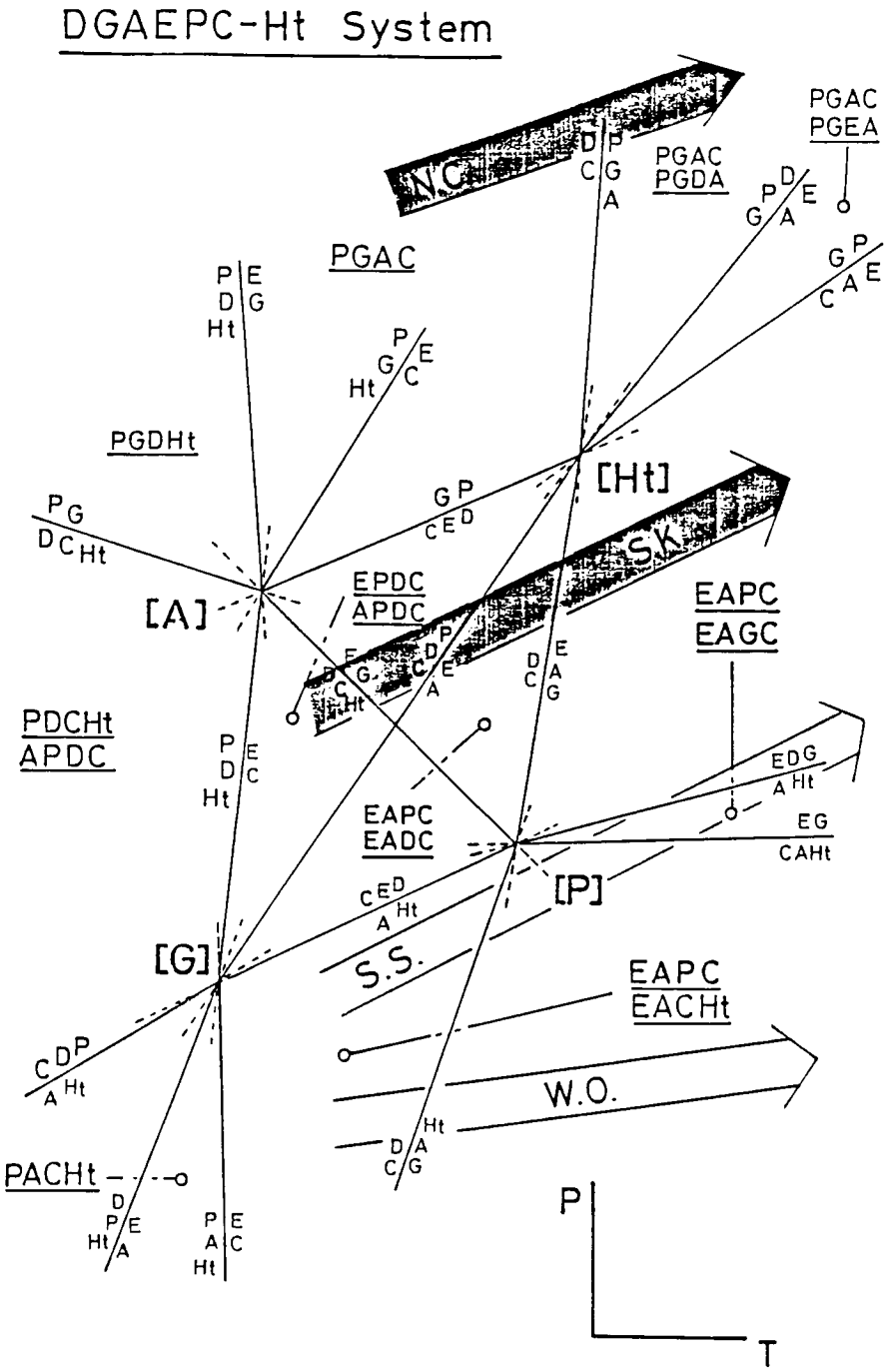

EAC-Ht assemblage with EAPC assemblage in his Zone III of Western Otago. The petrogenetic grid for four component system indicates that the Zone III of Kawachi (1975) belongs to L-P subfacies of the pumpellyite-actinolite facies same as the Sanbagawa belt of Shikoku. Brown (1977a) described that EAC-Ht assemblage is predominant after the disappearance of pumpellyite in high-grade part of Western Otago. As sodic amphibole-hematite assemblage was reported from the higher-grade part of Shikoku (Otsuki, 1980), the metamorphic pressure of the Sanbagawa belt in Shikoku is slightly higher than that of Western Otago (trend W.O. in Fig. VI-6).

Common occurrence of sodic pyroxene was reported from Calabria among the three metamorphic belts of the pumpellyite-actinolite facies mentioned above. De Roever (1972) emphasized the common occurrence of lawsonite-albite-chlorite assemblage associated with magnesioriebeckite and aegirine-augite and he concluded that the mineral assemblage of Calabria represented the lawsonite-albite facies (Winkler, 1965). Since the definition of this facies of Winkler (1965) is obscure, the lawsonite-albite facies is defined as the P-T field represented by the common occurrence of LAC (lawsonite-actinolite-chlorite) assemblage in metabasites for the grid of metamorphic facies of ACF system (Fig. V-7). De Roever (1972) reported the occurrence of following three phases assemblages, ELC, EPC, LPC, and

EAC. These assemblages are considered to be stable under the pumpellyite-actinolite facies or the greenschists facies of our definition for the ACF system. He described that EAGDC assemblage occurred with EAPC assemblage. This five phases assemblage represents the univariant reaction (2) for the ACF-F3 system which subdivides the pumpellyite-actinolite facies into M-T/H-P and H-T/H-P subfacies. Chemical variation of sodic pyroxenes from Calabria ($0.10<X_{Jd}<0.15$, and $0.3<X_{Ac}<0.7$) is very similar to that of the Kanto Mountains. Although the grid of metamorphic facies for lawsonite-bearing four component system is not produced, we regard that the metamorphic condition of Calabria is very similar to that of the Kanto Mountains. High-modal amount of lawsonite in Calabrian metabasites probably owes to high-Al_2O_3 content (about 20 wt%) of host rocks.

EAPC assemblage was not found in New Caledonia, Franciscan and Western Alps, that were considered to belong to the typical high-pressure facies series (Miyashiro, 1961 and 1973; Brown, 1977a). Black (1977) described that PGAC and LPGC assemblages are predominant in lower-grade part of the lawsonite zone, and omphacite-almandine assemblage replaces them in the epidote zone. The petrogenetic grid for four component system with seven phases indicates that PGAC assemblage is stable in high-pressure field of the pumpellyite-actinolite facies and the sodic pyroxene-chlorite facies. The lawsonite zone of New Caledonia

requires higher-pressure than that of the metamorphic path of the Kanto Mountains.

LGC+omphacite assemblage is predominant in type II and type III metabasites of Franciscan belt (Borg, 1956; Coleman & Lee, 1963; Ernst, 1965; Brown & Bradshaw, 1979). Since Jadeite + quartz assemblage occurs in metagraywackes associated with type II metabasites in Cazadero (Coleman & Lee, 1963) and Panoche Pass (Ernst, 1965), metamorphic pressure of type II of Franciscan is higher than that of New caledonia.

(VI-4) Metamorphism and tectonic significance of tectonic blocks.

(4-A) Metamorphism of the tectonic blocks

Many tectonic blocks were found from the Kanto Mountains; in the western part by Tanabe et al.(1982) and in the Tochiya Formation and the greenrock mélange of the eastern part (Hirajima, 1983a, 1984).

a) Sodic pyroxene-sodic amphibole-bearing rock

Amphiboles in this rock show a very wide chemical variation and various modes of occurrence. Some of sodic amphiboles occur as an intergrowth with actinolite with a distinct optical boundary, where the chemical composition changes discontinuously (Fig. IV-20b). This discontinuity corresponds to the miscibility gap. Other amphiboles have an intermediate composition within this gap. They are usually irregular and fine-grained with inhomogeneous composition even in a small single grain. Katagas (1974) and Brown (1974) described that the gap between actinolite and sodic amphibole existed in lower-grade glaucophane schists, but the gap between actinolite and riebeckite disappeared with increase of metamorphic temperature. Toriumi (1974, 1975) reported that the miscibility gap between actinolite and riebeckite existed in metabasites of the Kanna-gawa. However, this study pointed out that the gap between actinolite and riebeckite disappeared at the same stratigraphic horizon (Fig. IV-8). An intergrowth of

sodic amphibole and actinolite in this rock should have been formed under the lower-temperature condition than that of the Mikabu Greenrock Complex.

The compositional range of sodic pyroxenes in this rock is concordant to that of the second-stage sodic pyroxenes in the jadeite-quartz rock (Fig. IV-20a) with X_{Jd} (=0.2 in average) higher than that of the Mikabu Greenrock Complex (X_{Jd}=0.1 in average). Some sodic pyroxenes contact sodic amphibole and actinolite with a sharp boundary, but not with intermediate amphiboles. Hence it is considered that sodic pyroxene stably coexists with sodic amphibole and actinolite, but not with intermediate ones. These facts suggest that sodic amphibole and actinolite with distinct chemical gap were formed under the lower-temperature than that of the Mikabu Greenrock Complex, and that the formation pressure of these amphiboles and sodic pyroxene was higher than that of the Mikabu Greenrock Complex.

(b) Epidote-amphibolite

Epidote-amphibolite is mainly composed of hornblende, epidote, albite and sphene. The schistosity of this rock is mainly composed of columnar hornblende and epidote. Hornblende is replaced by actinolite along margins or rims. Barroisite is not found in this rock. Epidote is richer in Al than that of the Mikabu Greenrock Complex (Fig. IV-21). Many prehnite veins crosscut the schistosity of this rock. These mineralogical data indicates that this rock was formed

initially under the medium-pressure subfacies of the epidote-amphibolite facies (Miyashiro, 1973), and then suffered the low grade metamorphism which formed prehnite veins and actinolite mantling hornblende.

(C) Metagabbro and other blocks

Many other small blocks were found in the greenrock mélange. However, they were extensively deformed and altered by the veining of prehnite and carbonate. Hence it is difficult to estimate the original lithofacies, except for some blocks of metagabbro.

The greenrock mélange contains many blocks of metamorphic rocks whose grade are different from each other. It is obvious that these blocks were not formed in situ in the greenrock mélange. The metamorphism of the prehnite-pumpellyite facies is the only common character which was recorded in tectonic blocks, if not all of them, of the greenrock mélange. The prehnite-pumpellyite facies metamorphism had to have taken place after the mechanical mixture of metamorphic blocks in greenrock mélange.

(4-B) Timing of the prehnite-pumpellyite facies metamorphism in Klippes

In the Yorii area, prehnite occurs only in the rocks of Tochiya Formation, Kinshozan quartz-diorite and the greenrock mélange. In this area, this mineral was not found from the basement rocks, i.e., the Chichibu Group,

the Mikabu Greenrock Complex and the Sanbagawa schists, nor from younger covers of the Lower Miocene Yorii Formation and Middle to Upper Miocene Ogawa Formation. Distribution of prehnite indicates that the prehnite-pumpellyite facies metamorphism postdated the deposition of the Tochiya Formation (Miocene) and predated the Yorii and Ogawa Formations, i.e., Early Miocene.

Kosaka (1979) described that both the Tochiya Formation and the Kinshozan quartz-diorite formed a klippe which moved from north to south during late Cretaceous to Palaeocene. The distribution of prehnite indicates that the greenrock mélange is one of the constituents of the klippe and supports the klippe model of Kosaka (1979). However, the emplacement of the klippe should have occurred simultaneously or just after the prehnite-pumpellyite facies metamorphism; i.e., Early to Middle Miocene.

(4-C) Similarity and difference between the klippes in the Kanto Mountains and the Kurosegawa tectonic belt in Shikoku

Weakly metamorphosed sediments (Tochiya Formation), Paleozoic granites (Kinshozan-quartz-diorite), the tectonic block of the jadeite-quartz rock and the tectonic mélange which contains various kinds of metamorphic rocks (Greenrock mélange) are the fundamental members of the Kurosegawa tectonic zone in Kyushu, Shikoku and Kii Peninsula (Ichikawa et al., 1956; Maruyama, 1981; Hada and

Suzuki, 1983). In the Kanto Mountains, the affinities of the Kurosegawa tectonic zone are exposed here and there from Shimonita area (Arai et al., 1966; Tanabe et al., 1982), to Yoshimi Hill (Murai, 1965) along the WNW-ESE direction for a distance about 70 Km (Fig. II-2). This position exists about 20 Km to the north of the southern boundary of the Sanchu Graben which was regarded as the eastern extension of the Kurosegawa tectonic zone by Ichikawa et al.(1956).

Maruyama (1978) proposed that the Kurosegawa tectonic zone in Shikoku was formed by the diapir which was caused by the serpentinization of peridotite. Hada and Suzuki (1983) described that the boundary of the crustal structure between the typical continent and ocean is situated on the south side of the Kurosegawa tectonic zone by the geophysical data and pointed out that the formation process of the Kurosegawa tectonic zone is closely correlated to the present structure of the lower crust. However, the correlation between the structure of the lower crust and the affinities of the Kurosegawa tectonic zone in the Kanto Mountains has not been examined. The affinities in the Kanto Mountains overlay the Sanbagawa metamorphic rocks with a low angle thrust, and the amount of serpentinite is obviously less than that of Shikoku.

In Shikoku, the Kurosegawa tectonic zone was covered by the lower Cretaceous sediments (Maruyama, 1981), and the timing of the emplacement of serpentinite was considered to be mainly during the tectonic movements of the Nagahama-Ozu

and Hijikawa phases in middle Jurassic to early Cretaceous time (Hada and Suzuki, 1983). In the Kanto Mountains, the affinities of the Kurosegawa tectonic zone are unconformably covered by the lower Miocene sediments, and hence the age of emplacement is limited to early Miocene.

From the geologic and metamorphic view points, the trinity of the Tochiya Formation, Kinshozan quartz-diorite and the greenrock mélange is considered to have existed far from the present position before early Miocene. Kosaka (1979) regarded the Kinshozan quartz-diorite as one of the constituents of the Ryoke belt based on the lithofacies, and he proposed that the "decken" composed of the Tochiya Formation and the Kinshozan quartz-diorite moved from north to south. However, the Kinshozan quartz-diorite has a Paleozoic age (251±8 Ma; Ono, 1983). This rock type is not reported from the Ryoke belt. Therefore, there is no information on the moving direction of the klippe.

VII. Concluding remarks

The metamorphic aspects of the Kanto Mountains were summarized as follows:

1) The Sanbagawa metamorphism influenced the constituents of the Chichibu Group, the Mikabu Greenrock Complex, and the Sanbagawa schists in order of increasing metamorphic grade. The lowest-grade rocks of this metamorphism belong to the prehnite-pumpellyite facies. The metamorphic grade further increases from the sodic pyroxene-chlorite facies, through the high-pressure subfacies of the pumpellyite-actinolitefacies,to the epidote-amphibolite facies. Both the sodic pyroxene-chlorite facies and the high-pressure subfacies of the pumpellyite-actinolite facies are characterized by a mineral assemblage of low-X_{Jd} pyroxene and chlorite, and are newly proposed by this study. The Kanto Mountains is an example of such a hitherto unknown facies.

2) The constituents of the Atokura and Tochiya Klippes suffered the prehnite-pumpellyite facies metamorphism which postdated the Sanbagawa metamorphism. Further, many kinds of tectonic blocks were found from the Klippes. Some of them could not be formed by the Sanbagawa metamorphism. These petrographic data support the klippe model.

Acknowledgements

I am grateful to professor S. Banno, who helped me forward and gave me a through knowledge of the past and current problems concerning the phase petrology. I am deeply indebted to Mr. S. Uchida for a kind offer of his sample collection. Special thanks are due to prof. S. Banno and colleagues of Kyoto University and Kanazawa University for numerous encouraging discussion on the present problem and for moral and professional support.

Reference

Aiba, K., 1982: Sanbagawa metamorphism of the Nakatsu-Nanokawa district, the northern subbelt of the Chichibu belt in western central Shikoku. Jour. Geol. Soc. Japan, 88, 875-885. (J)

--------, Higashino, T., Sakai, C., & Banno, S., 1984: Electron microprobe analyses of rock-forming minerals from the Sanbagawa Metamorphic rocks, Shikoku. Part III. Nakatsu-Nanokawa and Yanadani-Mikawa Areas. Sci. Rep. Kanazawa Univ., 29, 65-90.

Albee, A.L., 1965: A petrogenetic grid for the Fe-Mg silicates of pelitic schists. Amer. Jour. Sci., 263, 512-536.

------------, & Ray, L., 1970: Correction factors for electron-probe microanalysis of silicates, oxides, carbonates, phosphates and sulphates. Analyt. Chem., 42, 1408-1414.

Arai, F., Hayama, Y., Hayashi, S., Hosoya, T., Ibe, H., Kanzawa, K., Kizaki, Y., Kim, G.J., Takahashi, K., Takahashi, T., Takei, K., Toya, K., Yamashita, N., & Yoshiba, K., 1963: OntheAtokura conglomerate in the Shimonita district, Gumma Prefecture. Earth Science, 64,18-31. (J)

---------, Hayama, Y., Hayashi, S., Hosoya, T., Ibe, H., Kanzawa, K., Kizaki, Y., Kubo, S., Nakajima, T., Takahashi, K., Takahashi, T., Takei, K., Toya, K.,

Yamashita, N., & Yoshiba, K., 1966: The Shimonita tectonic zone. Earth Science, 83, 8-25. (J)

Aumento, F., 1969: Diorites from the Mid-Atlantic Ridge at 45°N. Science, 165, 1112-1113.

Bailey, E.H., Blake, M.C., & Jones, D.L., 1970: On-land mesozoic oceanic crust in California Coast Range. Prof. Pap. U.S. Geol. Surv., 700-C, 70-81.

Banno, S., 1959: Aegirineaugites from crystalline schists in Sikoku. Jour. Geol. Soc. Japan, 65, 652-657.

---------, 1964: Petrologic studies on Sanbagawa crystalline schists in the Besshi-Ino district, central Shikoku. Jour. Fac. Sci. Univ. Tokyo, Sec.II, 15, 203-319.

---------, & Kurata, H., 1972: Distribution of Ca in zoned garnet of low-grade pelitic schists. Jour. Geol. Soc. Japan, 78, 507-512.

---------, Higashino, T., Otsuki, M., Itaya, T., & Nakajima, T., 1978: Thermal structure of the Sanbagawa metamorphic belt in the central Shikoku. Jour. Phys. Earth, 26, 345-356.

Bence, A.E., & Albee, A.L., 1968: Empirical correction factors for the electron microanalysis of silicates and oxides. Jour. Geol., 76, 626-634.

Binns, R.A., 1965: The mineralogy and metamorphosed basic rocks from the Willyama complex, Broken Hill district, New South Wales, Pt. I. Hornblendes. Min. Mag., 35, 306-326.

Black, P.M., 1970: Co-existing glaucophane and riebeckite-

arfvedsonite from New Caledonia. Amer. Min. 55, 1060-1064.

----------, 1973a: Mineralogy of New Caledonian metamorphic rocks. I. Garnet from the Ouégoa district. Contrib. Mineral. Petrol., 38, 221-235.

----------, 1973b: Mineralogy of New Caledonian metamorphic rocks. II. Amphiboles from the Ouégoa district. Contrib. Mineral. Petrol., 39, 55-64.

----------, 1974: Mineralogy of New Caledonian metamorphic rocks.III. Pyroxenes and major element partitioning between coexisting pyroxenes, amphiboles and garnets from the Ouégoa district. Contrib. Mineral. Petrol., 45, 281-288.

----------, 1977: Regional high-pressure metamorphism in New Caledonia; Phase equilibria in the Ouégoa district. Tectonophysics, 43, 89-107.

----------, & Brothers, R.N., 1977: Blueshists ophiolites in the melange zone, Northern New Caledonia. Contrib. Mineral. Petrol., 65, 69-78.

Brothers, R.N., 1970: Lawsonite-albite schists from northernmost New Caledonia. Contrib. Mineral. Petrol., 25, 185-202.

----------, 1974: High-pressure schists in Northern New Caledonia. Contrib. Mineral. Petrol., 46, 109-127.

----------, & Yokoyama, K., 1982: Comparison of the high-pressure schist belts of New Caledonia and Sanbagawa,

Japan. Contrib. Mineral. Petrol., 79, 219-229.

Brown, E.H., 1974: Comparison of the mineralogy and phase relations of blueschists from the North Cascades, Washington, and greenschists from Otago, New Zealand. Bull. Geol. Soc. Amer., 85, 333-344.

----------. 1977a: Phase equilibria among pumpellyite, lawsonite, epidote and associated minerals in low grade metamorphic rocks. Contrib. Mineral. Petrol., 64, 123-136.

----------. 1977b: The crossite content of Ca-amphibole as guide to pressure of metamorphism. Jour. Petrol., 18, 58-72.

----------, & Bradshaw, J.Y., 1979: Phase relations of pyroxene and amphibole in greenstone, blueschist and eclogite of the Franciscan Complex, California. Contrib. Mineral. Petrol., 71, 67-83.

Burnham, C.W., Holloway, J.R., & Davis, N.F., 1969: Thermodynamic properties of water to 1,000°C and 10,000 bars. Geol. Soc. Amer., Special Paper, 132.

Cann, J.R., 1970: Rb, Sr, Y, Zr, and Nb in some ocean-floor basaltic rocks. E.P.S.L., 10, 7-11.

Carpenter, M.A., 1980: Mechanisms of exsolution in sodic pyroxenes. Contrib. Mineral. Petrol., 71, 289-300.

Chichibu Research Group, 1961: On the Paleozoic formations and geologic structure of the Kanna-gawa district. Earth Science, 57, 1-11. (J)

Coleman, R.G., & Lee, D.E., 1963: Glaucophane-bearing

metamorphic rock types of the Cazadero area, California. Jour. Petrol., 4, 260-301.

----------, & Papike, J.J., 1968: Alkali amphiboles from the blueschists of Cazadero, California. Jour. Petrol., 9, 105-122.

Compagnoni, R., & Maffeo, B., 1973: Jadeite-bearing metagranites l.s. and related rocks in the Mount Mucrone area. (Sesia-Lanzo zone, Western Italian Alps) Schweiz. Min. Petr. Mitt., 53/3, 355-378.

Coombs, D.S., 1971: Present status of the zeolite facies. 'Molecular sieve zeolites-1', in Advances in chemistry series, No. 11, Amer. Chem. Soc., 317-327.

----------, Nakamura, Y., & Vuagnat, M., 1976: Pumpellyite-actinolite facies schists of the Taveyanne Formation near Loèche, Valais, Switzerland. Jour. Petrol., 17, 440-471.

Crowford, W.A., & Hoersch, A.L., 1972: Calcite-aragonite equilibrium from 50°C to 150°C. Amer. Min., 57, 995-998.

Curtis, L.W., & Gittins, J., 1979: Aluminous and titaniferous clinopyroxenes from regionally metamorphosed agpaitic rocks in Central Labrador. Jour. Petrol., 20, 165-186.

Deer, W.A., Howie, R.A., & Zussman, J., 1966: An introduction to the rock forming minerals. Longman, New York.

Ernst, W.G., 1962: Synthesis, stability relations and occurrence of riebeckite-arfvedsonite solid solutions. Jour. Geol., 70, 689-736.

----------, 1965: Mineral parageneses in Franciscan metamorphic rocks, Panoche Pass, California. Bull. Geol. Soc. Amer., 76, 879-914.

----------, 1971: Petrologic reconnaissance of Franciscan metagraywackes from the Diablo Range, Central California Coast Ranges. Jour. Petrol., 12, 413-437.

----------, Seki, Y., Onuki, H., & Gilbert, M.C., 1970: Comparative study of low-grade metamorphism in the Californian Coast Range and the Outer Metamorphic Belt of Japan. Geol. Soc. Amer. Mem. 124, pp.276.

Eskola, P., 1920: The mineral facies of rocks. Norsk Geol. Tidsskr., 6, 143-194.

----------, 1939: Die metamorphen Gesteine. In Die Entstehung der Gesteine, by T.F.W. Barth, C.W. Correns and P. Eskola, 263-407. Berlin: Julius Springer. Reprinted in 1960 and 1970.

Essene, E.J., & Fyfe, W.S., 1967: Omphacite in Californian rocks. Contrib. Mineral. Petrol., 15, 1-23.

Fyfe, W.S., Turner, F.J., & Verhoogen, J., 1958: Metamorphic relations and metamorphic facies. Geol. Soc. Amer., Mem. 73.

Fujimoto (Huzimoto), H., 1935: Geological study of the northern Kanto Mountains. Jour. Geol. Soc. Japan, 42, 137-151, 163-181. (J)

---------, 1937: The nappe theory with reference to the north-eastern part of the Kanto-mountainland. Sci. Rep., Tokyo Bunrika Daigaku, Sect. C, 6, 215-244.

---------, Watanabe, K., & Sawa, H., 1953: The nappe theory with reference to the northern part of the Kwanto-Mountainland. Bull. Chichibu Museum Natural History, 3, 1-42. (J)

---------, & Sakamoto, O., 1973: Further notes on the nappe structure of Kamiyama, one of the typical nappe blocks of the Kanto Massif. Bull. Chichibu Museum Natural History, 1-11. (J)

Geological Map of Japan,1978: eds.by O. Hirokawa, Geol. Sur. Japan.

Gouchi, N., 1983: Kamuikotan metamorphic rocks in the Kamuikotan gorge area, west of Asahikawa, Hokkaido. Jour. Japan. Assoc. Min. Pet. Econ. Geol., 78, 383-393. (J)

Hada, S., & Suzuki, T., 1983: Tectonic environments and crustal section of the outer zone of south west Japan. In Accretion Tectonics in the Circum Pacific Regions, edited by M. Hashimoto and S. Uyeda, 207-218.

Hallimond, A. F., 1943: On the graphical representation of the califerous amphiboles. Amer. Min., 26, 29-33.

Hara, I., Hide, K., Takeda, K., Tsukuda, E., Tokuda, M., & Shiota, T., 1977: Tectonic movement of the Sambagawa Belt. The Sambagawa Belt, eds. Hide, K., Hiroshima

Univ. Press, 307-390. (J)

Hashimoto, M., 1964: Omphacite veins in metadiabase from Asahine in the Kanto Mountains, Japan. Proc. Japan Acad., 40, 31-35.

----------, 1966: On the prehnite-pumpellyite metagreywacke facies. Jour. Geol. Soc. Japan, 172, 253-265. (J)

Henley, R.W., 1978: Arfvedsonite in basalt dykes, Buchans, Newfoundland. Amer. Min., 63, 413-414.

Higashino, T., 1975: Biotite zone of Sanbagawa metamorphic terrain in the Siragayama area, central Shikoku, Japan. Jour. Geol. Soc. Japan, 81, 653-670. (J)

Hirajima, T., 1983a: Jadeite+quartz rock from the Kanto Mountains. Jour. Japan. Assoc. Min. Pet. Econ. Geol., 78, 77-83.

----------, 1983b: The analysis of the paragenesis of glaucophanitic metamorphism for a model ACF system by Schreinemakers' method. Jour. Geol. Soc. Japan, 89, 679-691. (J)

----------, 1984: The greenrock mélange in the Yorii area, in the northeastern part of the Kanto Mountains. Jour. Geol. Soc. Japan, 90, ------(J)

----------, Hiroi, Y., & Ohta, Y., 1984: Lawsonite and pumpellyite from Vestgotabreen Formation in Spitsbergen. Norsk. Geol. Tidd., (impress)

Holland, T.J.B., 1980: The reaction albite = jadeite + quartz determined experimentally in the range 600-

1200°C. Amer.Min., 65, 129-134.

----------, 1983: The experimental determination of activities in disordered and short-range ordered jadeitic pyroxenes. Contrib. Mineral. Petrol., 82, 214-220.

Ichikawa, K., Ishii, K., Nakagawa, C., Suyari, K., & Yamashita, N., 1956: Die Kurosegawazone. Jour. Geol. Soc. Japan, 62, 82-103. (J)

Iijima, H., 1964: On the so-called Atokura Formation, near Mts. Medake and Odake (Part 1). Bull. Chichibu Museum Natural History, 12, 29-36. (J)

Inoue, M., 1974: Geologic structures of the Chichibu Terrain in the Kanto Mountains Land, Japan. Jour. Fac. Sci., Univ. Tokyo, Sec. II, 19, 1-25.

Johannes, W., & Puhan, D., 1971: The calcite-aragonite transition, reinvestigated. Contrib. Mineral. Petrol., 31, 28-38.

Kadota, O., & Tokunaga, S., 1982: On the geologic age of the Tochiya Formation, northwest of Ogawa-machi, Saitama Prefecture. Jour. Geol. Soc. Japan, 88, 637-640. (J)

Kanat, L.H., 1984: Jadeite from southern Oscar II Land, Svalbard. Min. Mag., 48, 301-303.

Katagas, C., 1974: Alkali amphiboles intermediate in composition between actinolite and riebeckite. Contrib. Mineral. Petrol., 46, 257-264.

Kawachi, Y., 1975: Pumpellyite-actinolite and contiguous

facies metamorphism in part of Upper Wakatipu district, South Island, New Zealand. New Zealand Jour. Geol. Geophys., 18, 401-441.

Kimura, T., 1977: Decollement between the Mikabu Green Rocks and the weakly metamorphosed Chichibu Meso-Paleozoic formation. Abstr. 84th meeting of Geol. Soc. Japan, 148. (J)

---------, & Yoshida, S., 1973: The basement structure of Neogene System in the Northeast Japan. Structural Geology on the crustal movement of the Tertiary Period in the Northeast Japan, 1-7. (J)

Klein, C., 1969: Two-amphibole assemblages in the system actinolite-hornblende-glaucophane. Amer. Min., 54, 212-237.

Koike, T., Igo, H., Takizawa, S., & Kinoshita, T., 1971: Contribution tothe geological history of theJapanese Islands by the Conodont biostratigraphy. Jour. Geol. Soc. Japan, 77, 165-168.

Korzhinskii, D.S., 1959: Physicochemical basis of the analysis of the paragenesis of minerals. Chapman and Hill, Ltd., London, pp.142.

Kosaka, K., 1979: Cretaceous and post-Cretaceous faultings in the northeastern Kanto Mountains. Jour. Geol. Soc. Japan, 85, 157-176. (J)

Koto, B., 1889: On the so-called crystalline schists of Chichibu. (The Sanbagawan Series) Jour. Coll. Sci., Imp. Univ. Tokyo, II, 77-141.

Kozima, Z., (Kojima, J.,) 1944: On stilpnomelane in greenschists in Japan. Proc. Imp. Acad., 20, 322-328.

Kuno, H., Yamasaki, K., Iida, C., & Nagashima, K., 1957: Differentiation of Hawaiian magmas. Japan. Jour. Geol. Geogr., 28, 179-218.

Kurata, H., & Banno, S., 1974: low-grade progressive metamorphism of pelitic schists of the Sazare area, Sanbagawa metamorphic terrain in central Sikoku, Japan. Jour. Petrol., 15, 361-382.

Laird, J., 1980: Phase equilibria in mafic schists from Vermont. Jour. Petrol., 21, 1-37.

----------, & Albee, A.L., 1981: High-pressure metamorphism in mafic schist from northern Vermont. Amer. Jour. Sci., 281, 97-126.

Leake, B.E., 1965: The relationship between tetrahedral aluminum and the maximum possible octahedral aluminum in natural calciferous and subcalciferous amphiboles. Amer. Min., 50, 843-851.

----------, 1968: A catalog of analyzed calciferous and subcalciferous amphiboles together with their nomenclature and associated minerals. Geol. Soc. Amer., Special paper No.98,

----------, 1978: Nomenclature of amphiboles. Amer. Min., 63, 1023-1052.

Liou, J.G., 1971: P-T stabilities of Laumontite, Wairakite, Lawsonite, and related minerals in the system

$CaAl_2Si_2O_8$-SiO_2-H_2O. Jour. Petrol., 12, 379-411.

Lyons, P.C., 1976: The chemistry of riebeckites of Massachusetts and Rhode Island. Min. Mag., 40, 473-479.

Maeda, S., 1954: Geologic structures of the eastern part of the Kwanto-Mountainland. Jour. Coll. Arts. Sci., Chiba Univ., 1, 160-165. (J)

Maruyama, S., 1978: Dismembered ophiolite in the Kurosegawa tectonic zone. Kaiyo-Kagaku, 10, 287-296. (J)

---------, 1981: The Kurosegawa melange zone in the Ino district to the north of Kochi city. Jour. Geol. Soc. Japan, 87, 569-583.

Misch, P., & Rice, J.M., 1975: Miscibility of tremolite and hornblende in progressive Skagit metamorphic suite, north Cascades, Washington. Jour. Petrol., 16, 1-21.

Miyashiro, A., 1957: The chemistry, optics and genesis of the alkali-amphiboles. Jour. Fac. Sci., Univ. Tokyo, Sec. II, 11, 57-83.

--------------, 1958: Regional metamorphism of the Gosaisho-Takanuki district in the central Abukuma Plateau. Jour. Fac. Sci., Univ. Tokyo, Sec. II, 11, 219-272.

--------------, 1961: Evolution of metamorphic belts. Jour. Petrol., 2, 277-311.

--------------, 1965: Metamorphic rocks and metamorphic belts. Iwanami-Shoten, Tokyo, pp.458.

--------------, 1973: Metamorphism and metamorphic belts. George Allen & Unwin, London, pp.492.

--------------, & Banno, S., 1958: Nature of glaucophanitic

metamorphism. Amer. Jour. Sci., 256, 97-110.

----------, & Seki,Y., 1958: Enlargement of the composition field of epidote and piemontite with rising temperature. Amer. Jour. Sci., 256, 423-430.

----------, Shido, F., & Ewing, M., 1969: Diversity and origin of abyssal tholeiite from the Mid-Atlantic Ridge near 24° and 30° North Latitude. Contrib. Mineral. Petrol., 23, 38-52.

Munhá, J., 1979: Blue amphiboles, metamorphic regime and plate tectonic modelling in the Iberian Pyrite Belt. Contrib. Mineral. Petrol., 69, 279-289.

Murai, T., 1965: On the garnet-amphibolites of the Yoshimi Hill, Saitama Prefecture, Japan. Sci. Rep. Saitama Univ., Ser. B, 5, 65-71.

Nakajima, T., 1975: Petrologic studies on the greenstones of the Sanbagawa southern marginal belt in central Shikoku, Japan. Master Theses of Kanazawa Univ., MS. (J)

----------, Banno, S., & Suzuki, T., 1977: Reaction leading to the disappearance of pumpellyite in low-grade metamorphicrocks of the Sanbagawa metamorphic belt in central Shikoku, Japan. Jour. Petrol., 18, 263-284.

Newton, R.C., & Smith, J.V., 1967: Investigations concerning the breakdown of albite at depth in the earth. Jour. Geol., 75, 268-286.

Nitsch, K.H., 1968: Die Stabilitat von Lawsonit.

Naturwissenschaften, 55, 388.

----------, 1971: Stabilitatsbeziehungen von Prehnit und Pumpellyit-haltigen Paragenesen. Contrib. Mineral. Petrol., 30, 240-260.

Okay, A.I., 1980a: Mineralogy, petrology, and phase relations of glaucophane-lawsonite zone blueschists from the Tavsanli region, northwest Turkey. Contrib. Mineral. Petrol., 72, 243-255.

----------., 1980b: Lawsonite zone blueschists and a sodic amphibole producing reaction in the Tavsanli Region, Northwest Turkey. Contrib. Mineral. Petrol., 75, 179-186.

----------., 1982: Incipient blueschist metamorphism and metasomatism in the Tavsanli region, Northwest Turkey. Contrib. Mineral. Petrol., 79, 361-367.

Okursch, M., Seidel. E., & Davis, E.N., 1978: The assemblage jadeite-quartz in the glaucophane rocks of Sifnos (Cyclades Archipelago, Greece). Neues Jahrb. Min. Abhdl., 132, 284-308.

Okubo, M., & Horiguchi, M., 1969: Geology of Mamba district. Quadrangle series, scale 1:50,000, Tokyo(8) No.26, Geol. Surv. Japan. (J)

Ono, A., 1983: K-Ar age of the Kinshozan quartz diorite from the Kanto Mountains. Jour. Japan. Assoc. Min. Pet. Econ. Geol., 78, 38-39. (J)

Otsuki, M., 1980: Petrological study of the basic Sanbagawa metamorphic rocks in central Shikoku, Japan. Ph.D.

Thesis of Tokyo Univ., MS

Rasse, P., 1974: Al and Ti contents of hornblende, indicators of pressure and temperature of regional metamorphism. Contrib. Mineral. Petrol., 45, 231-236.

De Roever, E.W.F., 1972: Lawsonite-albite facies metamorphism near Fuscaldo, Calabria (South Italy), its geological significance and petrological aspects. GUA papers of Geology 1,

Sakai, C., 1980: Biotite zone in the Sambagawa metamorphic terrain east of Onishi-machi, Kanto Mountains. Jour. Geol. Soc. Japan, 86, 517-524. (J)

--------, 1982: Time-pressure-temperature trajectory of the Sanbagawa metamorphism deduced from kinetics of crystallization and chemistry of garnet in pelitic schists. Master Thesis of Kanazawa Univ., MS

Sashida, K., Igo, H., Igo, H., Takizawa, S., Hisada, K., Shibata,T., Tsukada, K., & Nishimura, H., 1982: On the Jurassic radiolarian assemblages in the Kanto Mountains. News of Osaka Micropaleontologists Special Volume No. 5, 51-66. (J)

Sato, T., Takizawa, S., & Kodato, T., 1977: Revision of stratigraphy and structure of the Sakahara Formation at its type locality. Jour. Geol. Soc. Japan, 83, 631-637. (J)

Sciffman, P., & Liou, J.G., 1980: Synthesis and stability relation of Mg-Al pumpellyite, $Ca_4Al_5MgSi_6O_{21}(OH)_7$.

Jour. Petrol., 21, 441-474.

Seki, Y., 1957: Lawsonite from the eastern part of the Kanto Mountainland. Jour. Japan. Assoc. Min. Pet. Econ. Geol., 41, 155-163.

-------, 1958: Glaucophanitic regional metamorphism in the Kanto Mountains, central Japan. Japan. Jour. Geol. Geogr., 29, 233-258.

-------, 1960: Jadeite in Sambagawa crystalline schists of central Japan. Amer. Jour. Sci., 258, 705-715.

--------, 1969: Facies series in low-grade metamorphism. Jour. Geol. Soc. Japan, 75, 255-266.

-------, 1972: Lower-grade stability limit of epidote in the light of natural occurrence. Jour. Geol. Soc. Japan, 78, 405-413. (J)

--------, & Shido, F., 1959 : Finding of jadeite from the Sambagawa and Kamuikotan metamorphic belts, Japan. Japan Acad. Proc., 35, 137-138.

Silver, E.A., & Beutner, E.C., 1980: Melanges. Geology, 8, 32-34.

Sugiyama, R., 1943: On the so-called Atokura conglomerate of Simonita-mati, Gunma Prefecture. Bull. Tokyo Sci. Mus., 3, 1-37. (J)

Suzuki, M., 1977: On the Sambagawa metamorphic rocks of the western part in the Kanto Mountains, central Japan. The Sambagawa Belt, eds. Hide, K., Hiroshima Univ. Press, 207-216. (J)

Tagiri, M., 1977: Fe-Mg partition and miscibility gap

between coexisting calcic amphiboles from the southern Abukuma Plateau, Japan. Contrib. Mineral. Petrol., 62, 271-281.

Takasu, A., 1984: Prograde and retrograde eclogites in the Sambagawa metamorphic belt, Besshi district, Japan. Jour. Petrol., 25, 619-643.

Takayama, M., 1984: Geologic and petrologic study of the Sanbagawa metamorphic rocks in the Sanbagawa-Ayukawa area, Gunma Prefecture, central Japan. Graduation Thesis of Kyoto Univ., MS

Takizawa, S., & Sato, T., 1979: The character of the geologic structure in the northern part of the Kanto Mountains. Abstr. 86th meeting of Geol. Soc. Japan, 323. (J)

Tanabe, K., 1981: Petrologic studies of the Sanbagawa metamorphic terrain, the Kanto Mountains. Master Thesis of Chiba Univ., MS (J)

--------, Tomioka, N., & Kanehira, K., 1982: Jadeite-aragonite-bearing rocks from the Sanbagawa metamorphic terrane in the Kanto Mountains. Proc. Japan Acad., 58, 199-203.

Tanaka, K., & Fukuda, M., 1974: Geologic structure and metamorphic zoning of the northern extremity of the Sanbagawa metamorphic terrain in the Kanto Mountains. --with special reference of the occurrence of biotite-- Jour. Japan. Assoc. Min. Pet. Econ. Geol., 69, 313-

323. (J)

Thompson, J.B., Jr., 1955: The thermodynamic basis for the mineral facies concept. Amer. Jour. Sci., 253, 65-103.

---------, Laird, J., & Thompson, A.B., 1982: Reactions in amphibolite, greenschist, and blueschist. Jour. Petrol., 23, 1-27.

Toriumi, M., 1974: Actinolite-alkali amphibole miscibility gap in an amphibole composite-grain in a glaucophane schist facies rocks, Kanto Mountains, Japan. Jour. Geol. Soc. Japan., 80, 75-80.

--------, 1975: Petrological study of the Sambagawa metamorphic rocks, Kanto Mountains, central Japan. Bull. Univ. Mus., Univ. Tokyo, 9. 1-99.

Uchida, N., 1962: On the "Atokura Conglomerate" -Geological studies of the Shimonita district, Gumma Prefecture, part 2 - Jour. Geol. Soc. Japan, 68, 133-140. (J)

--------, 1966: On some problems of the geology in the northern part of the Kanto Mountains, central Japan. Seikei Ronso, 5, 3-22. (J)

-------, 1967: Mikabu tectonic line. Seiji-Keizai Ronso, Seikei Univ., 16, 510-535. (J)

--------, 1978: On the nappe theory with reference to the northern part of the Kanto Mountainland. -Review of the research- Jour. Geography, 187, 16-26. (J)

--------, 1981: Major-element petrochemistry of lavas and tuffs from the Sanbagawa and Chichibu terrane. -The northern Kanto Mountains, central Japan- Seikei

Ronso, 20, 1-138.

Watanabe, T., 1974: Metamorphic zoning of the Sambagawa and Chichibu belts in the Koshibu-gawa River area, Oshika district, central Japan, with special reference to pumpellyite-actinolite schist facies mineral assemblage. Jour. Geol. Soc. Japan, 80, 525-538.

---------, 1975: Aegirine-augite and sodic augite from the Sanbagawa and the Chichibu belts in the Oshika District, central Japan, with special reference to Na-metasomatism. Jour. Fac. Sci. Hokkaido Univ., Ser. IV, 16, no. 4.

Winkler, H.F.G., 1965: Die Genese der metamorphen Gesteine. Springer, Berlin, Heidelberg.

Yajima, T., Kajima, M., & Arai, Y., 1984: On the green-rocks on and around Mt. Maruyama, Yokoze Village, Saitama Prefecture. Jour. Geol. Soc. Japan. 90, 329-343, (J)

Yasudo Research Group, 1982: Stratigraphy and geologic structure of the Mikabu green rocks around Mt. Dohdaira in the Kanto mountains,central Japan. Earth Science, 36, 23-34. (J)

Yoshizawa, H, 1984: Petrologic study of the pumpellyite-actinolite facies rocks in the Oboke Area, Sanbagawa Metamorphic terrain in central Shikoku, Japan. Master Theses of Kyoto Univ., MS

Zen, E-An, 1966a: Construction of pressure-temperature diagrams for multicomponent systems after the method of

Schreinemakers-- A geometric approach. Geol. Surv., Bull. 1225.

-----, 1966b: Some topological relationships in multisystems of n+3 phases. I. General theory; Unary and binary systems. Amer. Jour. Sci., 264, 401-427.

-----, 1967: Some topological relationships in multisystem of n+3 phases. II. Unary and binary metastable sequences. Amer. Jour. Sci., 265, 871-897.

-----, 1974: Prehnite- and pumpellyite-bearing mineral assemblages, West side of the Appalachian Metamorphic belt, Pennsylvania to Newfoundland. Jour. Petrol., 15, 197-242.

-----, & Roseboom, E.H.Jr., 1972: Some topological relationships in multisystems of n+3 phases. III. Ternary systems. Amer. Jour. Sci., 272, 677-710.